UNIVERSIDADE TÉCNICA DE LISBOA

INSTITUTO SUPERIOR TÉCNICO

UMTS PERFORMANCE IN MULTI-SERVICE NON-UNIFORM TRAFFIC NETWORKS

Luís Miguel da Cruz Santo

(Licenciado)

Dissertation submitted for obtaining the degree of Master
In Electrical and Computer Engineering

Supervisor: Doctor Luís Manuel de Jesus Sousa Correia

Jury

President: Doctor Rui Manuel Rodrigues Rocha

Members: Doctor Américo Manuel Carapeto Correia

Doctor Luís Manuel de Jesus Sousa Correia

March 2005

To Susana and my parents

‘If you would be a real seeker after truth, you must at least once in your life doubt, as far as possible, all things. ’

(R. Descartes in *Discours de la Méthode*, 1637**)**

Acknowledgements

First, I would like to thank Prof. Luís Correia for having supervised this work and for the unique opportunity of the knowledge and experience sharing along the work. His dedication, discipline, constant support and guidelines were a key factor for the completion of an ambitious and comprehensive project such as a Master thesis.

A special thanks to the GROW team, in particular Allen Vasconcelos, Lúcio Ferreira, Filipe Cardoso, for all fruitful discussions and clarifications, and António Serrador for the crucial technical orientations in the software development phase.

To all Optimus colleagues with whom I shared my thoughts and doubts throughout these last three years, especially to Carlos Rodrigues for its constant encouragement and work reference without whom the finishing of this thesis would have been a much more difficult task. I would also like to thank Optimus management, namely Ana Claro and Judite Reis for the support, encouragement and providing the necessary availability to complete this thesis.

From Susana, I received constant encouragement, motivation and support, in first place for starting a Master Thesis, and then throughout the whole development of this work.

I would also like to thank my parents, my brother and all my friends for their unconditional and constant support throughout this journey.

Abstract

This work analyses the overall performance at the UTRAN FDD radio interface of multi-service non-uniform traffic networks, with the aid of a newly developed simulation platform. The traffic mix impact is analysed at system level (circuit switch calls blocking rate, average delay of packet switch packets/frames, mean bit rate obtained for packet switch data, etc.), either in the speech vs. data split or in the packet switch domain service distribution. Assessment of non-uniformity traffic generation patterns is investigated for two main site/user density scenarios.

Detailed assessment is provided and traffic mix performance impact is modelled, extrapolating network figures for non-uniform traffic scenarios. Impact of RRM strategies, such as channel switching, soft handover (active set window) and load control is analysed.

Eight different applications/services were considered and characterised for user traffic generation: Speech, Video-telephony, Streaming, Web Browsing, Location Based Services, Multimedia Messaging Service, E-mail, and File Transfer Protocol. Traffic source models, as well as call/session generation and duration processes, have been implemented for each of these applications.

From the statistical analysis of user traffic variations performed in this work, it has been verified that result convergence requires a minimum of 20 runs per scenario to allow a reasonable degree of confidence.

As expected, the performance indicators degrade with the increase of the data vs. speech split, reaching a five times higher average blocking rate when speech is reduced from 60 to 25% of the total traffic mix. Site/user density scenarios shown high impact on the considered population penetration for an average target blocking of 1%. It has been verified that, for instance, a high density scenario comprising 1% population penetration leads to approximately 1% blocking, while in a lower density scenario, equivalent blocking is achieved only when users reach 4% population penetration.

Keywords

UMTS, Multi-Service Traffic, Non-Uniform Traffic Distributions, Quality of Service, System Performance

Resumo

Neste estudo é analisado o desempenho da interface rádio do sistema UTRAN FDD na presença de um perfil de tráfego multi-serviços não uniforme, recorrendo ao desenvolvimento de uma nova plataforma de software – TRAFSIM3G. O impacto do perfil multi-serviços é aferido ao nível do desempenho do sistema (taxa de bloqueio de chamadas de comutação de circuitos, atraso médio dos pacotes/tramas de chamadas de comutação de pacotes, ritmos binários médios das chamadas de comutação de pacotes, etc.). O impacto da não uniformidade de tráfego é aferido recorrendo à definição de dois cenários com diferentes densidades de utilizadores e estações base.

O impacto da distribuição do perfil multi-serviços é investigado em detalhe, sendo feita uma análise quantitativa e qualitativa dos principais indicadores de desempenho de sistema. É também analisado o impacto das estratégias de gestão de recursos rádio como o *channel switching, soft handover* e controlo de carga.

Oito aplicações distintas são consideradas e caracterizadas na geração do perfil de tráfego por utilizador: Voz, Video-telefonia, *Streaming, Location Based Services*, Serviços de Mensagens Multimédia, *E-mail* e Transferência de Ficheiros. Modelos de tráfego fonte, bem como a geração e duração de chamadas e sessões são implementadas para cada uma destas aplicações.

Da análise das variações do perfil multi-serviços, verificou-se que um mínimo de 20 simulações para cada cenário são necessárias para se considerar a convergência dos principais indicadores tendo em conta a análise da evolução do(s) intervalo(s) de confiança.

Em linha com o esperado, os principais indicadores de desempenho (bloqueio e atraso médio) degradam-se na presença de um perfil multi-serviços polarizado para os serviços de dados, atingindo o bloqueio 5 vezes o valor obtido no cenário dominado pelo serviço de voz. Dos dois cenários de utilizadores/estação base infere-se uma diferença substancial, obtendo-se no cenário de baixa densidade a mesma taxa de bloqueio para uma penetração de população 4 vezes superior à considerada no cenário de alta densidade.

Palavras-chave

UMTS, Tráfego multi-serviços, Distribuições de Tráfego Não Uniforme, Qualidade de Serviço, Desempenho de Sistema

Table of Contents

List of Figures

List of Tables

List of Abbreviations

2G	2nd Generation Systems
3G	3rd Generation Systems
3GPP	Third Generation Partnership Project
AI	Acquisition Indicator
AICH	Acquisition Indicator Channel
AMR	Adaptive Multi Rate
AS	Active Set
ATM	Asynchronous Transfer Mode
Ax	Axial (or road sites)
BB	Base Band boards
BCH	Broadcast Channel
BH	Busy Hour
BER	Bit Error Rate
CAPEX	Capital Expenditures
CBD	Central Business District
CC	Common Channels
CCTrCH	Coded Composite Transport Channel
CDF	Cumulative Distribution Function
CE(M)	Channel Element (Module)
CN	Core-Network
CPICH	Common Pilot Channel
CRNC	Controlling RNC
CS	Circuit Switch
DCCH	Dedicated Common Channels
DCH	Dedicated Channel
DL	Downlink
DLL	Dynamic Link Library
DPCCH	Dedicated Physical Common Channel
DPCH	Dedicated Physical Channel
DPDCH	Dedicated Physical Data Channel
DRNC	Drift RNC
DSCH	DL Shared Channel

DTCH	Dedicated Traffic Channels
DU	Dense Urban
EFR	Enhanced Full Rate
EIRP	Equivalent Isotropic Radiated Power
FACH	Forward Access Channel
FDD	Frequency Division Duplex
FER	Frame Error Rate
FFM	Fast Fading Margin
FTP	File Transfer Protocol
GGSN	Gateway GPRS Support Node
GIS	Geographical Information Systems
GPRS	General Packet Radio Service
GSM	Global System for Mobile Communications
HLR	Home Location Register
HIMM	High Interactive Multimedia
IETF	Internet Engineering Task Force
IM	Interference Margin
IOT	Interoperability
IPDL	Idle Periods in DL
LNA	Low Noise Amplifier
LoS	Line of Sight
MAC	Medium Access Control
MCPA	Multi Carrier Power Amplifier
MHT	Mean Holding Time
MMM	Medium Multimedia
MP3	MPEG-1 Audio Layer-3
MPEG	Moving Picture Experts Group
MRC	Maximum Ratio Combining
MSC	Mobile Services Switching Centre
NLoS	Non Line of Sight
OPEX	Operational Expenditures
OVSF	Orthogonal Variable Spreading Factor
PA	Power Amplifier
P-CCPCH	Primary Common Control Physical Channel

PCH	Paging Channel
PCPCH	Physical Common Packet Channel
PI	Paging Indicator
PICH	Paging Indicator Channel
PRACH	Physical Random Access Channel
PS	Packet Switch
P-SCH	Primary Synchronisation Channel
QoS	Quality of Service
QPSK	Quadrature Phase Shift Keying
R99	3GPP Release 1999
RAB	Radio Access Bearer
RACH	Random Access Channel
RANAP	Radio Access Network Application Part
RB	Radio Bearer
RL	Radio Link
RNC	Radio Network Controller
RNS	Radio Network Sub-systems
RRC	Radio Resource Control
RRM	Radio Resource Management
RSCP	Received Signal Code Power
Ru	Rural (sites)
S-CCPCH	Secondary Common Control Physical Channel
SF	Spreading Factor
SGSN	Serving GPRS Support Node
SHO	Soft Handover
SIP	Session Initiation Protocol
SSC	Secondary Synchronisation Codes
SSHO	Softer Handover
S-SCH	Secondary Synchronisation Channel
SU	Suburban (sites)
SYS INFO	(Broadcasted) System Information
TD	Transmit Diversity
TDD	Time Division Duplex
TF	Transport Format

TFCI	Transport Format Combination Indicator
TFS	Transport Format Set
TMA	Tower Mounted Amplifier
TPC	Transmission Power Control
TRX/M	Transceiver Module
TTI	Transmission Time Interval
U	Urban (sites)
UARFCN	UTRA Absolute Radio Frequency Channel Number
UE	User Equipment
UL	Uplink
UMTS	Universal Mobile Telecommunication System
USIM	UMTS Subscriber Identity Module
UTRA	Universal Terrestrial Radio Access
UTRAN	UMTS Terrestrial Radio Access Network
VC++	Visual C++®
VLR	Visitor Location Register
VoIP	Voice over IP
WCDMA	Wideband Code Division Multiple Access
WWW	World Wide Web

List of Symbols

α	DL orthogonality factor
Δf	Signal bandwidth
φ	Road orientation with respect to the direct radio path
υ	Channel activity factor
ρ	Slope of propagation distance coefficient
σ	Standard deviation of the slow fading margin (indoor and outdoor)
σ_{in}	Standard deviation of the building penetration losses
σ_{out}	Standard deviation of the outdoor shadow fading
η_{DL}	DL load factor
η_{UL}	UL load factor
b	Building separation
C_m	Hata correction for urban/metropolitan centres
d	Distance
E_b	Bit energy
E_c	Energy per chip
f	Frequency
F	Receiver noise figure
F_{feeder}	Feeder chain (feeder and jumpers) noise figure
F_{LNA}	LNA noise figure
F_{NodeB}	NodeB noise figure
G_{div}	Diversity Gain
G_e	Emitting antenna gain
G_{feeder}	Feeder gain (attenuation)
G_{LNA}	LNA gain
G_P	Processing gain
G_r	Receiving antenna gain
$G_{Rx\text{-}chain}$	Receiver chain gain due to LNA insertion
G_{SHO}	Soft handover gain
h_{BASE}	NodeB radiation height
h_{Mobile}	UE height
h_{Roof}	Height of buildings (including rooftop)

i_{DL}	Other-cell to own-cell interference ratio (DL)
I_0	Interference spectral density
i_{UL}	Other-cell to own-cell interference ratio (UL)
K	Rice factor
L_0	Free space loss
L_c	Losses between the emitter and the base station antenna
L_{ind}	Indoor penetration losses
L_{msd}	Multiple screen diffraction loss
L_p	Total propagation attenuation
L_{ptot}	Total system attenuation
L_{rts}	Roof-top-to-street diffraction and scatter loss
L_u	Body Loss
M	Total system margins
M_{CC}	Common Channels margin
M_{FF}	Fast fading margin
M_{SF}	Slow fading margin
M_{SF_SHO}	Slow fading margin in case of SHO
N	Total noise power
N_l	Number of links
N_0	Spectral noise density
N_u	Number of users
P_{cov}	Cell Area Coverage probability
P_{out_SHO}	Equivalent outage probability in case of SHO
P_r	Available receiving power at antenna port
P_{Rx}	Received power at receiver input
P_t	Available power at antenna port
R_b	Bit rate
W	Chip rate
w	Width of roads

List of Software

- MathCAD 7 Professional, Mathsoft
- MapBasic® 6.0, MapInfo® Corporation
- MapInfo® Professional 7.5, MapInfo® Corporation
- Microsoft VC++ 6.0, Microsoft Corporation

1. Introduction

1.1 Overview

When this thesis was initiated, UMTS (Universal Mobile Telecommunication System) trends in Europe were more uncertain than ever. Operators, specially "green field" ones, were quitting the "dream" that lead to license bidding during 1999 and 2000, claiming lack of technology, market and investment. Expressions like "uncertain demand" or "regulators relaxing licence requirements" were general findings in every economical/technological publication when addressing UMTS.

Despite the picture of uncertainty, the industry has made some progress in the last 12 months, and discussion now focuses increasingly on the question of when and not if, with some launches already on track. Isle of Man network and Monaco Telecom were the only live networks launched in early 2003, although Q3-2003 was pointed as the "big launch" date with roughly 15 new UMTS networks launching [Wool02].

The consecutive specification change requests in 3GPP (Third Generation Partnership Project [3GPP02a]) were pointed as one of the responsible causes for the technological delay on the available commercial equipment, arising compatibility, and performance issues for the operators willing to deploy UMTS. Delay on terminals development and mass market production was (and still is) also pointed as one of the key blocking points for massive UMTS deployment, leading to limited performance and high cost devices. Interoperability (IOT) between suppliers and backwards compatibility with legacy networks, such as GSM (Global System for Mobile Communications) with GPRS (General Packet Radio Service), are other two issues that most operators add to the technical difficulties list.

UMTS initial deployment will be focused on business and population high-density areas, requiring that terminals are able to roam from UMTS to GSM/GPRS in areas where UMTS will not be present. While the auction processes of 2000 demonstrated hope and expectation for upcoming 3G services, the return for the huge licence fees paid is a long way off.

Now, in late 2004, UMTS operators are launching their networks, with auspicious customer numbers already crossing the 5 digits barrier, and commercial launches in most European countries. Nevertheless, little vision on what will be the killer application set and its true

impact on network performance and associated dimensioning requirements is available mainly because of low statistical validity of existing network traffic.

Besides the investigation and study effort on UMTS performance and dimensioning as included in [MaZe02] or [AdCo02], the complexity of the multi-service and associated QoS (Quality of Service) mechanisms modelling still presents areas for future improvement given its importance to system performance modelling. The non-uniform traffic impact on system performance is also of main interest, as operators will face its consequence as traffic arises in UTRAN (UMTS Terrestrial Radio Access Network).

From the operator viewpoint, big interest is put on more accurate system performance and QoS assessment as a function of the multi-service and non-uniform traffic aspects. As more complex services are implemented over the UMTS infrastructure, more complex shall be its modelling to accurately dimension network resources in order to meet the required QoS.

Other important aspect to retain is the network cost estimations, tightly bounded with the dimensioning process and associated with target system performance (blocking, delay, average bit rate, etc.), and where accurate network resource needs predictions are required. NodeBs are one of the main components of costs in a full UMTS deployment and can represent approximately 40% of total costs. Within the NodeB scope, it is of major importance to model the impact of the traffic mix (multi-service) and of the non-uniform traffic distribution in the NodeB dimensioning, mainly number of carriers, power amplifiers and base band processing units, as they represent approximately 60% of total NodeB cost.

Operators are aware that a correct radio network dimension modelling associated with clear system performance objectives is mandatory for an efficient business case formulation, in order to efficiently estimate the associated capital expenditures (CAPEX), already enlarged by high license fees.

The PS (Packet Switch) and CS (Circuit Switch) QoS management and dimensioning is also a subject where improvements can also be inferred as the available classical traffic models do not answer to complex resource handling algorithms that boost UMTS radio interface coverage and capacity, but increasing system dimensioning complexity.

Given these major highlights, this thesis intends to go a step forward in developing a novel approach to user generation algorithms and system performance assessment of multi-service non-uniform UMTS traffic networks.

1.2 State of the Art and Innovation

Several research groups and projects are (or have been recently) focussed on multi-service non-uniform UMTS traffic networks performance aspects (at different levels), namely:

- **ETSI** (European Telecommunications Standards Institute) and **3GPP** (3rd Generation Partnership Project) [3GPP04c], on UMTS inter-working;
- **IST-MOMENTUM** (MOdels and SiMulations for NEtwork PlaNning and ConTrol of UMTS) [MOME00] deals with the dimensioning of UMTS radio networks in an optimum way, taking into account the relationships between services demand, traffic capacity and network performance;
- **IST-ARROWS** (Advanced Radio Resource Management for Wireless Services) [ARRO04] aiming at providing advanced Radio Resource Management (RRM) and QoS management solutions, for both UMTS modes, TDD (Time Division Duplex) and FDD (Frequency Division Duplex), to support integrated voice and data services;
- **IST-SEACORN** (Simulation of EnhAnced UMTS access and CORe Networks) [SEAC04] addressing real-time and large-scale simulation and visualisation technologies;
- **IST-SOQUET** (System fOr management of QUality of sErvice in 3G neTworks) [SOQU04] objective is to develop QoS concepts using multi-dimensional QoS inputs and generating perceived QoS outputs for managed multi-media services over 3G networks.

Recent Ph.D. works on traffic dimensioning ([Ribe03]) provided several analysis approaches to the main study subject of this thesis, proposing a practical framework to characterise the traffic offered to multimedia wireless systems targeting to proper dimensioning and optimisation of the system for a particular demand scenario.

Although many simulations have been described in literature for multi-service UMTS networks ([MaZe02], [SoLa03]), their typical starting point assumes that the active user layers are known inputs, with few mentions on definition of those inputs, both quantitative and qualitatively, based on existing (real) demographic data as well as on previous knowledge of voice traffic distribution on the network. This aspect is proposed to be explored along this thesis, as real usage scenarios are built upon 2G/2.5G traffic experience and used to create a rich multi-service set (also known as traffic mix), and assessing different site/user density scenarios to evaluate the non-uniform impact in overall network performance.

Most of available simulators treat traffic analysis based on density maps, where network performance is normally inferred by Monte-Carlo analysis (e.g., Netact from Aircom/Nokia [NOKI04]), lacking the time-domain analysis where RRM features impact can strongly change available network resources. On the other hand, time-domain simulators (e.g., UTRAPlan from Southern Poro Communications [UTRA04]) focus normally at cell level, allowing detailed algorithm modelling but lacking the network performance level approach required by operators.

The main contribution of this work to innovation is the joining of these two approaches. The space and time-domain analysis in just only one platform where UMTS scenarios are built from user and service generation/characterisation up to the specificities of the radio frame (time domain), where main RRM algorithms and UMTS main features, such as soft handover and power control are included, allowing a quantitative and qualitative system performance analysis of multi-service non-uniform UMTS networks.

1.3 Motivation and Contents

Wireless operators adopting third-generation (3G) technologies and those migrating from 2G/2.5G to 3G face a number of challenges related to traffic modelling, demand characterisation, and performance analysis, which are key elements in the processes of designing, dimensioning and optimising their network infrastructure.

Traditional traffic modelling assumptions used for CS voice traffic no longer hold true with the convergence of voice and data over PS infrastructures. Self-similar models need to be explored to appropriately account for the burstiness that packet traffic is expected to exhibit in all time scales. The task of demand characterisation must include an accurate description of the multiple user profiles, traffic source modelling, and service classes the network is expected to support, with their distinct geographical distributions, as well as forecasts of how the market should evolve over near and medium terms.

The appropriate assessment of QoS becomes a more complex issue, as new metrics and more intricate dependencies have to be considered when providing a varying range of services and applications that include voice, real-time, and non-real time data associated with development

of complex RRM strategies and algorithms that make modelling a complex (but required) task.

All those points have to be considered by the operator to obtain a proper dimensioning, resource allocation, and rollout plan for system deployment. Additionally, any practical optimisation strategy has to rely on accurate estimates of expected system performance in the presence of a specific multi-service profile. The assessment is proposed via performing a set of UMTS simulations case studies using the proposed framework, in order to discuss validation and sensitivity of main network indicators to the multi-service and non-uniform aspects of the offered traffic.

It is also proposed to investigate techniques that can be used to improve capacity, by optimising system variables such as network topology, sector RF configurations (e.g., TMA (Tower Mounted Amplifier)) and RRM parameters, presenting additional case-study simulations to exemplify and illustrate those topics, when relevant to overall system performance.

Although it is a valid argument that data traffic is still negligible on those networks today, it is also true that large investments are being made to migrate those networks towards offering a variety of multimedia services. The only means to get a return on that investment includes proper dimensioning of the systems to support data traffic, with appropriate QoS without sacrifice of the existing voice subscribers. In that sense, the main benefits expected from the work presented here are to:

- allow dimensioning guidelines and performance assessment, therefore leading to a more reliable business case analysis (capital and operational expenditures) for operators planning to migrate to UMTS Networks;
- provide a framework to design a proper rollout plan for the system deployment, by inferring on multi-service non-uniform traffic impact on performance indicators, such as blocking and PS data service rates;
- provide guidelines for efficient resource allocation based on expected demand and growth, associated with RRM performance impact

In a time where optimisation of investment vs. technological performance of UMTS networks is a “must”, the scope of the work developed target at modelling and quantifying the impact of different usage scenarios of WCDMA (Wideband Code Division Multiple Access) radio

interface, namely considering different user distributions, different services set per user and its impact on cell coverage, capacity and QoS.

This document is composed of five chapters, besides the current one, and seventeen annexes. The following chapter is dedicated to UMTS general system description, emphasising the relevant areas to this thesis' studies. Link budget, services, QoS and WCDMA radio aspects are analysed in detail, as a basis for the work developed. Chapter 3 includes the description of the application and services considered along the work, with corresponding radio bearer (RB) mapping and detailed description on traffic source models, finally, the non-uniform user generation algorithm is described. In Chapter 4, the simulator description is provided, detailing the input/output formats along with the main simulator (TRAFSIM3G – TRAFfic SIMulator for 3G networks) implemented features, Chapter 4 also presents important assessment on the simulator parameterisation and its validation. Chapter 5 gathers all simulation scenarios results and includes the preliminary conclusion and trends analysis. Conclusions and further suggestions of work to be done are drawn in the final chapter.

A very complete set of annexes is provided with auxiliary information that might complement the understanding of the main text and includes all exhaustive data analysis for each of the simulation scenarios considered. Annexes A to D include FDD channels, link budget, propagation model and common channels dimensioning considerations. Annexes E and F relate to traffic source model statistical description and validation of implemented source code. Annex G and H include the GIS (Geographical Information Systems) tables with population data characterisation, sites plan, etc.. In Annex J, TRAFSIM3G user manual is provided with full description on configuration parameters and practical hints for its usage. Annexes K and L include all TRAFSIM3G input and output flat files structure and contents. Annexes M and N include the service tables definition for the simulated scenarios and finally in Annexes O, P and Q data analysis of all scenarios is presented.

2. Radio Interface and Capacity Aspects

In this chapter, one presents relevant UMTS and WCDMA concepts required to introduce the analysis and studies regarding the thesis' main subject. The first section addresses the UTRAN architecture, focusing on the elements and aspects that will interact with traffic processing, especially at the radio interface level. The second section introduces the UMTS services concept and QoS considerations. The latest sections focus on WCDMA UTRA FDD (Frequency Division Duplex) physical layer overall description and WCDMA aspects regarding coverage and capacity modelling, such as link budget and load equation.

2.1 System Architecture

UMTS is the third generation system as specified by 3GPP, defining two main radio interface modes: UTRA (Universal Terrestrial Radio Access) FDD and TDD (Time Division Duplex) [3GPP02b]. This thesis will only focus on the UTRA FDD mode. Network elements are grouped in three functional areas [3GPP02b]:

- UTRAN (UMTS Terrestrial Radio Access Network)
- CN (Core-Network)
- UE (User Equipment)

The UTRAN block handles all radio related functionalities while CN is responsible for switching and routing calls (voice, data) to external networks, and UE is responsible for user and network radio communications. When comparing to 2G, UE and UTRAN present a new set of protocols, while CN can be viewed as an upgrade to the current GSM/GPRS CN.

UTRAN consists of two main elements: the NodeB, generally known as base station and, the RNC (Radio Network Controller). NodeB converts the data flow between Iub (interface defined between the NodeB and the RNC [3GPP02c]) and Uu (interface defined between the UE and the NodeB [3GPP02d]) interfaces, it is also responsible for the RRM (Radio Resource Management) algorithms. The RNC controls the radio resources, concentrating all the information (user, network) to deliver to CN, through Iu interface (interface defined between the CN and the RNC [3GPP02e]).

The UE consists of two parts: the mobile radio terminal used for communication over the Uu interface and the USIM (UMTS Subscriber Identity Module), which is a smart card holding subscriber identity, authentication algorithm, authentication and encryption/ciphering information [3GPP02f].

The typical CN configuration for Release 99 [HoTo01] consists mainly of the GSM/GPRS typical components, such as HLR (Home Location Register), MSC/VLR (Mobile Services Switching Centre/Visitor Location Register) related to CS call processing and SGSN/GGSN (Serving GPRS Support Node/Gateway GPRS Support Node) handling PS calls.

UMTS specifications (developed by 3GPP) are organised in several releases, each referring to a specific architecture solution and sequential in time. The releases defined until now are [3GPP02g]:

- Release 99 (also known as R3), specified in [3GPP02h], freeze in March 2000
- Release 4, specified in [3GPP02i], freeze in March 2001
- Release 5, specified in [3GPP02j], freeze in June 2002
- Release 6, not yet freeze (formal date was March 2004)

The work developed in this thesis will focus on R99 specifications and concepts.

UTRAN consists of one or more RNS (Radio Network Sub-systems), each containing an RNC and one or more NodeBs. RNCs are connected to each other via the Iur interface [3GPP02k]. The RNC is the element responsible for the control of radio resources in UTRAN, interfacing with the CN (CS and PS respectively MSC and SGSN) and terminates the RRC (Radio Resource Control) protocol [3GPP02l] that defines the messages and procedures between the UE and UTRAN.

The RNC connected to a NodeB (Iub termination) is named as the Controlling RNC (CRNC). The CRNC is responsible for the code allocation (new radio links), load, congestion and admission control (of its cells). When one UE uses resources from two distinct RNSs, the RNCs involved have two separate logical roles: Serving RNC is the RNC terminating the Iu connection (user data and corresponding RANAP (Radio Access Network Application Part) signalling [3GPP02m]), while the drift RNC (DRNC) is other RNC that controls cells used by the UE. The DRNC only performs macro diversity combining and splitting, routing transparently the information through Iub and Iur interfaces. The UTRAN architecture is presented in Figure 2.1.

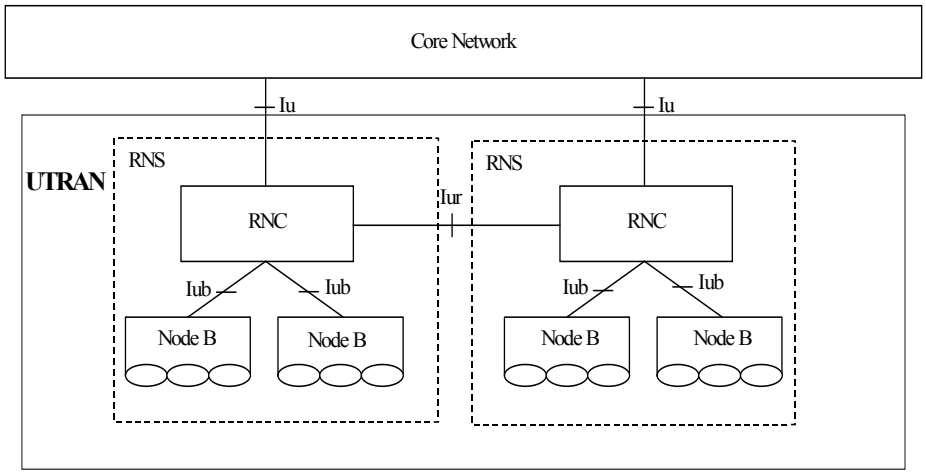

Figure 2.1 - UTRAN architecture (extracted from [3GPP02b]).

The NodeB main function is to perform the air interface (Physical Layer - L1) processing, coding and interleaving, synchronisation, rate adaptation, spreading, etc. [3GPP02n]. Some RRM tasks are performed by the NodeB, such as inner loop power control. NodeB architecture is not specified in 3GPP, depending on supplier implementation, nevertheless, three main important blocks should be referenced related to NodeB traffic processing capabilities [PMCS02a]:

- Base-band boards (BB), usually known as Channel Element Modules (CEMs), which are responsible for coding, interleaving, spreading and scrambling in the Downlink (DL). In the Uplink (UL), they are responsible for de-coding, de-interleaving, de-spreading, de-scrambling, closed loop power control, RACH preamble detection (Random Access Channel), etc.;
- Transceiver Module(s) (TRM or TRX) is the unit that performs modulation/de-modulation, frequency conversions (up/down) and performs analogue to digital (and *vice-versa*) conversion, etc.;
- Multi Carrier Power Amplifier (MCPA) performs the DL power amplification received from the transceiver modules. It presents typical power values from 43 to 45 dBm, and normally supports more than one 5 MHz channel (multi-carrier characteristic).

2.2 Services in UMTS

Expectations around new 3G services to be offered over UMTS are very high. Among the awaited 3G advantages are the always-on feature, the possibility of offering personalised services, location-aware services, real-time and flexible, easier, better, faster and with the possibility to offer a high level of QoS.

One of the main drivers of 3G is the expected convenience of accessing information and services anywhere, anytime, stationary or on the move, demand for general and personalised data services. Mobile entertainment is expected to grow, e.g., mobile games, mobile music and downloading of mobile cartoons and icons. Mobile gambling and betting is often considered as an early example of mobile commerce. Mobile music will include MP3 music or music clips/ring tone download, used in conjunction with the mobile Internet.

From the technical perspective, UMTS brings new higher user bit rates up to 384 kbps, allowing support of new demanding services, such as video telephony and high bit rate data transfer. Even without the clear definition of what the set of services in UMTS will be, and assuming fast changes in concept and development, the system architecture is dynamic to handle user service requests. Voice services typically account for over 90% of mobile operators' revenues, but by 2005/6 data/non-voice services are expected to generate 50% of revenues [FORU02].

CS bearers will handle delay-critical applications, such as voice or video telephony, although it is expected that QoS functions will evolve fast in the PS domain. UMTS allows the negotiation of the radio bearers, generally characterised by its throughput, delay, data error rate, etc., adapting system resources to the target QoS.

Bearer services provide the capability for information transfer between access points, and involve only low layer functions. Each network contributes to the end-to-end QoS perceived by the end-user. PS and CS domains provide a specific set of bearer capabilities: CS bearer services are described in [3GPP02x], while PS ones (GPRS) are described in [3GPP02y]. Bearer services are characterised by a set of end-to-end characteristics with requirements on QoS. It shall be possible to negotiate/renegotiate the characteristics of a bearer service at session/connection establishment and during an on going session/connection [3GPP02u].

It shall be possible for one application to specify its traffic QoS requirements to the network by requesting a bearer service with any of the specified traffic type, traffic characteristics, maximum transfer delay, delay variation, bit error and data rates. It shall also be possible for the network to satisfy these requirements without wasting resources on the radio and network interfaces due to granularity limitations in bit rates [3GPP02u].

Moreover, it shall be possible for one mobile termination to have several active bearer services simultaneously, each of which could be connection oriented or connectionless. The only limiting factor for satisfying application requirements shall be the cumulative bit rate per mobile termination at a given instant in each radio environment [3GPP02u]:

- at least 144 kbps in rural outdoor radio environment;
- at least 384 kbps in urban/suburban outdoor radio environments;
- at least 2048 kbps in indoor/low range outdoor radio environment.

The layered architecture of a UMTS bearer service is defined in [3GPP02v]. Each bearer service offers its individual services provided by the lower layer bearers. The work developed along the thesis will focus on Radio Bearer Service and UTRA FDD Service Layers Aspects.

When defining the UMTS QoS classes, also referred to as traffic classes, the restrictions and limitations of the air interface have to be taken into account. The QoS mechanisms provided in the cellular network have to be robust and capable of providing reasonable QoS resolution. There are four different QoS classes [3GPP02v]: **Conversational**, **Streaming**, **Interactive** and **Background**. UMTS classes' characterisation is summarised in Table 2.1 [3GPP02v].

Table 2.1 - UMTS QoS Classes.

Traffic class	Conversational Conversational RT	Streaming Streaming RT	Interactive Interactive best effort	Background Background best effort
Fundamental characteristics	Preserve time relation (variation) between information entities of the stream Conversational pattern (stringent and low delay)	Preserve time relation (variation) between information entities of the stream	Request response pattern Preserve payload content	Destination is not expecting the data within a certain time Preserve payload content
Example of the application	Voice	Streaming video	Web browsing	Background, e-mail

The main distinguishing factor between these QoS classes is how delay sensitive the traffic is: Conversational class is meant for traffic that is very delay sensitive, while Background is the most delay insensitive traffic class [3GPP02v].

Conversational and **Streaming** classes are mainly intended to be used to carry real-time traffic flows. The main difference between them is how delay sensitive the traffic is. Conversational real-time services, like voice (CS or VoIP (Voice over IP)), video telephony, are the most delay sensitive applications and those data streams should be carried in Conversational class [3GPP02v].

Speech codec in UMTS uses the AMR (Adaptive Multi Rate) technique, presenting bit rates from 4.75 to 12.2 kbps (equivalent to the EFR (Enhanced Full Rate) GSM codec). AMR groups information in three distinct bit groups (A (high content), B and C), tolerating 1% FER/10^{-4} BER (Frame Error Rate/Bit Error Rate) for A type bits without voice deterioration. Video Telephony has similar delay requirements as speech, but with stringent BER requirements. UMTS has specified ITU-T H.324M and H323/IETF SIP (Internet Engineering Task Force - Session Initiation protocol) for video telephony over CS and PS bearers respectively [HoTo01].

The Streaming class was thought to support services as, for instance, video streaming (e.g., web broadcast or video on demand). Video streaming is played in the destination equipment (personal computer, suitable user equipment, etc.) by means of a suitable media player, which does not have to receive all the stream of data (ideal for low speed internet access) before being able to process it and display it to the user. Hence, this kind of service is not as delay-sensitive as the former ones, due to the queuing performed by the final application.

Interactive and **Background** classes are mainly meant to be used by traditional Internet applications like WWW, E-mail, Telnet, FTP and Online News. Due to looser delay requirements, compare to Conversational and Streaming classes, both provide better error rate by means of channel coding and retransmission. The main difference between Interactive and Background is that Interactive is mainly used by interactive applications, e.g., interactive Web browsing, while Background is meant for background traffic, e.g., download of E-mails or background file downloading. Traffic in the Interactive class has higher priority in scheduling than Background one, so background applications use transmission resources only when interactive applications do not need them, optimising radio resources where the bandwidth is low compared to fixed networks [3GPP02v].

WCDMA UEs inform the network upon connection setup of its capabilities for UL and DL, allowing the network to optimise services and QoS provisioning. UE Radio Access Capabilities are specified in [3GPP02w].

2.3 Air Interface

UTRA/FDD for Europe is designed to operate in the following paired bands [3GPP02o]:

- 1920 – 1980 MHz: UL
- 2110 – 2170 MHz: DL

The chip rate is 3.84 Mcps, and transmit to receive frequency separation is typically 190 MHz (minimum transmit to receive frequency separation is 134.8 MHz and the maximum value is 245.2 MHz) [3GPP02o]. The nominal channel spacing is 5 MHz, adjustable in 200 kHz steps. The occupied channel bandwidth shall be less than 5 MHz based on a chip rate of 3.84 Mcps [3GPP02o]. The UTRA Absolute Radio Frequency Channel Number (UARFCN) designates the carrier frequency. The value of the UARFCN in the UMTS band (both UL and DL) is defined as 5 times the channel frequency in MHz (UARFCN is an integer) [3GPP02o].

Spreading is applied to the physical channels, consisting of two operations. The first is the channelisation (or spreading) operation, which transforms every data symbol into a number of chips, thus, increasing the bandwidth of the signal. The number of chips per data symbol is called the Spreading Factor (SF). The second operation is the scrambling operation, where a scrambling code is applied to the spread signal [3GPP02q].

Channelisation codes (UL and DL) are Orthogonal Variable Spreading Factor (OVSF) ones that preserve the orthogonality between a user's different physical channel in UL and DL. OVSF codes can be defined by using the code tree defined in [3GPP02q]. The channelisation code for the Primary CPICH (Common Pilot Channel) is fixed to $C_{ch,256,0}$, and the channelisation code for the Primary CCPCH (Common Control Physical Channel) is fixed to $C_{ch,256,1}$. Channelisation codes for all other physical channels are assigned by UTRAN.

All UL physical channels are subjected to scrambling with a complex-valued scrambling code [3GPP02q]. The DPCCH/DPDCH (Dedicated Physical Common/Data Channel) may be scrambled by either long or short scrambling codes, there being 2^{24} long or 2^{24} short UL

scrambling ones, assigned by higher layers [3GPP02q]. DL scrambling codes are divided into 512 sets each of primary and 15 secondary ones, in a total of 8192. There is a one-to-one mapping between each primary and the 15 secondary scrambling codes in a set, such that the i^{th} primary scrambling code corresponds to the i^{th} set of secondary ones. The set of primary scrambling codes is further divided into 64 groups, each consisting of 8 primary ones. Each cell is allocated one and only one primary scrambling code, repeated for every 10 ms radio frame. All (DL) common control channels are always transmitted using the primary scrambling code, while other DL physical channels can be transmitted with either the primary scrambling code or a secondary one from the set associated with the primary scrambling code of the cell.

In the UL and DL, the complex-valued chip sequence generated by the spreading process is QPSK (Quadrature Phase Shift Keying) modulated as described in [3GPP02q].

2.4 Channels

Three types of channels have been defined within UTRAN [3GPP02p]:

- Logical channels: Services offered by Layer 2 (L2) to higher layers. Logical channels are mapped onto Transport channels by the MAC (Medium Access Control) layer, being part of L2 [3GPP02p].
- Transport channels: Services offered by Layer 1 (L1) to the higher layers. A Transport channel is defined by how the data is transferred over the air interface (i.e., interleaving depth, channel coding, etc). Transport channels are mapped onto physical channels by L1 [3GPP02r].
- Physical channels: Used in the radio interface between L1 peers entity. Physical channels correspond to different radio frame types and content [3GPP02r].

Logical channels correspond to the different types of information provided by UTRAN radio protocols, each one being defined by which type of information is transferred. A general classification of logical channels comprises two groups:

- Control Channels are used for the transfer of control plane information only;
- Traffic Channels are used for the transfer of user plane information only.

Because of the transmission characteristics on the radio interface (interference, fading, shadowing, etc.), the radio part is the weakest link in a UMTS network. To ensure a given

QoS, as required by the applications, a number of mechanisms (coding scheme, etc.) must be implemented to make data exchanges reliable. The concept of transport channel corresponds to these mechanisms and a transport channel represents the way information is transmitted over the radio interface, therefore, the transport channel is representative of the quality of service provided by the radio part of the RAB (Radio Access Bearer).

The Transport Format Set (TFS) is a list of different Transport Formats (TF), and it is used by UTRAN to choose at any moment the most suitable format to transmit data over the radio interface, so as to use radio resources as efficiently as possible. The choice of a TFS and the related TF attribute values are determined for each TTI (Transmission Time Interval) by the UTRAN MAC layer, according to the RAB QoS attributes passed at RAB Assignment.

A physical channel may bear several transport channels and a transport channel may be born by several physical channels. The Coded Composite Transport Channel (CCTrCH) is defined as the multiplexing of several transport channels that can be supported by one or several physical channels on the radio interface. Some physical channels are used only by the physical layer of the radio interface [3GPP02r]. Table A.1 in Appendix A summarises all physical channels and its main characteristics.

There are two types of UL dedicated physical channels, the Dedicated Physical Data Channel (UL DPDCH) and the Dedicated Physical Control Channel (UL DPCCH). The DPDCH and the DPCCH are I/Q code multiplexed within each radio frame. The UL DPDCH is used to carry the DCH (Dedicated Channel) transport channel and its spreading factor may range from 256 down to 4. The UL DPCCH is used to carry control information generated at L1, existing one and only one UL DPCCH on each radio link. Each radio frame of length 10 ms is split into 15 slots, each of length T_{slot} (2560 chips), corresponding to one power-control period. The spreading factor of the UL DPCCH is always equal to 256, i.e., there are 10 bits per UL DPCCH slot.

There is only one type of DL dedicated physical channel, the Dedicated Physical Channel (DL DPCH), within each DPCH, dedicated data generated at L2 and above, i.e., the dedicated transport channel (DCH) is transmitted in time-multiplex with control information generated at L1 thus the DL DPCH can be seen as a time multiplex of a DL DPDCH and a DL DPCCH. Again, each frame of length 10 ms is split into 15 slots, each of length T_{slot} (2560 chips), corresponding to one power-control period. The spreading factor may range from 512 down to 4.

For signalling and synchronisation procedures, information needs to be exchanged between network and UEs recurring to common channels. Additional details on common channels are provided in Annex D.

The Common Pilot Channel (CPICH) is a non-modulated code channel, which is scrambled with the cell specific scrambling code which main function of CPICH is to help UEs to estimate channel properties and phase reference for other DL channels [3GPP02r]. Measurements for handover and cell selection/reselection are performed on CPICH power levels, having this later direct impact on cell coverage and load balance. There are two types of common pilot channels: Primary and Secondary (used for example in Adaptive Antennas solutions) [3GPP02r].

The Synchronisation Channel (P-SCH and S-SCH) is a DL signal used for cell search procedure. The SCH consists of two sub channels, the Primary and Secondary. The P-SCH (the same for every cell in the system) consists of a modulated code of length 256 chips, transmitted once every slot. The Secondary SCH consists of repeatedly transmitting a length 15 sequence of modulated codes of length 256 chips, the Secondary Synchronisation Codes (SSC), transmitted in parallel with the Primary SCH. This sequence on the Secondary SCH indicates which of the code groups the cell's DL scrambling code belongs to [3GPP02q].

The Primary Common Control Physical Channel (P-CCPCH) is a fixed rate (SF=256) DL physical channels used to carry the BCH (Broadcast) transport channel. No TPC (Transmission Power Control) commands, no TFCI (Transport Format Combination Indicator) and no pilot bits are transmitted. The Primary CCPCH is not transmitted during the first 256 chips of each slot; instead Primary SCH and Secondary SCH are transmitted during this period [3GPP02r]. P-CCPCH power setting is critical since, if decoding fails, terminals are not able to access system information (SYS INFO), such as RACH access channels information.

The Secondary Common Control Physical Channel (S-CCPCH) is used to carry the FACH (Forward Access Channel) and PCH (Paging Channel) transport channels. The FACH and PCH can be mapped onto the same or separate Secondary CCPCH's. If FACH and PCH are mapped onto the same Secondary CCPCH, they can be mapped onto the same frame, sparing NodeB Power Amplifier resources.

The Physical Random Access Channel (PRACH) is used to carry the (transport channel) RACH. It carries UL information, such as request to set up a RRC connection or to carry

small amounts of user information and it is always received from the entire cell using open loop power control. The Acquisition Indicator Channel (AICH) is a fixed rate (SF=256) physical channel used to carry Acquisition Indicators (AI). Acquisition Indicator AI_s corresponds to signature *s* on the PRACH signalling the UE of its good reception. The computation may result in a positive, negative or no acknowledge [3GPP02r]. The Paging Indicator Channel (PICH) is a fixed rate (SF=256) physical channel used to carry the paging indicators. The PICH is always associated with an S-CCPCH to which a PCH transport channel is mapped [3GPP02r]. If a paging indicator (PI) in a certain frame is set to "1" it is an indication that UEs associated with this paging indicator and PI should read the corresponding frame of the associated S-CCPCH. When a PI is detected, the terminal decodes the next PCH frame (transmitted on S-CCPCH) to see if paging message is intended for it.

It is important to note that the mapping between logical channels and transport channels is not fixed by 3GPP, and its implementation is dependent whether several choices are possible, which is the case for DCCH and DTCH channels (Dedicated Common/Traffic Channels). The correspondence between transport channels and physical channels is, on the contrary, performed by UTRAN physical layer, and offers no flexibility, since a given transport channel can only be supported by one type of physical channel [3GPP02r].

2.5 Physical Layer Procedures

In UMTS physical layer, several procedures are essential for system operation, such as synchronisation, power control, random access/paging, transmit diversity and IPDL (Idle Periods in DL) location method [3GPP02s] and measurements.

Measurements are performed by the physical layer with varying degrees of averaging and accuracy, filtered at Layer 3 (L3), and sent to the RNC over the interfaces: Iub or Iur in the case of NodeB measurements, Uu interface for the UE [3GPP02t]. The RNC is able to process these measurements and make use of them for different purposes, such as handover, load control, radio resource management, etc..

Three synchronisation general procedures are defined within 3GPP. Cell search, where the UE searches for a cell and determines the DL scrambling code and common channel frame synchronisation of that cell. Radio frame timing of all common physical channels can be determined after cell search. The P-CCPCH radio frame timing is found during cell search

and the radio frame timing of all common physical channels are related to that timing as described in [3GPP02r]. For the dedicated channels (DPCCH/DPDCH), synchronisation primitives are used to indicate the synchronisation status of radio links, both in UL and DL.

In the Random Access procedure, the UE will send initially preambles on the Physical RACH. The preamble is composed of two parts known as the preamble part and the message part. Before transmitting the message part of the preamble, the UE waits for an acknowledge from the network on the AICH confirming that the network understood the UE.

Once registered, the UE has been allocated a paging group. Paging Indicator signals appear periodically in PICH channel when there are paging messages for any of the terminals belonging to that paging group.

Transmit Diversity (TD) allows a decrease in the required E_b/N_0 (bit energy per spectral noise density ratio) in the UE receiver due to the coherent sum of the two transmitted waves and gain against fast fading effects. Coherent sum in the receiver is not perfect due to inaccurate channel estimation. Diversity fast fading gain is highly dependent on UE speed and channel characterisation. In 3GPP, there are two types of TD: open loop and closed loop that includes two different modes (mode 1 and 2) [3GPP02s].

The power management is a crucial issue for any CDMA system, and UMTS is one of them. Power management is two folded: it is made of the power allocation on one hand, and of the power control on the other. Power control procedures are used when one or more radio links are being or have been set up between the UE and one or more NodeBs. Their objective is to configure/reconfigure and to control the power of the traffic channels (dedicated or common) either in DL or UL. Open loop power control is applicable only in UL; it sets the initial UL transmission power and it is used on PRACH, PCPCH and DPCCH physical channels. Outer loop power control is applicable in both UL and DL; it sets the target quality value for the inner loop power control (in the NodeB for UL inner loop and in the UE for DL inner loop). The update rate is at most every frame (10 ms), i.e., 100 times per second. Inner loop power control, applicable in both UL and DL, controls the transmitter output power using power control commands (TPC). The inner loop power control is much faster than the outer loop one. Its update rate is at most every time slot (0.667 ms), i.e., at most, 1500 times per second, the UE power and NodeB power can be changed.

The global power control procedure is basically split into two subparts: open loop and closed loop power control. The open loop initiates the power control process, thus, it always precedes any closed loop, for both UL and DL. The closed loop notion encompasses inner and outer loops (a closed loop process means that there is a feedback to a command).

2.6 Link Budget

The UMTS link budget is used to calculate the cell range, for a given capacity. Cell range is evaluated by applying a propagation model translating a maximum allowable pathloss per user into a distance.

In WCDMA, the difficulty comes from the fact that all users must share NodeB output power as a function of their location in the cell, and that the number of users depends on the cell range. Unlike GSM, UL and DL UMTS link budgets are highly correlated to system capacity, and should aim at link balance. In terms of initial coverage definition, and regarding typical system asymmetries, such as UE and NodeB transmit powers, in low/medium load conditions UL is the coverage-limiting link.

In this section, one will address UMTS specificities regarding link budget, namely Interference Margin (M_I), Fast Fading Margin (FFM), Soft Handover (SHO) Gain and DL link budget differences. The detailed link budget description can be found in Annex B.

Due to the WCDMA intrinsic coverage/capacity relation, the M_I (Interference Margin, also referenced as "noise rise") aims at compensating the cell range reduction (cell breathing effect) due to cell-increased interference due to cell traffic increase, known as cell load (cell load is detailed in Section 2.7). Adopting an M_I value according to an expected maximal cell load in all cells, within a common area/environment, gives a larger investment at the beginning, but avoids coverage holes as the load increases. In UL, the M_I is given in function of UL cell load (η_{UL}):

$$M_{I[\mathrm{dB}]} = -10 \cdot \log\left(1 - \eta_{UL}\right) \tag{2.1}$$

The maximum realistic UL cell load is said to be around 50% [HoTo01], corresponding to an M_I of 3 dB. For higher values the system becomes unstable since the UL M_I curve between load and noise rise becomes highly non-linear.

In order to maintain the link quality (E_b/N_0), the fast power control in WCDMA compensates the fast fading of the propagation channel, for the UE at low speed when the power control algorithm can follow for the channel variations very closely and interleaving gain is low.

However, at the cell edge, the transmission power of the UE is close to its maximum and a saturation phenomenon can occur. The fast power control can no longer correct for the entire fast fading effects, therefore, the quality of the connection decreases. In order to correct the limited dynamics of the power control, a margin shall be included in the link budget [SLWJ99]. It is shown in [SiLW99] that the margin required can be significantly reduced due to soft-handover (SHO), therefore, a much lower margin can be used than that given in [SLWJ99]. Typical values for Fast Fading Margin (FFM) are 2 to 5 dB [HoTo01]. Analysis of fast fading margin is shown in Annex B, based on results from [SLWJ99] and [SiLW99], where the proposed variation of FFM is from 0 to 3.6 dB.

The possibility to receive the same UE signal by two different links allows decreasing base station E_b/N_0 targets. Besides, different power control algorithms tend to reduce UE output power when the UE is in SHO, providing higher gain against fast fading. Since UE output power determines the amount of interference to adjacent cells, and the received NodeB power determines the amount of interference to other users in the same cell, SHO brings a gain on capacity. Another important diversity technique is softer handover (SSHO) micro diversity. The UE transmitted signal is received by two antennas on the same NodeB, which could be processed using MRC (Maximum Ratio Combining) micro diversity technique.

SHO gain depends on environment, i.e., distance attenuation coefficient and UL signals correlation (UL diversity). As an example, in rural environment where fading can be considered less important, SHO presents lower gain due to high correlation on diversity signal received at the NodeB. In dense urban environments, where fading takes an important role, the NodeB receive signal is less correlated, therefore, presenting higher gain.

Dense urban, urban and suburban environments correlation is around 0.5, while for rural environments is around 0.7. Soft handover gain can be thought of as the difference between the fading margin required to achieve a given QoS of a single server system and that required to achieve the same QoS (cell area reliability) of n-server system (typically n equals 2). SHO gain theoretical approach is detailed in Annex B. Typical values considered for soft handover gain is between 2 and 5 dB [HoTo01]. Theoretical SHO obtained values vary from 3 to 4.5 dB (Annex B).

The UMTS UL frequency band does not exceed the 2 GHz, allowing empirical COST231-Hata and COST231-Walfisch-Ikegami models to be used for cell range calculations [DaCo99] as UL is normally the coverage limiting link. Both models are improved versions of the well-known models Okumura-Hata ([OOKF68] and [Hata80]) and Walfisch-Ikegami ([WaBe88] and [IkYU84]). For DL link budget, the same models are used although out of its validation range, the 200 MHz separation presents negligible pathloss differences.

The COST231-Hata model shall be used for large and small macro-cells, when the base station antenna height is above rooftop levels adjacent to the base station. This model must not be used for micro-cells (NodeB antennas below rooftop level) and for distances below one km. COST231 Walfisch-Ikegami model shall be used for small macro and micro-cells (i.e., for distances below 5 km). However, the model requires parameters, such as building heights, road widths, building separation and road orientation with respect to the direct radio path. Detailed models description and applicability ranges are presented in Annex C.

Within the typical propagation environments, COST231-Walfisch-Ikegami is adequate for cell range calculation in Dense Urban (DU), Urban (U) and Suburban (SU) clutters, where cell range is generally below or in the order of 1 km. For Axial (Ax) or Rural (Ru) cells, range and propagation environment leads to recommended use of COST231-Hata model.

It is important to note that for DL calculations (2110 to 2170 MHz) the models are used out of the frequency validity range (800-2000 MHz), although usage of such frequencies provides acceptable precision.

Considering the UL link budget, one can deduce the DL mean path loss by assuming link balance, which is valid for low/medium capacity cells. When DL traffic is high, cell range can be limited by NodeB amplifier (MCPA) power. There is no “truly” DL link budget, since the DL power to be allocated to the user will highly depend on the location of the users in the cell, the interference generated in the other cells and the traffic carried.

As in UL, one can then define a DL cell loading. This parameter is related to the part of interference that is considered to evaluate the power per user in DL and it is also related to the capacity of a cell, the latter being the result of asymptotic capacity multiplied by the DL cell loading.

In DL, other differences arise, such as higher noise figure on the UE (typically 5 to 8 dB compared with 3 to 5 dB in the NodeB) and the absence of diversity in the reception due to

small size UEs. Nevertheless, transmit diversity reduces the required UE E_b/N_0. In DL, the available power for traffic is highly dependent on common channels power configuration. These channels are needed for the setup of communications in all the coverage area of the respective cells. A fraction of the available power in the NodeB is used by common channels, requiring an optimised and strategic usage of this scarce resource. The common channels power also contributes to the overall interference level, since orthogonality between codes is not perfect, mainly due to multipath. The power allocated to each common channel is a compromise for an effective reception in all cell areas and minimising the MCPA power usage.

In Annex D, one presents a method to calculate the total DL power used by common channels based on link quality equations, allowing estimation of the amount of power available for user traffic. CPICH channel power allocation is the most sensitive one, since handover, cell selection and other physical procedures depend on this specific channel performance (E_c and E_c/I_0 - Energy per chip, and Energy per chip to Interference spectral density ratio).

2.7 Capacity and Interference

In UL, capacity is obtained by the "N-pole" formula corresponding to the maximum number of users that can be connected to the BS, taking into consideration the noise generated by them at the BS reception. When η_{UL} becomes closer to unity, the corresponding noise rise approaches to infinity (pole capacity). The UL load factor can be written as:

$$\eta_{UL} = (1 + i_{UL}) \cdot \sum_{j=1}^{N} \frac{1}{1 + \dfrac{W/R_{b\,j}}{(E_b/N_0)_j \cdot \upsilon_j}} \tag{2.2}$$

where:

- W: chip rate
- υ_j: activity factor of user j (normally 0.67 for speech and 1.0 for data [HoTo01])
- $R_{b\,j}$: bit rate of user j (dependent on service)
- i: other-cell to own-cell interference ratio
- $(E_b/N_0)_j$: bit energy per spectral noise density ratio of user j

Interference from other cells is taken in account in (2.2) by the other-cell to own-cell interference ratio (i), which depends directly on cell environment, cell isolation (macro/micro) and antenna pattern topology (omni/sectored). Simulations in [WLSH99] propose 0.66 for i in a 65º antenna tri-sectorial network configuration. The required $(E_b/N_0)_j$ is derived from link level simulations or equipment design measurements, and dependent on service, bit rate, multipath fading channel (mobile speed) and receive diversity. It includes soft handover and power control gains.

DL capacity is very difficult to model in a simple way. Like in UL, there is a notion of maximum theoretical capacity ("asymptotic capacity"), corresponding to the maximum number of users that can be served in a cell of a range given by the UL maximum allowable pathloss and assuming that BS can offer an infinite power to all the users. As a main difference from UL, several connections share the same resource (MCPA power), interference from serving cell is received through the same propagation channel as the signal (in UL interference generated be each UE to other UEs in cell have in general different propagation conditions), and different UEs experience different interference from neighbouring cells depending on location.

Nevertheless, it is expected that in DL there is a similar non-linearity in the required transmission power as a function of the loading, as in UL. DL cell loading can be calculated as [HoTo01]:

$$\eta_{DL} = \sum_{j=1}^{N_l} \upsilon_j \cdot \frac{(E_b/N_o)_j}{W/R_{b\,j}} \left[\left(\left(1-\overline{\alpha_j}\right)+i_{DL\,j}\right)\right] \tag{2.3}$$

where:

- N_l: number of radio links (1+SHO overhead)
- $\overline{\alpha_j}$: average orthogonality factor in DL (typically 0.4 to 0.9 [HoTo01])

Due to multipath, orthogonality among codes is lost, contributing to overall interference as perceived by the user. In DL, the SHO transmission is modelled as having additional connections (N_l) in the cell. The required transmission per user can be estimated assuming average values for path loss, orthogonality and i_{DL}. Dependency of transmit power with path loss, orthogonality and own-to other cell interference ratio is detailed in [SHLW00].

Total power in NodeB Power Amplifier (PA) can be estimated for traffic channels by [HoTo01]:

$$PA_{pwr} = \frac{N_{rf} \cdot W \cdot \overline{L} \cdot \sum_{j=1}^{N_L} \upsilon_j \cdot \frac{(E_b/N_0)_j}{W/R_{bj}}}{1 - \overline{\eta_{DL}}} \tag{2.4}$$

where:

- N_{rf} :is the noise spectral density of the UE receiver
- $\overline{L}$:is the average cell path loss

Note that PA power resource is normally limited to the nominal available power, with typical figures around 20 W, per cell. As UMTS is a multi-carrier system, some supplier offer PAs with 40 W, already allowing the usage in two different carriers in the same device. We will consider the standard 20 W PA available at each cell. Note that due to traffic asymmetry regarding the cell distribution, it is interesting to model in future studies the dynamic PA allocation strategies, where instead of having three 20 W independent PAs, a pool of 60 W is shared among all sectors, allowing a more effective PA power distribution and minimising power shortage in cells with high average path loss.

UMTS capacity assessment is composed of three main components; UL and DL load, PA power availability and OVSF code usage. Call admission and load control RRM are the main responsible algorithms that maintain these parameters within the range that guarantees a stable operation. All these aspects are simulated and its main impact analysed as function of the service mix offered to the network.

3. Service Characterisation and Traffic Source Models

In this chapter, the services[1] and applications that are considered in the present work are described. A detailed characterisation and parameterisation of traffic source models, as well as of generation and duration processes, for each considered application is also presented. Secondly, system considerations are detailed in order to introduce the application set, and the traffic source models associated with each application. After the application characterisation, radio bearer mapping options and radio layer related models (RRM and propagation) description is addressed. In the final section, spatial user generation algorithms and assumptions are described.

3.1 Services and Applications

UMTS aims at offering a large variety of services, having different usage and distribution according to the customer segments and environments characterising a scenario. Accurate traffic demand characterisation in such a diversified scenario is a non-trivial but crucial component of the deployment of UMTS radio network.

The foreseen variety of services, the enormous set of possibilities of their use, and the lack of solid marketing information, makes the task of traffic estimation a very difficult and challenging one. In this way, a realistic estimation of location-variant demand distribution for mobile users is essential to generate and optimise a realistic network configuration that satisfies this demand.

Within the present work, a typical set of services and applications will be considered as user service characterisation and consequently used for data patterns generation. This set should be heterogeneous enough, in order to translate the multiplicity of services, applications and traffic patterns that UMTS will bear with the objective of identifying the traffic mix impact in UMTS performance.

UMTS offers the technical possibility to provide a broad set of services and applications with different characteristics and target users. Data transfer, video-telephony, and multiple applications for E-commerce are foreseen, among many others, for deployment within

[1] Service and application definition as per ITU-T recommendations [EURE00].

UMTS, which constitutes a novelty in mobile communications. Killer application(s) definition is an issue since the beginning of 3G formulations, and still remains an unknown as main UMTS commercial networks are still in an early launch state.

Service and applications formulation/characterisation focus on the DL due to expected bias to what regard the traffic volume as also the higher impact that the traffic mix will have in UMTS system performance. When applicable, references to possible UL system limitation(s) are referenced and quantified. The option to mainly focus on DL system aspects is also present in similar works dealing with UMTS traffic mix impact in system performance [MaZe02].

The application set considered in this thesis is based in previous works on non-uniform user generation [VaCa02], [FeAl02] which formulation is also the framework for the non-uniform user generation. The applications set considered in this work as its definition/scope is presented in Table 3.1. As mentioned before, the application set was chosen as a subset of the set considered in [VaCa02], where some applications were considered as redundant to the study in what regard the service type (source model) and radio bearer characteristics that will support it. The service set considered in this thesis is the one proposed in [FeCo03], where a traffic mix is proposed covering the four traffic classes presented in Section 2.2. Work reported in [FeCo03] is based on the IST-MOMENTUM project [MOME00] that focused on UMTS radio planning aspects such as user profile, mobility scenarios, etc..

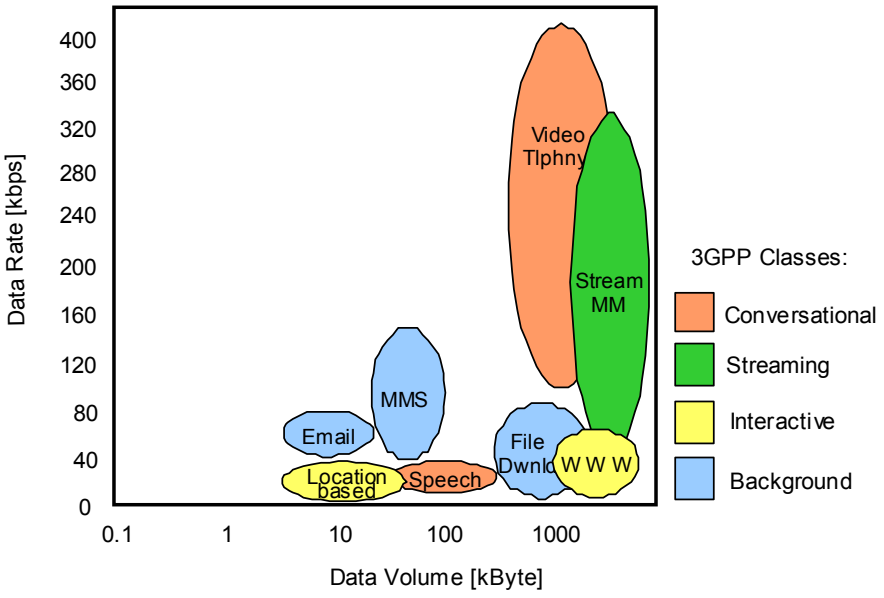

Figure 3.1 – Service Set bit rate range and DL session volume (extracted from [FeCo03]).

The application to service mapping proposal is based on the application content requirements and characterisation to what regards its source model. This type of simulation approach allows typical application deployment scenarios to be mapped directly onto the simulator inputs.

The set of 8 services (grouped by respective 3GPP traffic class), as described in [FeCo03] and used to characterise the user services set, is presented in Table 3.2. Only MMS was considered in the application set considered in this thesis, as SMS presents a subset of MMS capabilities (text only); MMS (text, image) is also considered as dominant UMTS messaging service [UMFo03]. Interactive gaming was considered to have a streaming profile, as interactive class might not provide temporal content in near real time gaming applications.

In [UMFo03], a specific set of services is proposed and compared in Table 3.2 with proposed service set. A very close match can be found from both studies, re-enforcing the service set selection/definition where no real data is still available for set validation.

Table 3.1 – Application set definition.

Application	Description
Voice Call	One to one voice communication with at least GSM voice quality, and connection expectations (at all mobility levels).
Video Call	One to one voice and video communication. Face to face calls will usually be made while the user is stationary, but moving in vehicles at any speed.
Video/Audio on Demand	Browsing for a short video/audio clip (e.g., news, advertisement or sports) of an event, and then watching it, stationary or moving.
Web Browsing, Chat, LBS, Interactive gaming	Downloading of mixed media. It is one of the nowadays most popular multimedia applications, also with large future foreseen acceptance (e.g., Mobile Internet). This information contains text, extensive graphics, video and audio sequences. It gives access to a wide number of areas: Communications and community (E-mail, calendar and chat), information (news, weather, and directories), lifestyle (events, restaurants, movies, and games), travel (hotel listings, location-based services (LBS), device type, and advertising).
E-mail, MMS and SMS	A process of sending messages in electronic form. These messages are usually in text form. However, they can also include images and video clips.
FTP	Application with FTP functionalities, allowing interactive browsing of directories and transfer of files.

Table 3.2 – Service set definition.

Traffic Class	Service Category	Service Category as in [UMFo03]	Information Type	Application(s) Mapping
Conversational	Speech-telephony	Simple Voice	Sound	Voice Call
	Video-telephony	Rich Voice	Video, Sound	Video Call
Streaming	Streaming Multimedia	Customised Infotainment/ Mobile Internet Access	Video, Sound	Video/Audio on Demand, Interactive Gaming
Interactive	Web Browsing	Mobile Internet Access	Multimedia	Web Browsing (WWW), Chat
	Location Based Services (LBS)	Location-Based Services	Multimedia	Personal LBS
Background	Multimedia Messaging	Multimedia Messaging Service (MMS)	Data, Sound	MMS, SMS
	E-mail	Mobile Internet Access	Text, Multimedia	E-mail
	FTP	Mobile Internet Access	Text, Multimedia Files	FTP (Data Server Access)

Based on the application/services set definition and their capabilities, adequate radio bearers are defined in UTRAN. The Radio Access Bearer Service is characterised by a number of attributes such as Traffic Class, Maximum Bit Rate, Guaranteed Bit Rate, SDU Error Ratio, Residual BER, Transfer Delay, etc. [3GPP04a].

A complete service capabilities listing is provided in [Agui03] where bit rates, traffic class, switching type, asymmetry, etc.. Within this work, services where mapped onto most common RABs available in UTRAN. The complete listing of supported RABs considered in R99 can be found in [3GPP04a].

The radio bearer mapping considered reflects the service capabilities requirements as defined in [Agui03]. Little information is available to what regard expected operator's services strategy and RAB mapping proposals. An example of an operator's strategy can be found in [IIRC03], where an application/service set and RAB mapping proposal is presented. The nominal mapping used in this work is presented in Table 3.3. Within this thesis, different RAB mappings as the ones here proposed will be used in order to evaluate system performance dependence on its selection.

As explained in Chapter 4, RRM features such as load control will impact on the nominal mapping, namely for interactive/background type traffic where the change of the radio bearer (normally its rate reduction) is performed to cope/minimise high load conditions in cells.

Table 3.3 – RAB Mapping.

Application	Service	Traffic class	Nominal Rate [kbps][2]	CS/PS
Voice Call	Speech-telephony	Conv.	UL:12.2 DL:12.2	CS
Video Call	Video-telephony	Conv.	UL:64 DL:64	CS
Audio on Demand	Streaming Multimedia	Stream.	UL:16 DL:64	PS
Video on Demand	Streaming Multimedia	I/B[3]	UL:64 DL:384	PS
Interactive gaming	Streaming Multimedia	I/B	UL:64 DL:128	PS
Web Browsing	Web Browsing	I/B	UL:64 DL:128	PS
Chat	Web Browsing	I/B	UL:64 DL:64	PS
LBS	LBS	I/B	UL:64 DL:64	PS
MMS (SMS)	Multimedia Messaging	I/B	UL:64 DL:64	PS
E-mail	E-mail	I/B	UL:64 DL:128	PS
FTP	FTP	I/B	UL:64 DL:384	PS

The next section will describe traffic source models for each service, making also reference to the criteria that lead to the proposed RABs.

3.2 Traffic Source Models

Any optimisation study of UMTS, e.g., at the level of the radio network, requires the introduction of service traffic source models, in order to predict the user's generated load in the network, based on multi-service traffic modelling. The central idea of traffic modelling lies in constructing models that capture the important statistical properties of services.

[2] Only values in DL are taken in consideration to traffic mix performance assessment. UL link budget considered in this thesis limits its rate to 64 kbps as commercial UEs (typically) only provide this maximum UL rate.

[3] 3GPP do not distinguish interactive from background traffic class in RABs definition [3GPP04a] as Background can be viewed as a subgroup of interactive class.

Some work has been done to evolve traffic source models to models for 3G mobile wireless networks services, but most existing traffic models are presented for wireline data networks, such as ATM or IP. Several works in traffic source models characterisation for wireless systems, and particularly UMTS networks, can be found in [Serr02], [Dias03] and [Agui03], which framework was based in the IST-MOMENTUM project studies. The traffic source models characterisation considered in this thesis are proposed in [SeCo03] and [Serr02].

The following subsections provide an overview of the selected traffic source models for the applications/services set described. The selection criteria were based on the source models that presented analytical tractability and suitable example parameters for the UMTS FDD system in study. Additional source models are referenced when applicable and assessment of its performance is delivered.

3.2.1 Speech and Video-Telephony

Conversational type services are characterised by their symmetric or quasi-symmetric nature, where the inherent QoS allows a very small delay (200 ms). As this thesis focus on system performance and radio resource dimensioning aspects (load, power and codes), speech and videoconference are modelled as a simple classical model, since its switching mode (CS) characteristics reserves in most NodeB architectures the resources are reserved during the whole call period (e.g., baseband processing units , usually named channel elements).

Voice and video calls (CS data services also apply) are generated according to a Poisson process with duration given by a (negative) exponential distribution. Mean call time (also known as Mean Holding Time - MHT) was set differently to speech (60 s) and video-telephony (120 s), as the later is expected to last more than a voice call due to the video content. Detailed distribution expressions can be found in Annex E.

Speech coding in UMTS uses the Adaptive-Multi Rate (AMR) technique, implementation details being found in [3GPP04b]. The AMR speech coder is a single integrated speech codec with eight source rates from 4.75 to 12.2 kbps, and a low rate background noise-encoding mode. The higher AMR rate (12.2 kbps) was chosen as it is widely available in commercial deployments, and more adequate AMR implementation would require knowledge of E_b/N_0 figures for each coding rate.

3GPP has specified that the transmission of video-telephony in third generation mobile systems, using CS connections, shall follow ITU-T H.324M (also referenced as 3G-324M) while for PS connections, ITU-T H.323 and IETF (Internet Engineering Task Force) SIP (Session Initiated Protocol) are two main candidates [HoTo01]. Actually, most video-telephony services are implemented over the CS type codec, with 64 kbps rate as it is the maximum typical rate available at 2G/3G MSC.

In [VaRF99], a measurement-based voice traffic model is described, which captures not only the ON-OFF behaviour, previously described, but also the effect of voice encoder, compression device, and air interface characteristics in CDMA mobile communication systems. Nevertheless, its characterisation does not fit the AMR behaviour, regarding either the Time to Transmit Interval (TTI) of 20 ms (10 ms) or the OVSF speech allocation that can vary from SF 512 to 128 [SeCo03], while speech AMR RAB typically maintains SF 128, even for the different rates.

Concerning IP based voice communications, [DiLS01] and [VaRF99] describe possible traffic models similar to the previous voice models, as birth-death processes, with a Poisson distributed arrival process and exponential distributed call duration. UMTS FDD is not likely to provide VoIP services, as CS support is available from day one. On the other hand, TDD commercial solutions are PS oriented, and VoIP is delivered in early solutions [IPWL04].

Extensive investigation on video-telephony models is presented in [Agui03] based on VBR models (Gamma Beta Auto-Regressive (GBAR) Model [Heym97]) mainly focused on ATM networks and low bit rate streaming video model from [NyJO01]. Neither of these models was considered, especially due to their non-applicability in the envisaged video-telephony CS type traffic.

3.2.2 Web Browsing, and Location Based Services

Interactive type traffic is generated when a user performs an information request to remote equipment, typically a server. A typical example of this type of traffic is the access to a web server (web browsing). Several models have been proposed for web browsing traffic, like those described in [Agui03]. Within the present report, one will describe the model adopted by 3GPP for UMTS, as presented in [ETSI98b]. Specific parameterisation of the model

allowed adapting its performance to web browsing, LBS, or streaming profiles, as proposed in [SeCo03]. Detailed distribution expressions can be found in Annex E.

The model considers a sequence of packet calls during a WWW browsing session, initiating a packet call when requesting an information entity. During a packet call, several packets may be generated, constituting a bursty sequence of packets. WWW browsing sessions are highly asymmetric with typical bias in the DL. In these types of sessions, a packet call corresponds to the downloading of a WWW document (e.g., web page with images, text, applets, etc.). After the document is downloaded, a reading time interval (by the user) is experienced [ETSI98b]. A typical WWW session is shown in Figure 3.2.

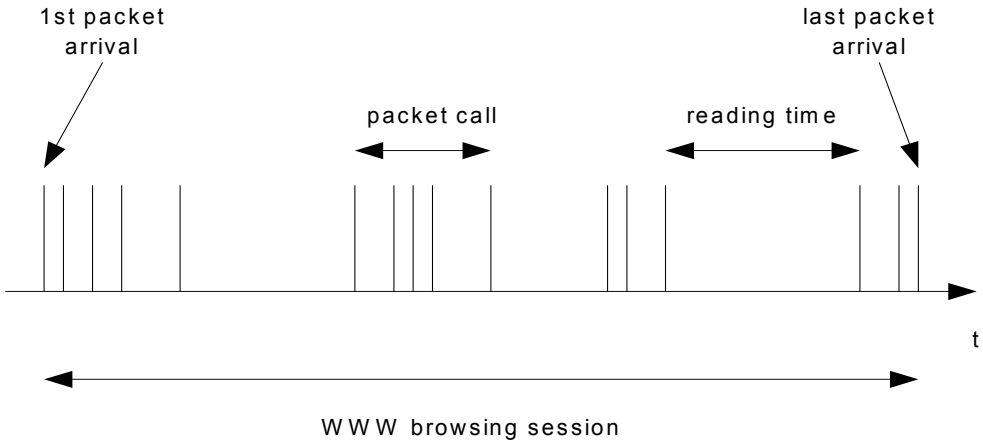

Figure 3.2 - Typical WWW session (extracted from [Agui03]).

The following parameters must be modelled, in order to catch the typical behaviour of the general model. The geometrical distribution is used (discrete representation of the exponential distribution), for discrete time scale simulation purposes.

- Session arrival process: The arrival of session set-ups to the network is modelled as a Poisson process. For each service there is a separate process.
- Number of packet call requests per session, N_{pc}: This is a geometrically distributed random variable.
- Reading time between two consecutive packet call requests in a session, D_{pc}: This is a geometrically distributed random variable. Note that the reading time starts when the last packet of the packet call is completely received by the user. The reading time ends when the user makes a request for the next packet call.
- Number of packets in a packet call, N_d: Different statistical distributions can be used to generate the number of packets. It can be a geometrically distributed random variable. It must be possible to select the statistical distributions that describe best the traffic

case under study. An extreme case would be that the packet call contains a single large packet, case used to emulate streaming type traffic [SeCo03].

- Time interval between two consecutive packets inside a packet call, D_d: This is a geometrically distributed random variable. Naturally, if there is only one packet in a packet call, this variable is not needed.
- Packet size, S_d: The packet size is defined as $S_d = \min\left(P_a, M_{ps}\right)$, where P_a is a Pareto distributed random variable and M_{ps} is the maximum allowed packet size (66 666 bytes).

The inter arrival time is adjusted in order to get different average bit rates at the source level. According to the values for α_p and k in the Pareto distribution, the average packet size μ_{Sd} is 480 bytes. Therefore, the average requested file size is $\mu_{Nd} \cdot \mu_{Sd}$ = 25 × 480 bytes = **12 kB**. Table 3.4 gives default mean values for the distributions of typical WWW browsing services.

Table 3.4 - Parameter values for web browsing model (adapted from [ETSI98b]).

Packet based information types (WWW browsing)	μ_{Npc}	μ_{Dpc} [s]	μ_{Nd}	μ_{Dd} [s]	**Parameters for S_d distribution**
UDD 64 kbps	5	4-12	25	0.0625	k = 81.5 α_p = 1.1
UDD 144 kbps				0.0277	
UDD 384 kbps				0.0104	

3.2.3 Streaming Multimedia and Multimedia Messaging

Streaming type services are characterised by a continuous flow of data capable of supporting substantially higher end-to-end transmission delays and fluctuation (jitter) than for conversational type services. The nature of the traffic in streaming services is clearly non-symmetric, since it refers to the download and simultaneous processing of huge data files, such as video. Furthermore, a larger fluctuation of packet arrival time is allowed although the use of intermediate buffers at the reception allows a nearly full cancellation of this fluctuation, assuring a constant data rate to the applications. Examples of this type of traffic are: video on demand and MP3 streaming [Agui03].

Advanced streaming source modelling is described in [Agui03], referring to MPEG-4 and H.263 encoded video (GOP GBAR model [FrNg00], is a generalisation of the GBAR model

for video conferencing referenced in Section 3.2.1). Within this thesis, as proposed in [SeCo03], the streaming source model is evolved from web browsing one, by setting average number of packet calls within a call to 1 and considering a null reading time between packets.

MMS and SMS can be modelled by an ON-OFF model (generation is a Poisson type process). The major difference between SMS and MMS is the average volume of each one (160 B and 30 kB respectively) and the average number session per hour. The volume is exponential distributed [SeCo03]. Detailed distribution expressions can be found in Annex E.

3.2.4 E-mail and FTP

Background type traffic corresponds typically to data transfer applications that do not demand an immediate response/reaction from the user. Typical examples of applications that generate this type of traffic are: e-mail, FTP, music download (e.g., Napster) and Telnet [Agui03]. The models proposed and already addressed in [Agui03] and [SeCo03] are synthetic traffic ones for UMTS based on measured trace data [KlLL01].

The traffic model proposed in [KlLL01] uses the notion that a user who runs non real-time applications (e.g., HTTP, Napster, e-mail) follows a characteristic usage pattern, and that a single user may run different applications that may be concurrently active, e.g., WWW browsing while downloading Napster music files.

Each application is completely described by its statistical properties, which comprise of an alternating process of ON and OFF periods with some application specific length or data volume distribution, Figure 3.3. Moreover, within each ON-period the packet arrival process is completely captured by the packet inter arrival times and the corresponding packet sizes. Detailed distribution expressions can be found in Annex E.

In this model, the single user traffic model is employed on three different levels:

- Session-level: it describes the dial-in behaviour of the individual users, characterised by the session inter arrival time distribution and the session data-volume distribution.
- Connection-level: it describes for each individual application the corresponding distribution of connection inter arrival times and connection data volume, respectively.
- Packet-level: it characterises the packet inter arrival time distribution and the packet size distribution within the application specific connections.

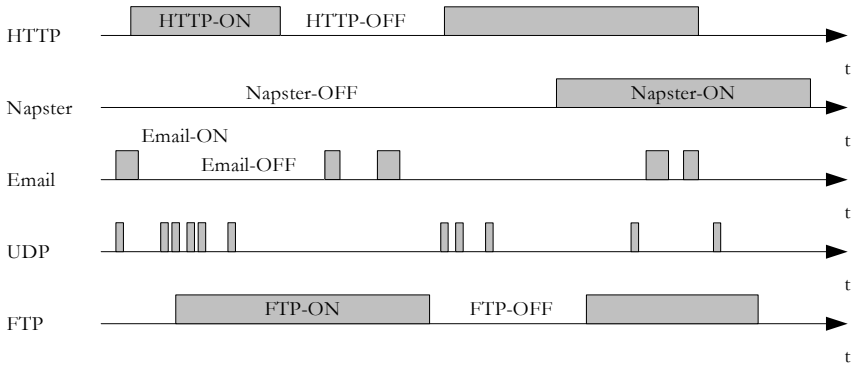

Figure 3.3 - Classification of non-real time IP traffic streams (extracted from [KlLL01]).

Table 3.5 presents a summary of the traffic source models described in the previous sections (inputs/outputs). Models will only be applied in DL, as mentioned in Section 3.1.

Table 3.5 - List of traffic source models.

Service	Traffic Source Models	Input Parameters	Output Parameters
Speech/Video Telephony	Classical Voice (ON-OFF) Model	Session rate. Mean Holding Time (MHT)	Speech start and duration
Web Browsing / LBS / Streaming	Web Browsing Model	Target bit rate and statistical parameters from real trace data	Number of packet calls per session. Reading time between packet calls. Number of packets within a packet call. Inter arrival time between packets within a packet call. Packet size
Multimedia Messaging	ON-OFF	Average packets size	Packet size
E-mail and FTP	e-mail/FTP *n* kbps (*n*=64, 144, 384)	Target bit rate and statistical parameters from real trace data.	Session inter arrival times / data volume. Connection inter arrival times / data volume. Packet Inter arrival time and sizes

3.3 Non-Uniform User Generation

3.3.1 Geographical Information Systems

This section focuses on the strategy and tools used to generate (spatially) users and their service characterisation. Due to flexible handling of geographical and socio-economic population characterisation, the selection of a Geographical Information Systems (GIS) software platform was a natural one. GIS is a concept to visualise, manipulate, analyse and display spatial data, combining layers of information on a region, and allowing advanced merge and query capabilities.

Several tools are available in the market (Arc View [ARCV03], MapInfo® [MAPI03], etc.) MapInfo® being chosen as the GIS, especially because of higher availability of information tables and the BASIC programming capabilities through MapBasic®. Other important GIS potentialities are:

- import/export from/to many formats;
- work with raster (pixel grid) and vector data;
- query, select and combine data;
- automatic reports.

The option of a GIS solution for the non-uniform user generation was driven by the flexibility on handling population data from any place, of any size and the easy handling of data to create non-uniform user/traffic traffic scenarios. An application responsible for the user geographic distribution and application was developed in MapBasic® – TRAFSIM3G. Additional and detailed information on GIS layers implemented in TRAFSIM3G is presented in Section 4.2.

3.3.2 User Generation Algorithms

User generation algorithms presented in TRAFSIM3G are based on previous works from [VaCa02] and [FeAl02]. The concept behind these two works is to create a certain service distribution based on demographic indicators, such as age, family's wealth, and education. The geographical user distribution is modelled by defining an overall penetration percentage over the total population present in the analysis area. Geographical user's distribution is achieved by assigning different user generation weights depending on the clutter characterisation (Dense Residential, Green Areas, CBD[4], Services Areas, etc.). All this information is handled through GIS tables using the concepts described in Section 3.3.1.

Both works ([VaCa02] and [FeAl02]) focused on the non-uniform traffic aspects. The former assessed UMTS performance dependencies, namely cell radius and traffic cell breathing effects. The latter is a tuning process of the non-uniform generation algorithm by evaluating its performance against real network voice traffic (GSM data).

[4] Central Business District – services and enterprises area

Other traffic characterisation works, namely [UMFo03] use similar items to predict/characterise the UMTS traffic offering. In this late example, besides the location profile (geographical/clutter penetration), demographic indicators, such as industry, occupation, and income are considered. Unfortunately, one year after [FeAl02], there are still no networks presenting statistical valid traffic amounts, or even clear ideas on the traffic mix to consider. This thesis uses the same approach as [VaCa02], including improvements proposed in [FeAl02], such as present population consideration (instead of residents only). The user generation/characterisation process takes into account the following demographic and geographic inputs (detailed GIS tables and data assumptions are shown in Annex G and Annex H):

- Population (Present population[5] [InNE01]).
- Population Characterisation (Age, Education, Economical Aspects – average salary rating [InNE01] and [DGCI02]).
- Clutter characterisation (Dense residential, Residential, CBD, etc. [CaML02]).
- Application/service penetration per demographic indicator (age, salary and education – Annex G).
- Application to radio bearer mapping and radio bearer details (Annex I).

Within the algorithm, the number of active users (district level) is defined by the population penetration rate (in fact it also includes utilisation rate), explicitly defined in TRAFSIM3G application (TRAFSIM3G reference guide is presented in Annex J). From the set of radio bearers considered (refer to Table 3.3) and from the application/services weights assigned (Annex H), a vector containing the radio bearer distribution per district is obtained by:

$$\boldsymbol{D}=k_1\left(p_{<20}\times\boldsymbol{v_{11}}+p_{20<<64}\times\boldsymbol{v_{12}}+p_{>64}\times\boldsymbol{v_{13}}\right)+k_2\left(p_{sem}\times\boldsymbol{v_{21}}+p_{obrig}\times\boldsymbol{v_{22}}+p_{\sec}\times\boldsymbol{v_{23}}+p_{\sup}\times\boldsymbol{v_{24}}\right)+k_3\left(\boldsymbol{v_3}\right) \quad (3.1)$$

Where:

- $\boldsymbol{D}$ is an array with the radio bearer distribution at district level,
- k_1, k_2 e k_3 are coefficients to introduce different weighting at age, education and wealth indicators respectively (configured in TRAFSIM3G application – Annex J),
- $\boldsymbol{v_{I1}}$, $\boldsymbol{v_{I2}}$, $\boldsymbol{v_{I3}}$ are arrays in GIS tables (referring to age population characterisation) shown in Annex G,

[5] From [FeAl02] expected that BH would occur during the day, were for the Lisbon city scenarios the present population shall account for residents and commuters. Detailed population analysis is presented in Annex G.

- v_{21}, v_{22}, v_{23} e v_{24} are arrays in GIS tables (referring to education population characterisation) shown in Annex G,
- v_3 is the array corresponding to population wealth indicator shown in Annex G,
- $p_{<20}$, $p_{10<<64}$ e $p_{>64}$ are the age population distribution (Annex G)
- p_{sem}, p_{obrig}, $p_{\sec}$ e $p_{\sup}$ are the education population distribution (no basic education, basic, High-school and University levels - Annex G)

The default application distribution settings were taken from [VaCa02] [FeAl02] and presented in Annex H. Due to software development implications in the second TRAFSIM3G module (VC++ module, with detailed description in Chapter 4), it was decided to restrict only one service to a user.

In addition to the radio bearer rate, the mapping proposed in Table 3.3 was implemented in TRAFSIM3G by the definition of a GIS table (see Annex I), where for each application the traffic source model and RAB physical layer main characteristics important for the application are detailed. One should note that besides the radio bearer rate, the source model distribution is taken into account for user generation.

After calculating the percentage of users of a certain RAB, with a certain source model, users are uniformly distributed along the district area, but in different proportions depending on the clutter occupation type (Dense Residential, Green Areas, Roads, etc). The used distribution is also taken from [VaCa02] [FeAl02] and summarised in Annex G.

The clutter distribution percentage in a district, along with the percentage defined in Annex G, leads to the number of users in a certain clutter. Within the clutter polygon (in GIS solutions, areas such as a clutter zone delimitation are usually named as a polygon), the geographic user location is random. One should note that irregular clutter polygons lead to high simulation times as random coordinates generation might lead to out of the polygon locations.

In order to summarise the user generation characterisation information, Section 4.2.2 shows all the items used to characterise the user services and location, and that input into the TRAFSIM3G VC++ module, where the real time system simulation is performed.

In Figure 3.4, a 0.5% population penetration/utilization TRAFSIM3G mapping output example is presented, where user's location is represented by a flag with its colour associated to the assigned RB.

Table 3.6 – User characterisation parameters.

Parameter	**UE index**	**Longitude**	**Latitude**	**DL RAB type**	**DL RAB type**	**Clutter type**	**Prop. Channel**	**Source Model**
Type	int	float	float	string	int	int	int	int
Range	1…49999	dec W	dec N	PS/CS[rate]	1…7	1…7	1,2	6…14
Example	1	-9.15129	38.7317	PS128	6 (128 kbps)	7 (Green Areas)	1 (Ped A 3km/h)	9 (Streaming)

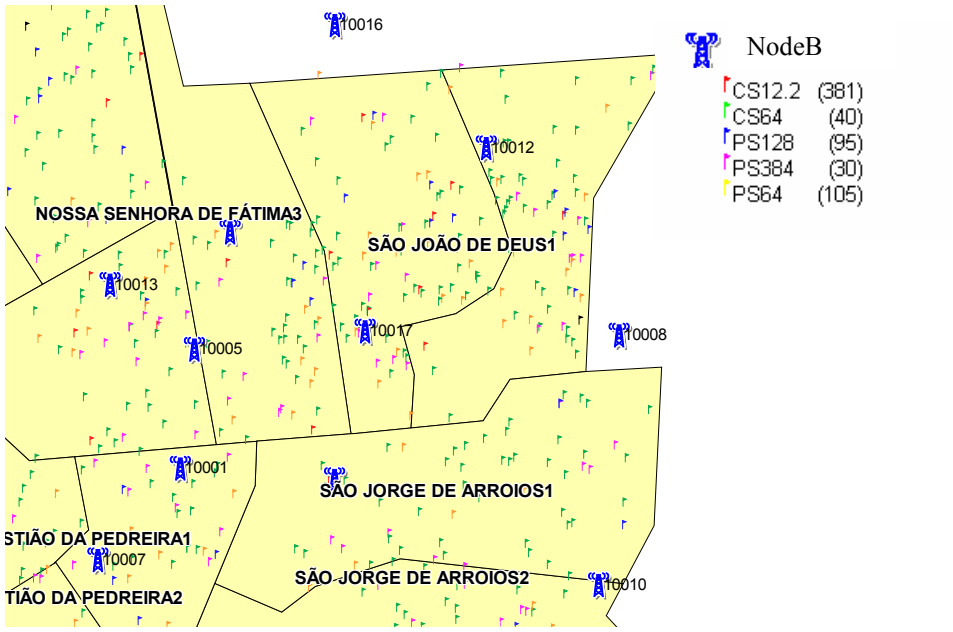

Figure 3.4 – User generation example, for Lisbon high-density area (population/sites).

MapInfo®, associated with MapBasic®, proved to be valuable and adequate tool for the concept used in the user generation and characterisation, specially the geographical specific calculations, allowing a flexible platform that can load any network or demographic scenario tables. It provided sufficient mathematical support to the user generation process and UL link budget calculation, but showed limited availability of more complex mathematical functions such as the one required for slow fading margins calculation. These late where implemented in VC++ DLLs and called from MapBasic® code.

4. TRAFSIM3G Simulator Description

The present chapter provides a functional description of the simulator platform developed within the scope of this thesis, with the main objective of allowing the evaluation of the impact of multi-service non-uniform traffic in UMTS FDD system performance. After introduction to the simulator scope and objectives, details in the GIS and VC++ modules implementation are presented. The last section shows simulator parameter analysis, validation of main RRM algorithms and preliminary scenarios performance requisites assessment.

4.1 Simulator Overview

For the purpose of evaluating the impact of non-uniform UMTS traffic mix, mainly from a system performance viewpoint (e.g., bit rates, delay, blocking, etc.), a complete simulator tool was implemented: **TRAFSIM3G**. The main goal underlying the development of the simulator was to build a platform enabling the following four main tasks:

- to create a non-uniform UMTS network traffic pattern and user traffic profile;
- to develop adequate traffic source models for the foreseen applications, and map application characteristics in a network Radio Bearers;
- to implement a UMTS simulator with all relevant mechanisms of Call Admission Control (CAC), handover (soft and softer (SHO/SSHO)), Power Control (PC), etc., and consequent system performance analysis;
- to simulate the main RRM algorithms that will affect original traffic source models, and to implement hardware dimensioning and NodeB processing main characteristics (carriers and Channel Elements).

As referenced in Section 3.3.1, the option to use a GIS programming language (MapBasic®), as best solution to implement the non-uniform user generation/characterisation, lead to the need to select a different programming language for the UMTS system module, where the frame level granularity would require faster and flexible programming languages. VC++ was selected for the UMTS simulator, using object-oriented programming (e.g., each UE/NodeB is considered as an object).

The UMTS simulator (VC++) can be run from the MapBasic® application, allowing in the same application to run the complete calculation flow. Both applications are linked with a flat

file set, where the user can easily change the inputs that feed the UMTS simulator, reducing the need to run every time a user scenario generation. The output of the UMTS simulator is also a set of flat files that can be triggered in the application options. As default, a set of main system performance indicators, such as UE and NodeB performance, is automatically generated.

The overall program has approximately 3 000/11 000 MapBasic®/C++ code lines, and constitutes a flexible and easily upgradeable platform for the simulation of different traffic mix and user generation scenarios. Two main functional blocks, GIS and VC++ engines, constitute the simulator, Figure 4.1.

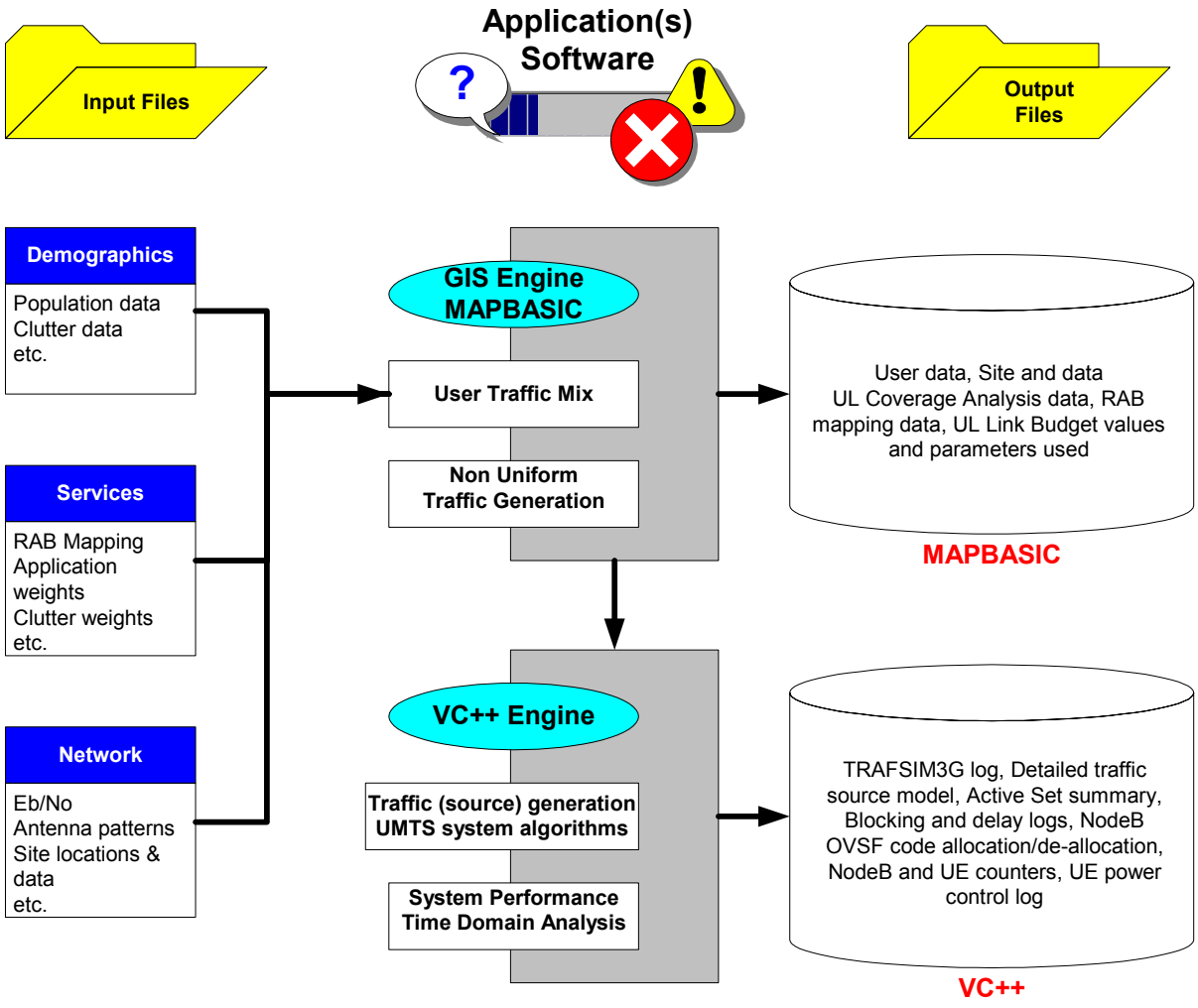

Figure 4.1 – Simulator module and generic file structure.

4.2 GIS Engine

4.2.1 GIS Module Diagram

The GIS engine calculation flow and file structure is shown in Figure 4.2.

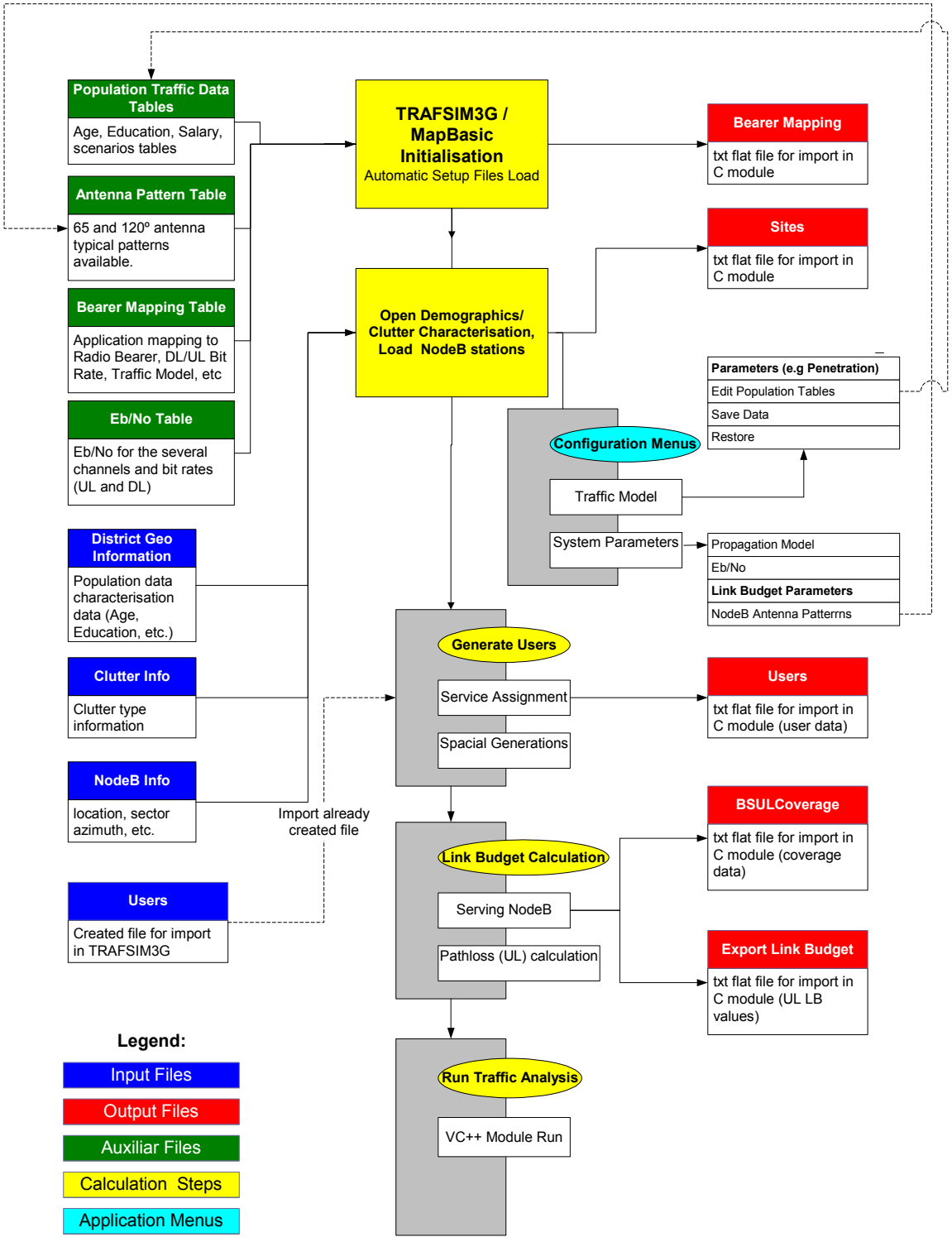

Figure 4.2 - GIS Engine flow, input/output files and application structure.

The TRAFSIM3G application is run from the MapInfo® executable file (MBX file), and from it the VC++ module can be initialised (optionally, it can be run alone as an executable file). Note that the MapInfo® platform is a requirement to handle GIS table's information that input the simulator, providing the flexibility and ease of use. GISs platforms are widely used in operator's radio planning groups, and so the MapInfo® application requirement should not be an obstacle if used in this context. In Figure 4.3 a snapshot of the application and main menu is shown (reference and user manual can be found in Annex J).

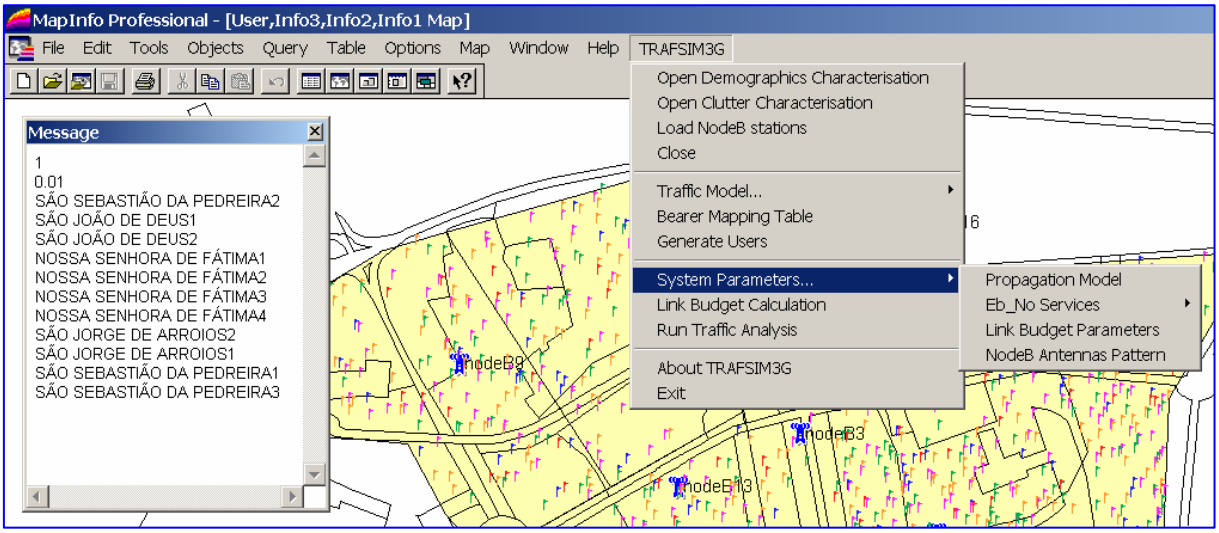

Figure 4.3 – TRAFSIM3G GIS application (output, main menu and mapping windows).

In the start-up, TRAFSIM3G.MBX loads automatically the following MapInfo® tables, included in TAB extension files (please refer to Figure 4.2):

- population traffic data tables (service dependence on demographics);
- antenna pattern (standard load is 65º horizontal beam antennas aperture);
- bearer mapping table (relation between service/application and radio bearer service that supports that service, automatic table export to text file format for input on VC++ module);
- E_b/N_0 table for link budget calculation purposes.

On initialisation, and to start using the application, the tool user is requested to locate/open the main input files for user generation that contain demographic information:

- district population (demographical and geographical) characterisation;
- district clutter characterisation (clutter location and type);
- NodeB location and configuration (site location, sector number, azimuth, etc.).

After loading the district and site information, the tool user has the ability to generate a user/service scenario or load an existing user file according to the generation algorithm described in Section 3.3, originating a text file with user generation data for input in the VC++ module. After the sites table is loaded, an automatic text output with site's information is generated for input into the VC++ module.

When the user generation process is finished, the UL coverage analysis function is run, analysing each user coverage conditions and creating the summary to an output file. Automatic with the UL coverage text file, the parameter values taken in the link budget are exported to this file for further processing in the VC++ module if applicable, along with the service cell radius. One should note that all outputs from MapInfo® have a flat version, and a dated version for storing and simulation tracking purposes.

After obtaining all the GIS tables (users, sites, UL coverage and Link Budget), the tool user can run the VC++ module from TRAFSIM3G menu (Run Traffic Analysis), and then proceed to the time domain analysis of the simulation. Additional menus are available to control table edition, link budget/propagation model parameters, etc..

The two main control menus in GIS engine are (detailed in Section 4.2.4):

- Traffic Model
    - Parameters (pop. penetration, demographic indicators weights, etc.);
    - Edit Population data (table edition);
    - Save Data (tables changes);
    - Restore (table defaults).
- System Parameters
    - Propagation Model (COST 231-WI parameters);
    - E_b/N_0 Services (table edition);
    - Link Budget Parameters (margins, TMA, etc.);
    - NodeB Antenna Pattern (65 and 120º antenna option).

Additionally, some auxiliary or informative options are available:

- Close (Reset to District/NodeB tables);
- Bearer Mapping Table (Display RB mapping and bearer characteristics);
- About TRAFSIM3G (Author and Supervisor identification);
- Exit (Quit application).

4.2.2 GIS Engine Input Data

This section describes the contents of each file used and the type of the variables included as some general comments on the options taken. Full file information format with numerical examples or assigned values is provided in Annex K.

When starting TRAFSIM3G, the GIS engine loads the service tables, where for each application a usage profile is defined, based on the demographic criteria assumed, it being age, education, salary and the environment scenario utilisation defined by a penetration per clutter type. Each table reflects the structure of the district information availability, e.g., age characterisation is done in 3 segments (refer to Section 3.3 for further clarifications). The table formats for age, education, salary and scenarios are presented in Annex K. The traffic mix scenarios are created acting on these percentages by giving different weights to specific applications that are then mapped in a specific MOMEMTUM model. Scenarios table provides the user distribution percentage for the clutters defined in the GIS information layers, Figure 4.4. The age, education, salary and scenarios values are shown in Annex H.

Salary Browser

Application	DL_Rb_kbps	Low	Medium
voice	12,2 (CS)	95	87
audio-on-demand	64 (PS)	0	0
video-telephony	64 (CS)	0	2
video-conf	64 (PS)	0	0
m-commerce	64 (PS)	0	0
video-on-demand	384 (PS)	0	0
web-browsing	128 (PS)	0	1
chat	64 (PS)	1	2
file storing	384 (PS)	0	0
		0	0
		0	1
		0	0
		0	0
		3	5
		1	3
		0	0
		0	0
		0	0
		0	0

Scenarios Browser

Clutter	Penetration_%
Dense Residential	30
Light Residential	15
Mixed Buildings	25
Terciary Buildings	20
Industrial Buildings	5
Roads	4
Green Areas	1

Age Browser

Application	DL_Rb_kbps	Age_20	Age_20_to_64	Age_64
voice	12,2 (CS)	44	48	90
audio-on-demand	64 (PS)	9	2	0
video-telephony	64 (CS)	5	9	2
video-conf	64 (PS)	0	0	0
m-commerce	64 (PS)	0	0	0
video-on-demand	384 (PS)	3	2	0
web-browsing	128 (PS)	6	12	5
chat	64 (PS)	9	5	0
file storing	384 (PS)	0	0	0
turistic info	64 (PS)	0	0	0
personal LBS	64 (PS)	1	7	2
travelling assistance	64 (PS)	0	0	0
emergency	12,2 (CS)	0	0	0
MMS	64 (PS)	13	4	0
interactive gaming	128 (PS)	4	2	0
FTP	384 (PS)	2	7	0
e-mail	128 (PS)	4	4	1
file download	384 (PS)	0	0	0
electronic journal/books	128 (PS)	0	0	0

Figure 4.4 – Input GIS tables' examples: age, scenarios and salary (fragment).

In order to be able to simulate different antenna beam width and its consequence on UMTS coverage performance, two (typical) NodeB antenna patterns are provided with TRAFSIM3G; 65º and 120º 3-dB horizontal beam-width antennas. The maximum gain value is provided in link budget menu, typically set at 17 dBi for 65º antennas and 14 dBi for 120º antennas. The reference to maximum gain value is defined as positive (no need to add negative sign).

Antenna pattern tables' format is detailed in Annex K. Antenna pattern values used are detailed in Annex I and its comparison is shown in Figure 4.5.

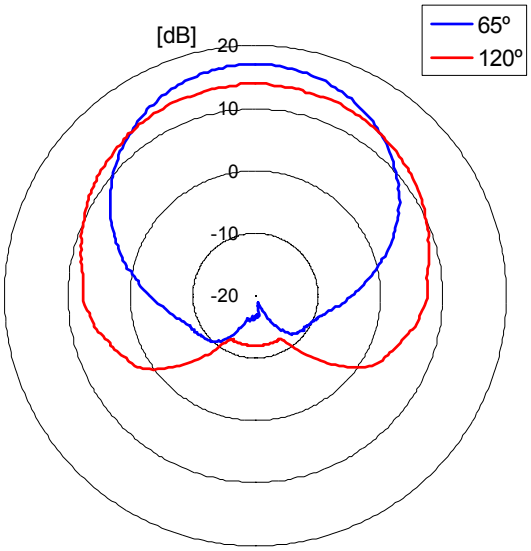

Figure 4.5 – Antenna patterns for 65 and 120º, shown for 17 and 14 dBi gain respectively.

RB mapping assumptions (detailed in Section 3.1) are included in the bearer-mapping table, also automatically input in TRAFSIM3G. This table provides the link between applications and its corresponding implementation in the network, namely bit rate for UL and DL, type of switching (CS or PS), QoS, transport channel information such as SF, TTI, coding, physical channel rate (from [3GPP02r]) and the assigned traffic source model (from [MOME00] and [SeCo03]) that will be used to generate its traffic patterns in VC++ module as explained further in Section 4.3. Bearer mapping table format and values are shown in Annex K and Annex I, respectively. In Figure 4.6, an example is shown for an application subset (please note traffic model and TFCS information columns).

BearerMapping Browser

Application	Service_Type	Bearer	Switching_Typ	QoS	ULrate_kbps	DLrate_kbps	Traffic_Model_Momentum
voice	VOICE	CS_C_UL_12.2kbps_DL_12.2kbps	CS	C	12.2	12.2	speech
audio_on_demand	MUSIC_ON_DEMAND	PS_IB_UL_64kbps_DL_64kbps	PS	IB	64	64	streaming
video_telephony	VIDEO_CONFERENCE	CS_C_UL_64kbps_DL_64kbps	CS	C	64	64	video
video_conf	REMOTE_MONITORING	PS_IB_UL_64kbps_DL_64kbps	PS	IB	64	64	streaming
m_commerce	MACHINE_2_CUSTOMER	PS_IB_UL_64kbps_DL_64kbps	PS	IB	64	64	www
video_on_demand	VIDEO_ON_DEMAND	PS_IB_UL_64kbps_DL_384kbps	PS	IB	64	384	streaming

BearerMapping Browser

Application	Service_Type	SF_UL	SF_DL	TTI_UL_ms	TTI_DL_ms	Coding_UL	Coding_DL	PHY_UL_Rb_kb	PHY_DL_Rb_kb
audio_on_demand	MUSIC_ON_DEMAND	16	32	20	20	0.333333	0.333333	240	240
video_telephony	VIDEO_CONFERENCE	16	32	40	40	0.333333	0.333333	240	240
video_conf	REMOTE_MONITORING	16	32	20	20	0.333333	0.333333	240	240
m_commerce	MACHINE_2_CUSTOMER	16	32	20	20	0.333333	0.333333	240	240
video_on_demand	VIDEO_ON_DEMAND	16	8	20	10	0.333333	0.333333	240	960

Figure 4.6 – Bearer mapping table (fragment).

Along with service characterisation, a table including all E_b/N_0 values for the different channel types (Pedestrian A) and speeds (3 and 120 km/h) is provided. These values are then considered in the UL/DL link budget calculations. E_b/N_0 table format is provided in Annex K and its values shown in Annex I. Service penetration and E_b/N_0 tables can be re-edited from TRAFSIM3G application as they are crucial for the user generation process. Nevertheless, standard values are automatically provided at application start-up. The next tables to input (see Figure 4.2) are the ones with the district, clutter and demographic information.

The main table contains all district area (area polygon), present population (typical busy hour is expected during working hours), age, education and salary. For the present population, and similarly to [FeAl02], one considers the population balance during working hours using commuting information for Lisbon city. District table format and values is shown in Annex K and Annex G, respectively. By crossing district demographics with service penetration, one will have a specific service set as detailed in Section 3.3. After population and district characterisation, the clutter/ground definition within the district is loaded. It includes the area polygons and allows calculating penetration levels defined in the scenarios table for each clutter for every district (table in Annex G); its format is presented in Annex K. In Figure 4.7, an example is provided where it can be seen all age, education and salary indicators of two Lisbon districts. In Figure 4.8, it is shown the clutter characterisation for the Olivais district area, where all clutter categories can be found from dense residential to roads.

FregLD Browser

District	Present_Populati	Age_20	Age20_64	Age_64	noEducation	Basic	Complementar	Degree	Salary
MARVILA_1	18,709	46.9099	41.1811	12.0542	15.3485	57.5994	19.8576	7.19445	Low
SANTA MARIA DOS OLIVAIS_2	33,914	30.6439	49.4593	20.042	11.4027	50.0733	20.2284	18.2956	Medium
MARVILA_2	19,000	46.9099	41.1811	12.0542	15.3485	57.5994	19.8576	7.19445	Low

Figure 4.7 – District table for Olivais and Marvila (Lisbon low density districts).

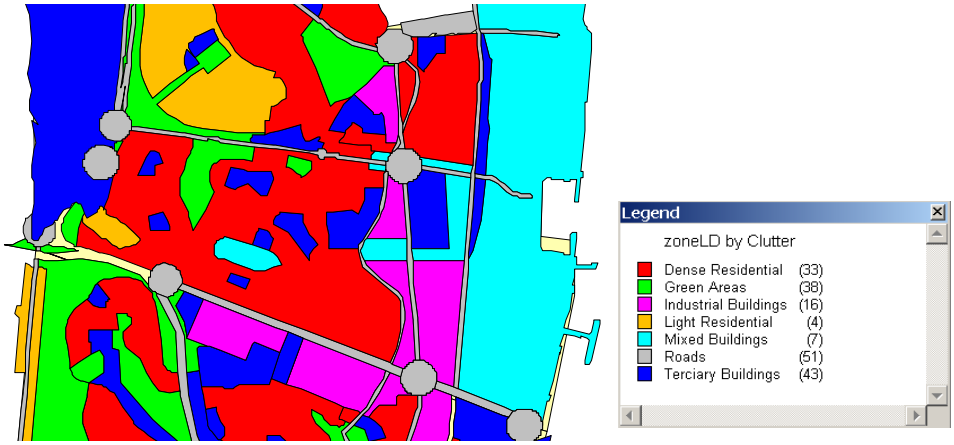

Figure 4.8 – Clutter plot for Olivais district area.

The final input phase is to enter the sites/NodeB locations and their basic configuration. It is extracted from [FeAl02], where an operator site locations plan is provided. NodeBs were considered to have standard 3 sectors and 20 W PAs. CPICH and common channel power assumptions (respectively 2 and 6 W) are detailed in Annex D. Site table format is shown in Annex K. To ease NodeB/cell identification, a numbering scheme with 6 digits was defined where the first 5 represent the NodeB code and the last is the sector/cell number. For example the site **10012** has associated three cells to it; 10012**1**, 10012**2** and 10012**3,** respectively sectors one, two and three.

4.2.3 GIS Engine Output Data

When running the user generation process or the UL link budget calculation (detailed in Section 4.2.4), TRAFSIM3G automatically generates table and .txt output files that will be used as input in the VC++ module. The automatic generated output files, as sites and bearer mapping info (see Figure 4.2), have the exact contents of the tables presented in Section 4.2.2, converted to a flat text file and with header information removed. The VC++ module will later import these files as described in Section 4.3.2.

The most important file (users.txt) includes all user generation information: location, service assigned, propagation conditions, etc.. Each user can be assigned 2 services (Multi-RAB - application percentage distribution for a certain population criteria, e.g., age, goes over 100 %. Users file format is shown in Annex K. One should note that all the services and propagation characterisation that will be used in the VC++ module, such as the traffic model (e.g., S1 or S2 MOMENTUM column) and channel type/penetration loss is available in this table. Besides the channel type, indoor penetration and the clutter in which the UE is located are available in specific columns. In Figure 4.9, one shows the TRAFSIM3G (mapping) output after user generation process where each colour represents a user in a specific RB and a fragment of the users table contents. Most of the information in users table was coded to an integer. As an example, channel type equal to one refers to pedestrian while two means a vehicular type channel. This coding is described in Annex K (Table Annex K.12).

The (UL) coverage analysis information for all UEs is gathered in BSULCoverage.txt file. It will allow the processing of the active set and soft handover management in the VC++ module. Up to 8 different NodeBs and 16 cells can be saved per UE (typical active set size is

less than 6 cells). One should note that TRAFSIM3G allows the change on the propagation model parameters as also the target UL rate. For all analysis, one has considered a UE with possible service when presenting a pathloss lower than the limit for the less stringent service available which is a signalling radio bearer (3.4 kbps) where SMS is carried. Since no E_b/N_0 values where available for signalling bearers, one has assumed a 5 dB margin (estimation based on the processing gain difference) over the pathloss calculated for speech AMR 12.2 kbps. The file format is presented in Annex K.

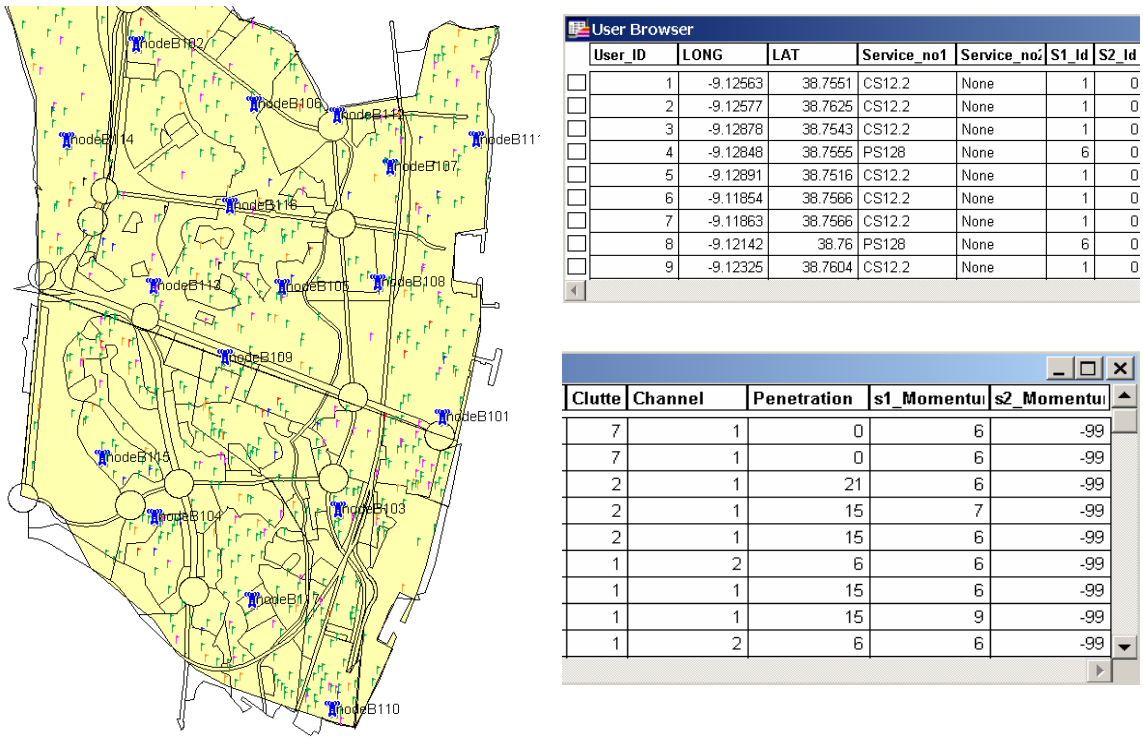

Figure 4.9 – Users table (mapping) and table fragment.

The VC++ module requires all information used in the link budget calculation, as also the (UL) cell radius values. All this information is gathered in the ExportLinkBudget file, which format is presented in Annex K. The next section describes in detail the main features available in the GIS engine, such as the table update aspects, user generation, propagation model and UL coverage analysis details.

4.2.4 GIS Engine Main Features

In parameters option from the traffic model menu, the tool user can adapt its generation process to apply to different population penetration and utilisation scenarios, or apply

different weights on the demographic aspects used in the generation algorithm. Significant work has been done in the generation process assessment ([VaCa02] and [FeAl02]), hence, focus on penetration/utilisation variations impact will be given in this thesis. Along with parameters, several options are also available in this menu with the aim of allowing user edition/save/restore of input tables.

The system parameter menu includes the propagation model and link budget parameters sub-menus. The propagation model options from [FeAl02] were updated with most relevant frequency channel on FDD and TDD sub bands. Since most tested scenarios are dense urban and urban, COST231 – WI option seems adequate for cell radius estimation. Extension to COST231-Hata model implementation in future works is proposed as a more adequate model to assess the propagation scenario in suburban or rural deployments.

The link budget parameters menu offers the opportunity to test several propagation and equipment scenarios, as all parameters are editable. It is worth to point the inclusion of the TMA option as a UL coverage enhancement strategy. This strategy has been used extensively in early UMTS launch, as coverage is expected to be limited in the UL as long as traffic (load) is kept low in the DL. Another reason is to minimise UE transmit power, as battery technology is still adapting to the high power requirements of UMTS (data) terminals. Link budget parameter window is shown in Figure 4.10. In Section 4.4, impact of TMA in UL coverage is shown.

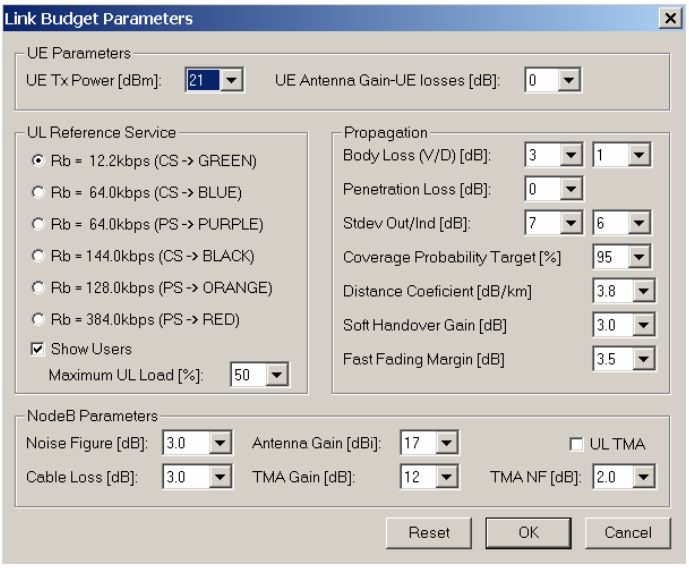

Figure 4.10 – Link budget parameters menu.

The UL coverage verification is evaluated following the scheme described in Figure 4.11. To start, a simple link budget for all possible services (RBs) is calculated based on the link budget parameters defined in the parameter menu window (Figure 4.10). From the cell radius and pathloss calculations, the figures for the less stringent service are extracted. For each user is then created a search area, which radius equals the maximum value possible (typically voice), and all NodeBs within that circle are analysed. For each NodeB, its distance and azimuth to the user is calculated, from antenna tables, and the gain is extracted. Finally, with distance, antenna gain and user penetration loss (included in the user table data) the total pathloss is calculated. A user is then considered to be covered if the total pathloss is less than the maximum path loss allowed plus a margin (5 dB) to allow only signalling coverage.

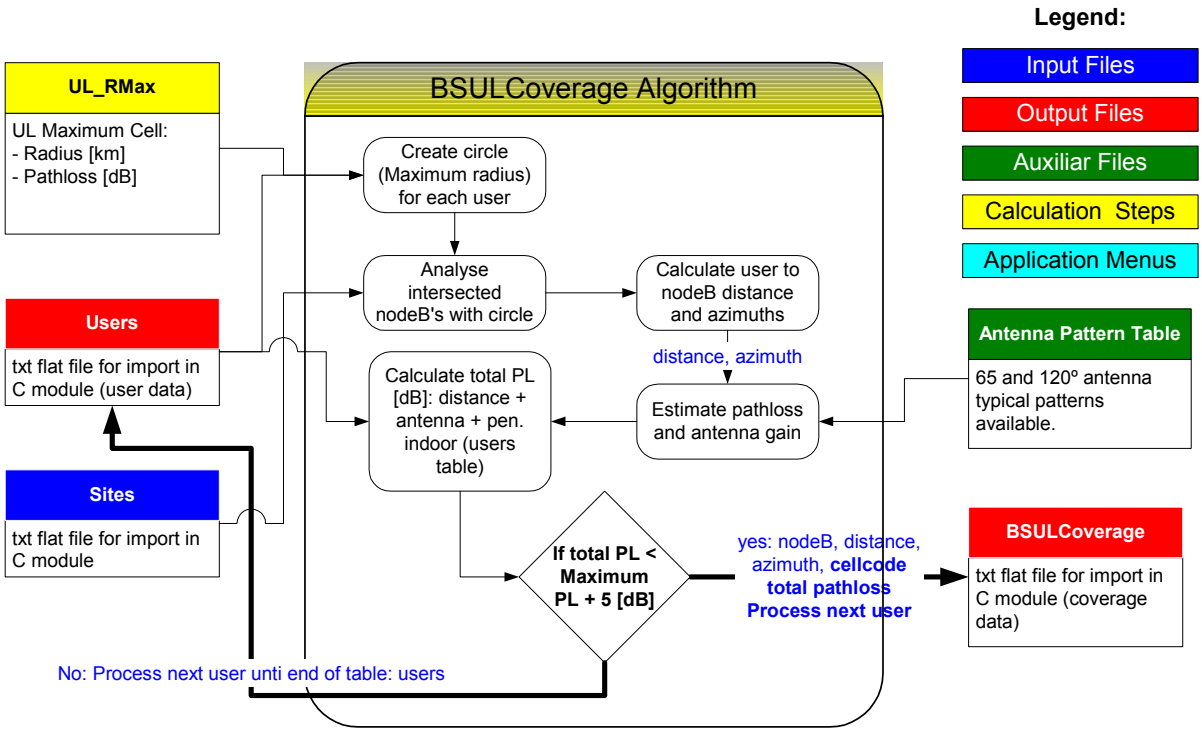

Figure 4.11 – UL coverage analysis method – BSULcoverage file creation process.

The propagation channel user characterisation was also enhanced from previous works. The approach taken here was to assign to each specific clutter, a typical distribution on the channel type (Pedestrian/Vehicular) and on the indoor penetration types (deep indoor, indoor light, indoor window and outdoor). With this approach, a more realistic scenario allows defining different sensitivities (E_b/N_0) depending on channel type and a non-uniform penetration loss distribution. By including vehicular users from the link budget perspective, and although mobility aspects are not modelled, impact on NodeB available power and load is evaluated. The assumed distributions on channel type and indoor penetration values are presented in

Table 4.1 and Table 4.2 respectively. The rational behind the defined values considers that voice users will use the system even if moving, but with lower figures if using CS64 or PS data services. As an extreme, the 384 kbps service was considered only as pedestrian, as defined by 3GPP. In roads, only vehicular users are considered, in opposition to green areas where only pedestrian ones were considered. The indoor penetration loss distribution is more dependent on the clutter type rather than service. As an example, roads considered only in car penetration levels (6 dB), while green areas where considered with an outdoor profile. Residential clutters were defined with higher deep indoor values than the ones including business or mixed usage buildings.

Table 4.1 – Channel type percentage distribution per service and clutter.

(DL) Radio Bearer	Channel	Dense Residential [%]	Light Residential [%]	Mixed B. [%]	Tertiary B. [%]	Industrial B. [%]	Roads [%]	Green Areas [%]
12,2 kbps, CS	Ped/Veh	60,40	60,40	70,30	70,30	70,30	0,100	100,0
64 kbps, CS	Ped/Veh	80,20	80,20	90,10	90,10	90,10	0,100	100,0
64 kbps, PS	Ped/Veh	80,20	80,20	90,10	90,10	90,10	0,100	100,0
128 kbps, PS	Ped/Veh	80,20	80,20	90,10	90,10	90,10	0,100	100,0
384 kbps, PS	Ped/Veh	100,0	100,0	100,0	100,0	100,0	0,100	100,0

Table 4.2 – Indoor penetration level percentage distribution per service and clutter.

(DL) Radio Bearer	Channel	Dense Residential [%]	Light Residential [%]	Mixed B. [%]	Tertiary B. [%]	Industrial B. [%]	Roads	Green Areas [%]
12,2 kbps, CS	DI/I/Out	30,50,20	20,60,20	40,50,10	40,50,10	30,50,20	Incar	0,0,100
64 kbps, CS	DI/I/Out	30,50,20	20,60,20	40,50,10	40,50,10	30,50,20	Incar	0,0,100
64 kbps, PS	DI/I/Out	30,50,20	20,60,20	40,50,10	40,50,10	30,50,20	Incar	0,0,100
128 kbps, PS	DI/I/Out	30,50,20	20,60,20	40,50,10	40,50,10	30,50,20	Incar	0,0,100
384 kbps, PS	DI/I/Out	30,50,20	20,60,20	40,50,10	40,50,10	30,50,20	Incar	0,0,100

User channel and penetration loss assignment impact is presented in Section 4.4, where it is shown the channel and indoor penetration distributions for different scenarios.

4.3 VC++ Engine

4.3.1 VC++ Module Diagram

The VC++ engine calculation flow and file structure is shown in Figure 4.12.

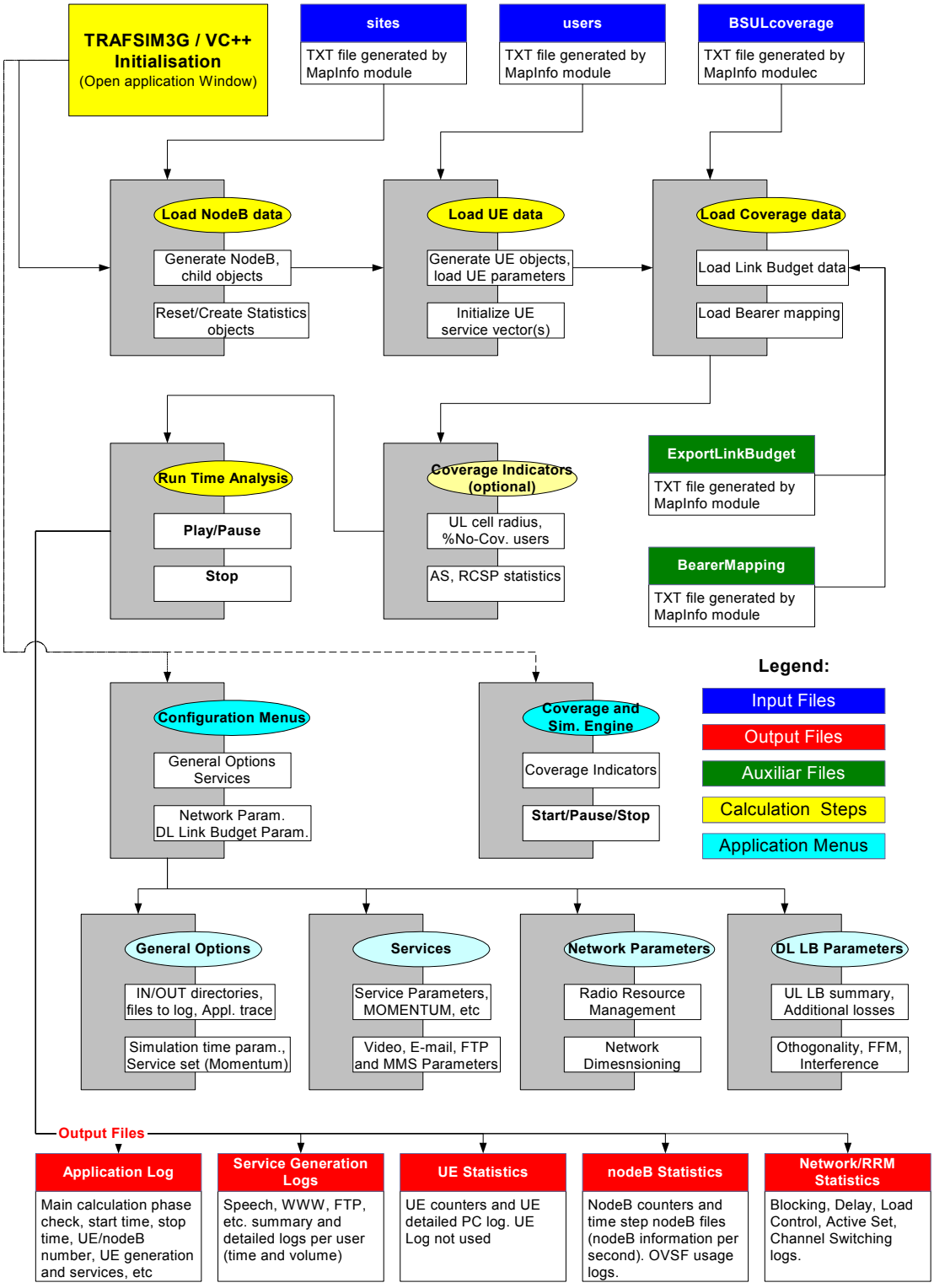

Figure 4.12 – VC++ Engine flow, input/output files and application structure.

The TRAFSIM3G VC++ module is responsible for the time domain analysis of the generated users/services. As it is an executable (.exe) file, it does not require any special software platform, as opposed to the MapInfo® module. In Figure 4.13, a snapshot of the application and main menu is shown (reference and user manual can be found in Annex J).

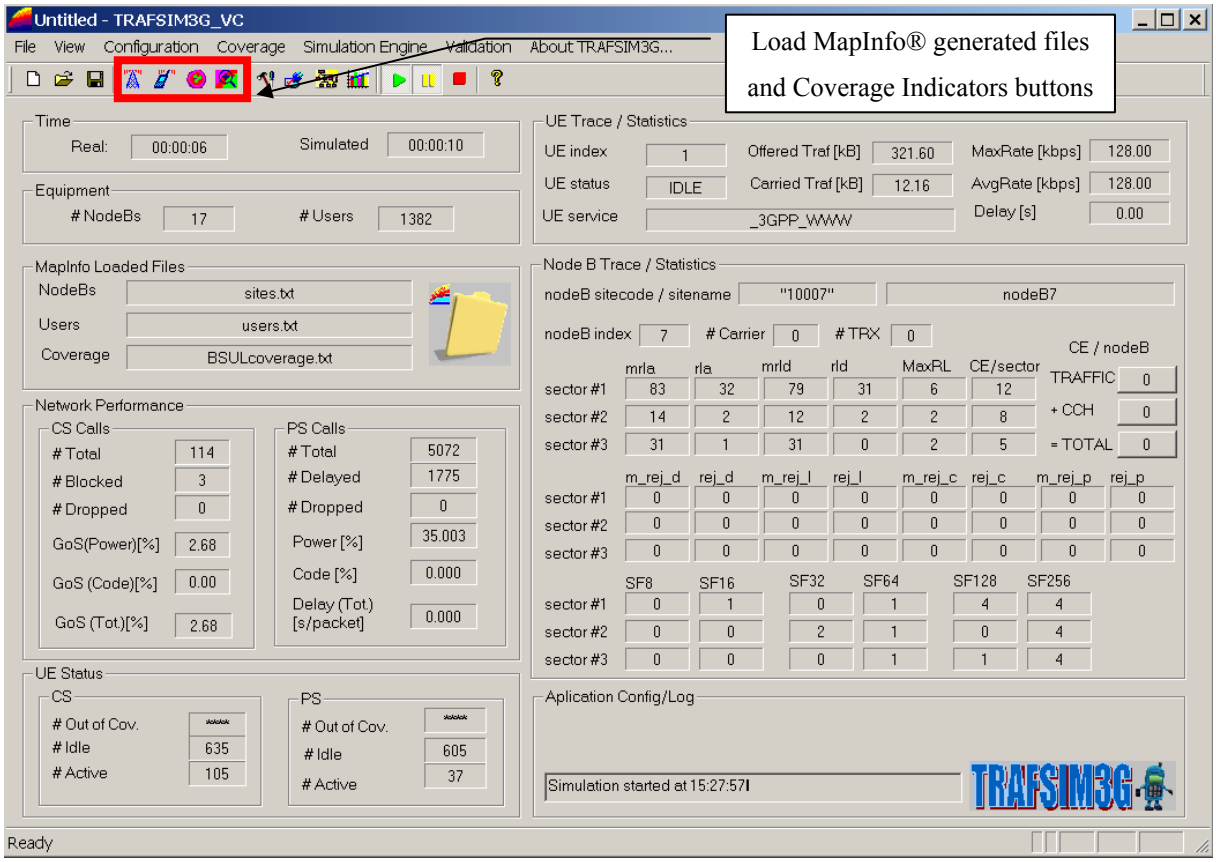

Figure 4.13 – TRAFSIM3G VC++ application (main window).

After running the VC++ module from the MapInfo® one (main application), the tool user shall load all info generated in MapInfo® and saved as flat text files (see Section 4.2.3), easily done by using the window buttons (see Figure 4.13). As shown in VC++ module diagram (Figure 4.12), file loading is sequential and includes the following files:

- sites (site location, NodeB and sectors parameters);
- users (user location, services, propagation channel, penetration loss, etc.) ;
- BSULcoverage (UL coverage data for all users: pathloss, #sites, etc.).

While loading BSULcoverage file, two additional files are loaded including UL link budget parameters (ExportLinkBudget) and radio bearer characteristics for each application /service considered (Bearer Mapping). Optionally, the user can quickly benchmark UL coverage by clicking on Coverage Indicators (see Figure 4.13), which is provided with an information

window (see Figure 4.14) including total number of users, users not covered, UL cell radius (import from MapInfo® files), active set statistics and CPICH RSCP statistics.

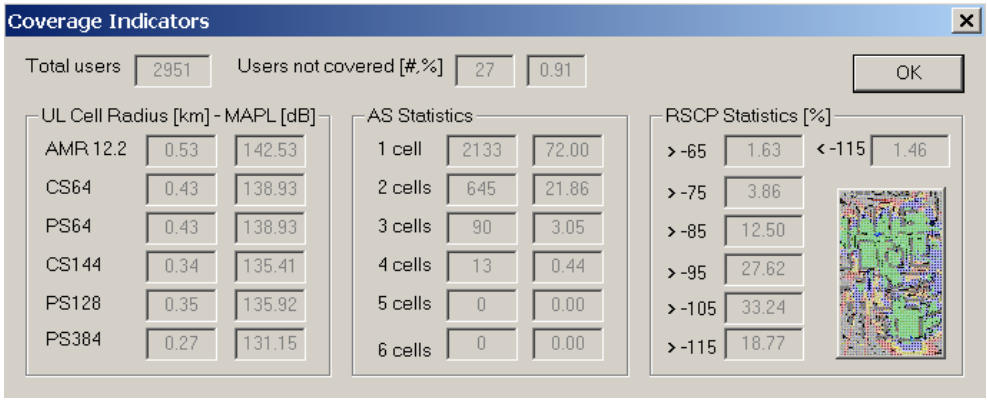

Figure 4.14 – Coverage indicators window – TRAFSIM3G VC++ module.

After loading all files, the tool user can start the time domain analysis by selecting the play button. The simulator will run until the simulation period expires (defined in General Options menu) or the user activates the pause (new click will resume simulator) or stop buttons. At start, the simulator will create a traffic profile for each user depending on its assigned service (the generated traffic profile is saved in a vectored structure containing time and volume distribution at the 10 ms radio frame level). The simulator includes a cycle representing each 10 ms frame where each user (traffic vector) is verified for traffic and according to its service needs; network resources are assigned (e.g., Call Admission Control verifying load, OVSF codes and PA power availability). The simulator algorithm is detailed in Section 4.3.3.

In the end of the simulation period, or at stop button click, a set of output files is generated. The output files type/contents to export are a configurable feature, included in General Options menu (see Annex J for full details). This way, the user can select strictly the files that provide specific information, minimising file storing/handling for bigger files (e.g., NodeB counters can be saved per second for detailed network evaluation). The output files from VC++ module include (detailed in Section 4.3.2):

- Application Log (calculation steps check, start/stop time, etc.);
- Service Generation (traffic parameters, time, volume per user, etc.);
- UE Statistics (UE counters, UE service, data volume, delay, etc.);
- NodeB Statistics (load, OVSF usage, PA power, traffic volume per RB, etc.);
- Network / RRM Statistics (blocking, delay, active set, etc.).

Additional menus are available to control and set the simulator operation:

- Configuration
  - General Options
  - Services
    - UMTS Forum (service parameters for HIMM, MMM, etc.)
    - 3GPP (MOMENTUM service parameters for speech, WWW, etc.)
    - SMS & MMS (service parameters)
    - E-mail, FTP and Video (service parameters)
  - Network Parameters
    - Radio Resource Management (SHO/PC parameters, etc.)
    - Network Dimensioning (Interference estimation method, etc.)
  - Link Budget Parameters (UL summary, orthogonality, interference, etc.)
- Coverage (Coverage Indicators window)
- Simulation Engine (Play, pause and stop actions)

In the services menu, the tool user can configure the traffic source model parameters. The RRM window includes all parameters used by algorithm, such as the active set definition, power control, channel switching, etc.. Network dimensioning allows the tool user to include FFM modelling or interference calculation method (detailed in Section 4.3.3). In Figure 4.15, RRM and fragment of 3GPP service parameters windows are shown.

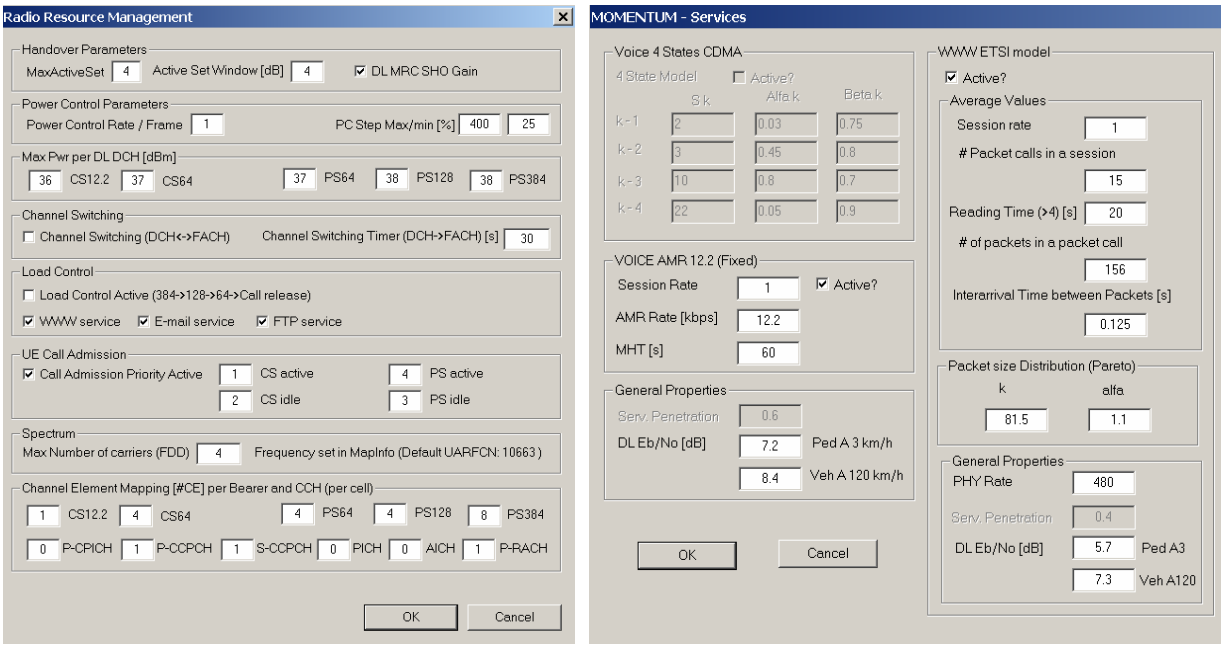

Figure 4.15 – RRM and MOMENTUM services parameters windows.

4.3.2 VC++ Engine Input/Output Data

As explained in Section 4.3.1, the input files of the VC++ module are the output ones from the TRAFSIM3G MapInfo® module, with exception of the fast fading margin file. The fast fading margin was retrieved from CDF values from a previous Ph.D. work on this subject [Card04]. The CDF values for pedestrian and vehicular channels are loaded in a text file for a Rice factor (*K*) of 3 and 6. The application will then run a uniform distribution and fetch from the file the corresponding margin value. The Rice factor to consider in each channel is defined in the link budget window (see Annex J).

The output files in the VC++ module are dependent on their activation in the General Options menu (see Annex J). Log files format and examples are shown in Annex L. A general log with start time, stop time information, success status on UE and NodeB object creation and UE traffic pattern generation is generated in each simulation and was used specially to retrieve simulation times. Its format is presented in Annex L.

Logs per application are intended to save all the traffic-generated patterns, keeping, at minimum, the frame time and number of frames occupied in the air interface by the service in question. The main objective of these files is to check the statistical characteristics of the traffic generation patterns as defined in Section 3.2 as they include, per user the number of sessions, session time, volume, etc., as detailed in Annex L. Traffic generation statistical validation is presented in Section 4.4. The detailed file (used in traffic models derived from 3GPP WWW, e.g., streaming) includes all granular packet level information as presented in Figure 3.2. Application log files examples are shown in Annex L along with the other output files herein described.

For the UEs, three files are available: one with detailed power control information of the trace UE, and two files with UE specific counter's information (see Annex L), one for all data and a second that only records data in the analysis period (60 minutes). As detailed in Section 4.4, for the busy hour simulation, it was needed to extend the simulation period to 70 minutes, because in the first minutes the number of active UEs is much smaller than the target average one. Note that it is desirable to remove the transitory behaviour of the first minutes where UEs are generated up to the BH average.

At the NodeB, also three files are available: one that includes the simulation aggregation counters, another file that saves all NodeB information periodically (period defined in General

Options menu), and a last one that is similar to the previous one, but only saves information within the data analysis period (time filtered). The file structure is the same for the three files (with exception of time column), and it is described in Annex L.

In order to allow a close tracking on NodeB traffic occupation, two files containing OVSF tree occupancy of each sector are available. One contains the allocations, and another the de-allocation, allowing by its subtraction (in time), to identify the number and type of radio links in a specific NodeB. The file structure is the same for the two files, and it is described in Annex L.

At the network performance level, two files record the blocking and PS delay figures. When such an event is triggered, the UE affected, service and additional data is recorded for future processing along with NodeB data. Note that the delay file can be extremely big, since any delay event will trigger a record (default is only to active blocking events logging); the file structure is the same for the two files. It is important to note that this table retrieves in the drop reason column the cause for a blocking event, such as (DL) load over defined threshold (70%), code blocking, insufficient PA power, over DL power allocation (per radio link) or simply by UL link budget limitation (distance). The active set information (per user) is recorded for future processing on SHO impact on performance, which format is detailed in Annex L.

Additionally, two files relating to channel switching feature and load control are available. Although these features were not completely implemented, these files are target to include, traffic patterns modified by channel switching and UE information in case of load control mechanism such as reason and values (similar to blocking/delay information). The development of such RRM mechanisms are proposed for future studies as they influence strongly the blocking and delay system performance figures.

4.3.3 VC++ Engine Main Features

This section details the main algorithms implemented in the VC++ module. The simulator architecture is evolved from the one used in previous works [Serr02], where UEs and NodeBs follow an object-oriented structure with specific functions responsible for the network emulation behaviour. This approach allowed to easily scale the network analysis in terms of node number and more important the functions (algorithms) that rule their relation(s).

In Figure 4.16, the main object (System) that controls the creation of UE and NodeB objects is shown, along with file data loading/export and the simulation engine time frame handling and controls. The UE object has two important child objects: one that includes all traffic data pattern information, and another that records counter/events data (also available for NodeB objects). Besides the counter child object, NodeB creates a BudgetMs object that includes data for each UE using resources in that NodeB. Additionally, a set of objects that gives support to variables and window contents is available from service characterisation (3GPP Services, E-mail_FTP and SMS_MMS_Video), DL link budget (FFM, CovIndicators and LinkBudgetPro) and simulator control data (Config_General, RRM and NetCalc). In this section, a detailed description on the most relevant algorithm is presented.

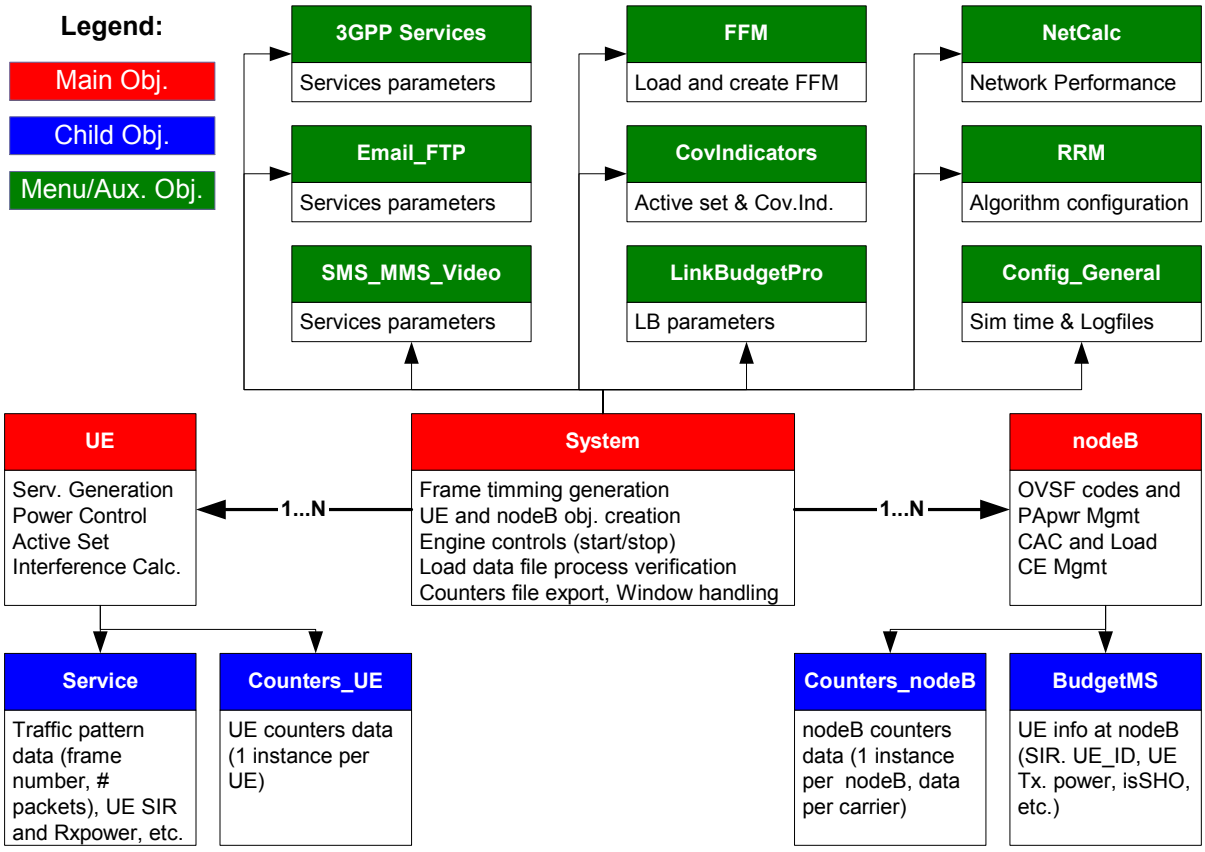

Figure 4.16 – Object structure, relations and main functions.

As mentioned previously, the time stamp used in simulations is the radio frame period (10 ms) that consequently models the traffic generation patterns adequately (e.g., data volumes below a frame capacity are rounded up). Several loops where conceived to cope with the desired simulation time, Figure 4.17. Each second corresponds to a 100 times frame cycle, where each UE and NodeB run a step function that is responsible for the data processing and NodeB resource request (UE-step) and for the DL power control algorithm (NodeB-step).

Step functions in NodeB and UE objects are nuclear to the simulator, and its main routines are detailed in Figure 4.18. DL power control algorithm operates at frame level, as traffic patterns were also with this granularity, and simulations can skip a 15 cycle calculation time for each frame allowing faster simulations time, but loosing some of the "transitory effects" that are a result of time slot power correction. In Section 4.4, the performance with both power control options is addressed.

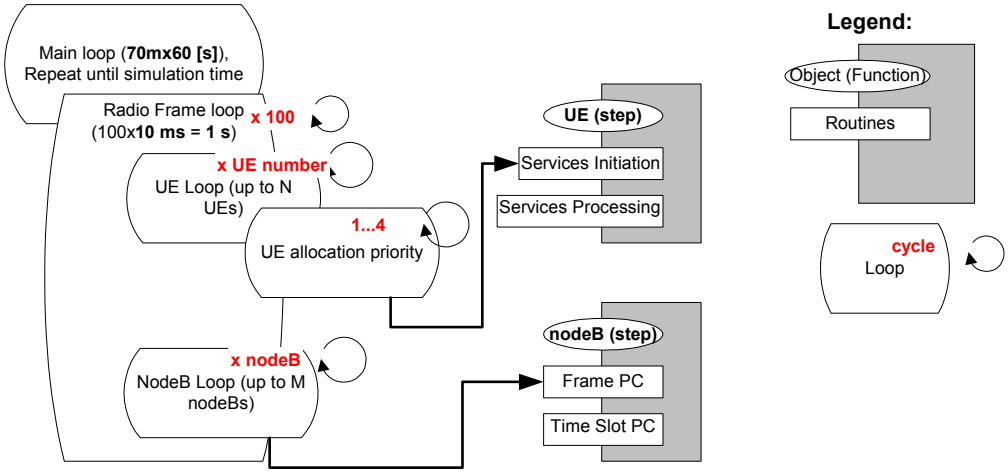

Figure 4.17 – Main time loops and processing functions (step).

Concerning the resource allocation order (in the same frame), a simple approach was taken ensuring that CS calls have higher priority than PS ones, and that on-going calls were prioritised over new calls (configuration in RRM window). This simplistic approach can be improved in future studies, as QoS is just seen at switching levels (CS/PS), while a more realistic approach would be to create different queues for conversational, streaming and interactive/background type services with different priorities in accessing network resources. In Section 4.4, the priority allocation performance along with CAC verification algorithms is shown. In Figure 4.18, the UE step cycle is shown with all its subroutines. In each frame, for every UE, considering its allocation priority and verifying if UL coverage meets the service requirements, it is verified if the UE has any data to transmit by checking the traffic pattern arrays that keep frame number and frame number to transmit information. In case of an initial frame, services are initialised and the traffic pattern arrays created (log files generation); if there is information in the service array, the UE tries to allocate resources in the NodeB.

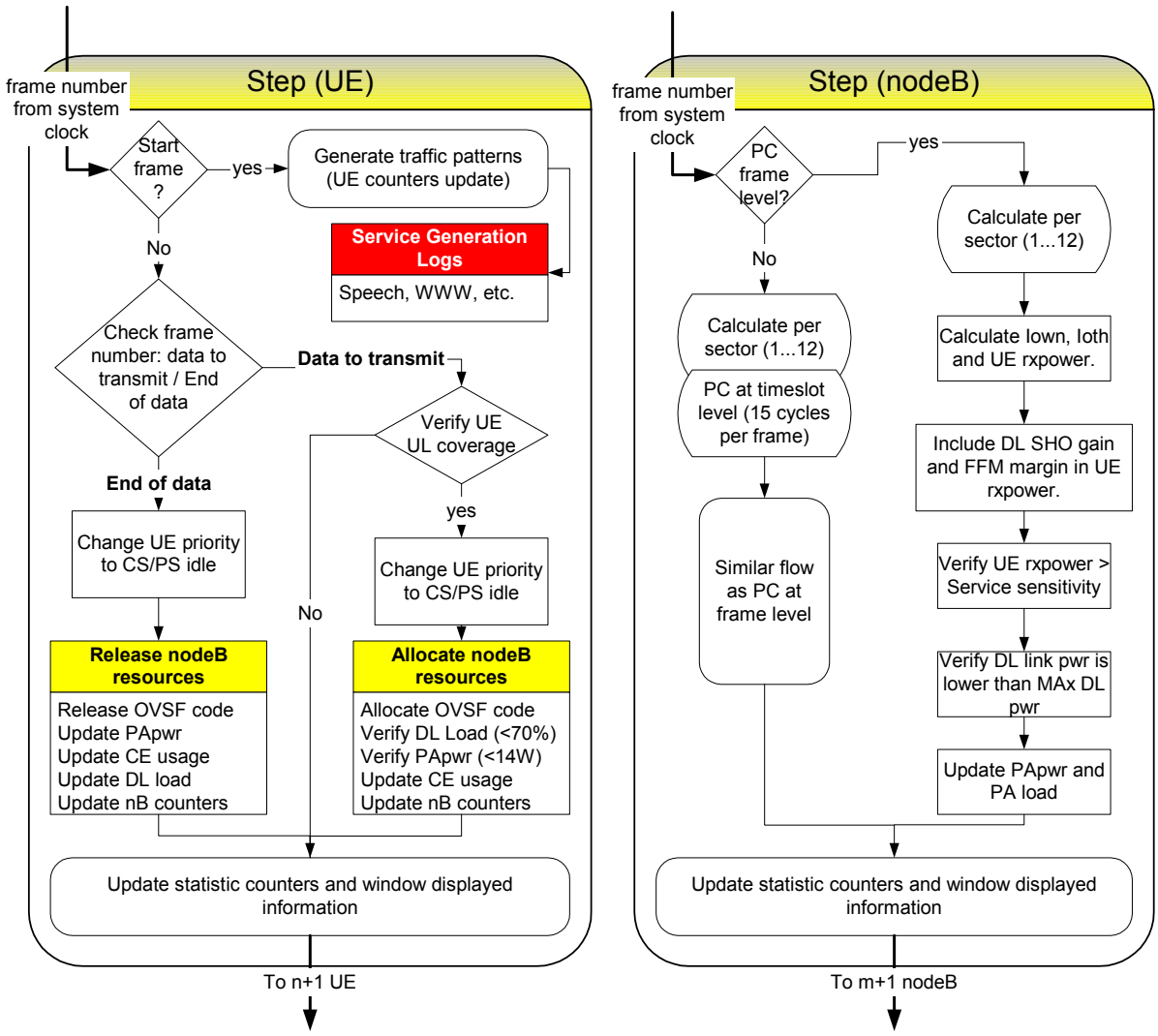

(a) UE (b) NodeB

Figure 4.18 – Details on step function (UE (a) and NodeB (b) objects).

In the step/UE function, allocation of resources in the NodeB is composed of a set of resources: OVSF codes, verification of total DL load below design value and available PA power. OVSF codes are allocated following a typical left to right algorithm (the tree is searched from left to right and allocated the first valid SF code). This approach, although not optimal, is similar to most vendor solutions due to simple implementation. Note that common channels were also included in the tree code usage (SF 256 and SF64 for S-CCPCH).

The DL Load CAC algorithm is based on (2.4), targeting to a maximum of 70%. The maximum DL load definition was taken considering the noise rise linearity up to this value and typical design figures from UMTS vendors. If one takes the noise margin curve and defines a linear trend, one obtains figures for the correlation in the order of 98.7, 97.9 and 95.8 % for 60, 70 and 80 % load, respectively.

For the PA power availability, a total common channel overhead of 6 W was considered, hence, 14 W are available for traffic. Each time a user asks for resources, the total PA power is calculated as per (2.5) and its limit verified.

Since it is also objective of this simulator to estimate the base band processing needs for the NodeBs, one has decided to use the channel element (CE) approach, where 1 unit is required for a speech call. For higher RBs, more CEs are required to process the user data, as defined in the RRM window (e.g., a 384 kbps RB requires 8 CEs). Most vendors follow this approach, as base band hardware is scalable like carriers or transceivers and must be dimensioned for the required QoS. Within this approach, common channels also required channel elements to process its information being it user data or only signalling.

Finally, and after allocation status, all counters from UEs and NodeBs are updated. For the release of resources, the process is opposite to this one, by releasing the used resources for main and SHO links.

As previously described, the allocation cycle is triggered by the UE object as it keeps the data traffic pattern arrays. The DL power control is then verified in the NodeB cycle (see Figure 4.18). The DL PC cycle starts by verifying if it is selected the frame or time slot approach, although with similar control mechanisms. A loop per all the active NodeB sectors (defined by 3 times the number of frequencies required) is started, and initially interference (own and other cell) is calculated and UE receive power estimated. Next, maximum ratio combining (SHO DL) gain and FFM are added to the UE received power (function of the channel type). After verifying the obtained value with service sensitivity, the PA power needed is estimated and check if maximum DL link power (set in RRM window per RB) is not reached.

The next section shows some tests and validation runs to validate the call admission routine here defined, with emphasis on DL load, allocation priority, PA power and maximum DL link power limit tests.

4.4 Parameter Analysis and Simulator Assessment

4.4.1 Users Generation – Penetration and Services

From the GIS module, several penetration values were run for a reference scenario (detailed in Section 5.2). The objective in this section is to show the module behaviour for several population penetration values, the service distribution mix, and the UE characterisation outputs. Two main geographical scenarios are studied in this thesis: a high traffic, high NodeB density in Lisbon CBD districts (HD) and a low traffic, low NodeB density (LD) in Olivais (a Lisbon residential area). These scenarios are detailed in Section 5.1, but mentioned here for parameter assessment purposes. From the total population present in each scenario, a traffic mix for 1, 2 and 3 % was generated and compared with expected theoretical values, Table 4.3.

Table 4.3 – Generated vs. Theoretical population.

Scenario - Total Pop. [inh]	HD – 156336			LD - 71623		
Penetration [%]	1	2	3	1	2	3
Theo. Pop. value [inh.]	1563	3127	4690	716	1432	2149
Generated Pop. [inh.]	1382	2951	4456	640	1337	2045
Deviation [%]	11.60	5.62	4.99	10.64	6.66	4.83
Real Penetration [%]	0.88	1.89	2.85	0.89	1.87	2.86

The deviation in generated population is due to the clutter non-uniform distribution in the analysed districts, with more critical for low penetration values (due to higher impact of numerical round), but intrinsic in the user generation process. This thesis mainly focus on 1 % (target) penetration, as it leads to network (CS) blocking values of 1 % as detailed in Section 4.4.5. As defined in Table 4.1, depending on the clutter the user is generated, a certain channel type and indoor penetration loss distribution is applied. For the LD scenario (0.5, 1, 1.5 and 2 %), the user channel and indoor penetration distributions (based on clutter distribution) were verified, and compared with theoretical estimates, showing a deviation below 1%, Table 4.4 and Table 4.5.

Similarly, and regarding the indoor penetration distribution (Table 4.2), the incar and indoor light penetration levels for the LD scenario were analysed in detail, again showing a deviation below 1%.

Table 4.4 – Channel type distribution validation.

Channel type / Penetration	0.5 %	1 %	1.5 %	2 %
Pedestrian [%]	84.46	84.69	84.66	83.40
Vehicular [%]	15.54	15.31	15.34	16.60
Pedestrian (Theoretical) [%]	83.99	84.13	84.26	83.80
Deviation [%]	**0.56**	**0.67**	**0.48**	**0.48**

Table 4.5 – Indoor penetration loss distribution validation.

Penetration Indoor Types / Penetration	0.5 %	1 %	1.5 %	2 %
Outdoor [%]	1.35	0.63	1.01	1.20
Indoor Light [%]	50.34	50.31	50.25	49.89
Deep Indoor [%]	32.77	33.75	33.40	32.31
Incar [%]	15.54	15.31	15.34	16.60
Incar deviation [%]	**0.00**	**0.00**	**0.00**	**0.00**
Indoor Light deviation [%]	**0.34**	**0.31**	**0.25**	**-0.11**

Far more important, is the validation of the service mix generation that is presented for speech, video and FTP in detail. RB and service type distributions were compared against theoretical expected ones for the HD scenario (1 % population penetration, averaged over 3 generations), and summarised in Table 4.6. All functions regarding user generation/characterisation and service mix definition are within the design expectations. Table 4.6 also presents the RB generation validation, as speech and video-telephony are the only applications to be mapped onto CS64 and CS12.2, respectively. For the PS 384 RB (includes FTP and video streaming applications), the average total percentage was 4.73 % compared with estimated 4.51 % value. Absolute deviation values are below 1 %, with exception of low penetration services, such as FTP or E-mail, where real distribution figures are slightly above theoretical estimates.

Table 4.6 – Service and RB distribution validation.

Service (Momentum)	RB	Distribution [%]	Theoretical [%]	Absolute Deviation [%]
Voice	CS 12.2	59.58	60.11	0.53
Video-telephony	CS 64	6.22	5.86	-0.36
FTP	PS 384	2.70	1.61	-1.10

4.4.2 Users Geographical Distribution and Link Budget Assessment

For the system performance analysis, it is important to quantify the geographical scenarios generation regarding user's distance and pathloss distributions. This objective is of key importance, as it allowed minimising the number of simulations, by verifying the strong correlation of the user distributions (distance and pathloss) for the same penetration value. One should note that pathloss invariance is of high importance, due to strong impact on PA power availability and interference issues. For the HD – 1 % scenario, 5 users generation were calculated and for each run the pathloss and distance cumulative (CDF) and density probability functions (PDF) were evaluated. In Figure 4.19, the pathloss and distance CDFs and PDFs for the first users generation are is shown. In Figure 4.19, it is interesting to note that the more continuous shape of the voice distribution is due to the higher number of speech service users, compared with any other service (around 60%), for example FTP, where user distribution shows a spike type distribution.

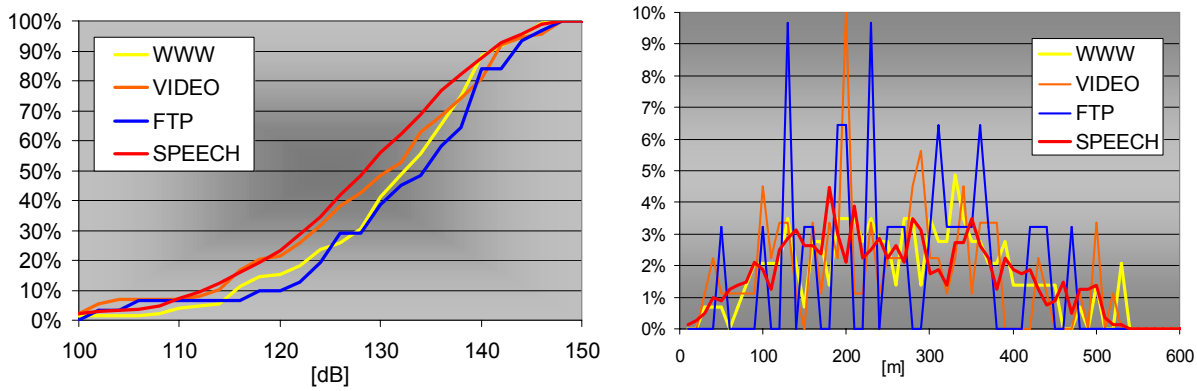

(a) Pathloss CDF (b) Distance PDF

Figure 4.19 – Pathloss CDF and distance PDF for HD-1%.

Taking the first simulation as reference, the average and standard deviation of distance and pathloss were compared for the remaining five ones. As shown in Figure 4.20 for the speech service, very similar distributions were generated for the 5 simulations. In Figure 4.21, the average pathloss variation for all the services in the 5 simulations is shown, revealing low variation for speech, and relevant variation for FTP service.

Afterwards, this analysis was extended to all services, by using the correlation of the CDFs as a main indicator for resemblance (first simulation taken as reference). Results show that correlation is higher than 98 % for pathloss and 98.5 % for distance. As previously

mentioned, worst correlation figures are obtained for low penetration services, such as e-mail and FTP. In Figure 4.22, pathloss and distance correlation values for the CDFs are shown.

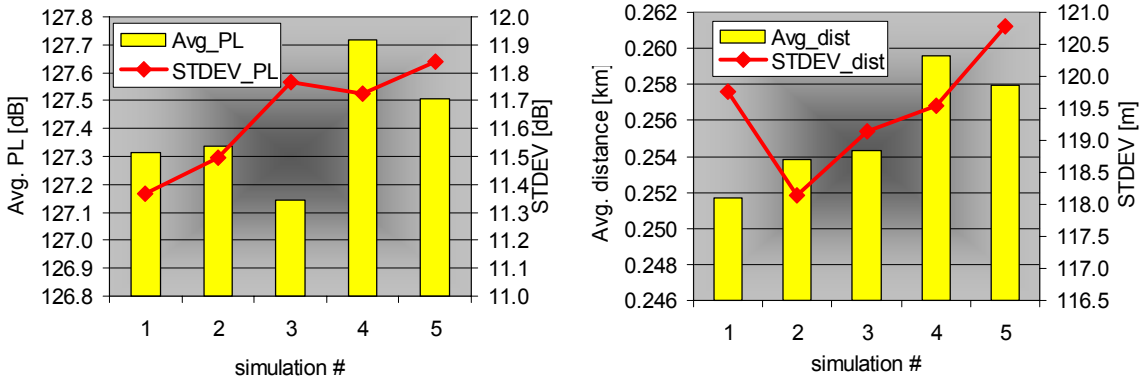

(a) Pathloss distribution (b) Distance distribution

Figure 4.20 – Speech pathloss and distance average/standard deviation (5 simulations).

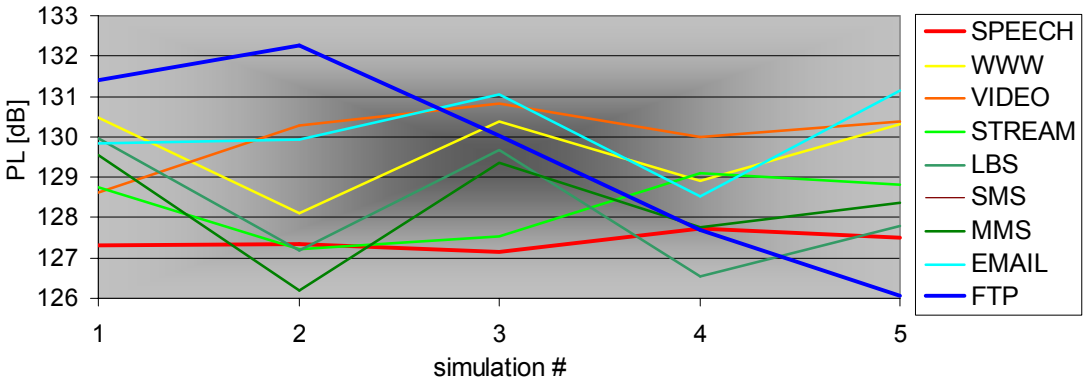

Figure 4.21 – Average pathloss (5 simulations – all services).

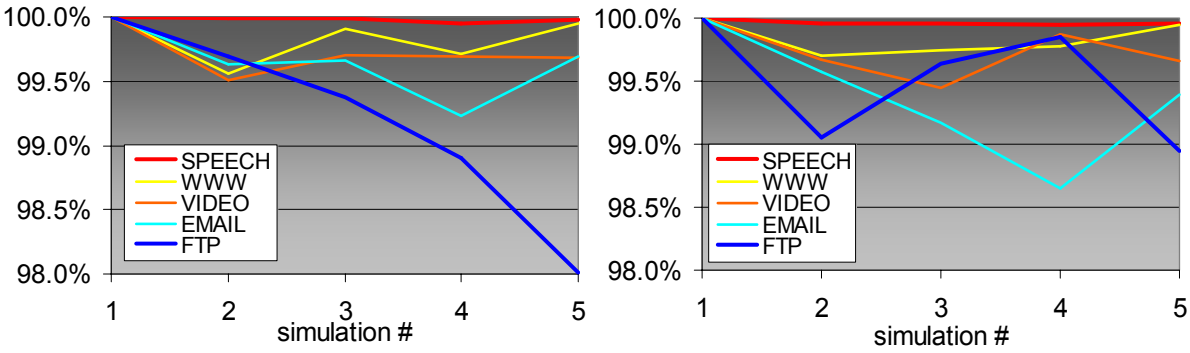

(a) Correlation (PL CDF) (b) Correlation (Dist. CDF)

Figure 4.22 – Correlation variation for pathloss and distance CDFs.

Besides the geographical tests, some analysis on UL coverage was performed, especially to assess TMA advantages in both HD and LD scenarios. It is important to note that site density in the LD scenario is lower than in the HD one, leading to a higher non-covered user's

percentage. In order to illustrate the TMA insertion impact, the user coverage percentage for both scenarios with and without TMA is shown in Table 4.7. One should note that this is just an UL coverage analysis, as system performance involving TMA is detailed in Chapter 0. It is interesting to note that for coverage reasons, the gain of TMA insertion in the HD scenario is residual, while in the LD one it allows to reduce the non-covered user's percentage in approximately 15 %. Regarding the maximum allowable pathloss (UL services: speech/CS64/PS64), it is expected that the 3.5 dB link gain is enough to neglect the effect of cable losses. Nevertheless, an insertion loss of approximately 0.7 dB is included to accommodate the TMA impact. Generally, the TMA insertion allows targeting CS64 service coverage, while with no TMA only speech service is possible, Table 4.7.

Table 4.7 – Coverage indicators summary for LD/HD and LD/HD with TMA scenarios.

Scenario	LD	LD_TMA	HD	HD_TMA
Population	1337	1337	1382	1382
Non-covered	332	131	11	2
Non-covered [%]	**24.83**	**9.8**	**0.8**	**0.14**
Maximum Pathloss – speech [dB]	142.5	146.0	142.5	146.0
Maximum Pathloss - CS64 [dB]	138.9	142.4	138.9	142.4
UL cell radius – speech [km]	0.53	0.65	0.53	0.65
UL cell radius - CS64 [km]	0.43	0.53	0.43	0.53

The TMA has also impact in the active set distribution, as the percentage of UEs with higher number of links will increase, increasing also the percentage of UEs in SHO. In Figure 4.23 the AS distribution, SHO percentage and RSCP statistics is shown for the 4 scenarios.

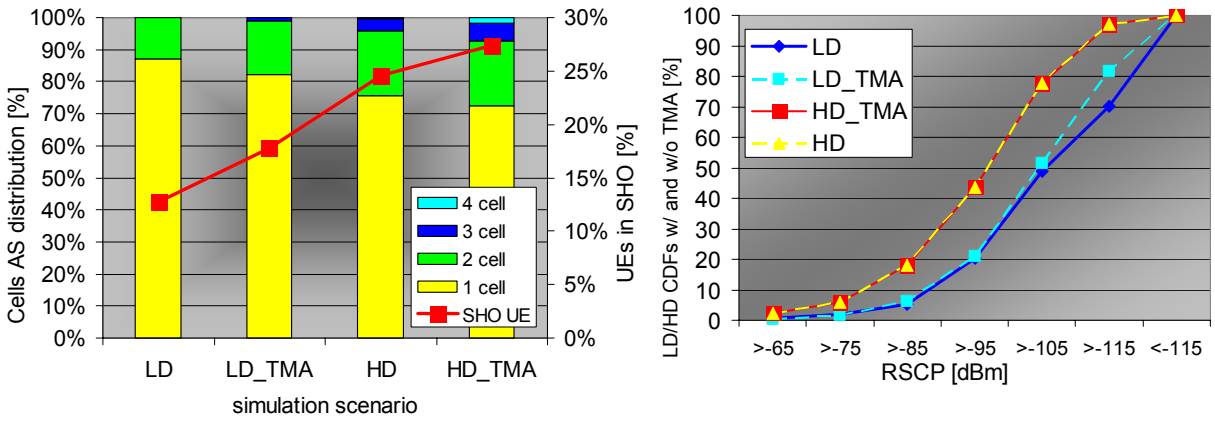

(a) Active set dist. and UE in SHO (b) RSCP CDFs for LH/HD

Figure 4.23 – Active set distribution and UE SHO percentage and RSCP CDFs.

One should note that this last indicator is just to shown similarity in terms of the simulations with and without TMA, as (DL) CPICH RSCP is not changed with TMA insertion (besides negligible TMA insertion loss). From the RSCP CDFs, the higher average pathloss for LD scenarios is also evident, by the right-shift on the curves. From the active set analysis, the increase of UEs with 3 and 4 links is clear, as the SHO percentage one: 39.5 % for LD and 11.7 % for HD.

In order to better illustrate the NodeB theoretical coverage with and without TMA, in Figure 4.24 it is plot the theoretical UL CS64 coverage for both scenarios with (green shading) and without TMA (red shading). The high area coverage percentage for the HD scenario is evident, while for the LD one non-covered areas can still be spot with relevant user density.

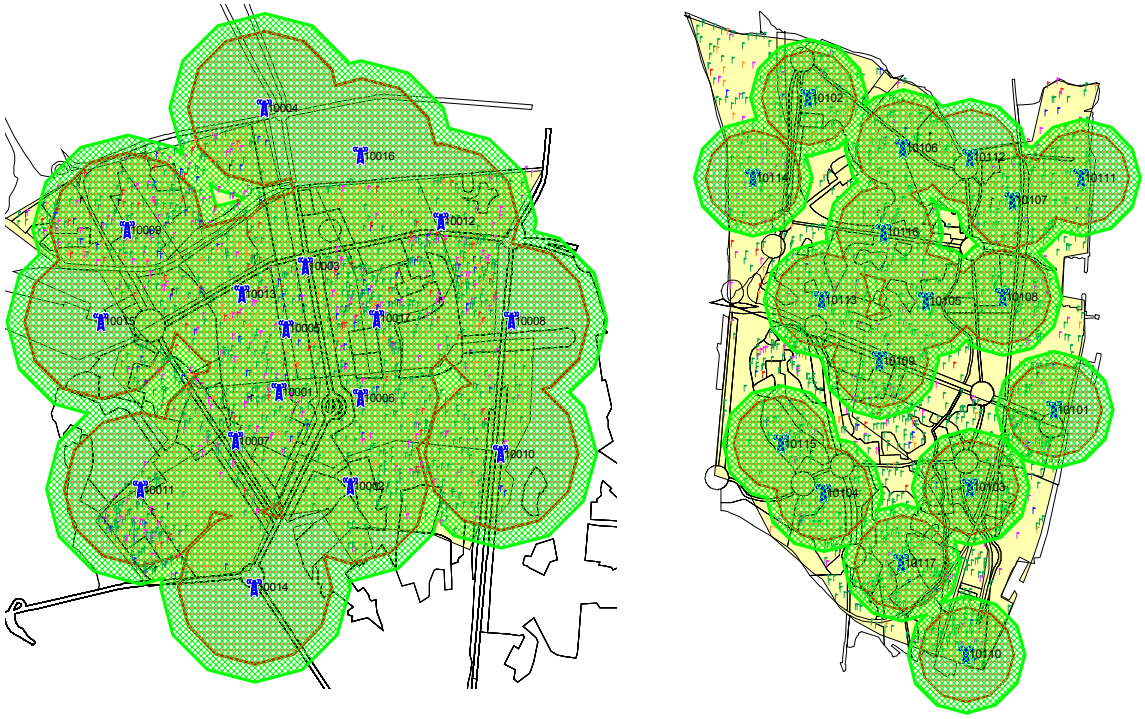

(a) HD scenario (b) LD scenario

Figure 4.24 – HD/LD CS64 UL coverage with and without TMA.

Another important aspect of the link budget implementation is the validation of the FFM distributions. By default, MapInfo® UL coverage analysis (pathloss) includes a fixed FFM as a function of the channel type (pedestrian/vehicular). It is an objective of this thesis to assess its impact on PA power availability and system performance. This way, the tool user can trigger, per frame, a generation of a FFM value that follows a Ricean type distribution with K factors of 3 or 6 dB, representing the ratio of the dominant component over the disperse ones.

As typical study scenarios are urban, the worst case FFM was selected, corresponding to the lowest K value.

In Figure 4.25, the theoretical and generated FFM distribution is shown, for a Pedestrian A 3 km/h scenario and K factor equal to 3 dB (typical urban propagation conditions where line of sight/direct components are the double of the disperse/non-line of sight ones). Impact of FFM in power control is detailed in Section 4.4.4.

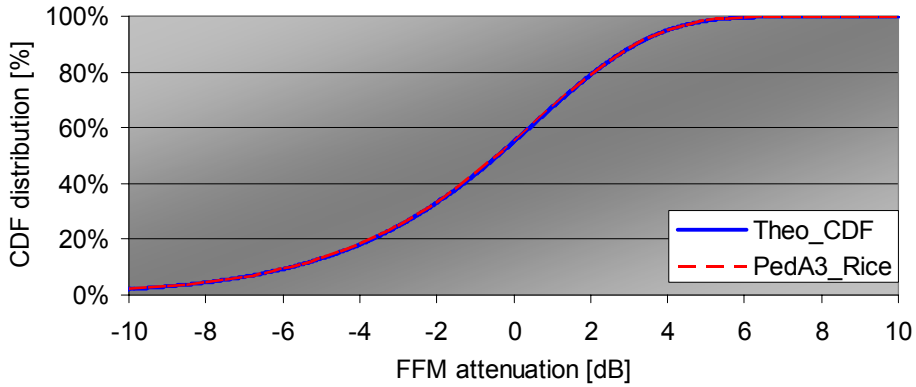

Figure 4.25 – FFM CDF (Rice, K=3) for Pedestrian A 3 km/h type channels.

4.4.3 Traffic Source Models Statistical Validity

This section focus on the verification of the characteristics of the developed statistical distribution functions defined in Section 3.2. The validation is mainly based on the correlation calculation of obtained CDF curves against theoretical ones (Excel CORREL(array1,array2) function is used). The information here processed can be extracted from the service generation logs available in the VC++ module, as detailed in Section 4.3.2. All detailed CDF verifications are shown in Annex F. The distributions here shown use the default parameters defined in Section 3.2.

For the uniform, Poisson and exponential distributions, one tested the generation of 20 000 speech users and analysed the respective CDFs by correlation figures with the theoretical CDFs above 99.99%. For the WWW type services [ETSI98b], the set of distributions were validated: session arrival is characterised by a Poisson process, packet size is a Pareto distribution, while other model parameters (number of packet call in session, reading time, etc.) are geometrically distributed. Similarly to speech, 5 000 WWW users were generated, and the generated traffic analysed. The CDF correlation for each of the tested distributions is

summarised in Table 4.8. With exception of the Pareto distribution (99.96 %), all the other CDFs correlation was above 99.99 %.

For the WWW service, random generation regarding the input parameter variation was also tested, namely the number of sessions (Poisson), this is shown for 1 and 10 sessions in Figure 4.26. For the WWW type services, the reading time is an interval between 4 and 12 s. As mentioned in Section 3.2.2, reading time was implemented recurring to a uniform distribution between 4 and 12 s. In Figure 4.26, validation of the obtained CDF is shown, comprised between the 4 and 12 s geometric distribution CDFs.

Table 4.8 – CDF correlation values for used distribution in traffic pattern generations.

Distribution Type	CDF Correlation [%]	Application example	Test application
Uniform	**99.9976**	Speech - start time	Speech
Exponential	**99.9990**	Speech - call duration	Speech
Geometric	**99.9957**	WWW - Number of packet in packet call	WWW
Lognormal	**99.9967**	E-mail, FTP - Data volume	FTP
Pareto	**99.9638**	WWW - Packet size	WWW
Poisson	**99.9998**	Speech - call generation	Speech
Weibull	**99.9961**	Speech - CDMA model	Not used

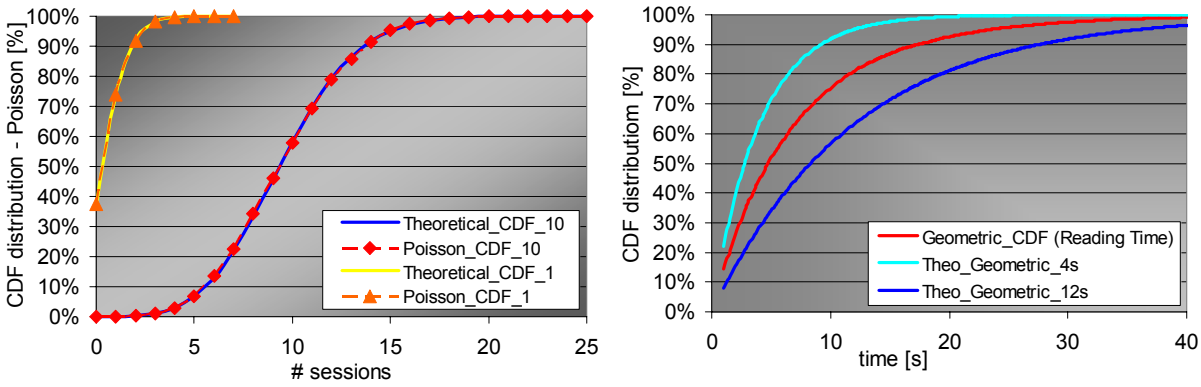

(a) Poisson CDFs validation (1 and 10 sessions) (b) Geometric CDF – Reading time (WWW)

Figure 4.26 – Poisson distribution and Geometric distribution for 4 and 12 s.

From the analysis of the CDF graphs (Annex F), one can conclude that for such a set of data, the CDFs present an acceptable approximation to the respective theoretical curves. The obtained values for correlation are acceptable to assume the liability of the above distributions for the intended simulation purposes, which encompass the generation of a number of samples of each statistical distribution in the order of 10^4.

4.4.4 RRM, blocking and delay

This section intends to demonstrate the good functioning of the implemented RRM algorithms, such as power control, handover, channel switching, call admission, and baseband capacity estimation. Associated with call admission algorithms, the respective blocking and delay calculation validations are also shown.

Handover was modelled in two main aspects: the number of radio links a UE/NodeB can simultaneously handle, and the impact on DL link budget as MRC gain is present. It being a static simulator, the active set is implemented by defining a SHO window value over the best server defined as the cell providing the higher CPICH RSCP. One should note that, ideally, the rank should have been done on E_c/N_0 figures rather than RSCP, but that would lead to a substantial increase on the calculation time, due to the need of estimating for each UE the transmitting power of each NodeB. Future work should expand its studies on identifying the impact of a more precise inter NodeB interference estimation (along a E_c/N_0 calculation) as in this thesis only taken its average value is taken (see (2.5)).

For the HD scenario (acceptable UL coverage without TMA), the impact in SHO statistics of the AS size was evaluated, as well as the SHO window, with the objective of defining the standard parameterisation for the simulations. By setting the AS size to maximum (6), and by varying the window from 2 to 6 dB, it can be concluded that and ideal 4 dB window targets to approximately 25 % UEs in SHO as proposed in [HoTo01], with mainly 4 links per UE (target AS size). Results are summarised in Figure 4.27.

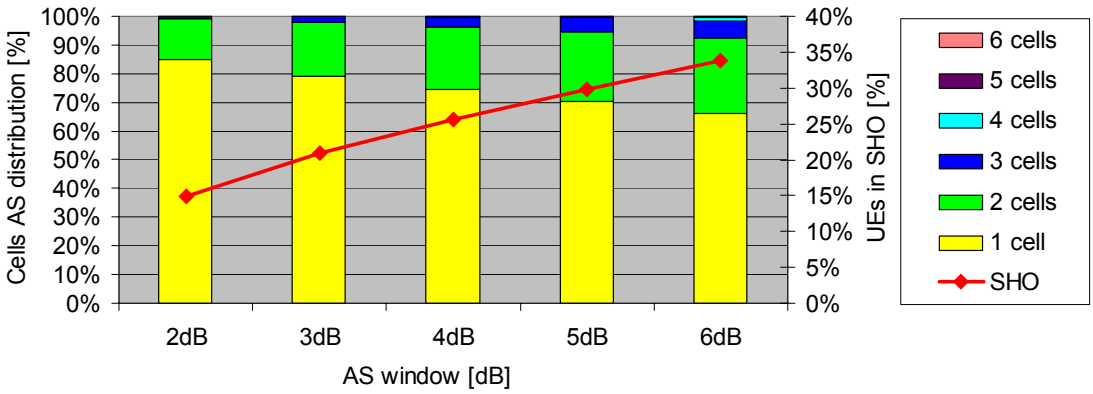

Figure 4.27 – Active set size and distribution in function of AS window.

Regarding the DL SHO gain modelling, a simple approach is considered, where a fixed value is assigned as a function of number of radio links. From typical MRC gain figures, values of 1, 1.5 and 2 dB gains were assumed for 2, 3 and more than 4 links, respectively.

DL power control was implemented to model two aspects: the inner loop corrections due to DL load increase and FFM (if random FFM option is enabled), and maximum DL link powers. Inner loop can be configured to be calculated either at each time-slot or at frame level; as mentioned in Section 4.2.4, frame level calculation allows a much faster simulation times. The maximum DL link power is implemented to avoid that single high pathloss users may be consuming all available PA power. Based on DL link budget, and assuming a DL load margin (similarly to UL), maximum link power can be estimated. Values used in simulation range from 36 to 38 dBm for CS 12.2 and PS 384 bearers, respectively, Table 4.9. Note that for PS128/384 maximum power is around 6 W, compared with the 14 W available traffic power.

Table 4.9 – Maximum DL link power.

DL Radio Bearer	CS12.2	CS64/PS64	PS128	PS384
Maximum Link Power [dBm]	36	37	38	38

The inner loop power control algorithm at time slot level was implemented following the approach described in [Serr02], where relative steps were applied (power up/down maximum variation is 400 % of current value and minimum value is 25 %). In order to assess algorithm performance, and including the FFM distribution modelling as defined in Section 4.4.2, one shows in Figure 4.28 a UE received power variation with two links, main and SHO during one frame (10 ms).

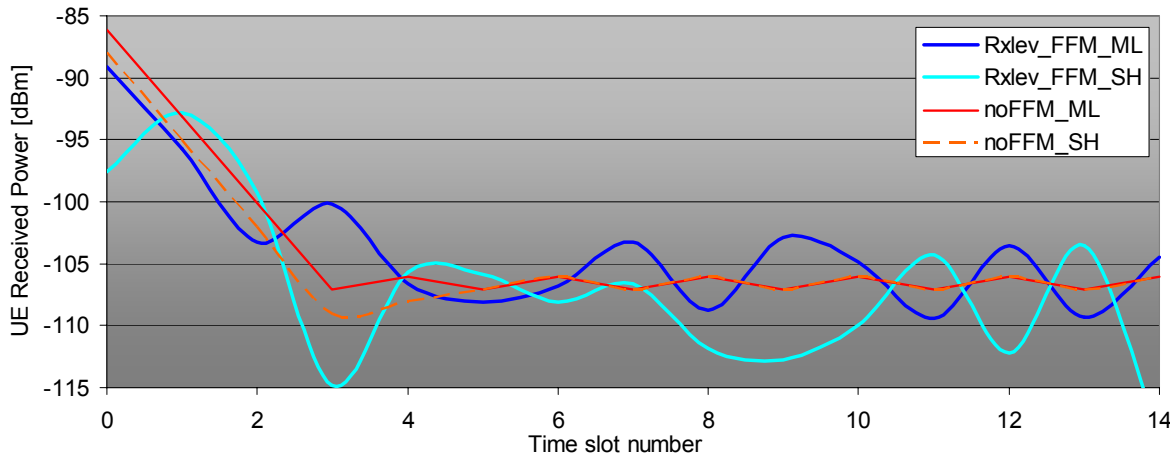

Figure 4.28 – Inner loop PC at time slot level with FFM effect.

It is worth to note the fast convergence of the inner loop PC algorithm, where after 4 time-slots the end frame level is achieved. Due to lower pathloss, the main link converge is faster

than SHO links. The FFM effect is clear in main (ML) and SHO links (SH), where UE received power convergence is never reached as FFM value is changing per time-slot.

In order to demonstrate the CAC algorithm, a 2-service scenario with 50 speech and 50 MMS users was set. The traffic pattern was modified for all UEs to start transmitting exactly at the same time, with speech call duration of 10 s and MMS size of 30 kB (375 frames – 3.75 s). All UEs were in the same location, meaning the same pathloss (135 dB) and only one link in the active set.

As expected, speech UEs were the ones to be first allocate NodeB resources, while MMS UEs needed to delay its transmission (CS call priority). Another important aspect is that only 39 speech UEs were accepted; this value is in accordance with the CAC load equation, where the 40^{th} UE would lead to an expected DL load of 70.1 %, value already above the defined dimensioning target (defined in the VC++ module LinkBudgetPro window).

Similarly, for PS64 (MMS), the maximum number of simultaneous users in the cell are 9 in the condition above. The CAC load control for speech can be verified in the number of SF128/SF32 codes allocated, Figure 4.29. From the DL load curves, a slight increase is noticed for the MMS users in instant 20 s. As only 9 MMS users can transmit simultaneously, the remaining ones will be delayed until CAC allows its transmission. As each MMS user will take 3.75 s to transmit, until instant 38.75 s the load will remain at its maximum, after which only 5 (MMS) UEs will transmit and DL load and PA power usage will drop. NodeB resources will then be release at instant 42.5 s (Figure 4.29). The 14 W available traffic power is enough to cope with the 135 dB pathloss, leading to a PA power load (ratio between allocate power and total PA power – maximum is also 70 % as 6/20 W are used to common channels).

Additionally, the same scenario was tested with a 140 dB pathloss. As expected, the maximum cell capacity is now limited by the PA power availability, reaching only a maximum of 34/7 users for speech and MMS services, respectively. The DL load reaches approximately 60 % while PA power load is near the 70 % limit, Figure 4.30.

The CS blocking is displayed correctly: 11/50 = 22 % for the first scenario, and 32 % for the second one. The average delay figures increased from 18.65 to 21.85 s as less simultaneous PS 64 calls are allowed.

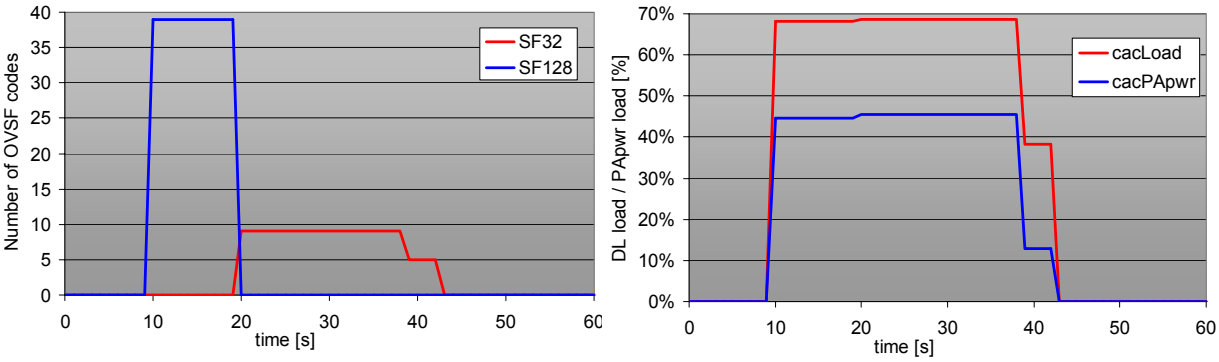

(a) OVSF code allocation per SF (b) DL Load and PA power load

Figure 4.29 - CAC algorithm – OVSF code usage and DL/PA power load for PL =135 dB.

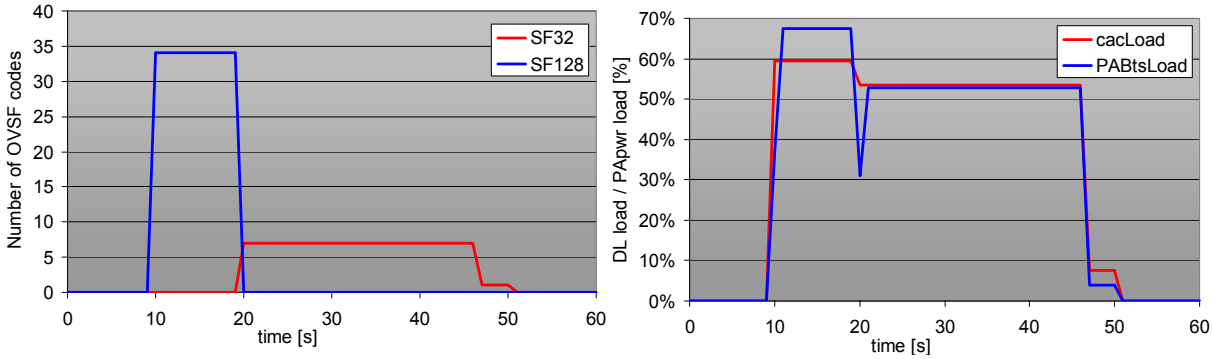

(a) OVSF code allocation per SF (b) DL Load and PA power load

Figure 4.30 - CAC algorithm – OVSF code usage and DL/PA power load for PL=140 dB.

Total baseband capacity is obtained by analysing the maximum simultaneous RBs, and consequently the maximum simultaneous CEs required to process the carried traffic. CEs are NodeB-pooled resources, hence, they are evaluated per NodeB rather than per cell. A CE overhead is required to process common channels information detailed in RRM window inputs. For the first scenario, a maximum 42 CEs is required as only 1 sector carried 39 voice calls plus 3 CEs for common channels.

TRAFSIM3G emulates the air interface capacity from the frame/packet perspective, allowing any UE to use NodeB resources if connected UEs (with on-going sessions) have no data to transmit. In reality, in early R99 implementations, most of the PS bearers are dedicated channels (DCHs), meaning that the NodeB resource will be kept reserved, even if there is no data to transmit. Nevertheless, if after a certain time the UE does not transmit/receive any data, or presents a very low data volume/rate, it is removed from the DCH RRC state and moved to the FACH state, where it assigned a SF64/32 code shared by all UEs in that state; this process is called channel switching. All the simulations were performed assuming

optimal DCH/FACH transitions, which is similar to a shared channel perspective. Nevertheless the tool user is able to define a timer in which the UE is still keeping the NodeB resources even if there is no data to transmit. After that timer expires, NodeB resources are released.

Other RRM important feature that is proposed for further studies is the load control concept. For interactive/background PS bearers, it is desirable to reduce PS rates in case of congestion or high DL/PA load. This feature can then be triggered at new call admission, readjusting the resource of on-going I/B PS calls, or in cell congestion/blocking. In the simulation, the PS RB reduction impacts in two main aspects: higher number of frames (lower rate), and lower UE received power as lower E_b/N_0 are required, Figure 4.31.

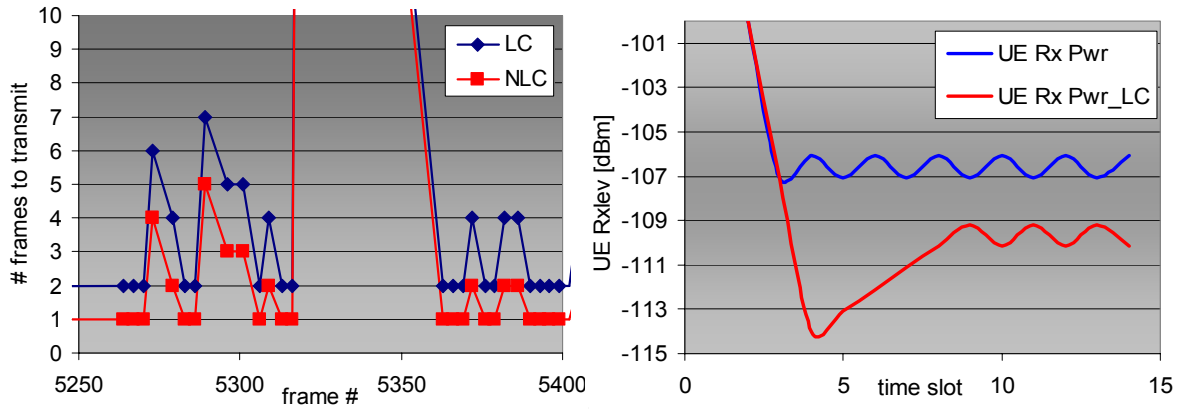

(a) # frames (b) UE Rxlevel

Figure 4.31 – Load control feature impact in frames to transmit and UE Rxlevel.

4.4.5 Number of Simulations and Results Convergence

The analysis of the several scenarios requires a statistical approach regarding the time variance and traffic pattern generation. In order to estimate the adequate numbers of simulations, a set of preliminary simulations were performed to identify the best compromise between result variation and simulation time.

A HD scenario was taken as a reference for a dense urban/urban area, penetration being varied between 0.5 to 3% in order to identify the population penetration that would lead to an average blocking of around 2 % and average delay within 1 s order. Five simulations were performed to identify the target study population. For these calculations, only cells with traffic were analysed, as border cells are not representative of the average network behaviour.

From the analysis of Figure 4.32, the 1 % penetration was selected as it lead to around 2.5 % blocking and an average delay value below 10 s. It is important to mention that with 1 %, maximum PA power is achieved, while for 0.5 % the test scenario does not trigger maximum power limitation conditions. In Figure 4.33 it is shown the simulation time for the studied penetrations, along with average delay and offered vs. carried traffic. In the simulator, delay is implemented by shifting the original traffic patterns (every frame) until resources are available to transport the offered traffic, originating higher simulation times for scenarios with high average delay. For 1 % penetration, simulation for the 70 minutes analysis period lasts approximately 1h10, increasing up to 8h15 for 3 % penetration.

As expected, total offered traffic (all services) shows a linear tendency with the penetration increase. Due to system blocking, the offered vs. carried traffic ratio decreases with penetration increase (see Figure 4.33). Given this analysis, it is proposed to set reference population penetration at 1 %, assessing in Chapter 0 the performance impact of the several traffic mixes.

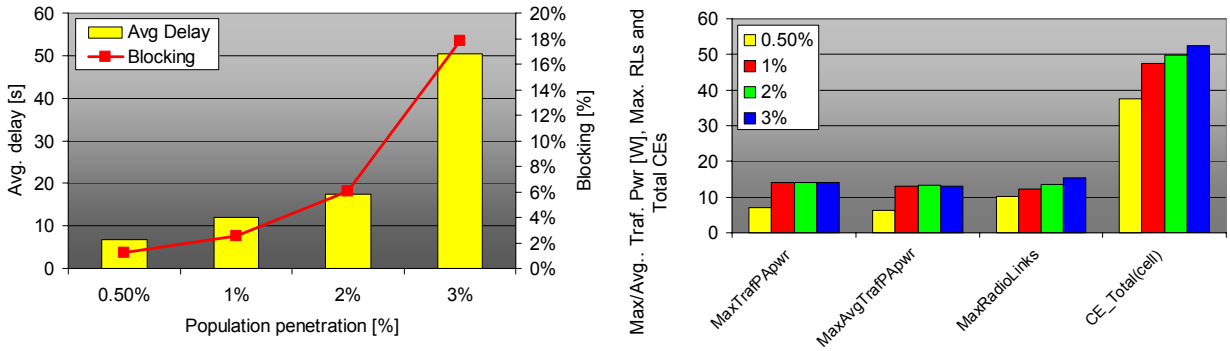

(a) Blocking and delay (b) Transmission parameter

Figure 4.32 – Blocking, Average Delay, PA power, Radio Links and total CEs.

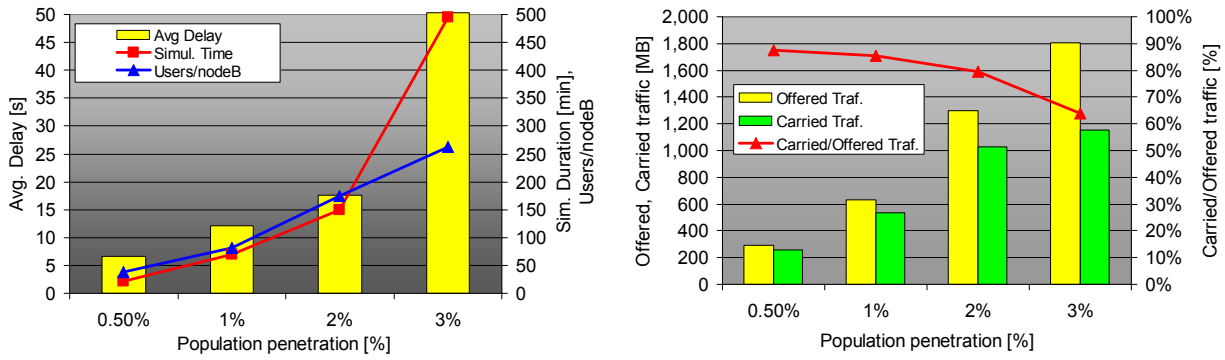

(a) Average delay, users/NodeB, sim. time (b) Offered vs. carried traffic

Figure 4.33 – Delay, Users per NodeB, simulation time and offered vs. carried traffic.

After fixing the penetration to 1 %, and for an initial traffic mix similar to the reference mix, one addressed the number of simulations required to assume convergence of results (reduction of standard deviation and 90 % confidence intervals) and minimum average blocking fluctuation. The test traffic mix is presented in Figure 4.34, showing a strong speech component of around 60 %, lead by WWW, streaming and videoconference services.

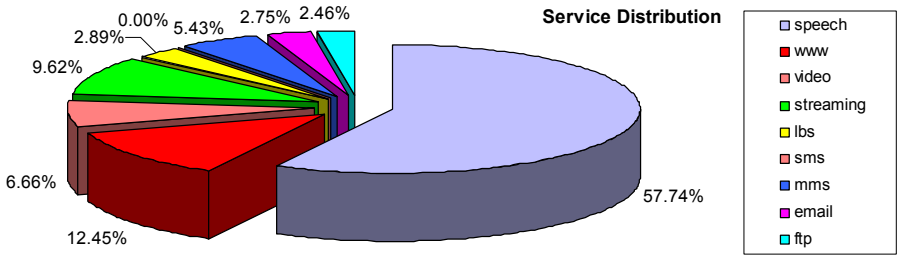

Figure 4.34 – Traffic mix used for result convergence analysis – 60% voice, 40% data.

In Figure 4.35, the blocking and average delay values obtained for the 30 simulations are shown. It is interesting to note some degree of correlation between blocking and delay, as expected. Then, one has aggregated the CS blocking figures for 5, 10, 15, 20, 15 and 30 simulations and compared the average standard deviation and the 5-95 % percentile (PERCENTILE Excel function used) to assess the numerical convergence, with results summarised in Figure 4.36.

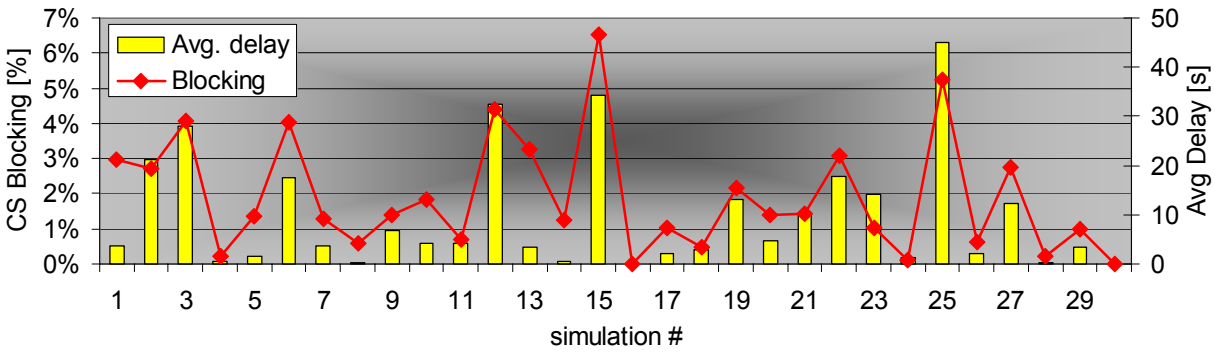

Figure 4.35 – Blocking and average delay values – 30 simulations.

From Figure 4.36, it clear that the 95 % percentile variation is residual when increasing from 25 to 30 simulations. Moreover, the standard deviation (of the average CS blocking) reduction is minimum, while the blocking value itself converges to around 1.5 %, pointing the optimum number of simulations between 20 and 25. By analysing the blocked calls for other parameters (load, PA power and distance) one concluded also on the convergence after 20

simulations. Without significant prejudice to the convergence of results, 20 simulations per scenario were chosen, leading to a total of around 24 h simulation times.

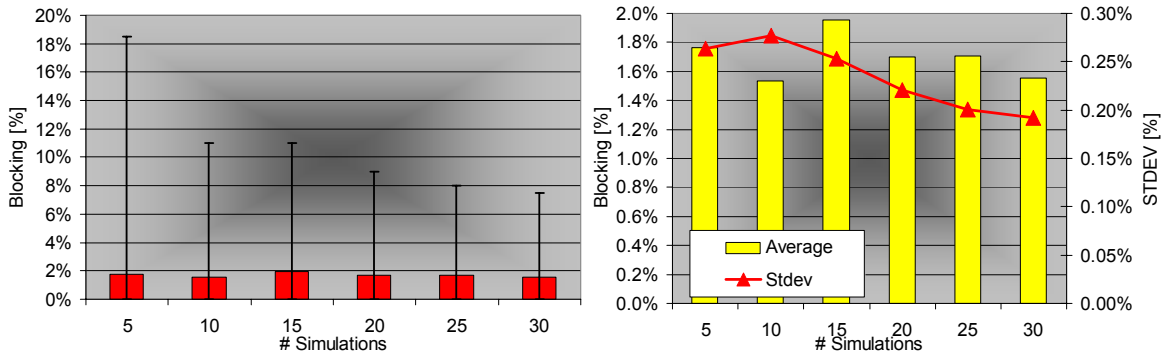

(a) Average and 90 % confidence interval (b) Average and stdev

Figure 4.36 – CS blocking parameters convergence.

As mentioned in Section 4.3, the 60 minutes (busy hour) simulations are achieved by simulating a real time of 70 minutes as approximately the first 10 minutes the traffic generator need to be neglected as is not stabilised yet. To evidence this, in Figure 4.37, the code allocation summary for the first 30 minutes is shown. Due the transitory effects approximately in the first 7 minutes (it depends on the traffic mix, see Figure 4.38), the total simulation duration was defined as 70 min, filtering out the first 10 min.

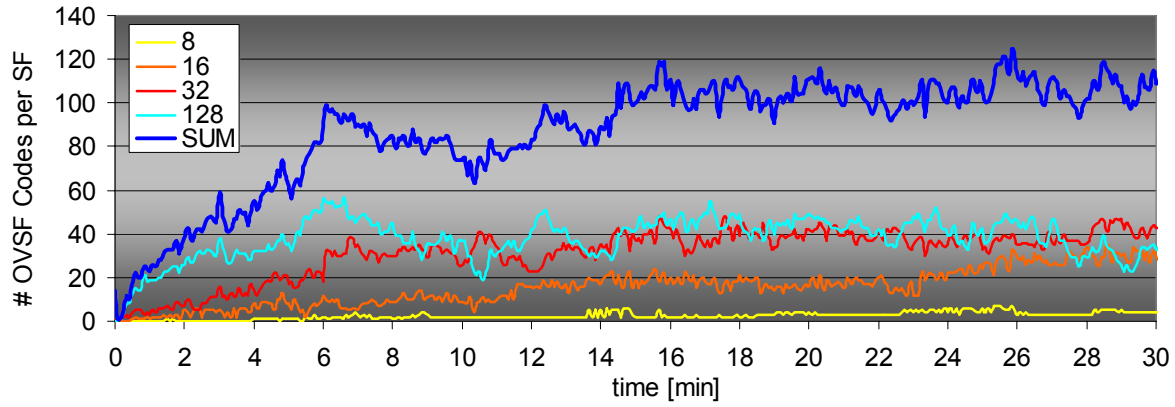

Figure 4.37 – OVSF code allocation (all network) for the first 30 minutes.

As shown in Figure 4.38, for the 60 minutes average, the filtered average (defined as the average from the initial instant to the end of simulation period) is similar to the average calculated over the total considered period, namely after the first 6 minutes, leading to the final value of 10 minutes. One should note that the 50 minutes average corresponds to the case of a 20 minutes guard period, which shows residual improvement in terms of average fluctuation, but would imply higher simulation times.

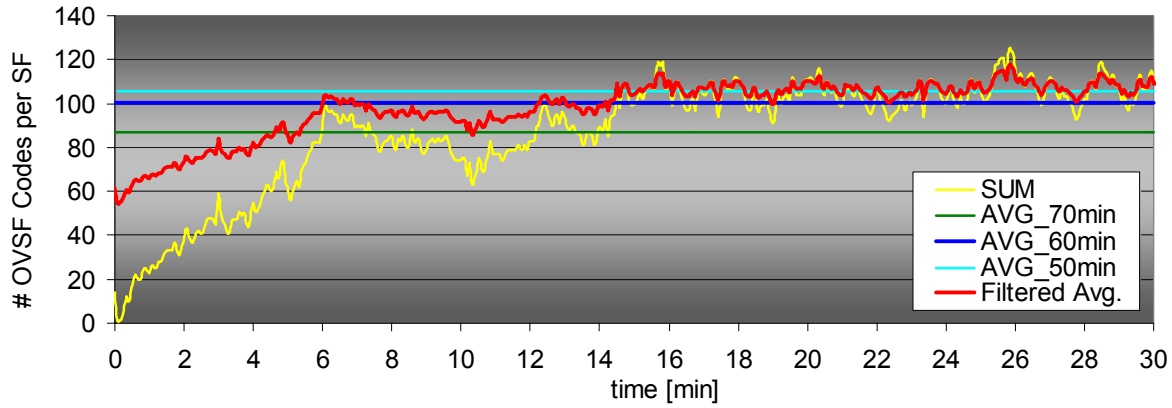

Figure 4.38 – OVSF code allocation average and filter period analysis.

The simulator platform was tested all main algorithms tested and validated, according to theoretical predefined scenarios. Nuclear calculations as the user and traffic generation processes distributions validation is assessed. Detailed evaluation is performed on the statistical distribution values in order to validate its main characteristics. Default scenario (population penetration) was identified and convergence requirements in terms of the number of simulations were obtained.

5. Results and Performance Assessment

The present chapter provides the simulation results analysis of all scenarios tested. After introduction to the scenarios characterisation (demographics and geography), details in the traffic mix composition are presented. Third section focuses on the analysis of the impact of speech vs. data split in the traffic mix, followed by the assessment in the service dominant scenarios. Lastly, HD and LD scenarios are compared, along with TMA impact assessment in the LD scenario.

5.1 Demographics and Geographical Study Areas

In order to analyse the non-uniform dependence of UMTS performance, two different areas in the city of Lisbon were selected, varying in population density, site plan density, and clutter/propagation characterisation. In each of these areas, different traffic mixes were set and network performance assessed. These two main areas were:

- High Traffic Density Area (HD) – CBD, with high user/NodeB density and a high data percentage on the traffic mix;
- Low Traffic Density Area (LD) – Residential/Mixed, oriented to a more residential traffic profile, where speech service still presents a significant weight on the traffic mix.

In order to compare as much as possible the two areas, the same number of NodeB was considered and population penetration changed to target for similar number of users (HD-1%, LD – 2%). Main demographic indicators of HD and LD scenarios are shown in Table 5.1.

The HD scenario includes 4 of the most populated districts (present population including workers and students) in Lisbon, S.Sebastião da Pedreira, S.João de Deus, Nª Sª Fátima and S.Jorge de Arroios, while the LD scenario was selected in Olivais and Marvila districts. District area, clutter distribution and site plan (from [FeAl02]) are shown in Figure 5.1.

It is clear from Figure 5.1 that clutter distribution is also a factor of difference in both scenarios, as LD presents a more varied clutter distribution, while HD is mainly composed of dense residential and services areas. In order to better quantify the clutter impact differences (implicit in the user channel type and indoor penetration distributions), in Figure 5.2, one

plots the user distribution among all the clutters for HD-1% and LD-2% (results are average on 5 user generation runs).

Table 5.1 – HD/LD main demographic indicators.

Parameter	HD	LD
Population [inh.]	156336	71623
Area [km^2]	4.88	14.82
# Sites	17	17
Pop. Density [inh./km^2]	**32018**	**4832**
Site density [sites/ km^2]	**3.48**	**1.15**
Pop./site	9196	4213
# Districts	4	2
Age Profile [%]	24.2 / 36.6 / 39	38.8 / 45.3 / 16.0
Education Profile [%]	8.0 / 34.6 / 20.8 / 36.5	13.4 / 53.8 / 20.0 / 12.7
Salary level	Medium-High	Low-Medium
Reference penetration [%]	1% - 1382	2% - 1337

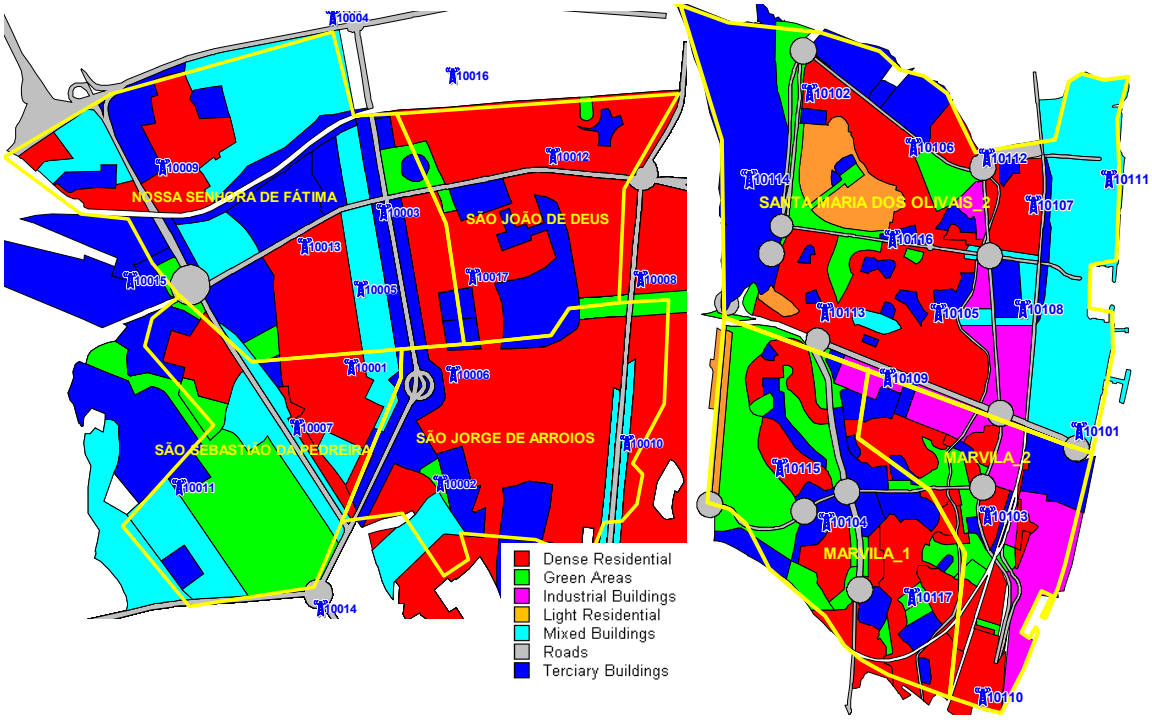

(a) HD (b) LD

Figure 5.1 – HD and LD districts, clutter distribution and site plan.

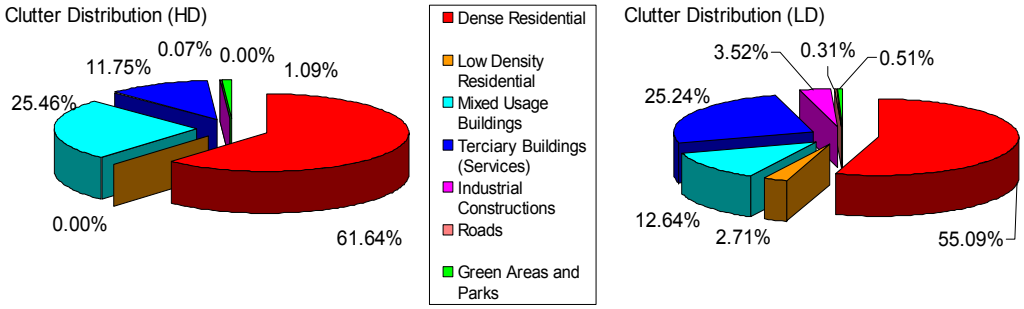

(a) HD (b) LD

Figure 5.2 – User clutter distribution – HD-1% and LD-2%, average over 5 runs.

Besides the clutter distribution, the different demographic indicators lead to different traffic mixes. For the reference service distribution according to age, education and salary indicators as proposed in [FeAl02] and [VaCa02], Table 5.2, the obtained traffic mix distributions for HD and LD scenarios is shown in Figure 5.3. In Figure 5.4, slight higher percentage on incar is noticed due to higher Vehicular type users.

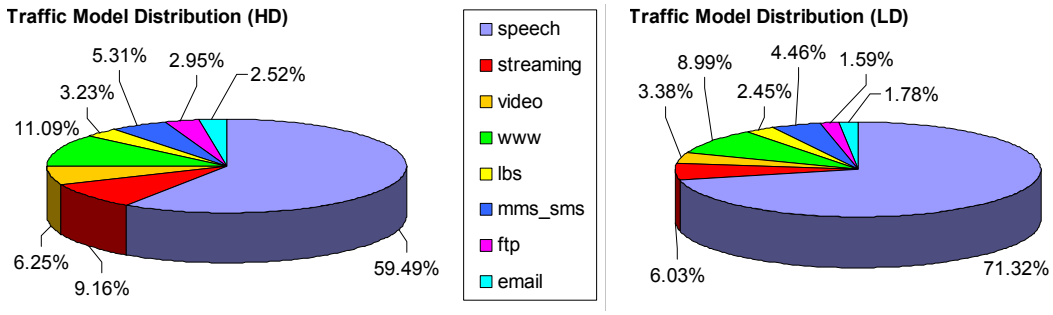

(a) HD (b) LD

Figure 5.3 – Traffic Mix for HD-1% and LD-2%, reference service distribution.

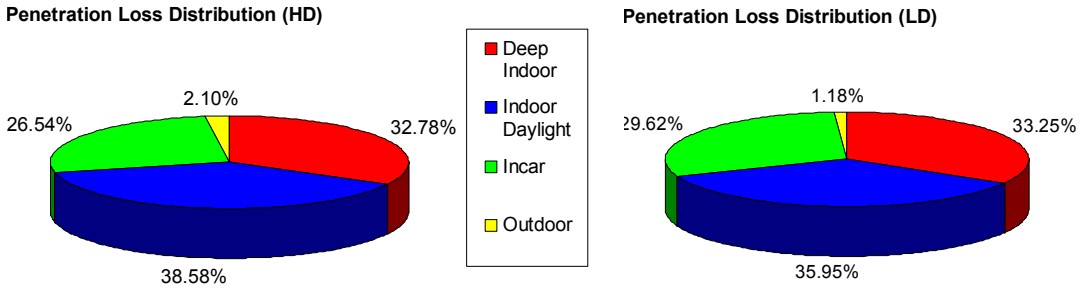

(a) HD (b) LD

Figure 5.4 – Indoor penetration distribution HD-1% and LD-2% (ref. service distribution).

Table 5.2 – Service distribution for age, salary and education demographic indicators.

Service Distribution			Age [%]			Salary [%]				Education [%]			
Application	DL rate [kbps]	Traf. Model	<20	<64	>64	Low	Med.	M/H	High	No	Basic	Compl.	Degree
voice	12,2 (CS)	speech	44	48	90	95	87	66	34	95	80	62	50
audio-on-demand	64 (PS)	streaming	9	2	0	0	0	2	7	0	3	4	2
video-telephony	64 (CS)	video	5	9	2	0	2	5	11	2	2	4	9
video-on-demand	384 (PS)	streaming	3	2	0	0	0	1	7	0	0	2	1
web-browsing	128 (PS)	WWW	6	12	5	0	1	4	10	0	2	9	13
chat	64 (PS)	WWW	9	5	0	1	2	6	5	0	1	6	4
personal LBS	64 (PS)	lbs	1	7	2	0	1	4	6	0	0	3	4
MMS	64 (PS)	mms_sms	13	4	0	3	5	6	7	0	7	4	4
interact. gaming	128 (PS)	streaming	4	2	0	1	3	4	5	3	5	4	2
FTP	384 (PS)	ftp	2	7	0	0	0	0	3	0	0	0	8
e-mail	128 (PS)	e-mail	4	4	1	0	0	2	5	0	1	2	4

5.2 Simulation Scenarios

As the main objective of this thesis is to assess the non-uniform traffic mix impact on system performance, a set of simulation scenarios was conceived in order to allow extrapolating dimensioning guidelines for a given traffic mix.

One of the main trends in UMTS traffic is the gradual PS data services increase, leading to a higher load than regular speech and video-telephony users. In order to assess the impact on the data vs. speech split, 4 main service distributions scenarios were created: a voice centric (VOC), reference (REF), data centric (DAC) and data mostly (DAM) scenarios. All these scenarios were launched in the HD area profile with a population penetration rate of 1 % as mentioned in Section 4.4.5. The services distribution tables referring to these four scenarios are presented in Annex M. In Figure 5.5 the speech/data split in terms of the RB distribution is shown (detailed values in Table 5.3).

The first set of simulations provides the trends on the dimensioning aspects regarding the speech/data split, but still does allow to evaluate the traffic mix impact as data services use the same service distribution for the four scenarios. Taking the DAC scenario as a starting point, 6 service centric ones were defined, where a specific service dominates the mixture with a relative weight over 20%; VC (video telephony), WW (WWW), ST (streaming), LB (LBS and MMS), EM (E-mail) and FT (FTP) as shown in Figure 5.6. The service distribution tables

referring to these scenarios are presented in Annex N. Note that the service-biased scenarios, besides the traffic source dominance, also imply a different RB mix, hence, network performance is modified. As an example, the FT scenario will trigger a higher PS384 kbps bearer penetration, as clearly shown in Figure 5.7, where the RB distribution is shown for all DAC scenarios (REF refers to the original DAC scenario from the first four mixes).

Table 5.3 – DL Radio Bearer Distribution.

BEARER	VOC	REF	DAC	DAM
CS12.2 [%]	79.12	68.21	55.77	36.08
CS64 [%]	3.03	4.60	6.41	9.36
PS64 [%]	8.72	13.36	18.71	27.19
PS128 [%]	6.97	10.71	15.09	22.33
PS384 [%]	2.16	3.11	4.02	5.04

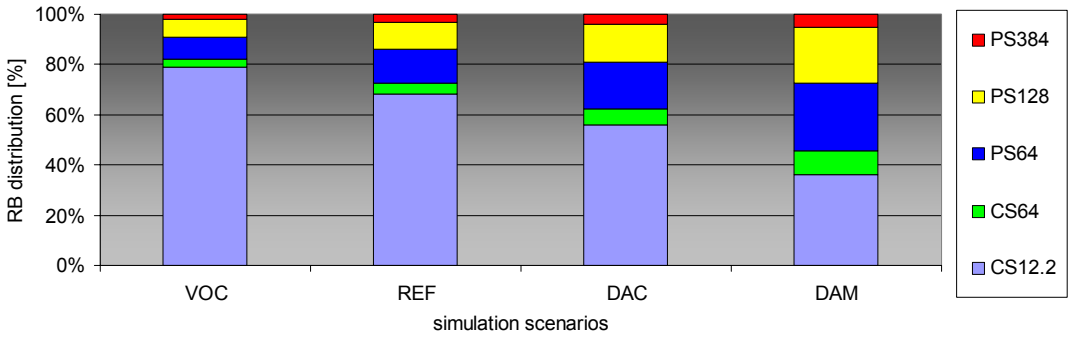

Figure 5.5 – Radio Bearer Distribution (from Service tables).

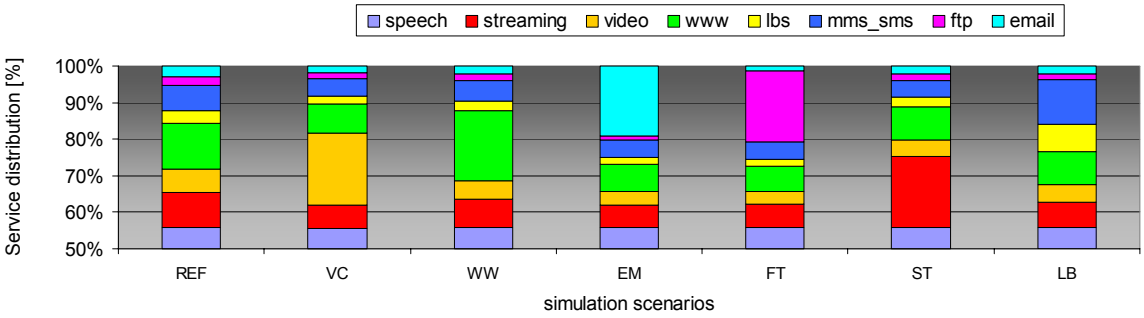

Figure 5.6 - Service distribution (from Service tables) for DAC scenarios.

After the traffic mix impact assessment, the non-uniform traffic and site density was studied by benchmarking in the same conditions the HD-1% and LD-2% scenarios characterised in Section 5.1. As the traffic mix for the LD scenario is less data oriented, it is desirable to investigate higher penetration values for LD scenario that match HD-1% performance (see Section 5.5).

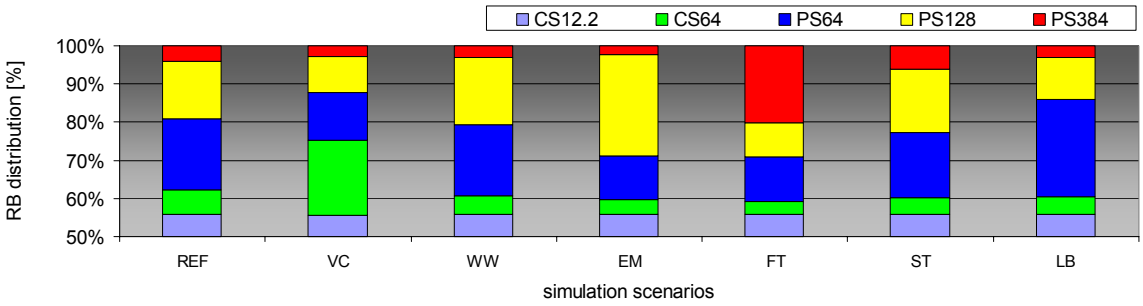

Figure 5.7 - Radio bearer distribution (from Service tables) for DAC scenarios.

Finally, a system performance assessment is performed to evaluate the impact of TMA in the LD-2% scenario, as adopting TMAs in every cell can minimise the high percentage of non-covered users. This analysis allows concluding on TMA impact on DL capacity, namely PA power and maximum DL link powers, as higher UL pathloss values are possible.

For all of the enumerated scenarios, 20 simulations were performed for a total of around 360 discrete simulations, leading to a simulation period of more than 700h[6] (roughly 29 days), and generating approximately 14 GB of compressed data.

5.3 Impact of speech vs. data split

In this section, the simulation outputs for the speech/data split scenarios are analysed: VOC, REF, DAC and DAM. Starting by the user generation profile, in Figure 5.8, the radio bearer and service distribution for the four scenarios are shown. Note that Figure 5.5, presents the distribution from the service table and not from the real user generation files. Speech weight varies from 72.5 to 26.8%, with uniform data distribution over the scenarios. From the data set, the dominant services are WWW, streaming and video-telephony.

As expected, for the several scenarios, no difference is noted in the user clutter distribution, but interesting differences are note at the channel type and indoor penetration losses distribution, as shown in Figure 5.9. With the data weight increase, pedestrian type users also increase, as for example PS384 will only be assigned pedestrian type channels (low data services penetration is expected for vehicular users). In terms of indoor penetration, the

[6] Simulations were mainly performed in Pentium IV 2GHz type processors with 512 MB RAM.

decrease of incar (due to vehicular channel reduction) leads to indoor light increase (it is expected that data users are mainly indoors).

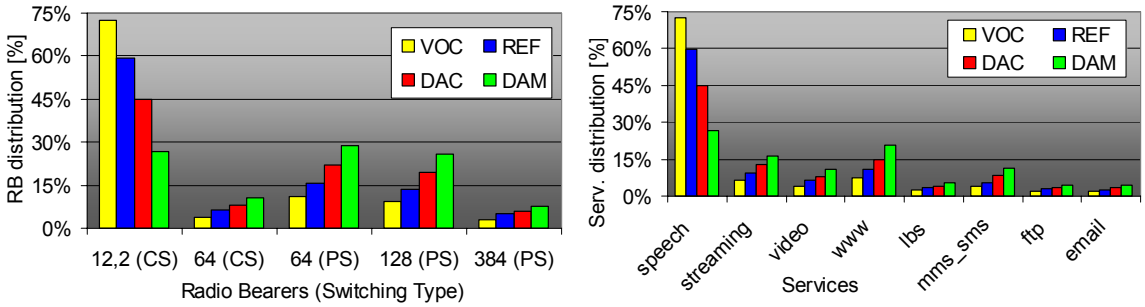

(a) Radio Bearer distribution (b) Service distribution

Figure 5.8 – RB and service distribution from user generation.

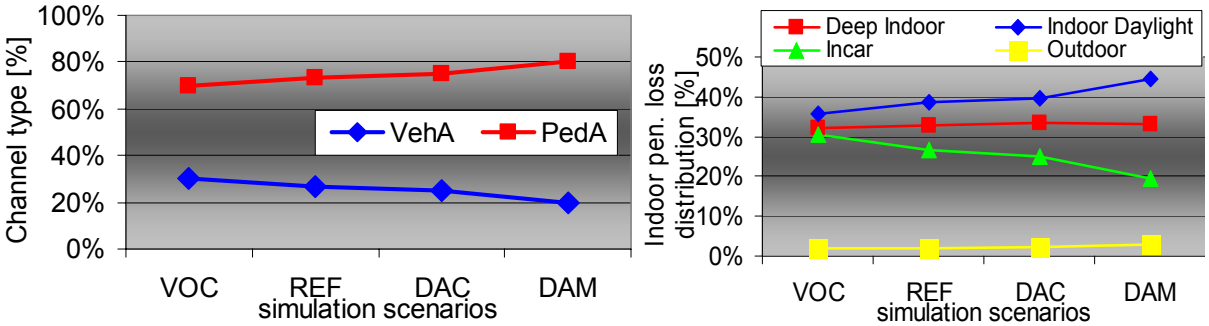

(a) Channel type (Pedestrian/Vehicular) (b) Penetration loss distribution

Figure 5.9 – Channel type and penetration losses distribution from user generation.

The first parameters to assess are the network blocking and average delay for each scenario. As expected, the reference scenario leads to around 1 % CS blocking, while the VOC one leads to a lower value. It is important to note the big variations in blocking and delay from simulation to simulation, which is illustrated in Figure 5.10 for REF and DAM scenarios.

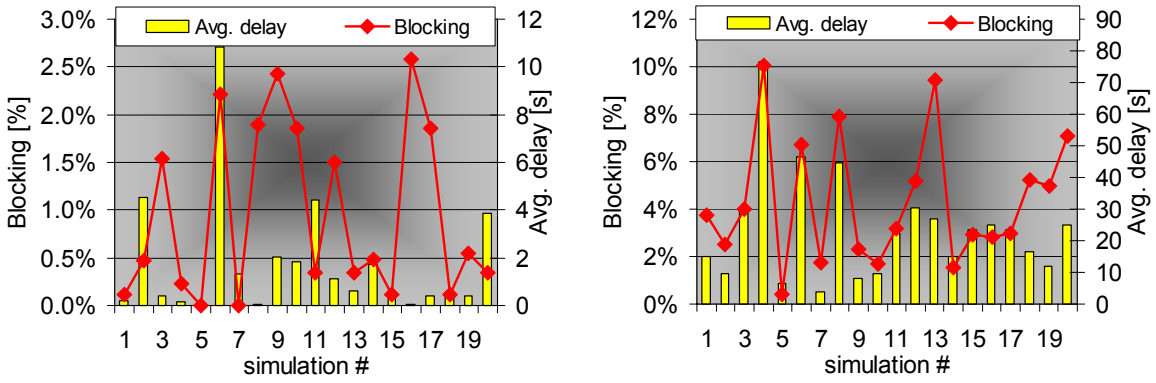

(a) REF scenario (b) DAM scenario

Figure 5.10 – CS blocking and Average delay for REF and DAM (20 simulations).

In order to quantify this variation, for blocking and average delay figures, the 90 % confidence interval along with average values are shown in Figure 5.11.

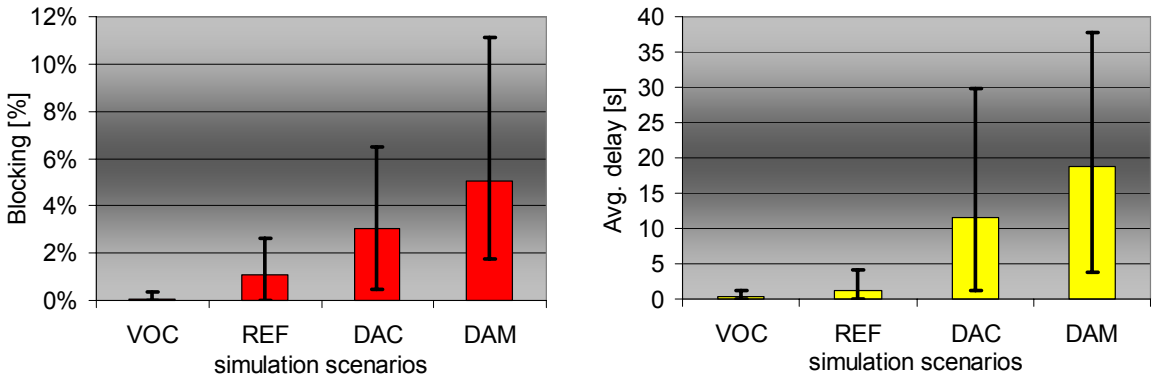

(a) CS blocking (b) PS delay

Figure 5.11 – Average CS blocking and PS delay, with 90 % confidence interval.

It can be concluded that the DAM scenario presents a blocking rate 5 times higher than the reference scenario and an average delay 15 times higher. The increase is due to higher data services volumes, which using higher RB, present less possible simultaneous connections.

Besides blocking and delay indicators, the offered vs. carried traffic was evaluated, as well as the normalised rate that is defined based on the average UE bit rate (associated with delay). This indicator shows the average maximum bit rate (e.g., 98 % means that 64 kbps connections had on average 0.98×64 = 62.72 kbps). The offered traffic was split by service for each scenario in order to allow evaluation of each service contribution to total data volume. Offered vs. carried traffic, normalised rate, and offered traffic split are shown in Figure 5.12 and Figure 5.13. As consequence of the average delay increase, the normalised rate drops as data weight increases. The offered vs. carried traffic ratio show a decrease trend with exception of DAC that is probably related with statistical traffic variation. From Figure 5.13 is also clear that data centric scenarios are mainly driven by WWW, streaming, video-telephony and LBS services to what regard data volume.

Other interesting indicator to analyse is the blocking and delay causes distribution. By its analysis, it can be inferred which are the main causes for call block or packet delay. If referring to CAC algorithm (detailed in Section 4.4.4), five parameters are verified; distance (UL path loss limitation), DL load, DL maximum link power, PA power and OVSF code shortage. In Figure 5.14, the blocking and delay causes partitioning is shown. Main radio link

allocation success rate is also presented for CS and for PS (for PS it is defined if the link can be assigned with no delay).

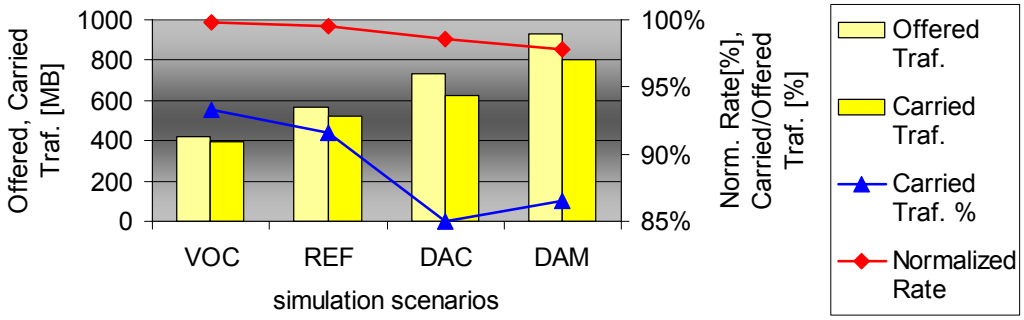

Figure 5.12 – Offered vs. carried traffic and offered traffic service split.

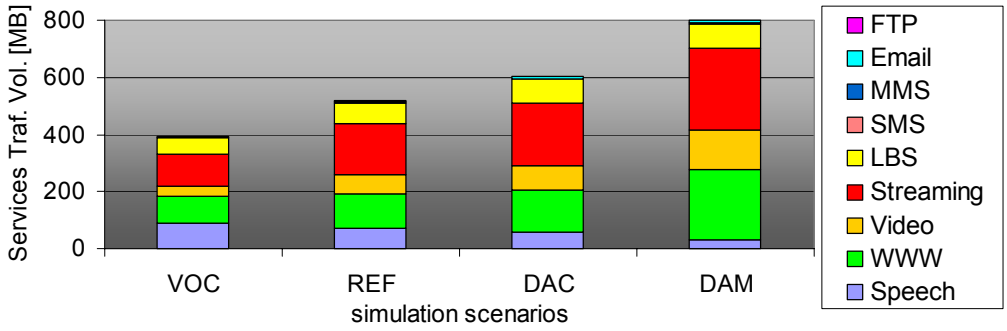

Figure 5.13 – Offered traffic service split.

As verified in Section 4.4.2, the HD scenario presents an acceptable UL coverage with average pathloss distribution, hence, the main blocking/delay cause is DL load. The increase of blocking related to distance is due to the increase of data services that require a 64 kbps UL, more stringent than voice (total CS blocking including distance is 0.34, 1.57 %, 4.25 and 6.48 %, respectively for the four scenarios). Regarding delay, and for the reference scenario, around 40 % of the packet transmit attempts do not suffer any delay. All the detailed output analysis graphs are presented in Annex O.

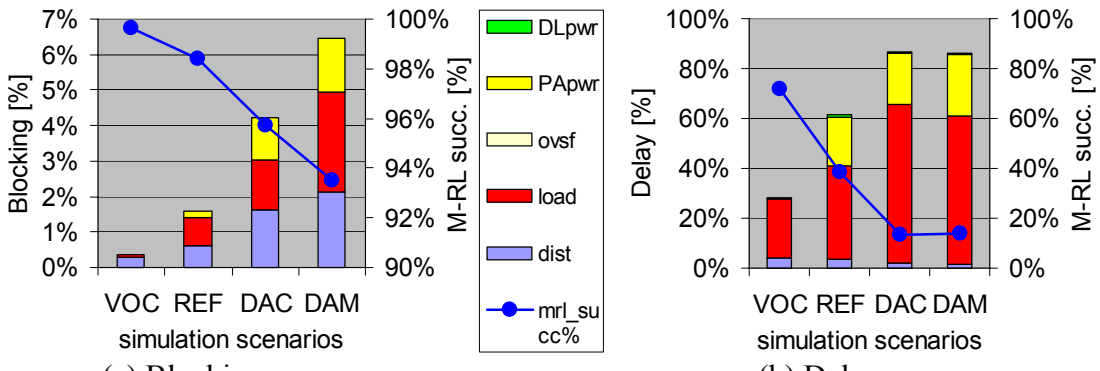

(a) Blocking causes (b) Delay causes

Figure 5.14 – Blocking and delay causes distribution.

One should note that distance blocking or delay are due to the NodeB distribution considered, and that way are treated separately when addressing the blocking and delay average figures. Nevertheless, these blocking calls are included in the causes detailed in

Figure 5.14. In order to better illustrate the distance drops impact, in Figure 5.15 one shows for the REF scenario (HD-1%) the blocking percentage including distance blocks compared with blocking calculated just for the load, PA power and codes limitation. It also presented in Figure 5.15 for reference the difference obtained for the busy hour (60 min) and the total obtained for the 70 min simulation period for CS blocking and average delay figures.

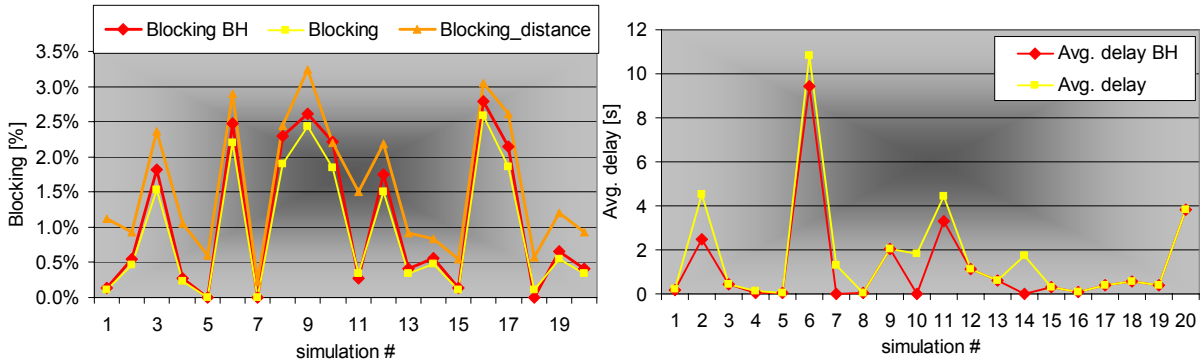

(a) Blocking (BH, 70min, distance) (b) Delay (BH, 70 min)

Figure 5.15 - Blocking and delay for REF with distance blocks included.

Another important aspect to consider is the SHO success rate (CS services) along with SHO percentage, Figure 5.16. As expected, the SHO percentage remains similar for the four scenarios (average 21.6 % and standard deviation equal to 1.4 %). Due to lower priority on allocation of SHO links, the allocation success percentage is slightly less (average 3 %) than the one for main link for all the scenarios. One should note that the allocation of SHO links can be as low as 92% while the main link success is over 99 % as shown in Annex O for the 20 simulations performed in the REF scenario (HD-1%).

One of the objectives of this thesis is to relate the baseband processing capabilities needs with the traffic mix and offered traffic characteristics. In order to investigate this aspect, radio link distribution (per SF), average PA power, maximum number of radio links (per cell) and channel element total (per cell) were analysed for the four scenarios. Results are summarised in Figure 5.17 (maximum and average refer to value in each of the 20 simulations performed).

From Figure 5.17, it is interesting to note that for DAM scenario, the high data component is evident in the average PA power increasing tendency. Regarding the number of radio links (total or per SF), a decrease in DAM comparing to DAC is identified. This is due the fact that

higher PS rate services are present in DAM scenario (e.g., SF8), leading to higher DL load factors (and higher PA power), hence, limiting the number of simultaneous radio links in the cells compared to DAC ones. This is also coherent with the fact that a lower number of maximum CEs (per cell) is required, but the average value is similar DAC scenario.

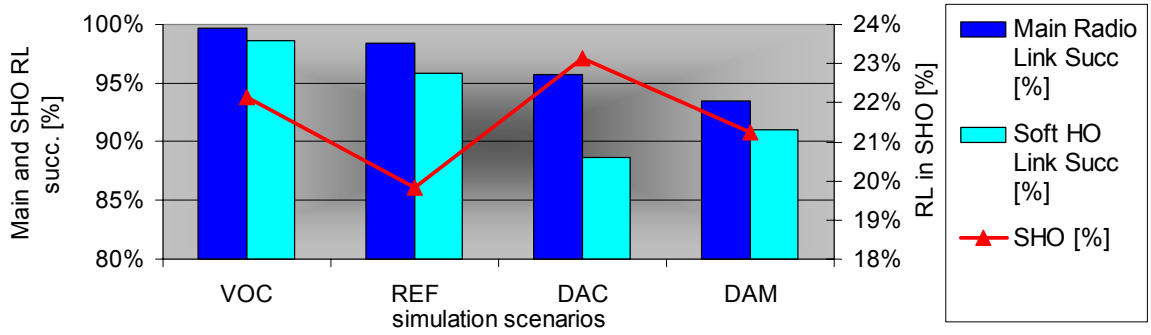

Figure 5.16 – Main and SHO radio link success and SHO percentage.

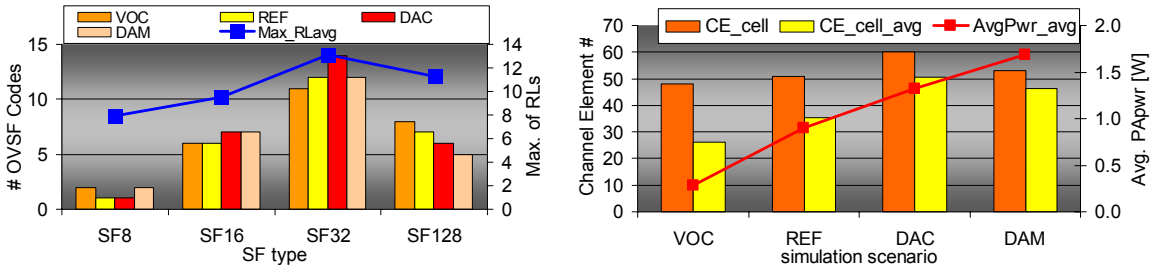

(a) Maximum RL per SF (b) PA power, CEs per cell

Figure 5.17 – Maximum RL per SF, Average PA power and CEs per cell.

One should note that baseband units are typically shared by all sectors of a NodeB (shared pooled resource), thus, the total CEs needed is obtained from inferring on the three sectors needs. Similar to the cell behaviour, for the DAC scenario the (maximum) requirement reach 150 CEs per NodeB, compared with the 90 CEs for the REF scenario, Figure 5.18.

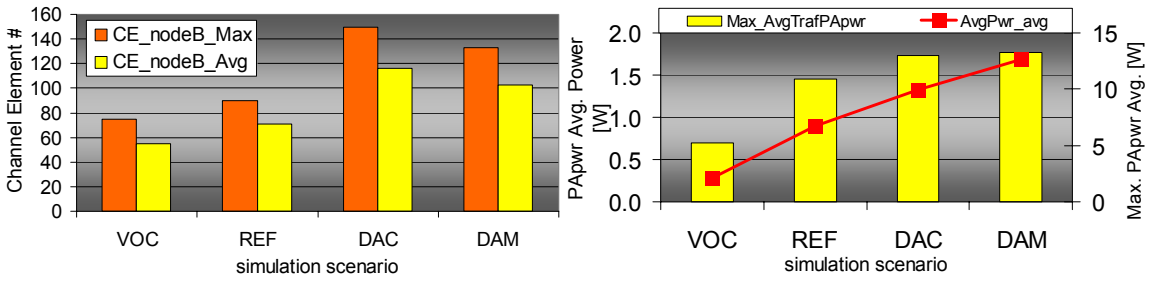

(a) NodeB CEs (b) PA power (cell)

Figure 5.18 – Maximum NodeB CE requirements and PA power (network and cell level).

This analysis shows how sensitive the baseband capacity is to the traffic mix, requiring a careful design to avoid hardware blocking in the (NodeB) CE pool. At the PA level, the decrease of speech lead in average to higher PA power usage (see Figure 5.18). This fact is mainly due to the higher power requirement of PS128/384 bearers.

As more data is present in the mix (DAC/DAM) the correlation between blocking, average delay and the complement of the normalised rate is higher, as can be easily seen in Figure 5.19, for the REF and DAM scenarios, these three indicators are shown for a decreasing order sort of blocking percentage for every simulation (remaining scenarios figures are available in Annex O). This behaviour is expected, as a high blocking normally is result of high PS data usage, and consequently to a more probable PS delay. The normalised rate is naturally bounded in this relation, as it is related with the PS services delay.

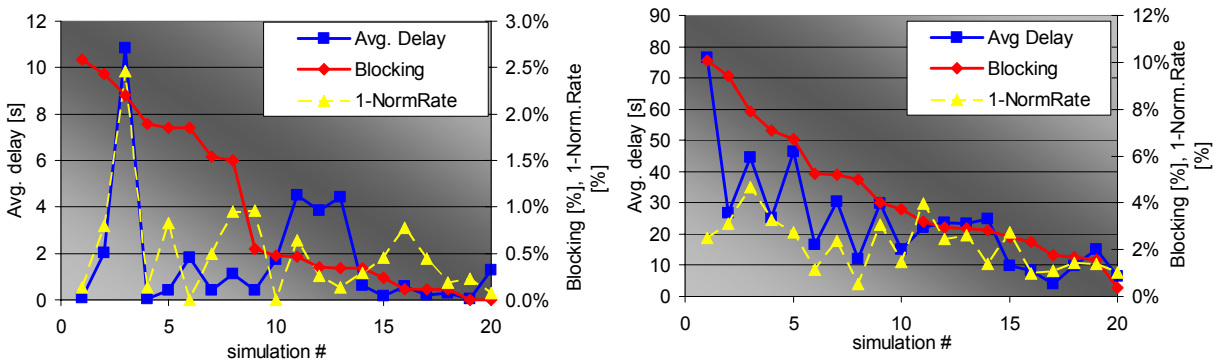

(a) REF (b) DAM

Figure 5.19 – Average delay, network CS blocking and complementary of normalised rate.

In order to better understand some of the trends found in the last indicators, a detailed DL load and PA power statistical characterisation was performed in the higher (MAX_BLOCK) and lower (MIN_BLOCK) average blocking simulations. The main indicators considered in this study are the average network DL load, the maximum DL load (loaded cell), the network average PA power and maximum PA power (cell level). This first study is also targeting at identifying the non-uniform traffic impact in the average network figures against its worst cell performance. The 90% confidence interval is shown along with the average, Figure 5.20 (remaining scenarios figures are available in Annex O).

As mentioned in Section 4.4, the maximum DL load is set to 70 % and maximum available traffic PA power is 14 W. It is interesting to note that network average load is around 12 % for the simulation presenting the higher average blocking CS probability, far from the 70 % maximum DL load, indicating the high non-uniformity of the traffic distribution as detailed

later in this section. The same applies to the PA power, where on average only 1.5 W is transmitted for the worst blocking simulation (see Figure 5.20). This values are analysed along the BH duration, where it interesting to plot its variation along the time. In Figure 5.21, load indicators from instant 10 to 70 minutes are shown (remaining scenarios figures are available in Annex O).

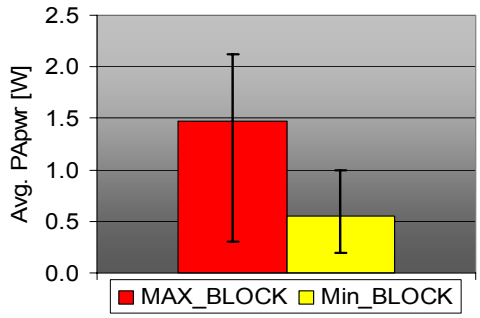

(a) Average network DL load

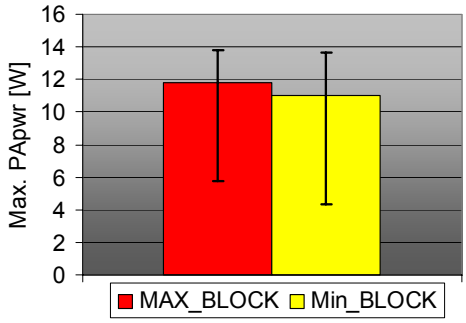

(b) Maximum cells DL load

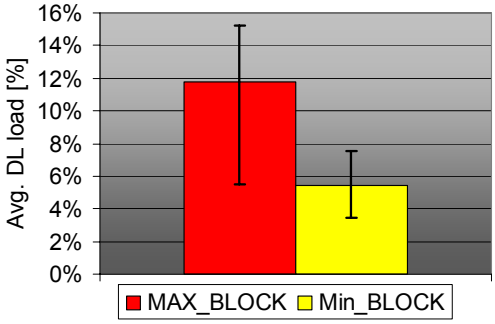

(c) Average network PA power

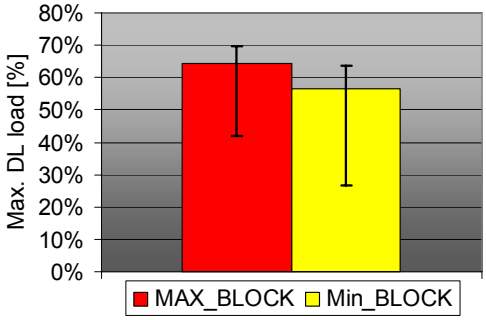

(d) Maximum cell PA power

Figure 5.20 – Average and maximum network load and PA power for DAC.

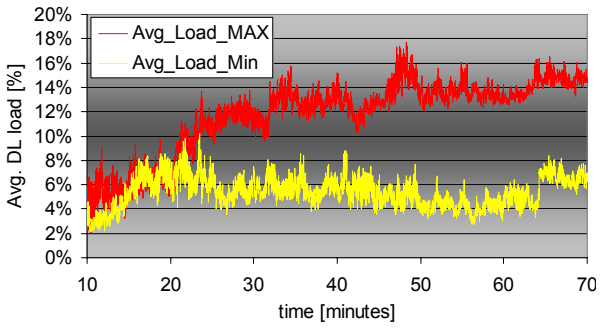

(a) Average network load

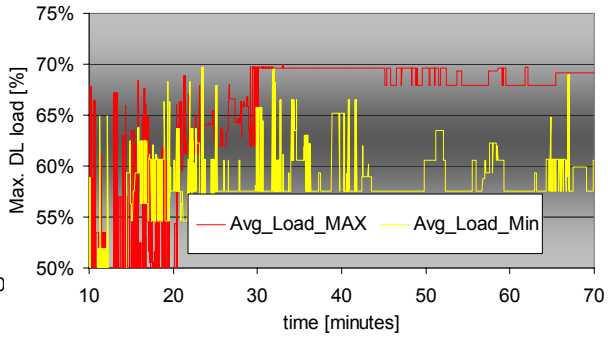

(b) Maximum cell load

Figure 5.21 - Average network load, Maximum cell load DAC in simulation period.

In Figure 5.22 and Figure 5.23, the DL load and PA power indicators are shown for the four scenarios. It is interesting to note that, for VOC and REF scenarios, the minimum and maximum blocking simulations provide similar figures for DL load/PA power, unlike the

DAC and DAM where values diverge rapidly. For the VOC scenario maximum load, it can be concluded that the maximum DL load (70 %) is not reached, leading to the very low blocking percentage. Only for DAM scenario, the 14 W PA power is fully used, while for the remaining three it presents lower values. As expected, along with the data weight increase vs. speech, the DL load and PA power increase either in minimum or maximum blocking simulations.

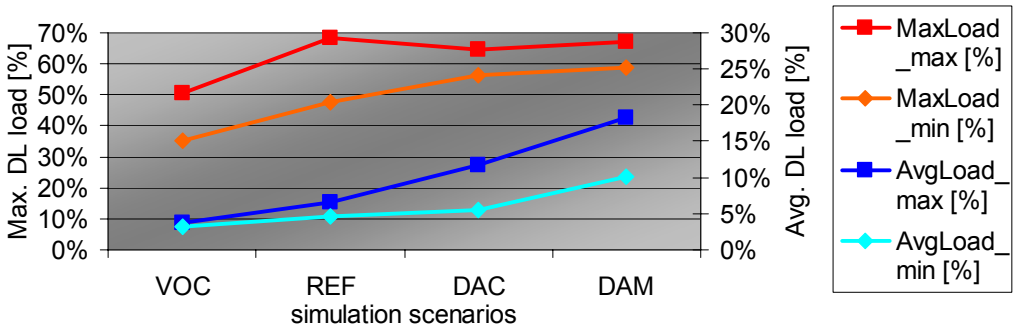

Figure 5.22 - Average network load and maximum cell load for the four scenarios.

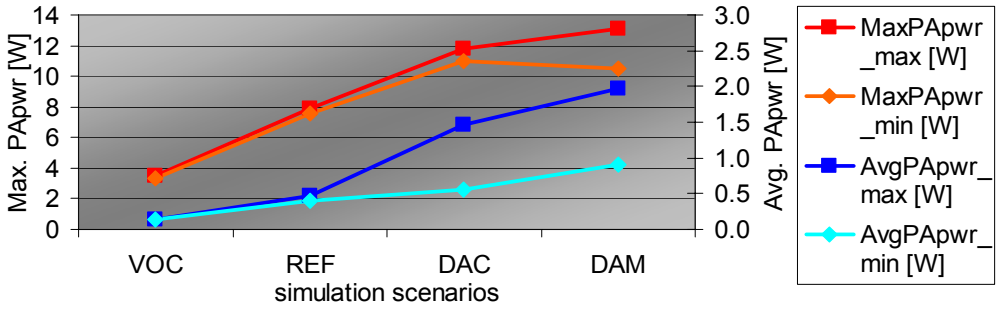

Figure 5.23 - Average network and maximum cell PA power for the four scenarios.

The non-uniformity assessment requires the analysis at the cell level, at least of a sample of the loaded cells in each scenario. Due to the approximate geographical invariance of the generated patterns, the cell set is the same for the four studied scenarios. After investigation on the cells offered volume and blocking for the DAC scenario, the following NodeB set was selected: 10012, 10013 and 10017 (NodeB/cell identification format detailed in Section 4.2.2), shown in Figure 5.24, along with a user generation (HD-1%). The first analysis performed is to correlate the total BH cell traffic in kilobyte (split by RB type) with cell blocking and the total CEs that are related with RL simultaneity, Figure 5.25.

From Figure 5.25, the correlation between the traffic volume and the CE number is evident, from the higher traffic volumes carried, or the cells with high data rates percentage (higher rates require higher number of CEs per call), normally a corresponding high CE number

applies. The blocking probabilities in Figure 5.25 are shown per cell (number in the figure), for the worst blocking simulation, reaching 50 % for the most stringent scenario (DAM). By inspection of Figure 5.25 and user distribution in Figure 5.24, it is easy to correlate the higher blocking/traffic volume for sectors 2 and 3 of 10012, and sector 1 of 10013 and 10017 sites. In these sites, it is clear the traffic non-uniformity impacts at the blocking level.

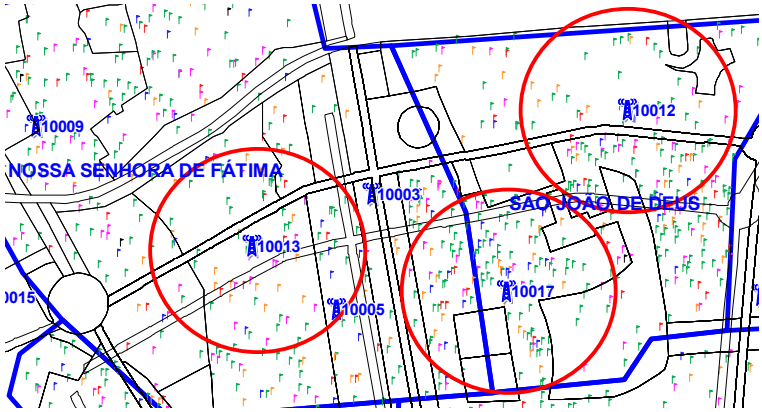

Figure 5.24 – Loaded cells/NodeB set (VOC, REF, DAC and DAM

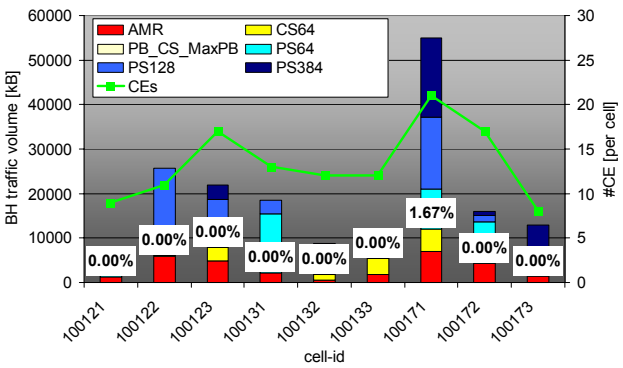

(a) VOC

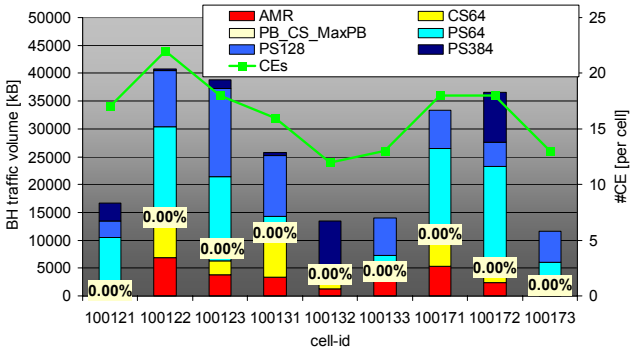

(b) REF

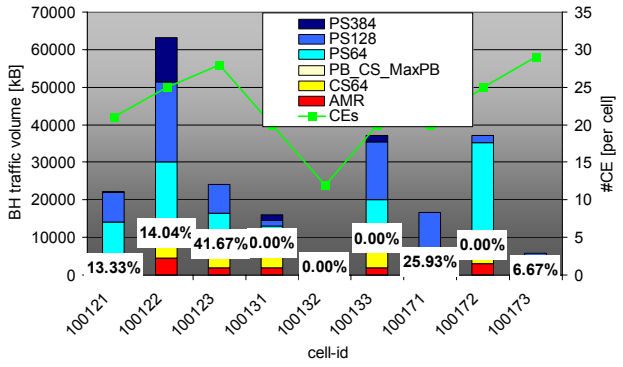

(c) DAC

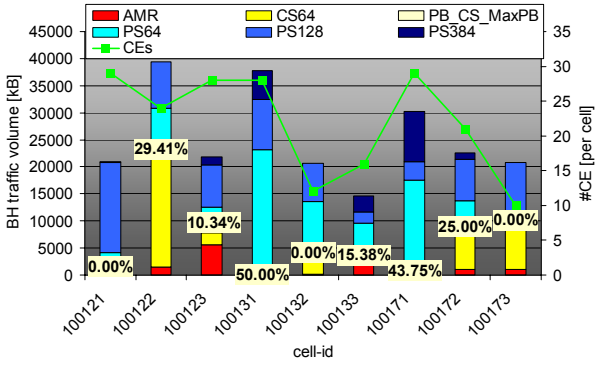

(d) DAM

Figure 5.25 – Cell traffic volume per RB, CE number and CS blocking rate (all scenarios).

Also, DL load, Figure 5.26, and PA power average, Figure 5.27 , are assessed.

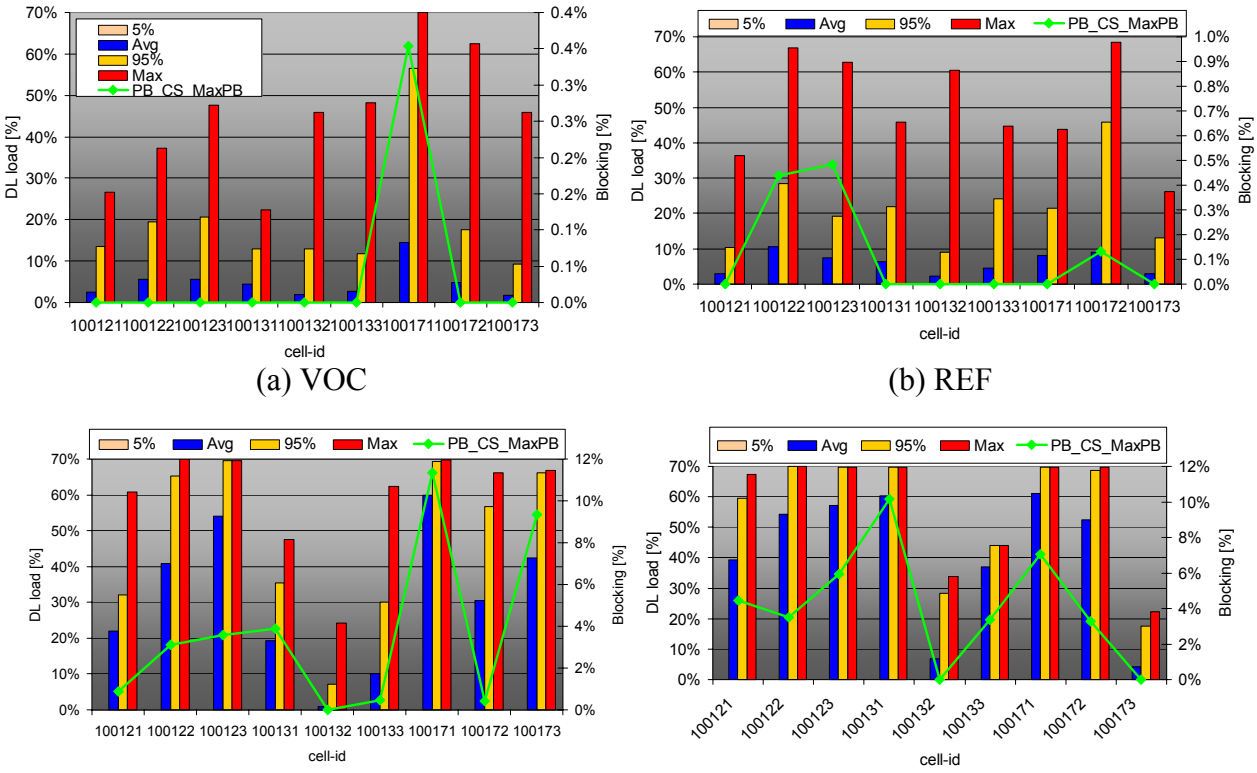

(a) VOC (b) REF

(c) DAC (d) DAM

Figure 5.26 – DL load average, 5/95% percentile and blocking for loaded sites.

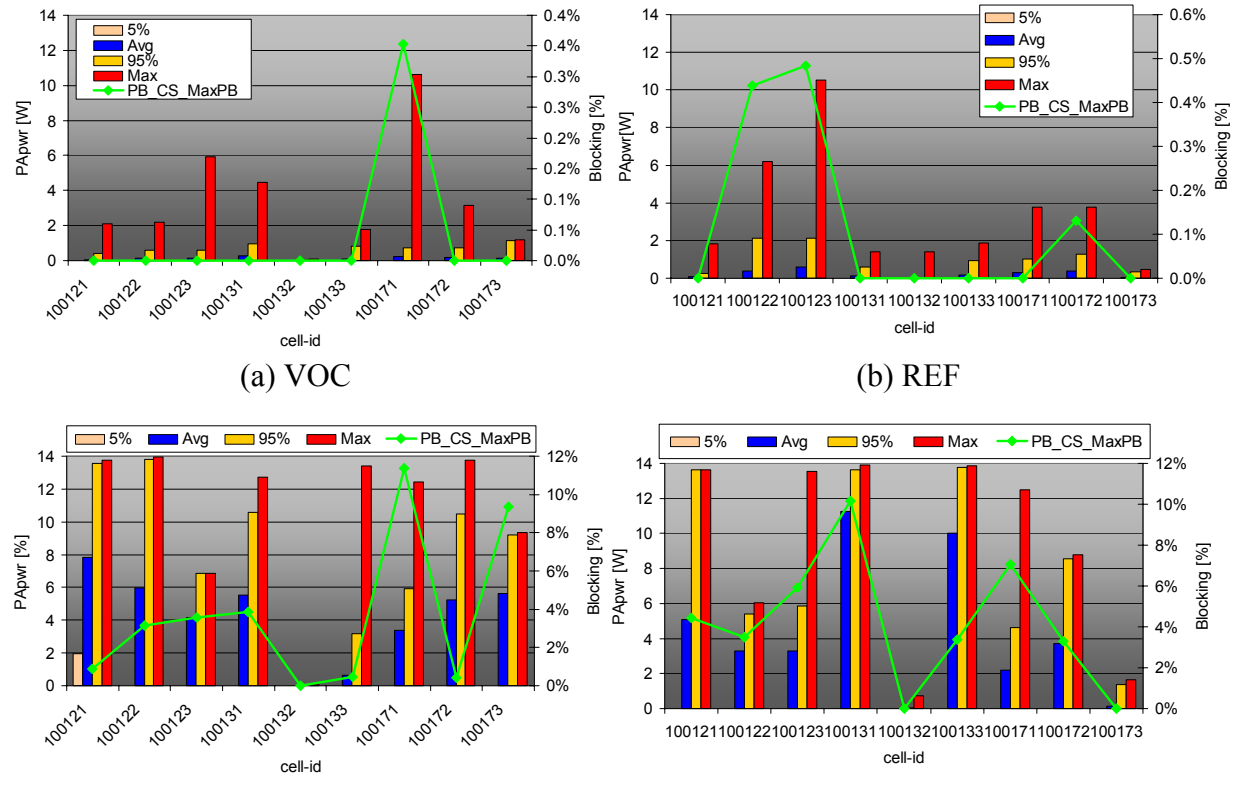

(a) VOC (b) REF

(c) DAC (d) DAM

Figure 5.27 – PA power average, 5/95% percentile and blocking for loaded sites.

Concerning the blocking causes, Figure 5.26 and Figure 5.27 provide a pretty good insight into cells limitations, namely the DL load one for all scenarios. DL load presents is the most critical limitation, as only DAC and DAM scenarios present PA power near the 14 W traffic limit. One should note that for a border site, such as 10012, the PA power limitation occurs is sectors 1 and 2 due to higher average pathloss. All values are shown along with the maximum, average and 95 % percentile, in order to better show the time variation of the indicator. It is expected that in the data oriented scenarios (DAC, DAM), the average (or 95% percentile) is closer to the maximum values when compared to VOC/REF scenarios.

To conclude the analysis on the four scenarios, and similarly to Section 4.4.5, for every scenario studied, convergence of the 20 simulations was tested and the average convergence and standard deviation reduction was verified. All scenarios convergence verification values are available in Annex O.

From results in presented in this section, one conclude on the strong blocking and delay dependence on the speech vs. data mix weight distribution. Moreover, DL load was identified as the most limiting capacity factor, along with PA power when addressing higher PS data traffic mixtures. Average cell PA power is also increasing with PS data increase due to higher DL link power requirements as spreading gain reduces for higher bit rate RBs. In the NodeB hardware, high impact is also evaluated regarding the CEs requirement to process without (hardware) blocking the offered traffic. SHO performance is also degraded by the increase of the data/speech ratio, with poor performance in the DAC scenario.

5.4 Influence of service predominance

From the first traffic mix scenarios, the blocking/delay indicators dependence on the speech vs. data split is clear. The next step is to infer on the data part of the traffic mix by defining a dominant service, and assessing its impact on the network performance indicators. In order to minimise the number of simulations, and assuming the DAC scenario as starting point, a similar study as shown in the last section is performed.

For the several scenarios, no difference is noted in the user clutter distribution, but interesting differences are noted at the channel type and indoor penetration losses distributions, as shown in Figure 5.28. Pedestrian type users' increase for PS384 services (e.g., FT) and in terms of

indoor penetration, the decrease of incar (due to vehicular channel reduction) leads to indoor light increase. The RB distribution is now driven by the dominant service; for example, the VC scenario shows a CS 64 RB percentage higher than 20 %, Figure 5.29, while speech weight is similar to all tested DAC scenarios. In Figure 5.30, the service dominance is clear for each of the created DAC scenarios.

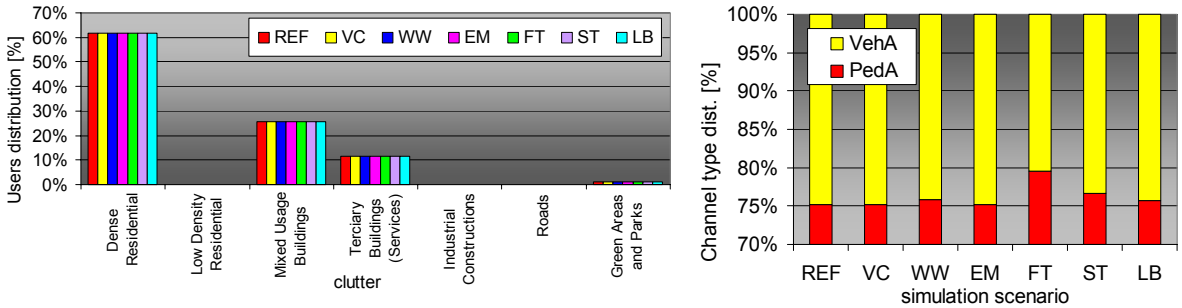

(a) Clutter distribution (b) Channel type distribution

Figure 5.28 - Clutter and channel type distribution for DAC scenarios.

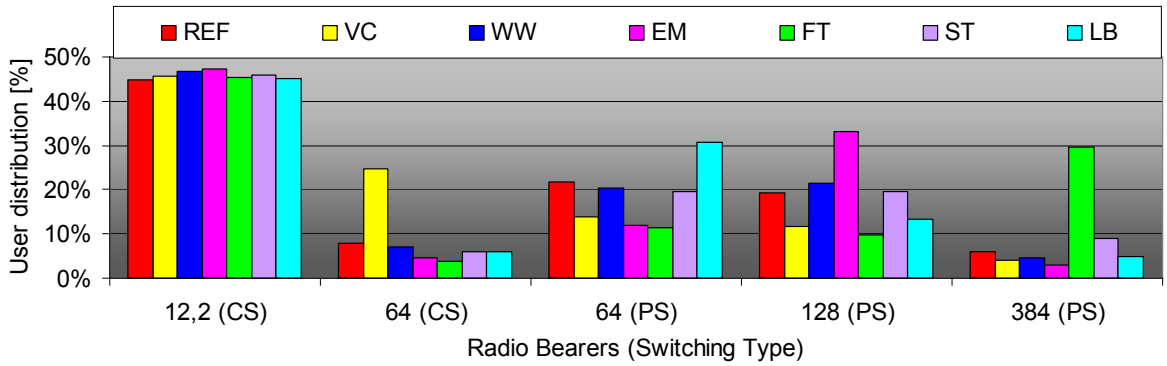

Figure 5.29 - RB distribution for DAC scenarios.

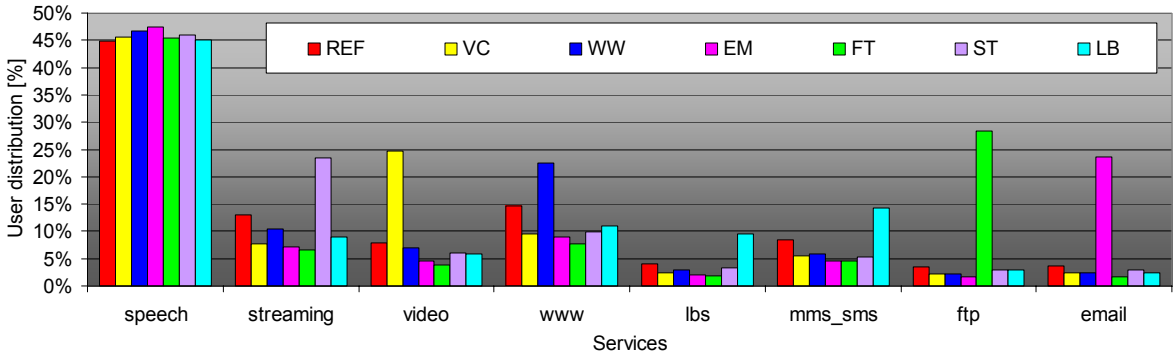

Figure 5.30 - Service distribution for DAC scenarios.

The analysis comprises the network blocking, Figure 5.31, and average delay, Figure 5.32, for each scenario (the 90 % percentile also shown). The reference scenario is now the DAC as characterised in Section 5.3, with approximately 3 % network blocking. Along with blocking

and delay performance, it is important to assess simultaneously the traffic volume distribution, Figure 5.34, and normalised rate, Figure 5.33.

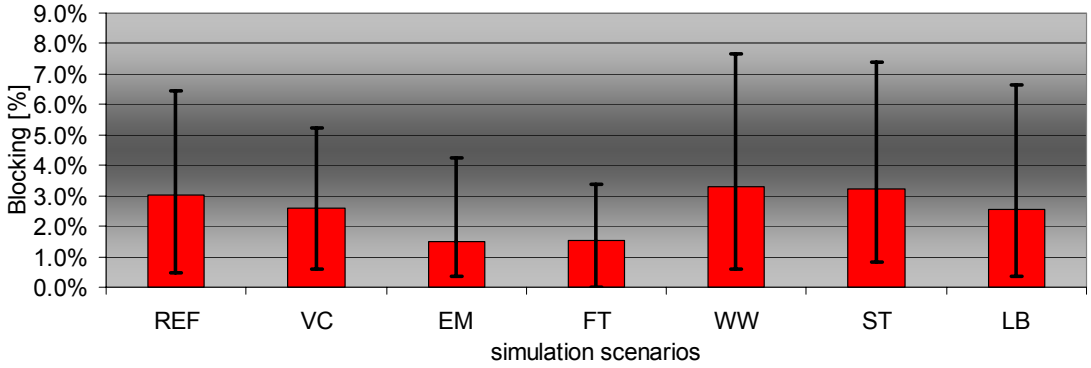

Figure 5.31 - Average network blocking rate for all DAC scenarios.

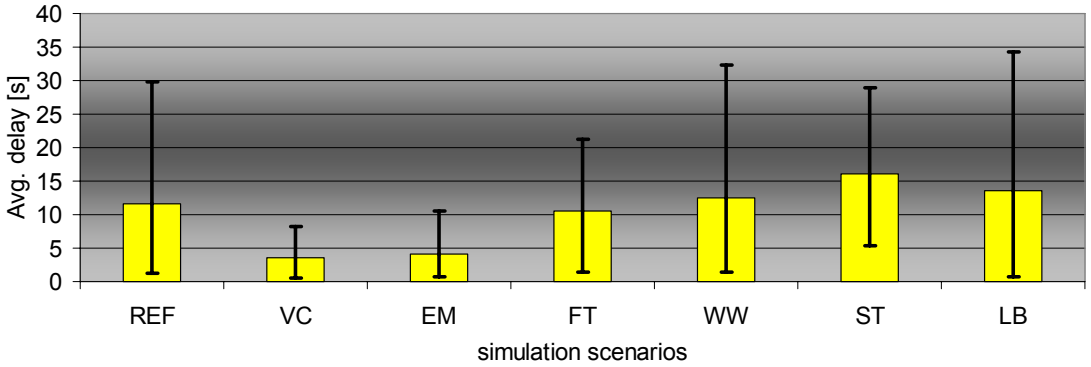

Figure 5.32 - Average delay for all DAC scenarios.

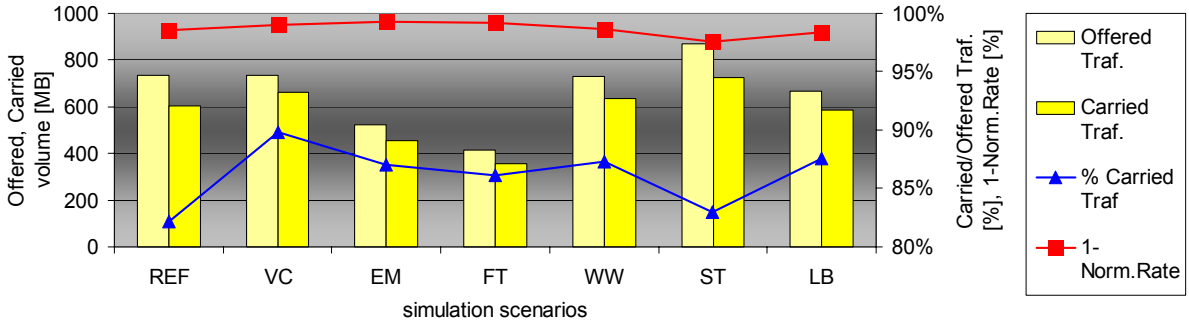

Figure 5.33 – Offered vs. carried traffic and normalised rate.

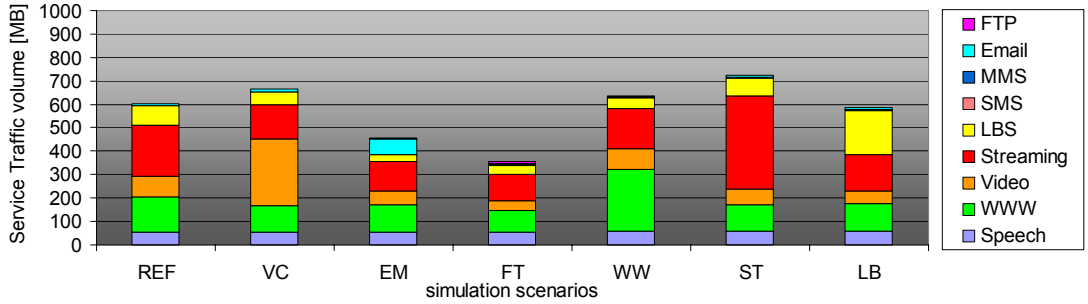

Figure 5.34 – Service volume distribution.

Concerning the average CS blocking rate, no big impact is noticed in VC and LB scenarios, as traffic volume is quite similar to the reference ones, and all these scenarios bias the lower CS or PS RBs (64 kbps) with lower performance impact. It is interesting to note the less sensitivity of the VC scenario, which shows a smaller 90 % confidence interval, as a main consequence of the priority of CS bearers against PS ones. For WWW and ST, associated with a slight higher traffic volume, the blocking rate also shows an increasing tendency (approximately 10 %) and a larger variation (90 % percentile) compared to reference (DAC) scenario. EM and FT services present the lowest blocking rate, mainly due to the low traffic volume, consequence of the source model modelling, as only one session for all services was considered. In fact e-mail and FTP traffic is expected to prevail along with WWW and streaming.

For the average network delay, interesting differences are noted in the REF (DAC), VC and LB comparison, since the CS switch dominance in video telephony service leads the delay to less than half of the figure for the other two scenarios. LB scenario shows a higher variation range, mainly due to the small packet/frame profile that characterises MMS and LBS services. Along with the higher blocking, WW and ST present the higher average delay figures. Also, it is interesting to note that the WWW source model being of more bursty nature, due to reading time uniform distribution, the average delay dispersion is higher than for ST scenarios. FTP services delay is high, compared with its low CS blocking rate, this fact being related with the absence of empty frames during data transmission (continuous frame usage) associated with a low RB simultaneity availability, as these services are mapped onto PS 384 kbps RBs. EM presents the lower average delay for the PS services.

From Figure 5.33, it can be concluded that no big impact exist in the carried traffic percentage, varying from 82 to 88 % of the offered traffic. The normalised rate curve shows also a similar trend to all studied scenarios, with worst performance for ST as it presents the worst blocking and average delay figures. Although presenting a higher average delay, and due to its nature, streaming services can easily accommodate packet delivery delays, being more sensitive to variations of the delay, which are higher for the WWW and LBS profiles.

E-mail and FTP source models, considering the default distribution/volume figures from [SeCo03], apparently are providing low volumes for both services, when compared with streaming or web services. Note that E-mail volume is growing, as attachments generated volume should be included. The increase on peer-to-peer traffic also drives the increase of big

files transfer (either in UL or DL), and its impact should be account when considering the FTP volume source models. The detailed impact of variation of the source model statistical characterisation is an important task that is proposed for further developments.

The blocking and delay causes distribution is shown in Figure 5.35 and Figure 5.36, respectively, where the dominance of DL load is clear as the main cause for blocking, with some DL power blocks for VC and WW, respectively, due to high pathloss (VC presents high distance blocks) for the former and due to high bit rate RBs (WW is biasing 128 kbps RBs) for the latter. One should note that blocking due to distance is manly due to CS64 users (video telephony), as UL coverage is defined for the lowest CS service (speech), explaining its higher weight for the VC scenario.

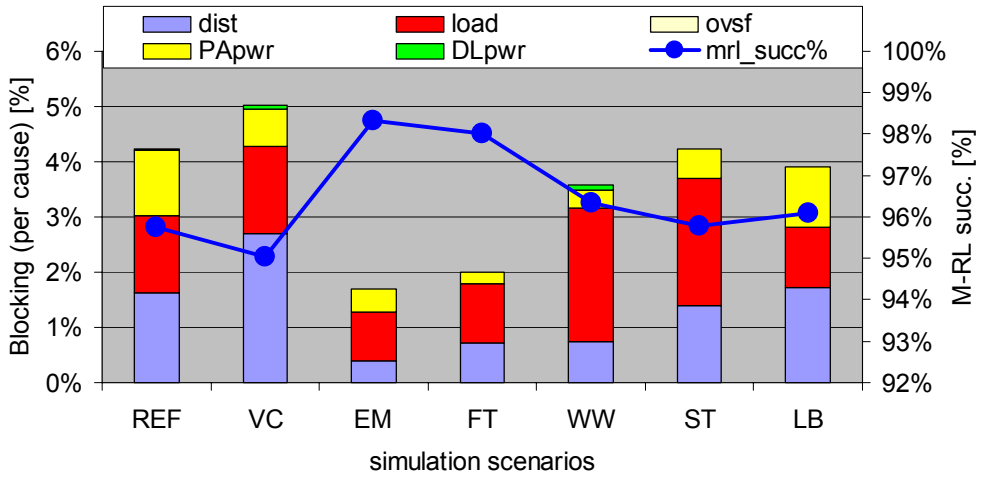

Figure 5.35 – Blocking cause's distribution for DAC scenarios.

As far as PS is concerned, delay is also mainly limited by DL load, Figure 5.36, where the percentage of allocated resources without delay ranges from 5 to 25 %. Note that these extremes happen in VC and FT scenarios as for the first one, the lowest PS traffic type percentage applies (CS64 dominant service) leading to a 25 % successful resource allocation without delay. The FTP case is by far the most stringent one regarding resource availability as main RB is PS 384 kbps, which presents the lowest users simultaneity capabilities due to natural WCDMA load limitation.

Another important aspect to consider is the SHO success rate (CS services) along with SHO percentage, see Figure 5.37. As expected, the SHO percentage remains similar for the four scenarios (approximately 22 % to 25 %). Due to lower priority on allocation of SHO links, the allocation success percentage is slightly less than the one for main link for all the scenarios,

namely VC, where the difference is higher due to CS dominance leading to SHO radio link blocking. EM and FT present better results, mainly due to the fact that the total carried traffic is lower than for the other scenarios.

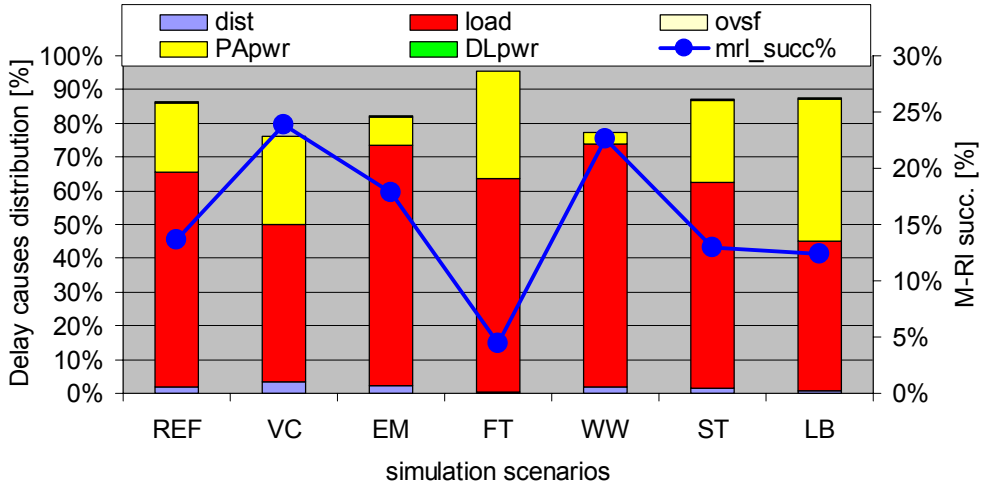

Figure 5.36 – Average delay causes distribution for DAC scenarios.

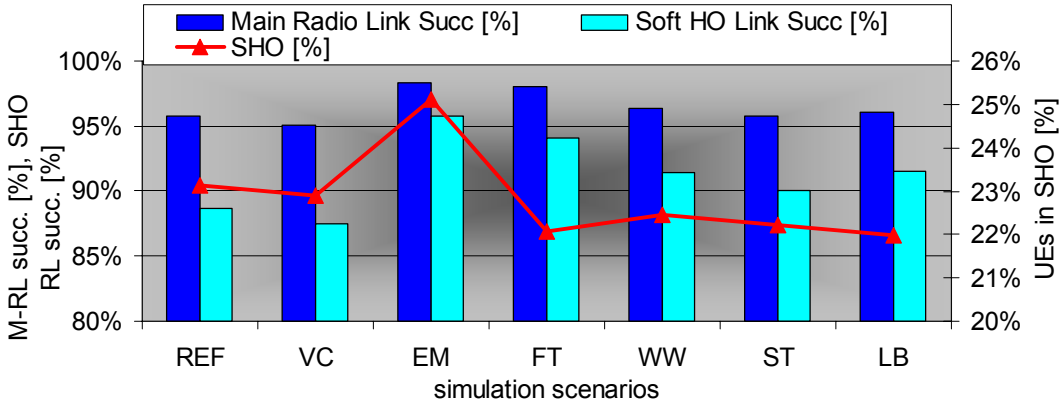

Figure 5.37 – Main and SHO radio link success and SHO percentage for DAC scenarios.

Concerning baseband processing capabilities needs with the traffic mix and offered traffic characteristics, radio link distribution (per SF), average PA power, maximum number of radio links (per cell) and channel element total (per cell) were analysed for all scenarios. Results are summarised in Figure 5.38 and Figure 5.39 (maximum and average refer to values in each of the 20 simulations performed). From Figure 5.39, there is no special trend for the average PA power with all scenarios reaching around 1.3 W. The same conclusion applies to the number of radio links (total or per SF) where minor changes are noticed. A lower number of maximum CEs (per cell) are required on average for FT, due to low number of users per cell, coming from PS384 kbps RB dominance. Note that although high bit rate RBs require more CEs, the total CEs for a scenario dominated by 64 kbps RBs will be higher, as the maximum

number of users exceeds the CE factor. As an example, a cell can handle 11 simultaneous PS 64 calls (22 CEs) while it only supports 2 simultaneous PS384 (16 CEs).

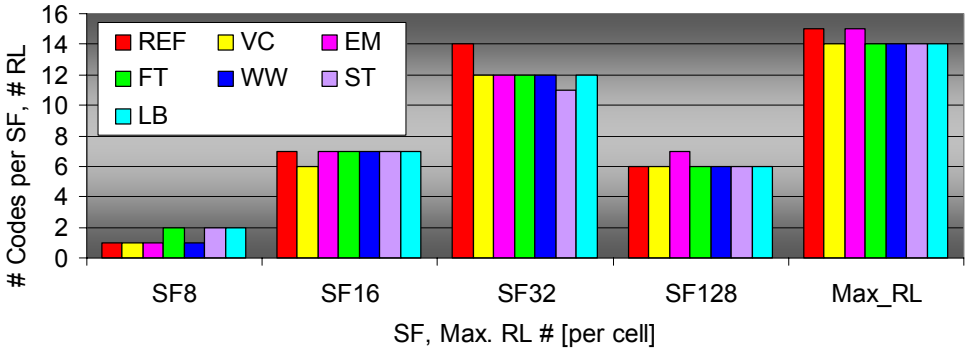

Figure 5.38 – Maximum RL per SF, maximum RL (average) for all DAC scenarios.

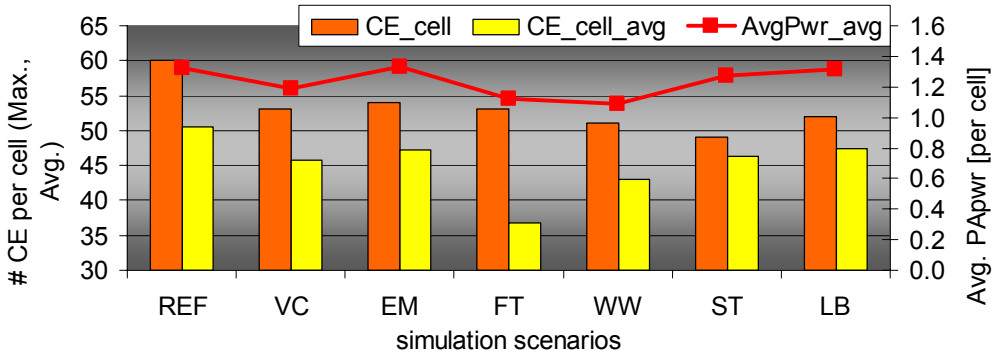

Figure 5.39 – Average PA power, CEs per cell for all DAC scenarios.

As explained in the last section, baseband units are shared by all sectors of a NodeB (shared pooled resource), thus, the total CEs needed is obtained from inferring on the three sectors needs, Figure 5.40.

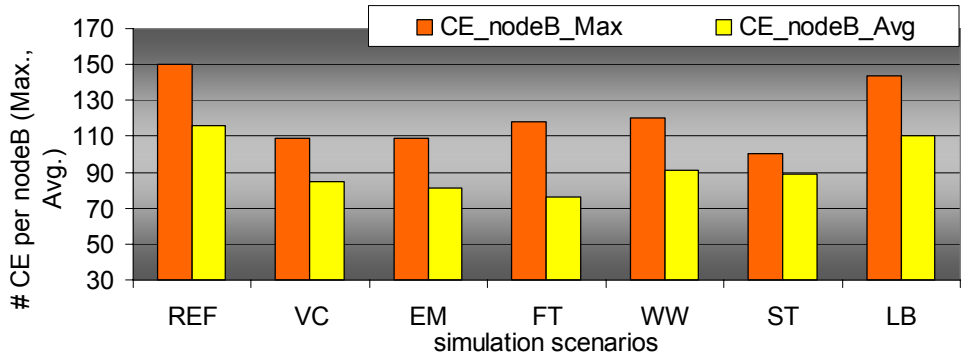

Figure 5.40 –CEs per nodeB for all DAC scenarios.

All tested scenarios lead to a lower maximum/average number of CEs required per NodeB, as the tested scenarios always bias a specific radio bearer. As identified, the DAC reference

scenarios RB distribution is similar to the scenarios where the PS64 RBs dominate, such as the LBS_MMS one, therefore, only this scenario presents NodeB CEs requirements similar to the reference one. At the PA level, the high bit rate of FT, and the LBS profile similar to the reference one lead to higher maximum average PA power usage, Figure 5.41.

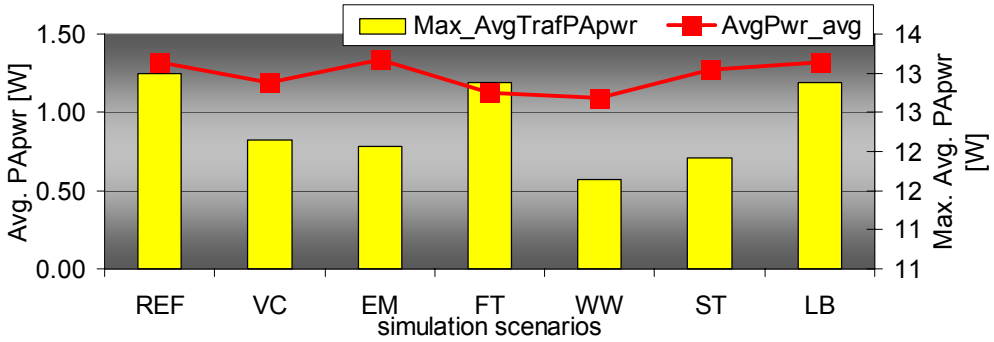

Figure 5.41 – PA power for all DAC scenarios.

In Figure 5.42 and Figure 5.43, DL load and PA power indicators are shown for the DAC scenarios. For EM the minimum and maximum blocking simulations provide similar figures for DL load/PA power, unlike the other scenarios where values diverge rapidly. As expected, all scenarios present a maximum load near the 70 % maximum target value. LB scenario presents the higher average DL load along with ST, WW and FT, due to the high rate services weight on traffic mix.

Only for scenarios with higher PS384 RB presence, the 14 W PA power is fully used, while for the remaining scenarios it presents lower values. Due to high volume and 384 RB high percentages, ST, LB and FT scenarios present the higher average PA power usage similar to the obtained in the reference (1.5 W).

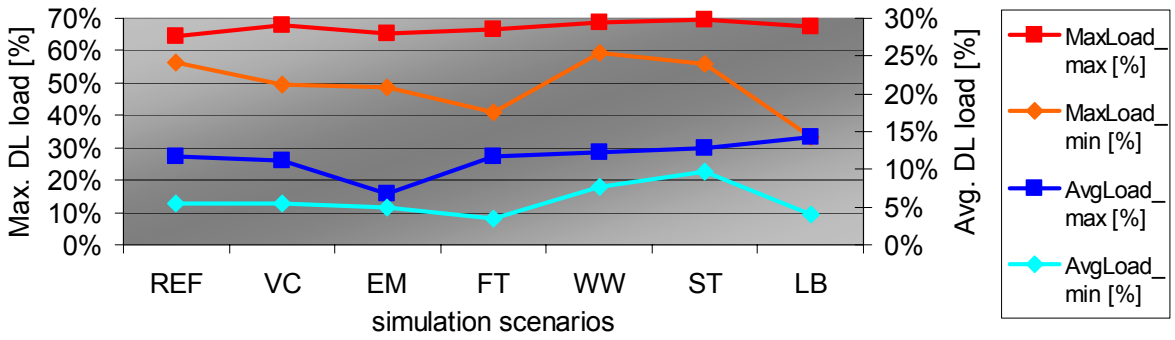

Figure 5.42 - Average network load and maximum cell load for DAC scenarios.

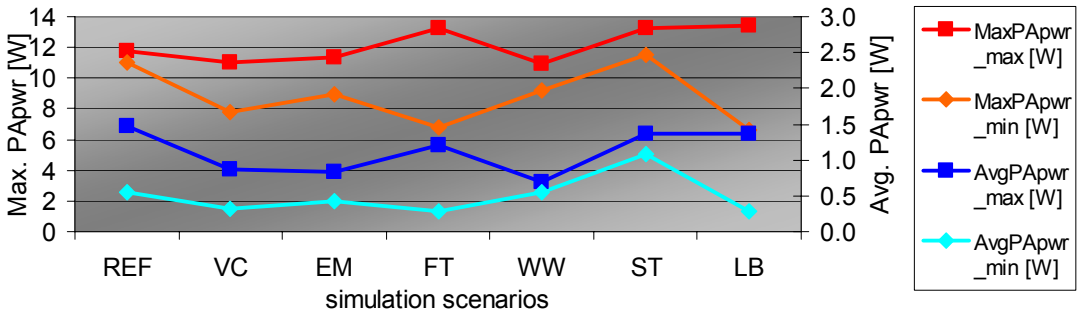

Figure 5.43 - Average network and maximum cell PA power for DAC scenarios.

From the simulations performed, it can be concluded that the WW and ST oriented scenarios show a slight increase in the blocking. Regarding delay, ST and LB presented the higher values. For the VC scenario is important to stress the lower delay impact as the service is carried over a CS RB. Concerning the system limitation, and due to 384 kbps RB dominance, the FT scenario presents a high PA power delayed call percentage along with a high cell PA power average. All scenario based on the DAC scenario showed similar CE requirements, with the dominant scenarios requiring less CE than the reference DAC scenario.

The WW and ST biased scenarios are in fact, the most probable one based on operators expectations [IIRC03], but present the worst blocking and delay performances, reinforcing the need of RRM to minimise load and PA power limitations (e.g. load and admission control).

5.5 HD vs. LD Scenario

5.5.1 REF, DAC and DAM Benchmark

In order to analyse the non uniformity impact, besides the cell level evaluation presented in last section, one need to study the impact of a different geographic scenario with lower site and user density (LD), but also with different clutter distribution, leading to a non uniform traffic generation, but of lower traffic density as defined for HD scenarios. The simulation process is similar to HD (20 simulations), but a population penetration of 2 % is considered, leading to 1337 users vs. 1382 from HD-1% scenario.

Since user density is lower than HD-1%, it was decided not to simulate the VOC scenarios, as it would lead to null blocking values. Besides user density, user demographic characteristics (see Annex G for LD demographical data) originate a more voice centric scenarios for the

same service distribution as HD, as shown in Figure 5.44 (see Annex H for district tables information), mainly due to lower average salary (medium-low) and lower education (low degree level penetration).

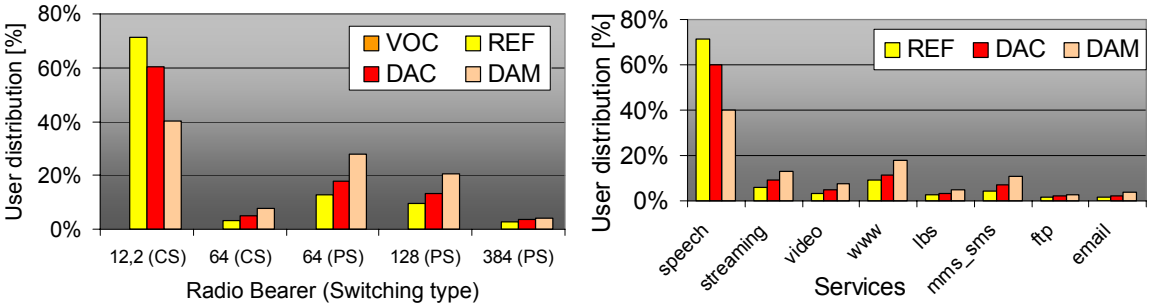

(a) Radio Bearer distribution (b) Service distribution

Figure 5.44 – RB and service distribution (LD – 2%, REF, DAC and DAM).

Comparing Figure 5.44 with Figure 5.8, it can easily be noticed that for the reference scenario one will have approximately 10 % additional users on speech service. No big impact is noticed at channel type distribution or indoor penetration distribution, comparing LD to HD (see Annex Q). As shown in Figure 5.2, a more uniform clutter distribution is present in the LD scenario, with no relevant differences either in channel type distribution or in indoor penetration loss distributions.

The first analysis is to assess the network blocking and average delay for each scenario. Note that now the reference scenario leads to much less than 1 % blocking, while even the DAM scenario leads to less than 1 %. For blocking and average delay figures, the 90 % confidence interval is also shown, along with average values, Figure 5.45.

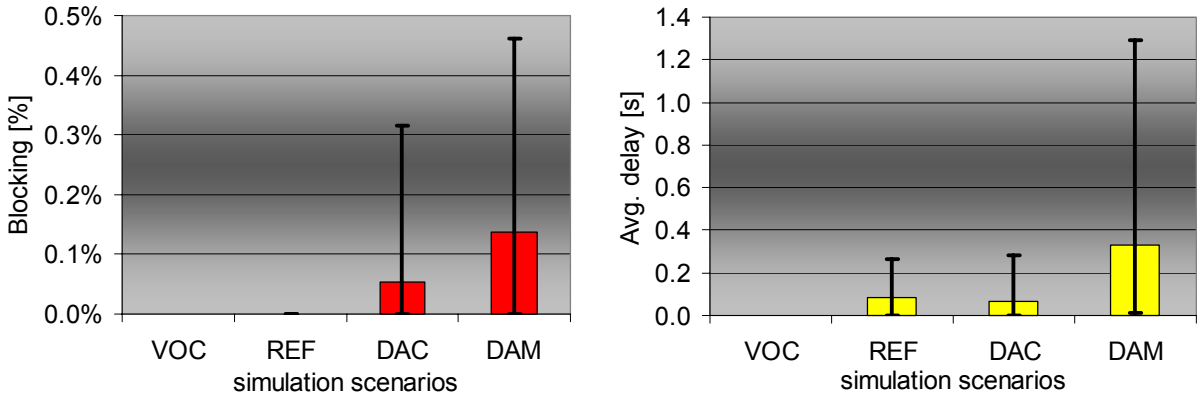

(a) Average CS blocking (b) Average PS delay

Figure 5.45 – Average CS blocking and average delay, 90 % confidence interval.

The low blocking and delay figures are mainly due to the fact that much less users can access the system, also present in lower network BH traffic volumes, shown in Figure 5.46, since the site plan is insufficient, as shown in blocking causes distribution (even assuming UL coverage enhancement with TMA, as demonstrated in Figure 4.24).

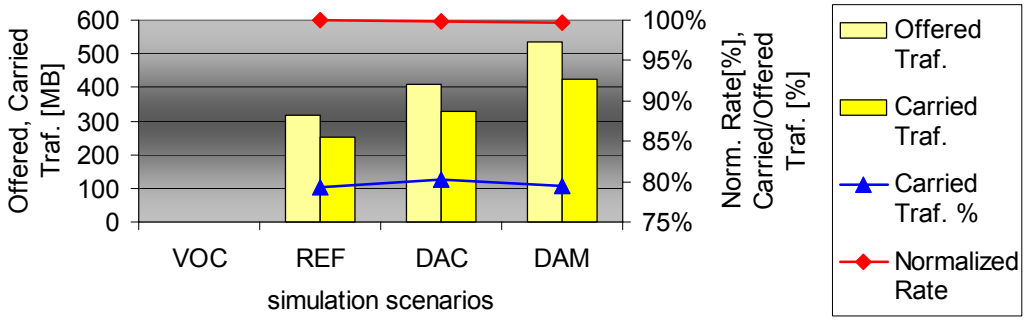

Figure 5.46 – Offered vs. carried traffic and offered traffic service split for LD scenarios.

The carried vs. offered traffic remains approximately 80 % for all scenarios, with a normalised rate close to unity with a light decrease as more data is present in the mix. Offered traffic split is shown in Figure 5.47, maintaining approximately the same distribution as Figure 5.13.

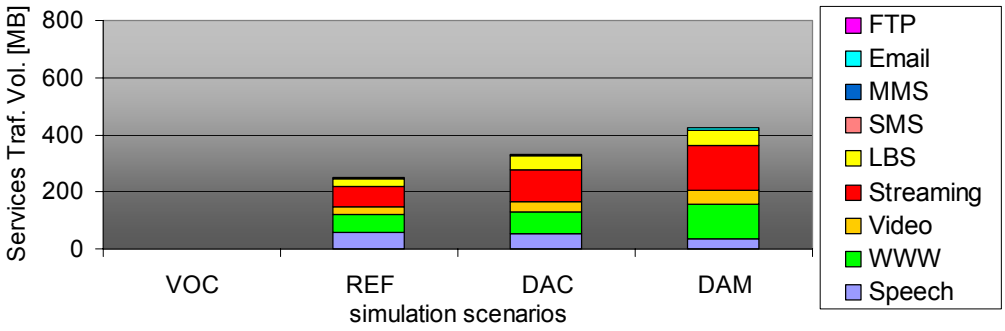

Figure 5.47 – Offered traffic service split for LD scenarios.

As verified in Section 4.4.2, the LD scenario presents a very poor UL coverage with high pathloss distribution, thus, the main blocking/delay causes are distance and PA power availability. Similar to HD, the increase of blocking due to distance is a consequence of the increase on data services that require a 64 kbps UL, more stringent than voice. Regarding delay, and for the reference scenario, around 30 % of the packet transmit attempts do not suffer any delay. All the detailed output analysis graphs are presented in Annex Q. In Figure 5.48, the blocking and delay causes partitioning is shown. The main radio link allocation success rate is also presented for CS and for PS (for PS it is defined if the link can be assigned with no delay).

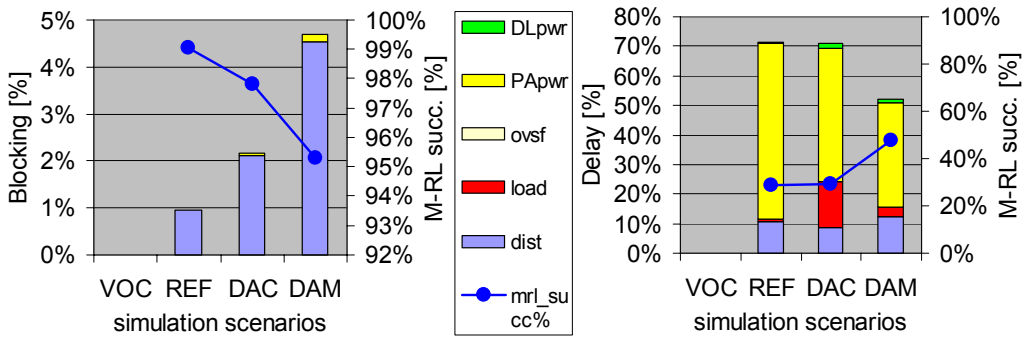

(a) Blocking causes (b) Delay causes

Figure 5.48 – Blocking and delay causes distribution for LD scenarios.

As expected, the SHO percentage remains similar for the three scenarios, now with a much lower value around 12 % as sites are sparse. Allocation success of SHO is very similar to the main link, except for the most data oriented scenario where a significant delta is found, Figure 5.49.

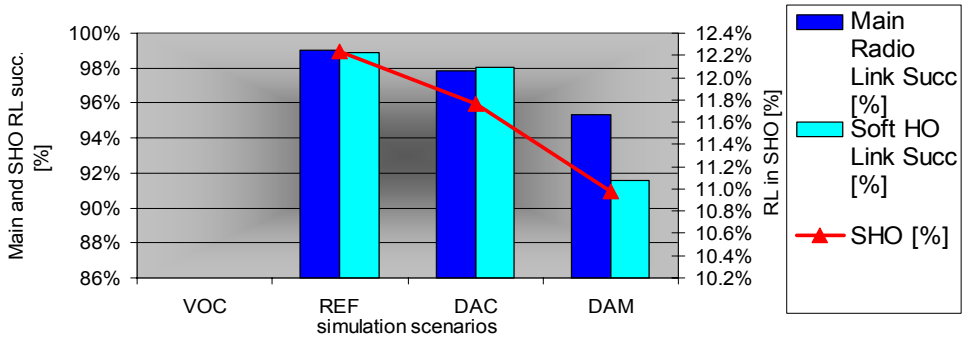

Figure 5.49 – Main and SHO radio link success and SHO percentage (LD).

In LD scenarios, baseband processing capabilities needs are shown along with radio link distribution (per SF), average PA power, maximum number of radio links (per cell) and total channel element per cell, Figure 5.50. As expected, radio links per SF are lower than for the HD scenario, namely for SF32 (PS64 kbps services) mainly due to the higher speech component in LD scenarios. Channel elements per cell and NodeB requirements are approximately half of the needed ones for the HD scenarios. Although LD is characterised by a lower network traffic volume, maximum PA power average is similar in both LD and HD, as LD average pathloss is higher than HD. Average PA power also follows half of the values obtained for HD, Figure 5.51.

Similar to HD, in Figure 5.50 it is interesting to note that for DAM scenario, the high data component is evident in the average PA power increasing tendency. Similar to the cell

behaviour, for the DAC scenario, the (maximum) requirement reaches 69 CEs per NodeB, compared with the 43 CEs for the REF scenario, Figure 5.51. Note that the scenario asymmetry assessment shows that for similar population penetration values, NodeB hardware configuration (baseband boards) will differ by an approximate factor of two with relevant costs for the operator deciding to start with unnecessary worst case configuration (e.g., 170 CEs vs. 69 in LD).

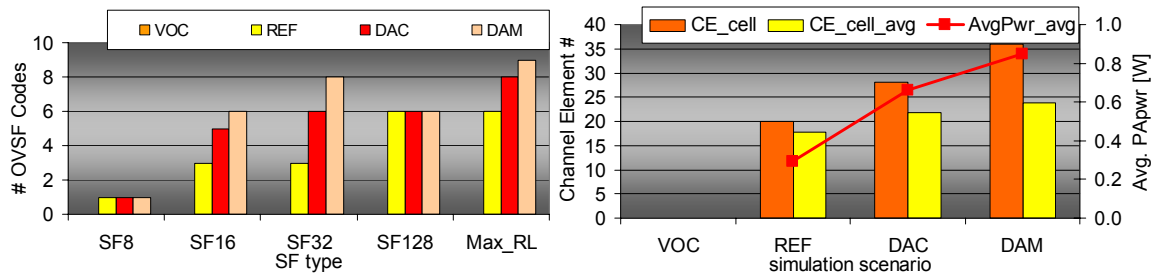

(a) RL per SF, maximum RL (b) PA power, CEs per cell

Figure 5.50 – Maximum RL per SF, Average PA power and CEs per cell (LD).

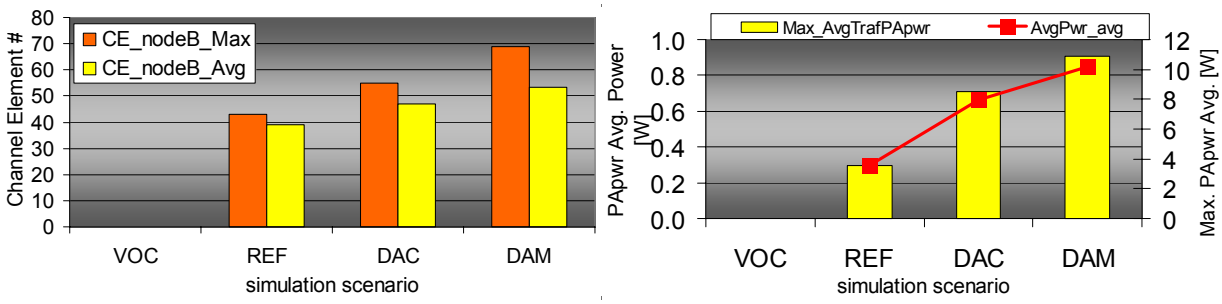

(a) NodeB CEs (b) PA power

Figure 5.51 –NodeB CE requirements and PA power (network and cell level).

In Figure 5.52 and Figure 5.53, DL load and PA power indicators are shown for LD scenarios. For all scenarios the minimum and maximum blocking simulations provide similar figures for the average DL load/PA power.

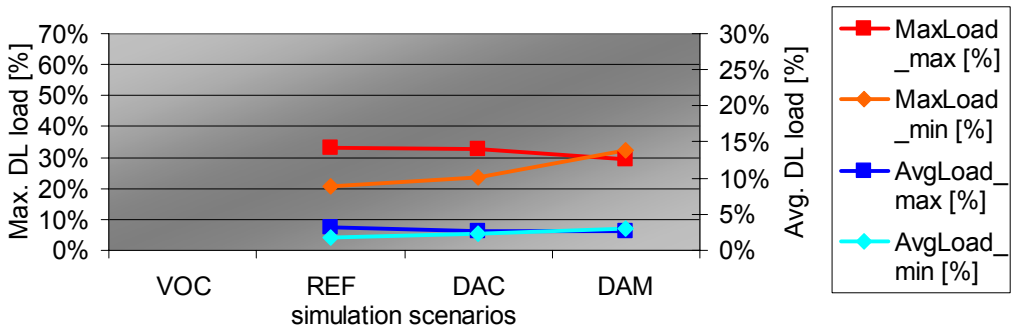

Figure 5.52 - Average network load and maximum cell load for LD scenarios.

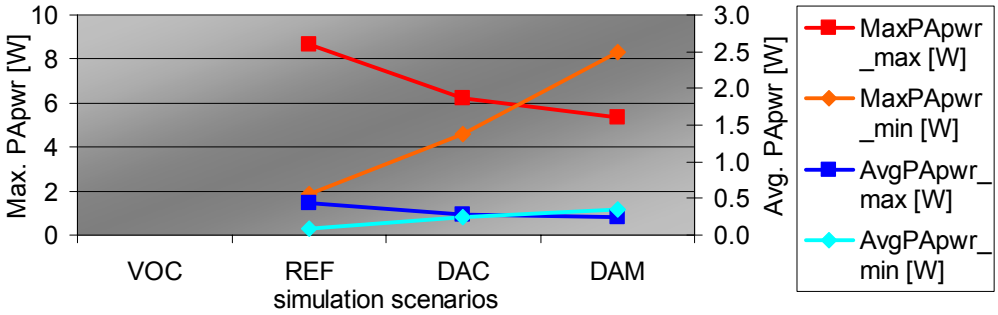

Figure 5.53 - Average network and maximum cell PA power for LD scenarios.

In all scenarios, the maximum load (70 %) is never reached leading to the very low blocking percentage due to DL load, but showing relevant PA power figures impacting the blocking rate due to PA power shortage.

5.5.2 LD Penetration and TMA Scenarios

As the LD scenario presents much lower blocking and delay figures, a 4% and 6% scenario were simulated, now taking the DAM service distribution as reference. Another aspect, considered as relevant, is the assessment of the network performance indicators, since the worst indicators were mainly related to poor (UL) coverage (high pathloss). As a consequence, a LD simulation set was run assessing the LD scenario performance impact of population penetration of 2, 4 and 6% along with the 2 % scenario assuming TMAs in all cells. From the theoretical point of view, the coverage area impact assuming TMA in UL is estimated, Figure 4.24. All the detailed output analysis graphs are presented in Annex Q.

Again, one starts by assessing the network CS blocking and average delay for each scenario. Note that now the reference scenario (LD_2 %) leads to much less than 1 % blocking, as shown in this section, while LD_6 % is now above 3 %, equivalent to HD-DAC-1% scenario. For blocking and average delay figures, the 90 % confidence interval is shown along with average values, Figure 5.54. The population penetration increase naturally leads to an increase in blocking and delay, as more traffic is offered to the network, Figure 5.55.

It is curious to see that the TMA impacts on service availability similarly as increasing the penetration to 6 %, as blocking rates are similar, but with TMA showing a lower variation (90 % percentile) since the user number is much lower, leading to lower variations. Average delay shows an increasing behaviour even from 6 % to 2 % with TMA. This effect is mainly

due to the higher packet delay in TMA scenario, where only 9 % of packets are served without any delay against 19 % in LD-6 % scenario.

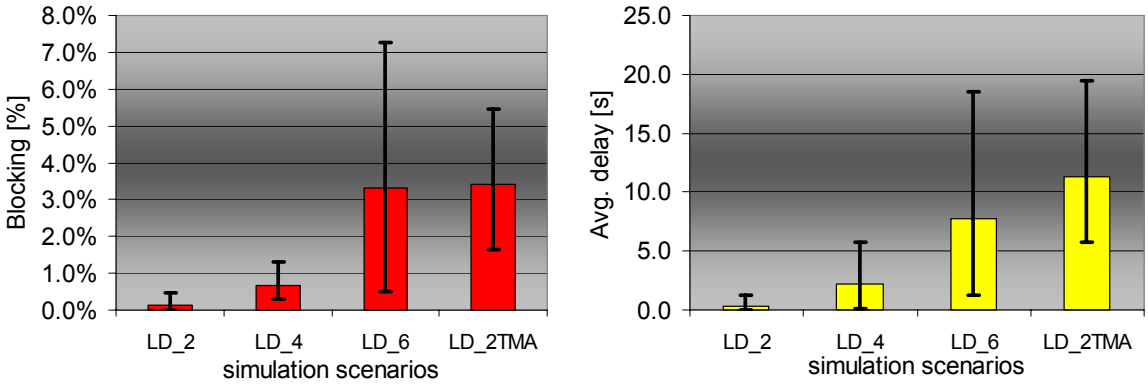

Figure 5.54 – Average CS blocking and average delay, 90% confidence interval.

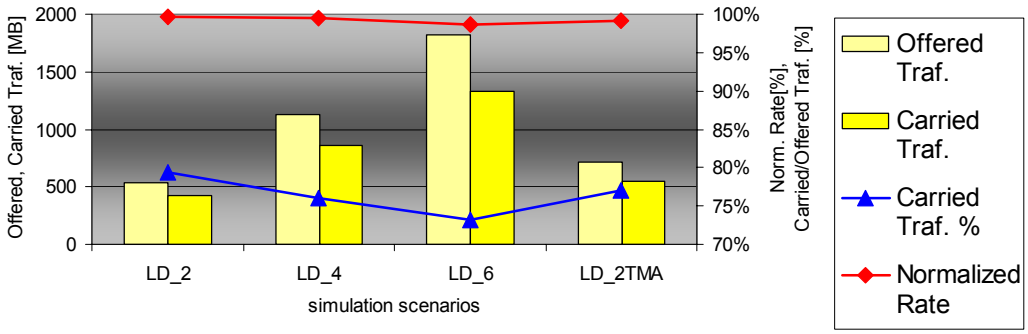

Figure 5.55 – Offered vs. carried traffic and offered traffic service split for LD scenarios.

The carried vs. offered traffic remains below 80 % for all new scenarios with a normalised rate close to unity, with a light decrease in the 6 % case due to higher delay. As expected, carried volume for the TMA scenario exceeds the value for LD-2% with no TMA in around 30 %, confirming the advantage of its deployment in site plans based on GSM site spacing, clearly insufficient to cope with service rates up to 384 kbps. Offered traffic split is shown in Figure 5.56, maintaining approximately the same distribution as Figure 5.13.

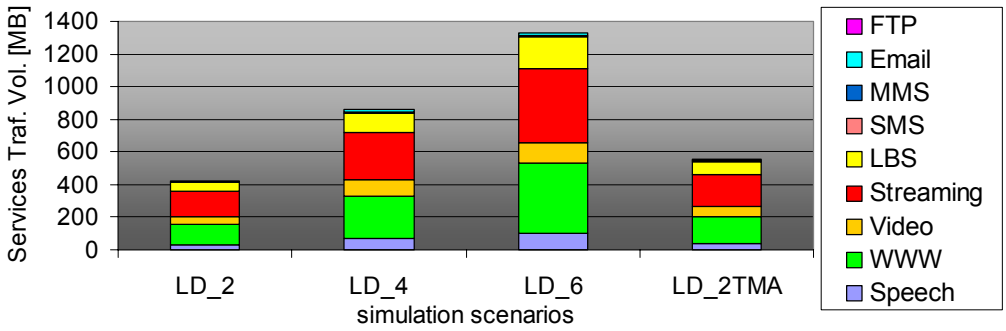

Figure 5.56 – Offered traffic service split for LD scenarios.

The increase of blocking due to penetration increase is seen from 2 to 6 %, although 4 % results are not conclusive, showing a different mix of blocking causes than the 6 % scenario. It is important to note that the TMA insertion reinforce the blocks due to power issues such as total PA power shortage (over 14 W) or violation of defined maximum DL Tx power per RB, showing a higher block weight on DL load limitations if compared with 6 % scenario. Concerning delay, the user's number increase naturally tends to reduce the distance drops weight, since it is more probable to have users covered that in lower penetration scenarios. The TMA scenario also presents high DL power delayed packets if compared with no TMA LD scenarios. The non delayed packet rate drops from around 50 % (2 %) to 9 % (2 % with TMA). In Figure 5.57, the blocking and delay causes partitioning is shown.

As expected, the SHO percentage remains similar for the three LD scenarios without TMA, but near 17 % for the TMA case as NodeB UL coverage increase leads to higher SHO areas. Note that SHO links success is naturally decreasing as penetration increases (2 and 6% scenarios). Important to note that main link success is similar in 2% penetration (TMA and no TMA case), but worst performance is found for TMA case as SHO areas increase as also the SHO failure rate, Figure 5.58.

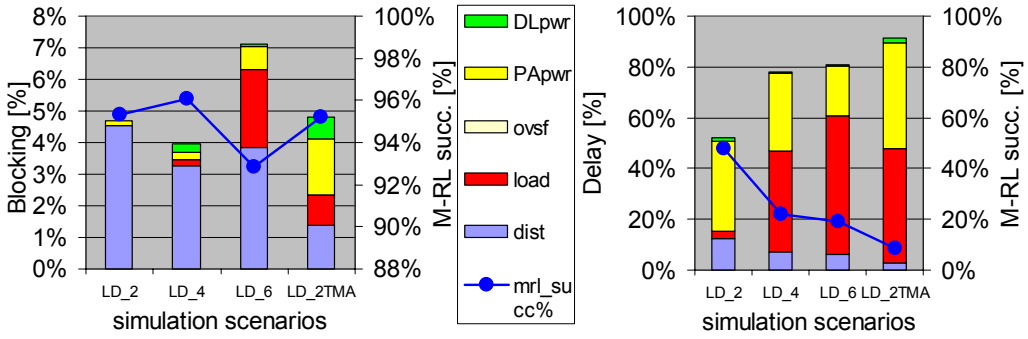

(a) Blocking causes (b) Delay causes

Figure 5.57 – Blocking and delay causes distribution for LD scenarios.

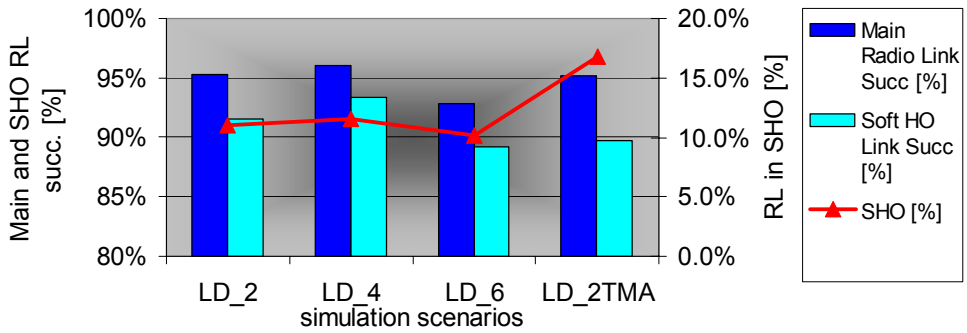

Figure 5.58 – Main and SHO radio link success and SHO percentage (LD).

In LD scenarios, baseband processing capabilities needs are shown along with radio link distribution (per SF), average PA power, maximum number of radio links (per cell) and channel element total per cell, Figure 5.59.

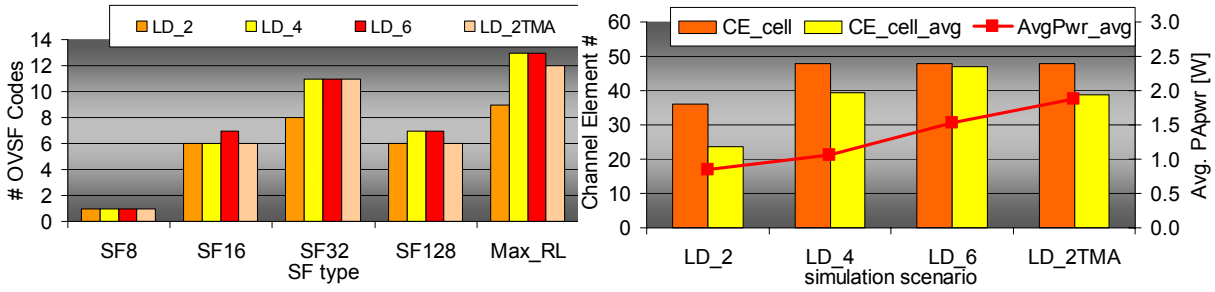

(a) Maximum RL per SF (b) PA power, CEs per cell

Figure 5.59 – Maximum RL per SF, Average PA power and CEs per cell (LD).

As expected, maximum radio links per SF are lower than for the HD scenario, but not much different from one scenario to another. Channel elements per cell and NodeB requirements show an increasing trend as penetration increases. TMA coverage extension strongly impacts on the number of CEs per cell, presenting a 68% increase for the LD-2% scenario. Another interesting fact is that as traffic volume grows (higher penetration), average CEs values tend to maximum CEs values per cell (high delay).

Average cell power of the TMA scenario is clearly higher than for the 6 % penetration one. This increase is expected as average UL maximum pathloss is increased, leading in an increase from 0.85 to 1.88 W. CEs per NodeB are approximately 112 units for the TMA case, with maximum average cell power reaching its maximum theoretical value near the 14 W, Figure 5.60.

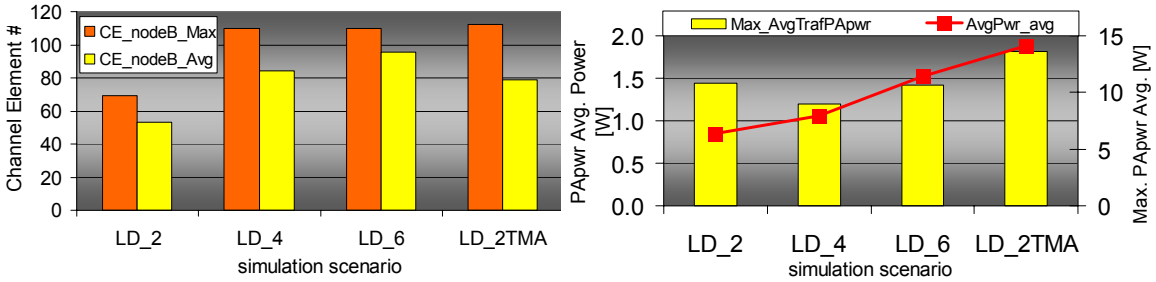

(a) NodeB CEs (b) PA power

Figure 5.60 –NodeB CEs and PA power (network and cell Maximum Average).

In Figure 5.61 and Figure 5.62, one shows the DL load and PA power indicators for the LD scenarios.

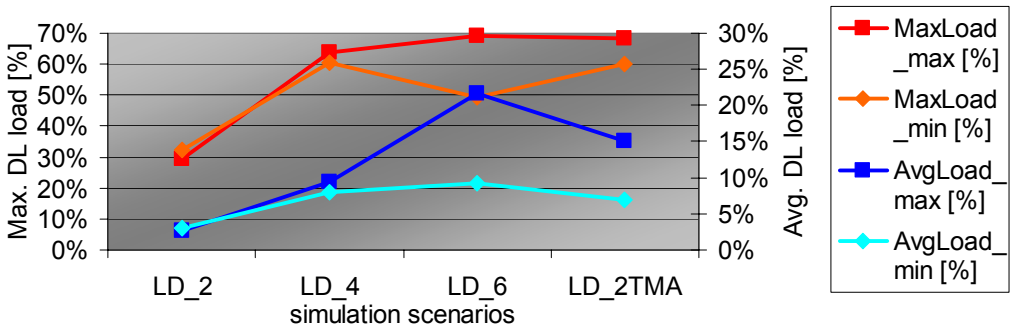

Figure 5.61 - Average network load and Maximum cell load for LD scenarios.

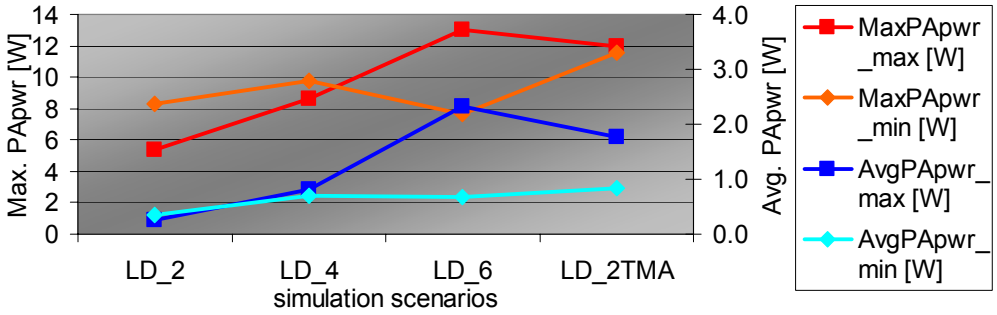

Figure 5.62 - Average network and maximum cell PA power for LD scenarios.

Differently from REF/DAC/DAM LD scenarios, the maximum load (70 %) is now reached, leading to significant blocking percentage due to DL load, but showing relevant PA power figures impacting on the blocking rate due to PA power shortage.

The benchmark on LD vs. HD shows an important performance difference when comparing the REF/DAC/DAM scenarios. The difference is mainly due to the different demographics and lower traffic volume as significant users do not have service as the site density is insufficient to guarantee a homogeneous coverage layout. Blocking and delay causes are mainly distance and PA power as LD scenarios present higher average pathloss. NodeB CEs requirements shows significant difference from LD and HD scenarios, reinforcing the advantages on careful dimensioning approaches, allowing significant savings in equipment.

From the several penetration LD scenarios, values show that LD penetration can be increased up to 4 % for similar blocking performance as HD ones. Besides the penetration impact, TMA assessment show important conclusions on its advantages in low NodeB density deployments. TMA scenario presents similar blocking as the 6 % LD without TMA, but significant changes in the blocking/delay causes distribution as DL link budget is now unbalanced due to UL TMA enhancement, impacting PA power and RB power availability.

6. Conclusions

The objective of this thesis was to analyse the overall performance of a multi-service non-uniform traffic UMTS (FDD) network, mainly focussing on capacity aspects of the radio interface. A one carrier system was considered, and NodeB dimensioning aspects, such as blocking, average delay and baseband processing capabilities requirements were investigated. The analysis was performed with the aid of a newly developed simulation platform, considering several scenarios in service and geographical configurations. Different approaches were followed for the analysis of the overall performance results, namely:

- analysis of the impact of users traffic mix variations (in order to analyse the impact of the statistical behaviour of user generated traffic on the overall performance);
- analysis of the impact of the number of users on specific scenarios, corresponding to different penetration percentages and considering coverage enhancements features/strategies (TMA);
- analysis of the impact of a given number of users with specific dominating traffic profiles on a non-uniform network scenario;
- analysis of similar traffic mixes in different site and demographic scenarios.

A key and novel approach in UMTS FDD network performance assessment of the present work is the multi-service non-uniform user generation algorithms, based on demographics/geographical data, jointly with the time-frame traffic generation and network performance evaluation.

This approach upgrades and gathers in the same software platform the user generation process, normally implemented over traffic density maps with limited multi-service handling, along with a frame level processing, allowing the implementation of specific RRM algorithms, which enable NodeB and UE performance analysis to a very detailed scope. Note that most commercial solutions opt to develop or put more emphasis in one of the main function of TRFSIM3G depending on its specificity; radio planning tools use traffic maps and normally implement a Monte Carlo approach to evaluate system performance based on the multi-service profile, but no time domain analysis is performed, mainly due to the computational effort involved. Other tools are specialised in RRM algorithms implementation (normally with a limited set, based on 3GPP available or specified algorithms), and present a

cell scope analysis rather than a network perspective which is required to assess multi-service and non-uniform traffic aspects together, as it is the main focus of this thesis.

As a first step for the development of the present work, the radio interface specificities of FDD (R99) have been studied, with the aim of establishing simple capacity models to be further implemented in the simulation platform. Additional investigation was performed on traffic source modelling, in order to best describe/characterise the multi-service traffic profile along with non-uniform user generation approaches.

In the implementation of TRAFSIM3G, namely to the interference and call admission modelling, several approximations were considered, in order to enable the desired analysis in the context of a Master Thesis. Nevertheless, there was always the concern that the taken approximations kept the essential characteristics of system behaviour. An example of the adopted approximations can be the air interface load estimation in DL for UMTS where a simplified inter-to-intra cell interference ratio figure is used, in order to ease the simulation process, otherwise each UE/NodeB contribution to other cells interference should have been calculated each frame, compromising the simulation time. Although the calculation of the inter-to-intra cell interference ratio is possible to be enabled with a higher calculation time, a small impact on final statistical analysis of the several scenarios would be obtained. Other approximations include, for example, "rounded" MAC frame durations for all services, neglecting all RLC/MAC specific buffering and retransmission specificities, and ideal (closed loop) power control as E_b/N_0 figures already include this effect.

Eleven different applications have been considered for user traffic generation: Voice Call, Video Call, Video and Audio on Demand, Interactive Gaming, Web Browsing, LBS, MMS, Chat, E-mail and FTP, representing all four service classes (with different QoS requirements) defined by 3GPP, and exploring the most probable combinations of radio bearer and traffic source models. These applications and the supporting services have been characterised in detail. In order to implement the user traffic generation mechanisms in the simulation platform, specific traffic source models, as well as call/session generation and duration processes, were necessary for each considered application. For this purpose, an extensive literature survey has been performed to obtain such traffic source models and respective parameterisation values. A complete mapping between the considered applications and traffic source models/Radio Bearers has been performed, but leaving a flexible structure to enable future studies and mapping.

The developed simulation platform, implemented in MapBasic® and Visual C++ programming languages, is based on two main functional blocks:

- GIS Engine, which is responsible for generating users and their associated applications/services along with UL coverage characterisation. The outputs of this block are user locations with respective service type and UL coverage analysis, such as pathloss and possible serving NodeB cells.
- Traffic Processing Engine, which is the main functional entity of the simulator, as it performs all the traffic generation and processing tasks along with RRM algorithms implementation. It receives the user information generated by the GIS Engine module (through a flat file structure) and processes its information according to defined RRM configured parameters, such as active set, SHO, etc..

For simplicity, the simulator only considers DL user traffic processing, disregarding the UL components, due to the high asymmetry of the majority of the considered applications, with a higher capacity demand in DL, and also because, in general, the DL component is capacity limited, opposed to the UL ones, which are usually interference/power limited. When applicable, references to possible UL system limitation(s) are referenced and quantified. The option to focus mainly on DL system aspects is also present in similar works dealing with UMTS traffic mix impact in system performance, e.g., [MaZe02].

Several tool user-defined inputs parameterise the simulator, enabling the simulation of different user generation profiles, including different demographic/geographical scenarios, applications and radio bearer mappings. The simulator provides several types of output indicators for overall network performance evaluation, namely CS (call blocking rate), PS (average delayed frames and normalised rate (average bit rate) at cell level) traffic statistics, traffic volume per application (all network), blocking and delay causes distribution, mobility indicators (main link, SHO links success rate and users in SHO percentage), baseband capacity required per cell and NodeB level (number of channel elements, including common channels), PA power usage (average and maximum values), DL load (average and maximum at cell/network level). Most of these indicators are also available at cell level, in order to assess the non-uniform traffic impact on overall performance.

The developed simulator tool constitutes a flexible and upgradeable platform, allowing, for example, an easy inclusion of different demographic/site/geographical scenarios or different

multi-.service profile. Hence, this simulation platform provides a complete functional framework for the evaluation of a multi-service non-uniform traffic UMTS (FDD) network.

All different scenarios (High Density (HD)/Low Density (LD) and multi-service variants) that are analysed in the present work are characterised according to their three main components: site/demographics, users and applications. In order to assess the impact on the data vs. speech split, 4 main service distributions scenarios were created: a voice centric (VOC), reference (REF), data centric (DAC) and data mostly (DAM) scenarios. All these scenarios were launched in the HD area profile with a population penetration rate of 1 %.

Three major performance indicators are considered for the overall performance analysis of these simulated scenarios: CS calls blocking rate, average delay of PS packets/frames, and mean bit rate obtained (normalised rate). Auxiliary parameters, helping in the results analysis, are also considered, namely the mobility, DL load and PA power usage statistics. When needed, a cell level indicator analysis is performed, in order to better understand network results trends.

Each simulation run (corresponding to one busy hour simulation) lasts approximately 80 minutes in a Pentium IV 2 GHz computer with 512 MB of RAM. The scenarios service mix impacts strongly on the simulation periods ranging, for example, from 70 to 250 minutes for HD-1% VOC and DAM scenarios, respectively. This effect is mainly related with the PS delay implementation approach, since on every PS delay, the user traffic vector, including frame number and packets to transmit, needs to be updated.

From the statistical analysis of user traffic variations performed in this work, it is verified that 20 simulation runs per scenario provide an already reasonable statistical behaviour, therefore, allowing the extrapolation of indicative error margins for results obtained from single simulation runs. Besides the number of simulation runs, investigation on population penetration figures (0.5, 1, 2, and 3 %) is performed in order to infer on the reference penetration value that leads to approximately to 1% service blocking for the HD scenario, which is 1 %.

From a network performance viewpoint, the error margins (i.e., 90 % confidence interval or standard deviation) observed for the performance indicators are acceptable. Note that the non-traffic uniformity induces a very asymmetric cell behaviour, requiring some caution when defining the minimum number of runs required for results convergence, establishing a trade-

off between accuracy and computation time. For the REF scenario (HD-1%) and considering 20 simulations, the standard deviation value is 0.21 % with an average blocking of 0.97 %. For all tested scenarios, blocking and delay standard deviation validation and 90 % confidence interval are evaluated (see Annex O). The obtained figures allow a reasonable degree of confidence on the results obtained with 20 simulation runs.

The first analysis concerning the HD demographic/site scenario is to assess the speech vs. data split impact on network performance, on the defined 4 service scenarios (VOC, REF, DAC and DAM) while keeping penetration to the 1 % reference value (1382 users/17 NodeB). The evolution of the performance indicators with the increase of the number of PS users behaves as expected, i.e., the calls blocking and the average packets/frames delayed increases, while the mean bit rate (normalised) decreases. As a consequence of the data driven scenarios, offered traffic volume also increases due to PS dominance over speech (CS64 video-conference although mapped to CS64 RB was considered as data type services).

The DAM scenario presents a blocking rate 5 times higher than the REF one, and an average delay 15 times higher. The increase is due to higher data services volume, which using a higher RB, present less possible simultaneous connections, mainly due to a higher DL load. Blocking and delay causes are mainly due to DL load along with PA power shortage for DAC and DAM scenarios, as DL power levels are higher for higher bit rates (lower SFs). Mobility is affected, as less SHO links are successful when more data dominates the mix, with users in SHO near 22 %. Average PA power and baseband capacity present an increasing trend up to the DAC scenario, naturally bounded by the higher weight of higher bit rate bearers. As expected, for DAC and DAM scenarios, a strong correlation between blocking, average delay and normalised rate is obtained.

After the first simulation set, DAC was defined as the reference scenario and 6 additional scenarios were created by polarizing the traffic mix to a source model, obtaining in the overall service distribution a weight higher than 20 % (VC (video telephony), WW (WWW), ST (streaming), LB (LBS and MMS), EM (E-mail) and FT (FTP)).

As far as the average blocking rate is concerned, no big impact is noticed in VC and LB scenarios, since the traffic volume is quite similar to the reference one and all these scenarios bias 64 kbps CS or PS RBs, with a lower performance impact. It is interesting to note the less sensitivity of the VC scenario, which shows a smaller 90 % confidence interval, mainly as a consequence of the priority of CS bearers against PS ones. For WW and ST, associated with a

slight higher traffic volume, the blocking rate also shows an increasing tendency (approximately 10 %) and a bigger variation (90 % percentile) compared to the DAC reference scenario. EM and FT services presented the lowest CS blocking rate mainly due to the low traffic volume, consequence of the source model modelling, as only one session for all services was considered. In fact, e-mail and FTP traffic is expected to prevail along with WWW and streaming.

For the average network delay, interesting differences are noted in the DAC, VC and LB comparison, since the CS switch dominance in video telephony service leads the delay to be less than half of the figure for the other two scenarios. The LB scenario shows a higher variation range, mainly due to the small packet/frame profile that characterises MMS and LBS services. Along with the higher blocking, WW and ST present the higher average delay figures. Also the WWW source model, being of a more bursty nature, due to a reading time uniform distribution, the average delay dispersion is higher than for ST scenarios. FTP services delay is high, compared with its low blocking rate, this fact being related to the absence of empty frames during the data transmission (continuous frame usage) associated with a low RB simultaneity availability as these services are mapped to PS 384 kbps RBs. EM presents the lower average delay for the PS services.

It can be concluded that no big impact exists in the carried traffic percentage, varying from 82 to 88 % of the offered traffic. The normalised rate curve shows also a similar trend for all studied scenarios, with a worst performance for ST, as it presents the worst blocking and average delay figures. Although presenting a higher average delay, and due to its nature, streaming services can easily accommodate packet delivery delays being more sensitive to variations on the delay, which are higher for the WWW and LBS profiles.

From the blocking and delay causes distribution the dominance of DL load is clear as the main cause for blocking, with some DL power blocks in VC and WW, due to the high pathloss (VC presents high distance blocks) in the former, and due to high bit rate RBs (WW is biasing 128 kbps RBs) in the latter. One should note that blocking due to distance is mainly due to CS64 users (video telephony), as UL coverage is defined for the lowest CS service (speech), explaining its higher weight for the VC scenario.

Finally, two demographic/geographical scenarios are compared, where site and user density differ strongly. For similar penetrations, LD scenarios (REF, DAC, DAM) present much lower blocking and average delay figures (DAM blocking and average delay of 0.14 % and

0.33 s respectively). Main drop causes are identified as distance (UL coverage) ones, as site density does not guarantee service continuity in all district area. In order to minimise deficient UL coverage, a LD-2% DAM scenario was set with TMAs, results pointing to additional 30 % carried volume, while maintaining blocking around 3.4 % and average delay in the order of 11 s, value aligned with HD-1% for DAC scenarios. The TMA consideration leads to higher block/delay causes, related to power shortage either in total PA power availability or in crossing maximum defined transmit power per RB.

Besides the reference scenario calculations (penetration from 0.5 to 3 %), the impact of the number of users is also analysed for the LD scenario (2, 4 and 6 %), maintaining the same applications scenario (DAM). The evolution of the performance indicators with the increase of the number of users behaves as expected, i.e., the calls blocking and the average packets/frames delayed increases while the normalised rate and carried to offered traffic volume ratio decreases. One should note that for the LD scenario with 6 % penetration, the blocking rate is still under the value obtained for HD-1% with the same application scenario. Note that these scenarios differ approximately in 3 times the number of users for a same number of NodeBs (17).

The studied scenarios show a significant dependence on the blocking and delay figures as function of the speech/data ratio, showing and increasing trend on blocking and delay as data services dominate the traffic mix. Associated with data increase, the blocking/delay causes distribution is mainly composed of DL load and PA power limitation due to higher RBs present in the network. The service dominant scenarios show lower impact in performance, with emphasis on WW and ST scenarios that present the higher blocking rate values. NodeB CEs requirements presented it maximum for the DAC scenario, with significant differences when addressing LD scenarios, reinforcing the need to adequate network dimensioning procedures to the expected network traffic density. TMA consideration proved to be an effective way to improve system performance, specially UL coverage, but introducing higher DL power limitation either at PA power and RB link TX powers.

This is not at all a finalised work, mainly due to the complexity of the subject as well as the variety of still possible studies underlying this Thesis. A wide range of issues can be improved, leading to the evaluation in a more realistic and detailed manner of the network performance in multi-service non-uniform UMTS FDD networks. Several improvements are proposed along this Thesis, focusing in improvements related either to the implemented

algorithms and programming structure, or related with future studies extending beyond the main scope of this work. The following paragraphs summarise some of these issues, which are left as suggestions for future investigation:

- Extension of the available propagation models to COST-231 Hata [DaCo99] to be used in the assessment of suburban, rural or axial network performance, as COST-231 WI is only adequate for dense urban/urban areas, where building structure is easily parameterised.
- Improvements in the CAC algorithm, as it only distinguishes CS and PS calls (on-going and starting calls), not providing a true PS QoS for streaming and Interactive/Background type traffic. Desirably, the resource allocation algorithm should include priority queues depending on the QoS type, and packets should be process according to its priority
- Conclusion of channel switching and load control algorithms, which already include several algorithm segments implemented in TRAFSIM3G, for their easy introduction in possible software platform evolutions. Inclusion of smart PA algorithms, such as shared PAs per cell, allowing a cell to use other cells PA to cope with high power requirements.
- Running of other scenarios, activating the inter-to-intra cell calculated figures and evaluating its impact in all studied scenarios.
- Performing of an in-depth analysis of other application scenarios, namely with different traffic profiles per user type, and their impact in the overall network performance. Extension to other site/user density scenarios namely suburban and rural.
- Enhancement of the traffic source models, both in type and parameterisation.
- Improvement of the traffic processing algorithms, namely with the implementation of additional carriers along with load control including traffic sharing among carriers.
- Inclusion of HSDPA (High Speed Downlink Packet Access) as a main DL boosting feature evolution for R5 UMTS networks, allowing the impact assessment of R99 and HSDPA traffic share in the same or different carriers for the issues of DL load, PA power and NodeB baseband capacity.
- Inclusion of specific QoS at user level, as more and more operators are forced to high QoS in specific segments, such as corporate and where pre-emption and priority access to UMTS networks will impact lower priority users.

Annexes

A. Physical Channels Description

In Table Annex A.1 a summary of R99 FDD channels main characteristics can be found.

Table Annex A.1 – Physical Channels in UMTS.

Channel	Definition	UL/DL	Characteristics
P-CCPCH	Primary - Common Control Physical Channel	DL	Fixed Rate. Broadcast continuously (System Information). Always scrambled by the Primary SC. Not transmitted during first 256 chips of each slot since time multiplexed with SCH. Sends OVSF to the UE.
S-CCPCH	Secondary - Common Control Physical Channel	DL	SF = 256 to 4. Always scrambled by the Primary SC. Not inner-loop power ctrl. Not always transmitted.
DPDCH	Dedicated Physical Data Channel	UL/DL	Traffic plus Signalling (Measurements, Mobility Management, Call Control, Radio Resource Control, etc)
DPCCH	Dedicated Physical Control Channel	DL	No transport channel associated. Signalling only, includes: TFCI, TPC, Pilot bits, FBI (UL only)
PRACH	Physical Random Access Channel	UL	Carries random access info of the UE accessing the network.
P-SCH	Primary Synchronisation Channel	DL	Common Channel. No transport channel associated. Not scrambled nor OVSF coded. Time multiplex with PCCPCH. Used for cell search procedure (Slot synchronization).
S-SCH	Secondary Synchronisation Channel	DL	Common Ch. No transport channel associated. Not scrambled nor OVSF coded. Time multiplexed with P-CCPCH. Used for cell search procedure (SC group identification).
P-CPICH	Primary Common Pilot Channel	DL	No transport channel associated. Fixed rate @ 30 kbps. Always scrambled by the Primary SC.
PICH	Page Indication Channel	DL	No transport channel associated. Fixed rate (SF=256).Used to carry the Paging Indicators (PI) informing the UE that paging info is available on the S-CCPCH. Always associated with an S-CCPCH (mapped with PCH).
AICH	Acquisition Indicator Channel	DL	No transport ch. associated. Fixed rate, SF=256. Always tx. Used by the network to confirm to the UE the reception of its access (PRACH).

B. Link Budget

Total propagation attenuation (L_p) can be generally defined for each link as (B.1) [Corr02]:

$$L_{p[\mathrm{dB}]} = P_{t[\mathrm{dBm}]} + G_{t[\mathrm{dBi}]} - P_{r[\mathrm{dBm}]} + G_{r[\mathrm{dBi}]} = EIRP_{[\mathrm{dBm}]} - P_{r[\mathrm{dBm}]} + G_{r[\mathrm{dBi}]} \quad \text{(B.1)}$$

where:

- L_p: total propagation attenuation
- P_t: emitting power at antenna port
- G_t: emitting antenna gain
- P_r: available receiving power at antenna port
- G_r: receiving antenna gain

The EIRP (Equivalent Isotropic Radiated Power) can be calculated using (B.2) or (B.3) if DL or UL is considered, respectively:

$$EIRP_{[\mathrm{dBm}]} = P_{Tx[\mathrm{dBm}]} + G_{t[\mathrm{dBi}]} - L_{c[\mathrm{dB}]} \quad \text{(B.2)}$$

$$EIRP_{[\mathrm{dBm}]} = P_{Tx[\mathrm{dBm}]} + G_{t[\mathrm{dBi}]} - L_{u[\mathrm{dB}]} \quad \text{(B.3)}$$

where:

- P_{Tx}: emitting power at antenna port
- G_t: emitting antenna gain
- L_c: Losses between the NodeB emitter and the antenna
- L_u: Body Loss

The reference NodeB antenna gain considered is 17 dBi (65º horizontal plane half-power beam width) for all environments. According to [ETSI98a], the UE antenna gain is specified as 0 dBi for all services and environments. It is expected that a UE station handling the high bit rates will not be used next to the ear. This is taken into account by increasing the gain to

2 dBi. The UE antenna gain will be manufacturer dependent and also may vary according to the type of terminal equipment, therefore it is assumed to be 0 dBi.

Four power classes have been defined for the UE output power for FDD mode [3GPP02z] and are presented in Table Annex B.1. For link budget calculations it is assumed 21 dBm for the maximum UE output power, since it is the most pessimistic case and also dependent on the manufacturers.

Table Annex B.1 - UE power classes.

Power Class	Nominal maximum output power	Tolerance
1	+33 dBm	+1/-3 dB
2	+27 dBm	+1/-3 dB
3	+24 dBm	+1/-3 dB
4	+21 dBm	± 2 dB

The NodeB maximum power is generally 20W (43 dBm) and it will be distributed among common and traffic channels. In Annex D common channels power allocation is proposed. Regarding user(s) channel power, it is generally limited to less than CPICH power, depending on the bearer service (typically 30 dBm).

Losses generated by feeders, connectors and all external equipment between the reception antenna and the NodeB are considered. As the number and type of RF (Radio Frequency) components (duplexers, diplexers, triplexers, etc.) will be dependent on the installed site configuration, for the estimation of the UL path loss it is considered 3 dB as a typical value for every site configuration and site height. No cable losses are considered for the UE (0 dB).

The human body absorbs energy, which reduces the antenna efficiency. A body loss margin is included in the link budget to take into account this “head effect”. A value of 3 dB is advised for voice services and 1 dB is considered for data services.

If receive diversity is used G_r must account for that extra gain, being substituted in (B.1) by (B.4), where G_{div} (in dB) is the achieved diversity gain.

$$G_{rdiv[\mathrm{dB}]} = G_{r[\mathrm{dB}]} + G_{div[\mathrm{dB}]} \tag{B.4}$$

Typical values for G_{div} are in the range 1…3 dB, depending on diversity type (spatial or polarisation) and correlation of received signals which is related to propagation environments characterisation. In urban type environments, due to low signal correlation, polarisation diversity delivers significant gain. Typical urban sites use polarisation diversity (cross-polarised antennas), requiring only one antenna per sector, minimising network cost and visual impact. Normally, equipment E_b/N_0 provide values already include diversity.

Transmit Diversity (TD) allows a decrease in the E_b/N_0 required in the mobile receiver due to the coherent sum of the two transmitted signals and gain against fast fading effects. Transmit diversity gain shall be treated as receive diversity gain but at the UE side. It is unlikely that TD will be used in early days since the system gain (typically in order of 2 dB) requires doubling of NodeB transmit RF equipment, such as transceivers (TRXs) and MCPAs.

The received power can be calculated by (B.5) for UL and by (B.6) for DL:

$$P_{RX[\mathrm{dBm}]} = P_{r[\mathrm{dBm}]} - L_{c[\mathrm{dB}]} \tag{B.5}$$

$$P_{RX[\mathrm{dBm}]} = P_{r[\mathrm{dBm}]} - L_{u[\mathrm{dB}]} \tag{B.6}$$

where:

- P_{RX}: receiver power at receiver input
- P_r: receiver power at antenna port

The receiver's sensitivity depends on the considered service and can be calculated by:

$$P_{RX\,\min[\mathrm{dBm}]} = N_{[\mathrm{dBm}]} - G_{P[\mathrm{dB}]} + E_b / N_{0[\mathrm{dB}]} \tag{B.7}$$

where:

- N: Total noise power given by (B.8)
- G_P: Processing gain given by (B.9)
- E_b/N_o: Required signal to noise ratio depending on the considered service

and:

$$N_{[\mathrm{dBm}]} = -174 + 10 \cdot \log\left(\Delta f_{[\mathrm{Hz}]}\right) + F_{[\mathrm{dB}]} + M_{I[\mathrm{dB}]} \quad \text{(B.8)}$$

$$G_{P[\mathrm{dB}]} = 10 \cdot \log\left(W / R_b\right) \quad \text{(B.9)}$$

where:

- Δf: Signal bandwidth. In UMTS it is equal to the chip rate (W) 3.84 Mcps
- F: Receiver's noise figure
- IM: Interference Margin given by (2.1)
- R_b: Bit rate associated to the analysed service

Processing gain values for the considered bit rates are shown in Table Annex B.2:

Table Annex B.2 - Processing gain.

Bit Rate [kbps]	12.2	64	128	384
G_p [dB]	25.0	17.8	14.8	10.0

The E_b/N_0 values are dependent on the bit rate of the service, the QoS required and the mobile speeds/environment type (see Table Annex B.3 for the channel types considered for each environment). Also the fact of considering the NodeB or the UE lead to different values, because the hardware implementation in the user equipment does not allow to achieve sensitivities as low as those achieved in the NodeB. Typical values range for NodeB E_b/N_0 are indicated in Table Annex B.4. Noise figure range values for NodeB and UE are given in Table Annex B.5 (Typical considered values are 3 and 8 dB respectively) [Corr02].

Table Annex B.3 - Environments and respective channel types.

Environment	Channel type
Dense Urban (DU)	Pedestrian A 3km/h
Urban (U)	Pedestrian A 3km/h
Suburban (SU)	Vehicular A 50 km/h
Rural (R)	Vehicular A 120 km/h
Axial (Ax)	Vehicular A 120 km/h

Table Annex B.4 - NodeB E_b/N_0 range values.

Service	Bit Rate [kbps]	E_b/N_0 [dB]
Voice	12.2	5.8 – 9.1
Circuit Switch	64	3.4 – 5.4
	128	2.8 – 4.7
	384	1.6 – 4.7
Packet Switch	64	3.0 – 7.3
	128	2.3 – 6.8
	384	1.9 – 6.2

Table Annex B.5 - Noise figure values for NodeB and UE.

Receiver Type	F [dB]
NodeB	2.0 – 5.0
User Equipment	5.0 – 8.0

The improvement in NodeB Rx sensitivity due to the inclusion of a TMA in the UL path is dependent upon the position of the TMA within the UL receiver chain. For gain maximisation one will consider the TMA close to the antenna, where G_x is the gain and F_x is the noise figure of the block. Given the above setup, the receiver sensitivity improvement ($G_{Rx\text{-}chain}$) is given by:

$$G_{Rx-chain[dB]} = F_{nodeB[dB]} + F_{feeder[dB]} - \left[10 \cdot \log \left[10^{\frac{F_{LNA[db]}}{10}} + \frac{10^{\frac{F_{feeder[dB]}}{10}} - 1}{10^{\frac{G_{LNA[dB]}}{10}}} + \frac{10^{\frac{F_{nodeB[dB]}}{10}} - 1}{10^{\frac{G_{LNA[dB]} + G_{feeder[dB]}}{10}}} \right] \right] \quad \text{(B.10)}$$

For a 12 dB gain LNA with 2 dB noise figure, the $G_{Rx\text{-}chain}$ is 3.5 dB.

Total propagation attenuation is calculated with the expressions presented so far. Once calculated the total propagation attenuation, maximum path loss can be evaluated taking into consideration the necessary margins of the system, as well as the additional soft handover gain. Having calculated maximum path loss, maximum cell radius estimation can be done using an appropriate propagation model. Total propagation attenuation relates with maximum path loss defined in (B.1) as in (B.11):

$$L_{ptot[\mathrm{dB}]} = M_{[\mathrm{dB}]} + L_{p[\mathrm{dB}]} \quad \text{(B.11)}$$

where:

- L_{ptot}: Total system attenuation
- M: Total system margins defined in (B.12)

and:

$$M_{[\mathrm{dB}]} = M_{SF[\mathrm{dB}]} + M_{FF[\mathrm{dB}]} + L_{ind[\mathrm{dB}]} - G_{SHO[\mathrm{dB}]} \quad \text{(B.12)}$$

where:

- M_{SF} : Slow fading margin
- M_{FF} : Fast fading margin
- L_{ind} : Indoor penetration losses
- G_{SHO} : Soft handover gain

Penetration losses and standard deviation considered are shown in Table Annex B.6:

Table Annex B.6 -Penetration types/losses and standard deviation.

Penetration Type/Environment	σ_{ind} [dB]	50% (building)	50% (ground floor)
Deep Indoor / DU	6	21 dB	28 dB
Indoor Light / U	5	15 dB	18 dB
Indoor Window / SU	4	6 dB	10 dB
In-car (+body loss) / Ax	4	10 dB	N/A
Outdoor / R	0	0 dB	N/A

The outdoor slow fading margin standard deviation (σ_{out}) is taken to be 7 dB [DaCo99], since it is expected COST231 – WI model usage in all environments except in R/Ax. One will consider figures for indoor coverage aiming at 50 % building coverage.

The Slow Fading margin (M_{SF}, also named as log-normal or shadow fading) is introduced in order to guarantee a certain coverage probability P_{cov} in the cell. The margin is the difference between the signal level necessary to cover the cell with a probability of coverage P_{cov} and the average signal at the cell edge. It depends on three parameters:

- P_{cov}: Coverage probability on the cell (95% for DU/U/SU and 90% for Ax/R)
- ρ: Slope of propagation distance coefficient (DU - 3,8; U/SU - 3,5; R/Ax - 3,2)
- σ : Standard deviation of the shadow fading. It includes the standard deviation of the building penetration losses σ_{in} and the standard deviation of the outdoor shadow fading σ_{out} as defined in (B.13) and shown in Table Annex B.7.

$$\sigma = \sqrt{\sigma_{in}^2 + \sigma_{out}^2} \tag{B.13}$$

$$P_{\text{cov}} = \frac{1}{2}\left[1 - erf(a) + \exp\left(\frac{1-2ab}{b^2}\right)\cdot\left(1 - erf\left(\frac{1-ab}{b}\right)\right)\right] \tag{B.14}$$

$$a = \frac{-M_{SF[\text{dB}]}}{\sigma_{[\text{dB}]}\cdot\sqrt{2}} \tag{B.15}$$

$$b = \frac{10\cdot\rho\cdot\log(e)}{\sigma_{[\text{dB}]}\cdot\sqrt{2}} \tag{B.16}$$

It should be noted that Jake's calculations are for a single cell and take no account of overlapping cell coverage effects that will in fact increase the probability of coverage. The gain due to this overlap is coverage is considered in the soft handover gain.

Table Annex B.7 - Slow fading margins.

M_{SF} [dB]	σ [dB]	DU_95%	DU_90%	U_95%	U_90%	SU_95%	SU_90%	R_90%	Ax_90%
Deep Indoor	**9.22**	**10.2***	6.5	10.5	6.8				
Indoor Light	8.60	9.3	5.9	**9.6***	6.1	9.6	6.1		
Indoor Window	8.06					**8.8***	5.5	**5.8***	**5.8***
Outdoor	7.00							**4.7**	4.7

In WCDMA cellular networks, the coverage areas of cells overlap and the UE is able to connect to more than just one serving cell. If more than one cell is detected, the location

* It is consider for each environment, an indoor coverage type, as noted in table B.7 by an asterisk.

probability increases and it is higher than the determined for a single isolated cell. In reality, signals from two NodeBs are correlated reducing estimated theoretical SHO gain.

Assuming M_{SF} as defined in (B.14), and defining the corresponding outage probability (P_{out}) for a single cell as (B.17), one can estimate an equivalent outage probability in case of SHO (P_{out_SHO}), calculating a new slow fading margin in case of SHO (M_{SF_SHO}) considering 50% correlation of the log-normal fading (B18) [LaWN02].

$$P_{out} = \frac{1}{2} \cdot \left(1 - erf\left(\frac{M_{SF}}{\sigma \cdot \sqrt{2}} \right) \right) \tag{B.17}$$

$$P_{out\_SHO} = P_{out} = \frac{1}{\sqrt{2\pi}} \cdot \int_{-\infty}^{+\infty} \exp\left(\frac{-x^2}{2} \right) \cdot \left[1 - erf\left(\frac{M_{SF\_SHO} - \sigma \cdot x / \sqrt{2}}{\sigma} \right) \Big/ 2 \right]^2 dx \tag{B.18}$$

SHO gain is the difference between M_{SF} and M_{SF_SHO}, show in Table Annex B.8 for the values considered in Table Annex B.7:

Table Annex B.8 - SHO gains.

SHO gain [dB]	DU_95%	DU_90%	U_SU_95%	U_SU_90%	R_Ax_95%	R_Ax_90%
Deep Indoor	4.5	4.2	4.5	4.2	4.6	4.2
Indoor Light	4.2	3.9	4.2	3.9	4.2	3.9
Indoor Window	3.9	3.6	4.0	3.6	4.0	3.7
Outdoor	3.4	3.1	3.4	3.1	3.4	3.2

In order to maintain the quality the fast power control in W-CDMA compensates the fast fading of the propagation channel. This is particularly true for the UE at low speed when the power control algorithm can follow for the channel variations very closely. For the case where the power control is not limited to an upper limit, a set of average E_b/N_0 values that are valid for the majority of the cell's area is obtained, where UEs are close enough to the NodeB that their maximum UL power limit is never reached.

In order to correct the limited dynamics of the power control in this case, a margin called the fast fading margin or TPC headroom is included in the link budget. From simulations presented in [SLWJ99] and [SiLW99] one will consider the following margins (Table Annex B.9). It is assumed that there will no users moving slowly near cell edge in R/Ax cells,

otherwise similar margins to DU/U or SU should apply, depending on speed/channel considerations.

Using the values described in this annex, the maximum pathloss for speech, CS64, PS128 and PS384 services and the environments considered is shown in Table Annex B.10.

Table Annex B.9 - Fast fading margins.

Environment	speed [km/h]	Channel type	M_{FF} [dB]
DU/U	2.7	Pedestrian A 3km/h	3.6
SU	54	Vehicular A 50 km/h	1
R/Ax	135	Vehicular A 120 km/h	0

Table Annex B.10 - Maximum pathloss.

Pathloss [dB]	DU	U	SU	Ax	R
Speech	122.0	128.1	129.7	141.2	142.7
CS64	119.2	125.3	127.9	137.0	140.5
PS128	117.2	123.3	124.7	134.5	138.0
PS384	113.5	119.6	122.2	130.7	134.2

C. Propagation Models

- **COST231-Hata Model Description**

COST 231 has extended Hata´s model to the frequency band 1500 to 2000 MHz by analysing Okumura´s propagation curves in the upper frequency band. Propagation loss (L_p) is given by (C.1) [DaCo99].

The model is restricted to:

- f : 1500... 2000 MHz (We will consider 1980 MHz (worst UL case))
- h_{Base}: 30 ...200 m (We will consider 30 m for DU/U/SU and 35 m for R/Ax)
- h_{Mobile}: 1 ...10 m (We will use 1.5m for all environments)
- d : 1 ...20 km

$$L_{p[\mathrm{dB}]} = 46.3 + 33.9 \cdot \log\left(f_{[\mathrm{MHz}]}\right) - 13.82 \cdot \log\left(h_{Base[\mathrm{m}]}\right) - a\left(h_{Mobile}\right) + \left(44.9 - 6.55 \cdot \log\left(h_{Base[\mathrm{m}]}\right)\right) \cdot \log\left(d_{[\mathrm{km}]}\right) + C_m \quad \text{(C.1)}$$

$$a\left(h_{Mobile}\right) = \left(1.1 \cdot \log\left(f_{[\mathrm{MHz}]}\right) - 0.7\right) \cdot h_{Mobile[\mathrm{m}]} - \left(1.56 \cdot \log\left(f_{[\mathrm{Mhz}]}\right) - 0.8\right) \quad \text{(C.2)}$$

where:

- h_{Base}: NodeB transmit antenna height
- h_{Mobile}: UE height
- f: frequency
- d: distance
- C_m: 0 dB (Medium sized and suburban centres with medium tree density), 3 dB for metropolitan centres

The application of the COST231-Hata-Model is restricted to large and small macro-cells, i.e., base station antenna heights above rooftop levels adjacent to the base station. Hata´s formula and its modification must not be used for micro-cells. Some corrections should be applied to (C.1) in order to use it in Suburban (C.3) and Quasi-Open Rural/Axial environments (C.4).

$$L_p' = L_p - 2 \cdot \left[\log\left(f_{[\mathrm{MHz}]}/28\right)\right]^2 - 5.4 \tag{C.3}$$

$$L_p' = L_p - 4.78 \cdot \left[\log\left(f_{[\mathrm{MHz}]}\right)\right]^2 + 18.33 \cdot \log\left(f_{[\mathrm{MHz}]}\right) - 35.94 \tag{C.4}$$

- COST231 Walfisch-Ikegami Model Description

Furthermore COST 231 proposed a combination of the Walfisch and Ikegami models. This formulation is based on different contributions from members of the "COST 231 Subgroup on Propagation Models". It is called the COST Walfisch-Ikegami-Model (COST-WI). The model allows for improved path-loss estimation by consideration of more data to describe the character of the urban environment, namely:

- Heights of buildings: h_{Roof}
- Widths of roads: w
- Building separation: b
- Road orientation with respect to the direct radio path: φ

The COST-WI model is restricted to:

- f : 800 ... 2000 MHz
- h_{Base}: 4 ... 50 m
- h_{Mobile} : 1 ... 3 m
- d : 0.02 ... 5 km

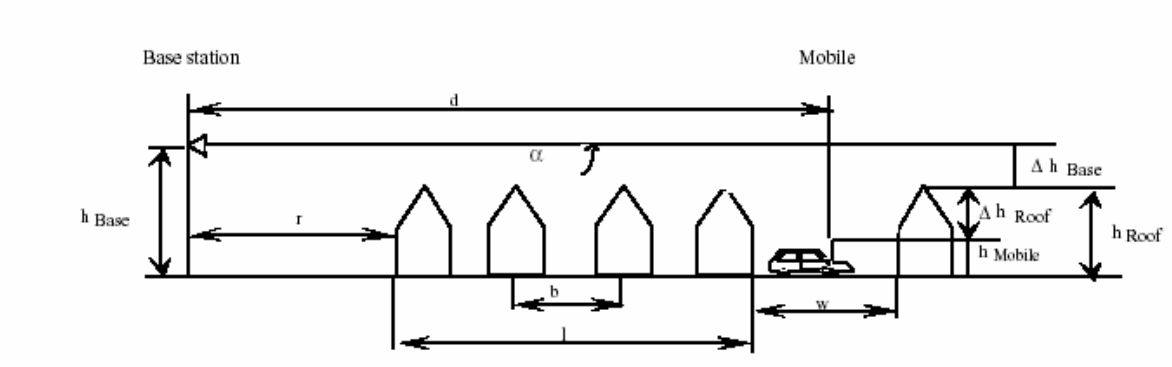

Figure Annex C.1 - COST-WI parameters.

The model distinguishes between line-of-sight (LOS) and non-line-of-sight (NLOS) situations. In the LOS case, between base and mobile antennas within a street canyon, a simple propagation loss formula different from free space loss is applied (C.5). The loss is based on measurements performed in the city of Stockholm [DaCo99]:

$$L_{p[\mathrm{dB}]} = 42.6 + 26 \cdot \log\left(d_{[\mathrm{km}]}\right) + 20 \cdot \log\left(f_{[\mathrm{MHz}]}\right) \qquad \text{for d}\geq 20\ \text{m} \tag{C.5}$$

where 42.6 derive from equality to free space loss equation at 20 m.

In the NLOS case the basic transmission loss is composed of the terms free space loss L_0, multiple screen diffraction loss L_{msd}, and roof-top-to-street diffraction and scatter loss L_{rts} (C.6).

$$L_p = \begin{cases} L_0 + L_{rts} + L_{msd} & \text{for } L_{rts} + L_{msd} > 0 \\ L_0 & \text{for } L_{rts} + L_{msd} \leq 0 \end{cases} \tag{C.6}$$

The free space loss (L_0) is given by (C.7):

$$L_{0[\mathrm{dB}]} = 32.4 + 20 \cdot \log\left(d_{[\mathrm{km}]}\right) + 20 \cdot \log\left(f_{[\mathrm{MHz}]}\right) \tag{C.7}$$

The term L_{rts} describes the coupling of the wave propagating along the multiple-screen path into the street where the mobile station is located. The determination of L_{rts} is mainly based on Ikegami's model. It takes into account the width of the street and its orientation. COST 231, however, has applied another street-orientation function than Ikegami (C.8):

$$L_{rts} = -16.9 - 10 \cdot \log\left(w_{[\mathrm{m}]}\right) + 10 \cdot \log\left(f_{[\mathrm{MHz}]}\right) + 20 \cdot \log\left(\Delta h_{Mobile[\mathrm{m}]}\right) + L_{Ori} \tag{C.8}$$

$$L_{Ori} = \begin{cases} -10 + 0.354 \cdot \varphi_{[\mathrm{deg}]} & \text{for } 0^{\circ} \leq \varphi \leq 35^{\circ} \\ 2.5 + 0.075 \cdot \left(\varphi_{[\mathrm{deg}]} - 35\right) & \text{for } 35^{\circ} \leq \varphi \leq 55^{\circ} \\ 4.0 - 0.114 \cdot \left(\varphi_{[\mathrm{deg}]} - 55\right) & \text{for } 55^{\circ} \leq \varphi \leq 90^{\circ} \end{cases} \tag{C.9}$$

$$\Delta h_{Mobile} = h_{Roof} - h_{Mobile} \tag{C.10}$$

$$\Delta h_{Base} = h_{Base} - h_{Roof} \tag{C.11}$$

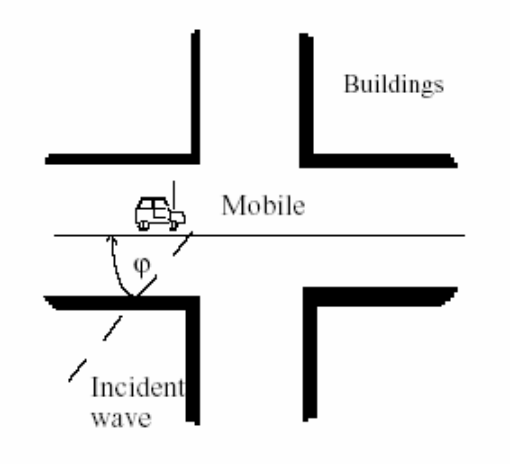

Figure Annex C.2 – Definition of the street orientation angle φ.

Scalar electromagnetic formulation of multi-screen diffraction results in an integral for which Walfisch and Bertoni published an approximate solution in the case of base station antenna located above the rooftops. COST 231 extends this model for base station antenna heights below the rooftop levels using an empirical function based on measurements. The heights of buildings and their spatial separations along the direct radio path are modeled by absorbing screens for the determination of L_{msd} (C.12):

$$L_{msd} = L_{bsh} + k_a + k_d \cdot \log\left(d_{[\mathrm{km}]}\right) + k_f \cdot \log\left(f_{[\mathrm{MHz}]}\right) - 9 \cdot \log\left(b_{[\mathrm{m}]}\right) \tag{C.12}$$

$$L_{bsh} = \begin{cases} -18 \cdot \log\left(1 + \Delta h_{Base[\mathrm{m}]}\right) & \text{for } h_{Base} > h_{Roof} \\ 0 & \text{for } h_{Base} \le h_{Roof} \end{cases} \tag{C.13}$$

$$k_a = \begin{cases} 54 & \text{for } h_{Base} > h_{Roof} \\ 54 - 0.8 \cdot \Delta h_{Base[\mathrm{m}]} & \text{for } d \ge 0.5 \text{ km and } h_{Base} \le h_{Roof} \\ 54 - 0.8 \cdot \Delta h_{Base[\mathrm{m}]} \cdot \dfrac{d_{[\mathrm{km}]}}{0.5} & \text{for } d < 0.5 \text{ km and } h_{Base} \le h_{Roof} \end{cases} \tag{C.14}$$

$$k_d = \begin{cases} 18 & \text{for } h_{Base} > h_{Roof} \\ 18 - 15 \cdot \dfrac{\Delta h_{Base}}{h_{Roof}} & \text{for } h_{Base} \le h_{Roof} \end{cases} \tag{C.15}$$

$$k_f = -4 + \begin{cases} 0.7 \cdot \left(\dfrac{f_{[\mathrm{MHz}]}}{925} - 1 \right) & \text{for medium sized city and suburban centres} \\ 1.5 \cdot \left(\dfrac{f_{[\mathrm{MHz}]}}{925} - 1 \right) & \text{for metropolitan centres} \end{cases} \tag{C.16}$$

The term k_a represents the increase of the path loss for base station antennas below the rooftops of the adjacent buildings. The terms k_d and k_f control the dependence of the multi-screen diffraction loss versus distance and radio frequency, respectively. If the data on the structure of buildings and roads are unknown the following default values are recommended:

$$h_{Roof} = 3_{[m]} \cdot \{\text{number of floors}\} + \text{roof\_height (3 m pitched; 0 m flat)} \quad \text{(C.17)}$$

- b: 20 ... 50 m
- w: b / 2
- φ: 90°

The estimation of path loss agrees rather well with measurements for base station antenna heights above rooftop level. The mean error is in the range of +3 dB and the standard deviation 4-8 dB [DaCo99]. However the prediction error becomes large for $h_{Base} >> h_{Roof}$ compared to situations where $h_{Base} >> h_{Roof}$. Furthermore the performance of the model is poor for $h_{Base} << h_{Roof}$.

The parameters b, w and φ are not considered in a physically meaningful way for micro-cells. Therefore the prediction error for micro-cells may be quite large. The model does not consider multipath propagation and the reliability of pathloss estimation decreases also if terrain is not flat or the land cover is inhomogeneous [DaCo99].

Using the values described in Annex B for the maximum pathloss for speech, CS64, PS128 and PS384 services and considering the models describing in this annex, the cell radius is shown in Table Annex C.1, considering COST231-WI for DU/U/SU and COST231- Hata for R/Ax:

Table Annex C.1 - Cell radius.

Range [m]	Speech	CS64	PS128	PS384
DU	211	178	158	126
U	346	292	259	207
SU	414	372	306	263
Ax	8325	6305	5340	4160
R	9194	7949	6732	5245

D. Common Channels Configuration

Being the NodeB power a limited resource, it is very important to optimise the common channel power settings leading to a maximisation of the power available for the connections but assuring that signalling and system information reaches all the cell coverage area. Due to the typical bias on the DL traffic load, the correct dimensioning of common channel is of major interest.

For the link quality formulation, one will consider as reference the 3GPP $E_c/I_{o\ target}$ for common channels. Assuming no power control for common channels (except for S-CCPCH when carrying FACH using open loop and RACH with open loop for initial power settings), the link quality for common channels (CC) is guaranteed for all mobiles over the cell (D.1) and defining DL interference factor as other-to-own-cell received power ration ($i_{DL,i}$) for mobile *i* (D.2):

$$E_c / I_{oCC,i} \geq E_c / I_{oCC,t\arg et} \tag{D.1}$$

$$i_{DL,i} = \frac{L_{BS,i}}{P_{BS}} \cdot \sum_{j=1, j\neq BS}^{N} \frac{P_{BS,j}}{L_{i,j}} \tag{D.2}$$

where:

- $L_{BS,i}$: pathloss for mobile *i*
- $P_{BS,j}$: *j* NodeB total transmitted power
- $L_{i,j}$: pathloss between NodeB *j* and mobile *i*

We suppose that for a mobile *i* at the edge of the cell ($i_{DL\ i} = i_{\ DL,max}$) the link quality is equal to target link for common channels except for synchronisation channels (P-SCH and S-SCH) since they are not scrambled and therefore no orthogonality factor applies. From [HoTo01] one can derive link quality (D.3) applied for a common channel CC (except SCH channels).

(D.3)

$$E_c / I_{o\ CC,i} = \frac{P_{CC} \Big/ L_{BS,i}}{\alpha_{CC} \cdot \left(P_{BS} - P_{CC} - P_{P-SCH} - P_{S-SCH}\right) \Big/ L_{BS,i} + \left(P_{P-SCH} + P_{S-SCH}\right) \Big/ L_{BS,i} + \sum_{j=1, j\neq BS}^{N} P_{BS,j} \Big/ L_{i,j} + P_{Nth}}$$

where:

- α_{CC}: common channel orthogonality factor (defined as unit complementary of α_j for matters of equation simplicity)
- P_{BS}: NodeB maximum (MCPA) power
- P_{CC}: common channel power
- $P_{P/S\text{-}SCH}$: SCH channels power
- P_{Nth}: Thermal noise power

Note that (D.3) formulation includes common channels specificity's such as non-scrambling of SCH channels. For common channel P-SCH and S-SCH equivalent to (D.3) are (D.4) and (D.5) respectively:

$$E_c/I_{o\,P-SCH,i} = \frac{P_{P-SCH}/L_{BS,i}}{\left(P_{BS} - 2\cdot P_{P-SCH}\right)/L_{BS,i} + \sum_{j=1,j\neq BS}^{N} P_{BS,j}/L_{i,j} + P_{Nth}} \quad \text{(D.4)}$$

$$E_c/I_{o\,S-SCH,i} = \frac{P_{S-SCH}/L_{BS,i}}{\left(P_{BS} - 2\cdot P_{S-SCH}\right)/L_{BS,i} + \sum_{j=1,j\neq BS}^{N} P_{BS,j}/L_{i,j} + P_{Nth}} \quad \text{(D.5)}$$

The term "$2.P_{x\text{-}SCH}$" in (D.4) and (D.5) reflect the fact that $P_{P\text{-}SCH} = P_{S\text{-}SCH}$ and since they are orthogonal are not considered as interference power. Channel activity factors for common channels are not introduced since one aim at calculating the instantaneous transmit power of common channels (only considered in capacity calculation regarding MCPA available power). For planning purposes, one want to guarantee that link quality is good all over the cell, specially for mobiles at the edge of the cell, taking maximum interference factor ($i_{DL} = i_{DL,max}$) and maximum path loss $L_{BS,i} = L_{CC,Maximum}$ Deducing from (D.3), (D.4) and (D.5) one can estimate common channels power as (D.6), (D.7) and (D.8):

(D.6)

$$P_{CC} = \frac{E_c/I_{o\,CC,target}}{1+\alpha_{CC}\cdot E_c/I_{o\,CC,target}}\cdot\left(\left(\alpha_{CC}+i_{DL,\max}\right)\cdot P_{BS} + \left(1-\alpha_{CC}\right)\cdot\left(P_{P-SCH}+P_{S-SCH}\right) + L_{CC,\max}\cdot P_{Nth}\right)$$

$$P_{P-SCH} = \frac{E_c/I_{o\,P-SCH,target}}{1+2\cdot E_c/I_{o\,P-SCH,target}}\cdot\left(\left(1+i_{DL,\max}\right)\cdot P_{BS} + L_{P-SCH,\max}\cdot P_{Nth}\right) \quad \text{(D.7)}$$

$$P_{S-SCH} = \frac{E_c/I_{o\,S-SCH,target}}{1+2\cdot E_c/I_{o\,S-SCH,target}}\cdot\left(\left(1+i_{DL,\max}\right)\cdot P_{BS} + L_{S-SCH,\max}\cdot P_{Nth}\right) \quad \text{(D.8)}$$

Several values of i_{DL} will be analysed regarding common channel power. Nevertheless is important to estimate its maximum value. Assuming a simplified hexagonal pattern with tri-sector sites, the maximal number of adjacent cells is 3, leading to i_{DL} approximately to 2.

Different common channels depending on its purpose should aim at different service areas. Common channels should be received besides the service coverage area of cells in order to allow the UE to synchronise and identify the new cell(s). Maximum common channels path loss can be defined as (D.9):

$$L_{CC,\max} = L_{prop,\max} + G_{MRC} + M_{CC} \tag{D.9}$$

where:

- $L_{prop,max}$: maximal path loss of propagation (less stringent service)
- G_{MRC}: maximum ratio combining gain (receiver E_b/N_0 reduction in Softer handover)
- M_{CC} is an additive margin to common channel CC including SHO threshold (M_{SHO}) and a CPICH/SCH margin ($M_{CPICH/SCH}$). M_{CC} for the different common channels is proposed in Figure D.1:

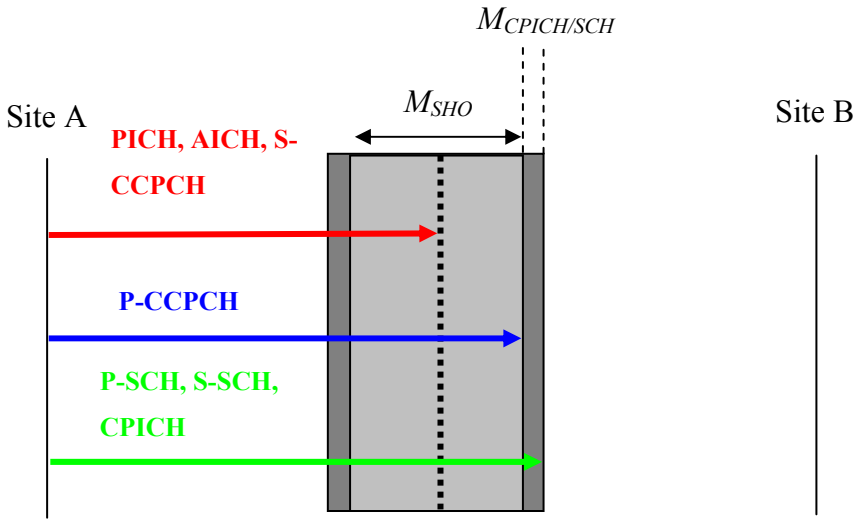

Figure Annex D.1 - M_{CC} margin definition.

We defined PICH, AICH and S-CCPCH exactly to be received within nominal cell coverage range. For P-CCPCH (BCH) one propose to extended it to the possible area were SHO can occur since in that condition the neighbour lists should still be heard by the UE. Last, in order to detect new cells we, CPICH and SCH should be present in slighter higher range than P-CCPCH, being adopted a margin of 1 dB. Along the simulations presented, the values used in calculations are according to Table Annex D.1 (otherwise stated):

Table Annex D.1 - Fixed parameters considered common channels calculations.

General Parameters	value	unit
Maximum BS power	20	W
M_SHO	3	dB
M_CPICH_SCH	1	dB
G_MRC	1.5	dB
Chip rate (W)	3.84E+06	cps
UE noise factor (N)	8.00	dB
CPICH_Ec/Io	-15	dB
PCCPCH_Ec_Io	-17	dB
SCCPCH_Ec_Io	-17	dB
P-SCH_Ec_Io	-20	dB
S-SCH_Ec_Io	-20	dB
PICH_Ec_Io	-20	dB
AICH_Ec_Io	-20	dB

The Common channels $E_c/I_{o,\ target}$ is estimated from [3GPP02z]. According to 3GPP, UE measured CPICH E_c/I_o>-20 dB. If considering common channels proposed setup in [3GPP02z], minimum channel power is referring to AICH (E_c/I_{or}= -15 dB). Considering that AICH and CPICH have SF=256, with target CPICH E_c/I_o equal to –15 dB. Using the methodology defined in this annex, the common channels setup to be used is summarised in Table Annex D.2, with CPICH power given in dBm and the other CC power given in reference to CPICH power:

Table Annex D.2 - Common Channels power setup.

Common Channel	CPICH [dBm]	PCCPCH	SCCPCH	P-SCH	S-SCH	PICH	AICH
DU	31.4	-2.0	-2.0	-4.0	-4.0	-5.0	-5.0
U	31.5	-2.0	-2.0	-4.1	-4.1	-5.0	-5.0
SU	31.5	-2.0	-2.0	-4.1	-4.1	-5.0	-5.0
R	32.4	-2.2	-2.4	-5.0	-5.0	-5.4	-5.4
Ax	33.6	-2.3	-2.8	-6.2	-6.2	-5.8	-5.8

From Table Annex D.2 values, it is assumed an average CPICH value of 2 W (33 dBm) in each cell, and total common channel power overhead is 30% of total PA power. If considering 20W default PA power, common channels power will be 6 W.

E. Traffic Source Models Statistical Description

This annex sums up all source model statistical description

- **Call/session generation and duration processes**

For a complete modelling of traffic sources, one must also characterise call/session arrivals and durations.

Generally, voice calls and data sessions, are considered to be generated according to a Poisson process [ETSI98b], where the probability, $p_{Po}[n,t]$, of generating n calls/session in a certain time interval t is given by:

$$p_{Po}[n,t] = \frac{(\lambda_c \cdot t)^n}{n!} e^{-\lambda_c \cdot t}, \quad \text{(E.1)}$$

where λ_c is the mean arrival rate of calls (*e.g.*, calls per second). $p_{Po}[n,t]$ represents the Poisson PF.

In general, it is also assumed that durations for voice calls and data sessions follow an exponential distribution [ETSI98b]. The corresponding PDF and CDF are given by (E.2) and (E.3), respectively:

$$P_E(t) = 1 - e^{-\mu_{CD} \cdot t}, \quad \text{(E.2)}$$

$$p_E(t) = \mu_{CD} \cdot e^{-\mu_{CD} \cdot t}, \quad \text{(E.3)}$$

where $1/\mu_{CD}$ is the mean call duration time. Equation (E.3) is usually referred to as the negative exponential distribution.

In Table Annex E.1, the generation and duration processes that will be used in the current work for each application are presented. Again, as with the traffic source models, scarce information can be found in the literature for parameterisation of these processes, mainly for advanced services and applications. Therefore, in this work some of these values will be arbitrated, with a reasonable practical sense.

Table Annex E.1 - Session/call generation and duration processes.

Service Class	Services	Applications	Arrival Rate in Busy Hour	Session/Call duration
Conversational	Speech telephony	Voice Call	Poisson	Exponential
	Video telephony	Video Call	Poisson	Exponential
Streamin	Streaming Video	Video on Demand	Poisson	Exponential
Interactive	Multimedia Communication Service	Web Browsing	Poisson	Given by source model
Background	Messaging Service	E-mail	Poisson	Given by source model
	Unrestricted Data Retrieval Service	FTP	Poisson	Given by source model

- **Source Models Statistical Description**

Mathematical description of the source models used can be found in most of the references used along this thesis, namely, [SeCo03], [Serr02] and [Agui03].

Table Annex E.2 - List of traffic source models.

Service	Traffic Source Models	Input Parameters	Output Parameters
Speech/Video Telephony	Classical Voice (ON-OFF) Model	Session rate. Mean Holding Time (MHT)	Speech start and duration
Web Browsing / LBS / Streaming	Web Browsing Model	Target bit rate and statistical parameters from real trace data	Number of packet calls per session. Reading time between packet calls. Number of packets within a packet call. Inter arrival time between packets within a packet call. Packet size
Multimedia Messaging	ON-OFF	Average packets size	Packet size
E-mail and FTP	e-mail/FTP *n* kbps (*n*=64, 144, 384)	Target bit rate and statistical parameters from real trace data.	Session inter arrival times / data volume. Connection inter arrival times / data volume. Packet Inter arrival time and sizes

F. Statistical Distributions Validation

In the present annex, a simple validation of each implemented statistical function is presented, based on a comparison with the respective theoretical PDFs/CDFs. For the implementation of statistical traffic source models, Random Number Generators (RNG) are essential. In the case of the traffic source models considered in the present report, 8 different RNGs were necessary for their implementation. More specifically, RNGs for the following statistical distributions were used: Uniform, Exponential, Geometrical, Normal, LogNormal, Pareto, Poisson and Weibul. The selected Uniform RNG algorithm is the VC++ standard function while the remaining RNG algorithms are based on transformations of this Uniform RNG. For each distribution, the CDF/PDF correlation is calculated based on discrete generate samples and the theoretical distribution expressions (see Table Annex F.1).

- **Uniform and Poisson Distribution Validation**

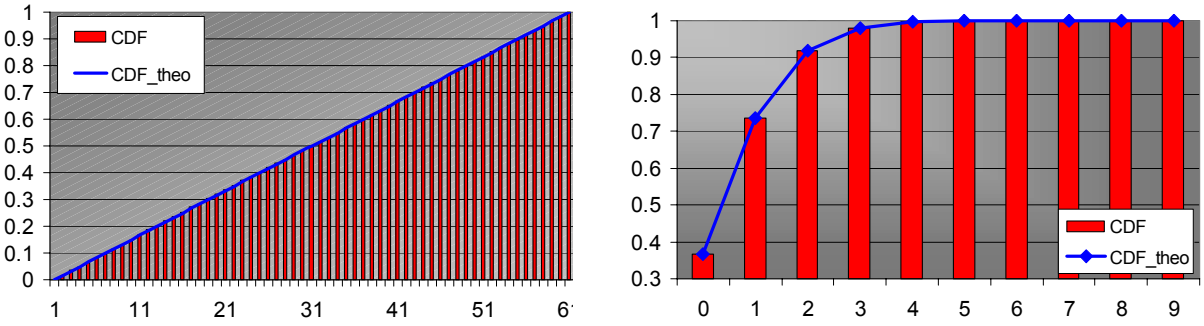

Figure Annex F.1 – Theoretical and generated CDFs (uniform and Poisson).

- **Exponential and Geometric Distribution Validation**

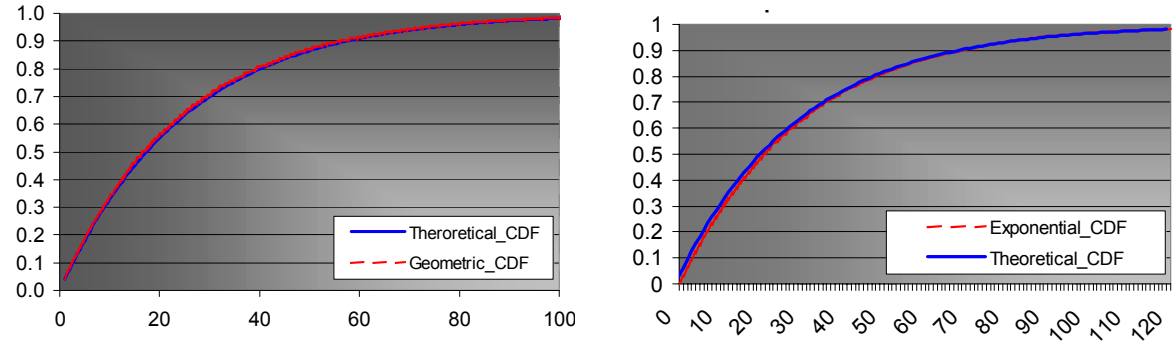

Figure Annex F.2 – Theoretical and generated CDFs for geometric and exponential.

- **Lognormal and Pareto Distribution Validation**

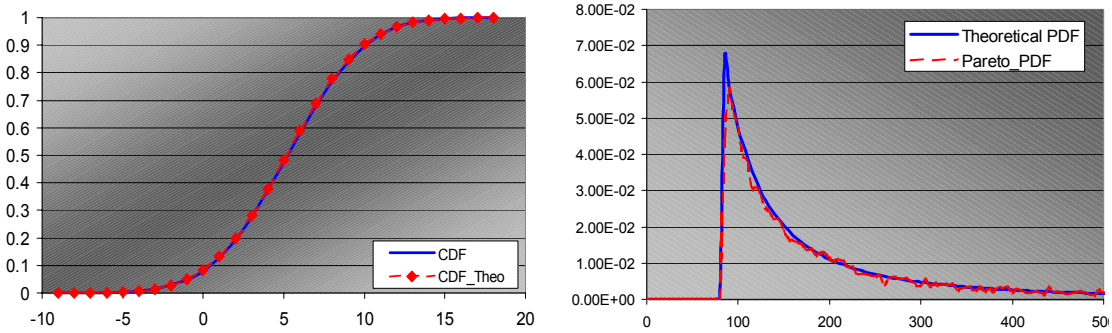

Figure Annex F.3 – Theoretical and generated CDF/PDF for lognormal and Pareto.

Table Annex F.1 - CDF correlation values for used distributions.

Distribution Type	CDF Correlation [%]	Application example	Test application
Uniform	**99.9976**	Speech - start time	Speech
Exponential	**99.9990**	Speech - call duration	Speech
Geometric	**99.9957**	WWW - Number of packet in packet call	WWW
Lognormal	**99.9967**	E-mail, FTP - Data volume	FTP
Pareto	**99.9638**	WWW - Packet size	WWW
Poisson	**99.9998**	Speech - call generation	Speech
Weibull	**99.9961**	Speech - CDMA model	Not used

G. Population and clutter data GIS tables

This annex includes the MapInfo® tables to characterise the HD and LD scenarios, namely district and clutter data. Due to limitation in MapInfo® array handling, and to allow high number of users generation (above 32000), districts were split in lower areas, with users proportional to its area and maintaining its demographic characteristics. District present population data and clutter tables are taken from [FeAl02] and summarised in Table Annex G.1 and Table Annex G.2.

- **HD District Tables**

Table Annex G.1 – HD scenario district information.

Pop. [inh]		Age [%]			Education [%]				Salary
District	Pop.	Age20	Age20to64	Age64	NoEduc.	Basic	Compl.	Degree	Qualitative
Nª Sra Fátima	15977	25.27	40.02	34.71	8.21	34.82	19.42	37.56	High
S. João de Deus	15977	22.95	33.34	43.71	6.7	31.91	22.28	39.11	High
S. Jorge Arroios	31954	23.82	36.97	39.07	8.67	40.22	22.36	28.75	Medium
S. Seb. da Pedreira	63908	23.82	36.97	39.07	8.67	40.22	22.36	28.75	Medium High

- **LD District Tables**

Table Annex G.2 – LD scenario district information.

Pop. [inh]		Age [%]			Education [%]				Salary
District	Pop.	Age20	Age20to64	Age64	NoEduc.	Basic	Compl.	Degree	Qualitative
Marvila	37709	46.91	41.18	12.05	15.35	57.6	19.86	7.19	Low
Olivais	33914	30.64	49.46	20.04	11.4	50.07	20.23	18.3	Medium

The following clutter types were considered; dense residential, light residential, mixed buildings, tertiary buildings, industrial buildings, roads and green areas, with GIS tables retrieved from [CaML02]. In Figure 5.1we show the tables GIS information and geographical polygons for HD and LD areas together.

H. Application Set GIS Tables (Services Penetration)

In Table Annex H.1 it is shown the reference service distribution as proposed in [FeAl02] and [VaCa02]. MapInfo® tables for Age, Salary and Education data are created with table contents.

Table Annex H.1 – Service distribution for REF scenario.

Service Distribution			Age [%]			Salary [%]				Education [%]			
Application	DLrate [kbps]	Traf. Model	<20	<64	>64	Low	Med.	M./H.	High	No Ed.	Basic	Compl.	Degree
voice	12,2 (CS)	speech	44	48	90	95	87	66	34	95	80	62	50
audio-on-demand	64 (PS)	streaming	9	2	0	0	0	2	7	0	3	4	2
video-telephony	64 (CS)	video	5	9	2	0	2	5	11	2	2	4	9
video-on-demand	384 (PS)	streaming	3	2	0	0	0	1	7	0	0	2	1
web-browsing	128 (PS)	WWW	6	12	5	0	1	4	10	0	2	9	13
chat	64 (PS)	WWW	9	5	0	1	2	6	5	0	1	6	4
personal LBS	64 (PS)	lbs	1	7	2	0	1	4	6	0	0	3	4
MMS	64 (PS)	mms_sms	13	4	0	3	5	6	7	0	7	4	4
interactive gaming	128 (PS)	streaming	4	2	0	1	3	4	5	3	5	4	2
FTP	384 (PS)	ftp	2	7	0	0	0	0	3	0	0	0	8
e-mail	128 (PS)	e-mail	4	4	1	0	0	2	5	0	1	2	4

From [FeAl02], a proposal for a multi-service profile based on an operator expectation is shown for comparison with Table Annex H.1 reference figures in. It is clear that refernce scenario is more voice centric than the proposed scenario.

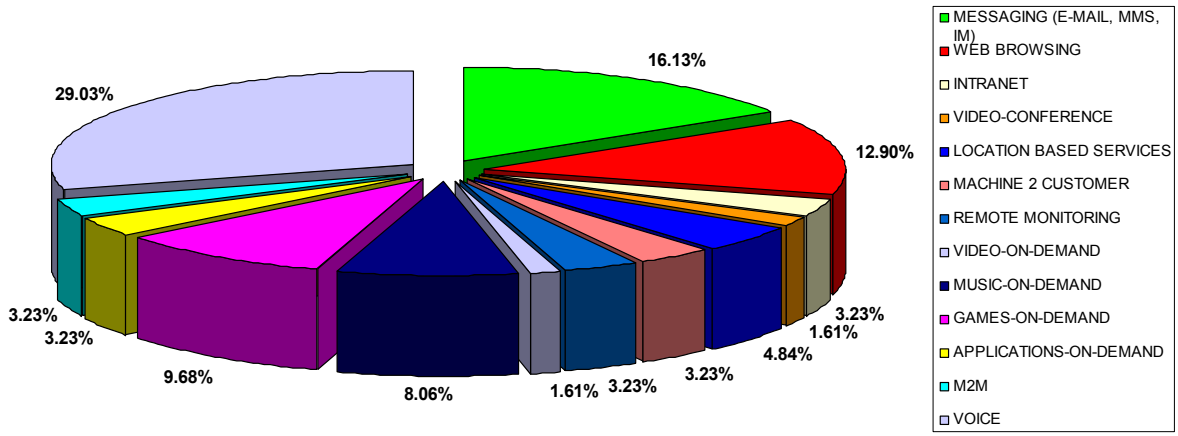

Figure Annex H.1 - Multi-service profile proposal ([FeAl02]).

I. Auxiliary GIS Tables

The main auxiliary GIS tables include:

- Site locations table (HD and LD scenarios), see Table Annex I.1 (I.2). These tables include sites latitude, longitude, sector azimuth, PA power, CPICH values and total common channels power.
- Antenna patterns, see Table Annex I.3. This table includes the antenna pattern relative gain values (radiation pattern description).
- Clutter distribution (Scenario table), see Figure Annex I.4. This table includes the clutter type assignment for each (clutter) polygon.
- Eb/N0 values table for pedestrian and vehicular type channels, see Table Annex I.4.
- Bearer Mapping Table (fixed), see Figure Annex I.2 and Figure Annex I.3.

Table Annex I.1 – HD site information.

Code	Name	CITY	X	Y	Z	S1_Az	S2_Az	S3_Az	PA_1	CPI_3	CCH_1
10001	nodeB1	LISBOA	-9.14845	38.7341	0	0	120	240	20	2	6
10002	nodeB2	LISBOA	-9.14385	38.7294	0	0	120	240	20	2	6
10003	nodeB3	LISBOA	-9.14676	38.7405	0	0	120	240	20	2	6
10004	nodeB4	LISBOA	-9.14939	38.7484	0	0	120	240	20	2	6
10005	nodeB5	LISBOA	-9.14797	38.7373	0	0	120	240	20	2	6
10006	nodeB6	LISBOA	-9.14318	38.7338	0	0	120	240	20	2	6
10007	nodeB7	LISBOA	-9.15125	38.7317	0	0	120	240	20	2	6
10008	nodeB8	LISBOA	-9.13348	38.7377	0	0	120	240	20	2	6
10009	nodeB9	LISBOA	-9.15822	38.7423	0	0	120	240	20	2	6
10010	nodeB10	LISBOA	-9.13416	38.731	0	0	120	240	20	2	6
10011	nodeB11	LISBOA	-9.15915	38.728	0	0	120	240	20	2	6
10012	nodeB12	LISBOA	-9.13802	38.7427	0	0	120	240	20	2	6
10013	nodeB13	LISBOA	-9.15085	38.739	0	0	120	240	20	2	6
10014	nodeB14	LISBOA	-9.15003	38.7243	0	0	120	240	20	2	6
10015	nodeB15	LISBOA	-9.15989	38.7377	0	0	120	240	20	2	6
10016	nodeB16	LISBOA	-9.14319	38.746	0	0	120	240	20	2	6
10017	nodeB17	LISBOA	-9.14032	38.7376	0	0	120	240	20	2	6

Table Annex I.2 – LD site information.

Code	Name	CITY	X	Y	Z	S1_Az	S2_Az	S3_Az	PA_PWR_1	CPICH_1	CCH_1
10101	nodeB101	LISBOA	-9.09569	38.7539	0	0	120	240	20	2	6
10102	nodeB102	LISBOA	-9.12141	38.7794	0	0	120	240	20	2	6
10103	nodeB103	LISBOA	-9.10444	38.7476	0	0	120	240	20	2	6
10104	nodeB104	LISBOA	-9.11979	38.747	0	0	120	240	20	2	6
10105	nodeB105	LISBOA	-9.1091	38.7628	0	0	120	240	20	2	6
10106	nodeB106	LISBOA	-9.1115	38.7753	0	0	120	240	20	2	6
10107	nodeB107	LISBOA	-9.10004	38.771	0	0	120	240	20	2	6
10108	nodeB108	LISBOA	-9.10106	38.7631	0	0	120	240	20	2	6
10109	nodeB109	LISBOA	-9.11391	38.7579	0	0	120	240	20	2	6
10110	nodeB110	LISBOA	-9.10488	38.7339	0	0	120	240	20	2	6
10111	nodeB111	LISBOA	-9.09287	38.7729	0	0	120	240	20	2	6
10112	nodeB112	LISBOA	-9.10453	38.7746	0	0	120	240	20	2	6
10113	nodeB113	LISBOA	-9.11994	38.7629	0	0	120	240	20	2	6
10114	nodeB114	LISBOA	-9.12721	38.7729	0	0	120	240	20	2	6
10115	nodeB115	LISBOA	-9.12424	38.7511	0	0	120	240	20	2	6
10116	nodeB116	LISBOA	-9.1135	38.7684	0	0	120	240	20	2	6
10117	nodeB117	LISBOA	-9.12246	38.7909	0	0	120	240	20	2	6

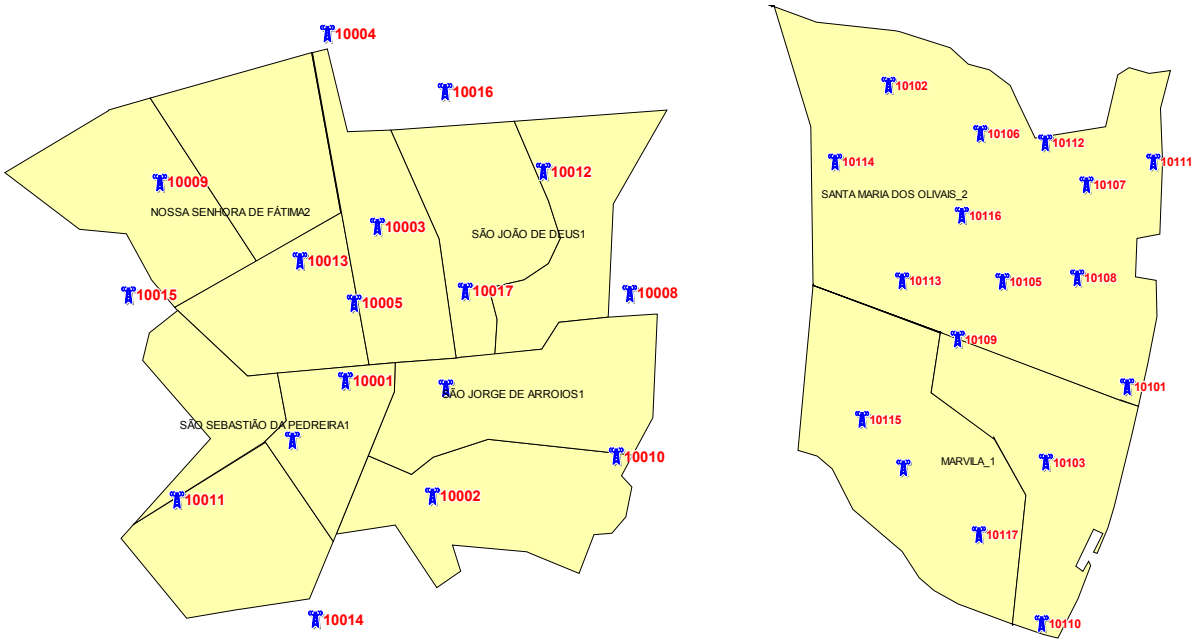

(a) HD scenario (b) LD scenario

Figure Annex I.1 – HD and LD districts and site plan.

Table Annex I.3 – 65 and 120º antenna table values (radiation pattern).

Az.	65º	120º	Az.	65º	120º	Az.	65º	120º	Az.	65º	120º	Az.	65º	120º	Az.	65º	120º
0	0.02	0	60	10.65	3.4	120	27.3	12.3	180	33.78	26	240	25.83	12	300	10.63	3.4
1	0.03	0.05	61	10.99	3.54	121	27.4	12.32	181	33.45	26	241	25.71	11.74	301	10.32	3.27
2	0.03	0.1	62	11.33	3.68	122	27.55	12.68	182	33.22	26	242	25.7	11.53	302	9.98	3.14
3	0.05	0.14	63	11.69	3.82	123	27.66	13.09	183	33.16	26	243	25.64	11.35	303	9.71	3.03
4	0.05	0.17	64	12.03	3.96	124	27.57	13.54	184	33.11	26	244	25.48	11.18	304	9.35	2.91
5	0.08	0.2	65	12.37	4.1	125	27.68	14	185	33.2	26	245	25.45	11	305	9.07	2.8
6	0.11	0.22	66	12.73	4.23	126	27.59	14.48	186	33.14	26	246	25.44	10.81	306	8.77	2.69
7	0.17	0.25	67	13.09	4.35	127	27.78	14.97	187	33.26	26	247	25.34	10.6	307	8.48	2.59
8	0.21	0.26	68	13.46	4.47	128	27.79	15.47	188	33.34	26	248	25.21	10.4	308	8.21	2.49
9	0.27	0.28	69	13.81	4.59	129	27.82	15.98	189	33.66	26	249	25.1	10.19	309	7.89	2.39
10	0.34	0.3	70	14.21	4.7	130	28	16.5	190	33.24	26	250	24.94	10	310	7.62	2.3
11	0.39	0.32	71	14.55	4.81	131	28.04	17.03	191	33.37	26	251	24.79	9.83	311	7.33	2.21
12	0.47	0.34	72	14.96	4.93	132	28.02	17.57	192	33.31	26	252	24.65	9.66	312	7.05	2.13
13	0.54	0.36	73	15.31	5.05	133	28.19	18.11	193	32.92	26	253	24.42	9.49	313	6.77	2.05
14	0.61	0.38	74	16	5.17	134	28.36	18.65	194	32.75	26	254	24.25	9.31	314	6.5	1.98
15	0.71	0.4	75	16.35	5.3	135	28.56	19.2	195	33	26	255	24.05	9.1	315	6.24	1.9
16	0.81	0.42	76	16.72	5.43	136	28.51	19.75	196	33.08	26	256	23.89	8.86	316	5.98	1.82
17	0.89	0.44	77	17.06	5.57	137	28.64	20.29	197	33.03	26.01	257	23.64	8.6	317	5.72	1.75
18	0.99	0.47	78	17.41	5.71	138	28.76	20.83	198	32.97	26.01	258	23.37	8.34	318	5.47	1.67
19	1.11	0.48	79	17.81	5.86	139	29.24	21.37	199	33.1	26.01	259	23.15	8.1	319	5.23	1.59
20	1.23	0.5	80	18.17	6	140	29.49	21.9	200	32.88	26	260	22.95	7.9	320	4.99	1.5
21	1.35	0.51	81	18.56	6.14	141	29.77	22.43	201	32.58	25.99	261	22.76	7.75	321	4.76	1.41
22	1.5	0.52	82	18.89	6.27	142	30.13	22.95	202	32.33	25.98	262	22.51	7.63	322	4.5	1.32
23	1.63	0.54	83	19.24	6.38	143	30.05	23.45	203	31.85	25.97	263	22.26	7.53	323	4.27	1.24
24	1.79	0.56	84	19.62	6.46	144	30.25	23.94	204	31.77	25.97	264	22.07	7.43	324	4.05	1.16
25	1.92	0.6	85	19.95	6.5	145	30.72	24.4	205	31.68	26	265	21.78	7.3	325	3.84	1.1
26	2.07	0.65	86	20.34	6.5	146	31.41	24.83	206	31.48	26.05	266	21.53	7.14	326	3.62	1.05
27	2.24	0.71	87	20.67	6.48	147	31.44	25.22	207	31.12	26.09	267	21.26	6.95	327	3.42	1.01
28	2.4	0.78	88	20.97	6.45	148	31.43	25.55	208	30.68	26.12	268	20.99	6.77	328	3.22	0.98
29	2.55	0.84	89	21.29	6.45	149	32.17	25.82	209	30.15	26.09	269	20.68	6.61	329	3.03	0.94
30	2.73	0.9	90	21.62	6.5	150	32.52	26	210	29.76	26	270	20.43	6.5	330	2.85	0.9
31	2.92	0.94	91	21.91	6.61	151	32.9	26.09	211	29.52	25.82	271	20.15	6.45	331	2.66	0.84
32	3.1	0.98	92	22.22	6.77	152	33.25	26.12	212	29.24	25.55	272	19.86	6.45	332	2.48	0.78
33	3.31	1.01	93	22.54	6.95	153	33.73	26.09	213	29.03	25.22	273	19.53	6.48	333	2.3	0.71
34	3.5	1.05	94	22.83	7.14	154	34.33	26.05	214	28.81	24.83	274	19.24	6.5	334	2.14	0.65
35	3.71	1.1	95	23.13	7.3	155	34.67	26	215	28.66	24.4	275	18.94	6.5	335	1.98	0.6
36	3.92	1.16	96	23.43	7.43	156	34.76	25.97	216	28.49	23.94	276	18.68	6.46	336	1.83	0.56
37	4.13	1.24	97	23.7	7.53	157	35.18	25.97	217	28.24	23.45	277	18.38	6.38	337	1.69	0.54
38	4.37	1.32	98	23.96	7.63	158	35.66	25.98	218	28.02	22.95	278	18.09	6.27	338	1.56	0.52
39	4.59	1.41	99	24.27	7.75	159	35.8	25.99	219	27.79	22.43	279	17.78	6.14	339	1.43	0.51
40	4.83	1.5	100	24.5	7.9	160	35.87	26	220	27.63	21.9	280	17.48	6	340	1.31	0.5
41	5.06	1.59	101	24.74	8.1	161	35.98	26.01	221	27.42	21.37	281	17.15	5.86	341	1.17	0.48
42	5.32	1.67	102	25.07	8.34	162	35.45	26.01	222	27.25	20.83	282	16.82	5.71	342	1.05	0.47
43	5.56	1.75	103	25.24	8.6	163	35.36	26.01	223	27.05	20.29	283	16.13	5.57	343	0.92	0.44
44	5.82	1.82	104	25.39	8.86	164	35.38	26	224	26.91	19.75	284	15.81	5.43	344	0.82	0.42
45	6.07	1.9	105	25.55	9.1	165	35.59	26	225	26.9	19.2	285	15.51	5.3	345	0.72	0.4
46	6.34	1.98	106	25.76	9.31	166	35.16	26	226	26.88	18.65	286	15.19	5.17	346	0.63	0.38
47	6.63	2.05	107	25.93	9.49	167	34.8	26	227	26.72	18.11	287	14.89	5.05	347	0.55	0.36
48	6.92	2.13	108	26.13	9.66	168	34.6	26	228	26.69	17.57	288	14.56	4.93	348	0.49	0.34
49	7.2	2.21	109	26.3	9.83	169	34.05	26	229	26.57	17.03	289	14.24	4.81	349	0.42	0.32
50	7.5	2.3	110	26.46	10	170	33.77	26	230	26.48	16.5	290	13.9	4.7	350	0.34	0.3
51	7.78	2.39	111	26.6	10.19	171	33.84	26	231	26.45	15.98	291	13.57	4.59	351	0.27	0.28
52	8.07	2.49	112	26.69	10.4	172	33.48	26	232	26.39	15.47	292	13.21	4.47	352	0.2	0.26
53	8.37	2.59	113	26.82	10.6	173	33.59	26	233	26.32	14.97	293	12.92	4.35	353	0.17	0.25
54	8.68	2.69	114	26.94	10.81	174	33.58	26	234	26.25	14.48	294	12.58	4.23	354	0.11	0.22
55	8.97	2.8	115	27.04	11	175	33.63	26	235	26.18	14	295	12.25	4.1	355	0.11	0.2
56	9.31	2.91	116	27.11	11.18	176	33.97	26	236	26.11	13.54	296	11.94	3.96	356	0.08	0.17
57	9.63	3.03	117	27.09	11.35	177	33.92	26	237	26.04	13.09	297	11.58	3.82	357	0.05	0.14
58	9.97	3.14	118	27.23	11.53	178	33.54	26	238	25.98	12.68	298	11.28	3.68	358	0.01	0.1
59	10.33	3.27	119	27.34	11.74	179	33.63	26	239	25.93	12.32	299	10.94	3.54	359	0.02	0.05

Table Annex I.4 – E_b/N_0 table values.

RB (Switching Type)	Propagation type	UL	DL
12,2 (CS)	Indoor	5.8	7.7
12,2 (CS)	Pedestrian	5.8	7.7
12,2 (CS)	Vehicular	6.9	8.0
64 (CS)	Indoor	4.1	6.7
64 (CS)	Pedestrian	4.2	6.7
64 (CS)	Vehicular	5.8	7.8
64 (PS)	Indoor	4.2	6.6
64 (PS)	Pedestrian	4.2	6.6
64 (PS)	Vehicular	5.5	7.3
128 (CS)	Indoor	4.0	5.9
128 (CS)	Pedestrian	4.2	6.0
128 (CS)	Vehicular	5.8	7.5
128 (PS)	Indoor	4.0	5.9
128 (PS)	Pedestrian	4.2	5.9
128 (PS)	Vehicular	5.5	6.3
384 (PS)	Indoor	4.0	6.5
384 (PS)	Pedestrian	4.2	6.7
384 (PS)	Vehicular	5.5	7.7

BearerMapping Browser

Application	Service_Type	Bearer	Switching_Typ	QoS	ULrate_kbps	DLrate_kbps	Traffic_Model_Momentum
voice	VOICE	CS_C_UL_12.2kbps_DL_12.	CS	C	12.2	12.2	speech
audio_on_demand	MUSIC_ON_DEMAND	PS_IB_UL_64kbps_DL_64kl	PS	IB	64	64	streaming
video_telephony	VIDEO_CONFERENCE	CS_C_UL_64kbps_DL_64kb	CS	C	64	64	video
video_conf	REMOTE_MONITORING	PS_IB_UL_64kbps_DL_64kl	PS	IB	64	64	streaming
m_commerce	MACHINE_2_CUSTOMER	PS_IB_UL_64kbps_DL_64kl	PS	IB	64	64	www
video_on_demand	VIDEO_ON_DEMAND	PS_IB_UL_64kbps_DL_384l	PS	IB	64	384	streaming
web_browsing	WEB_BROWSING	PS_IB_UL_64kbps_DL_128l	PS	IB	64	128	www
chat	MESSAGING	PS_IB_UL_64kbps_DL_64kl	PS	IB	64	64	www
file_storing	INTRANET	PS_IB_UL_64kbps_DL_384l	PS	IB	64	384	ftp
turistic_info	LOCATION_BASED_SERVI	PS_IB_UL_64kbps_DL_64kl	PS	IB	64	64	lbs
personal_LBS	LOCATION_BASED_SERVI	PS_IB_UL_64kbps_DL_64kl	PS	IB	64	64	lbs
travelling_assistance	LOCATION_BASED_SERVI	PS_IB_UL_64kbps_DL_64kl	PS	IB	64	64	lbs
emergency	VOICE	CS_C_UL_12.2kbps_DL_12.	CS	C	12.2	12.2	speech
MMS	MESSAGING	PS_IB_UL_64kbps_DL_64kl	PS	IB	64	64	mms_sms
interactive_gaming	GAMES_ON_DEMAND	PS_IB_UL_64kbps_DL_128l	PS	IB	64	128	streaming
FTP	INTRANET	PS_IB_UL_64kbps_DL_384l	PS	IB	64	384	ftp
email	MESSAGING	PS_IB_UL_64kbps_DL_128l	PS	IB	64	128	email
file_download	INTRANET	PS_IB_UL_64kbps_DL_384l	PS	IB	64	384	ftp
electronic_journal_books	APPLICATIONS_ON_DEMA	PS_IB_UL_64kbps_DL_128l	PS	IB	64	128	www

Figure Annex I.2 – Bearer mapping table.

BearerMapping Browser

Traffic_Model_Momentum	SF_UL	SF_DL	TTI_UL_ms	TTI_DL_ms	Coding_UL	Coding_DL	PHY_UL_Rb_kb	PHY_DL_Rb_kb
speech	64	128	20	20	0.333333	0.333333	60	60
streaming	16	32	20	20	0.333333	0.333333	240	240
video	16	32	40	40	0.333333	0.333333	240	240
streaming	16	32	20	20	0.333333	0.333333	240	240
www	16	32	20	20	0.333333	0.333333	240	240
streaming	16	8	20	10	0.333333	0.333333	240	960
www	16	16	20	20	0.333333	0.333333	240	480
www	16	32	20	20	0.333333	0.333333	240	240
ftp	16	8	20	10	0.333333	0.333333	240	960
lbs	16	32	20	20	0.333333	0.333333	240	240
lbs	16	32	20	20	0.333333	0.333333	240	240
lbs	16	32	20	20	0.333333	0.333333	240	240
speech	64	128	20	20	0.333333	0.333333	60	60
mms_sms	16	32	20	20	0.333333	0.333333	240	240
streaming	16	16	20	20	0.333333	0.333333	240	480
ftp	16	8	20	10	0.333333	0.333333	240	960
email	16	16	20	20	0.333333	0.333333	240	480
ftp	16	8	20	10	0.333333	0.333333	240	960
www	16	16	20	20	0.333333	0.333333	240	480

Figure Annex I.3 – Bearer mapping table (cont.).

Scenarios Browser

Clutter	Penetration_%
Dense Residential	30
Light Residential	15
Mixed Buildings	25
Terciary Buildings	20
Industrial Buildings	5
Roads	4
Green Areas	1

Figure Annex I.4 – Clutter user distribution (Penetration).

J. TRAFSIM3G – Reference and User Guide

- **Introduction**

This annex includes a quick reference guide, enabling tool users to quickly familiarize with the tool menus and functional procedures.

TRAFSIM3G is developed over MapInfo® and VC++ platforms, allowing generating a multi-service non-uniform traffic pattern, and performing a system performance analysis in the time domain. The tool user is required to previously install MapInfo® [MAPI03] application in order to run the main TRAFSIM3G executable (TRAFSIM3G.mbx).

The TRAFSIM3G software package includes 3 main components:

- TRAFSIM3G.mbx (MapInfo® executable file)
- TRAFSIM3GDLL.dll (Auxiliay DLL, including VC++ function to use with MapInfo®)
- TRAFSIM3G_VC.exe (VC++ executable file)

To run TRAFSIM3G application, the tool user just needs to open the .mbx file as all other will be run automaticaly from the TRAFSIM3G.mbx menus.

- **File structure**

To ease TRAFSIM3G usage, it is proposed to follow a specific folder structure as most file input/output routines include those by default. If copying the three TRAFSIM3G base files (.mbx, .dll and .exe), the tool user shall additionaly create in that same folder the following structure:

- Input (MapInfo® Tables data)
- Output (MapBasic® module outputs, where VC++ module will retrieve automatically data)
- Output_VC (VC++ module output files)

- **User Generation**

The user generation process can be enabled by a simple 4-click process, Figure Annex J.1.

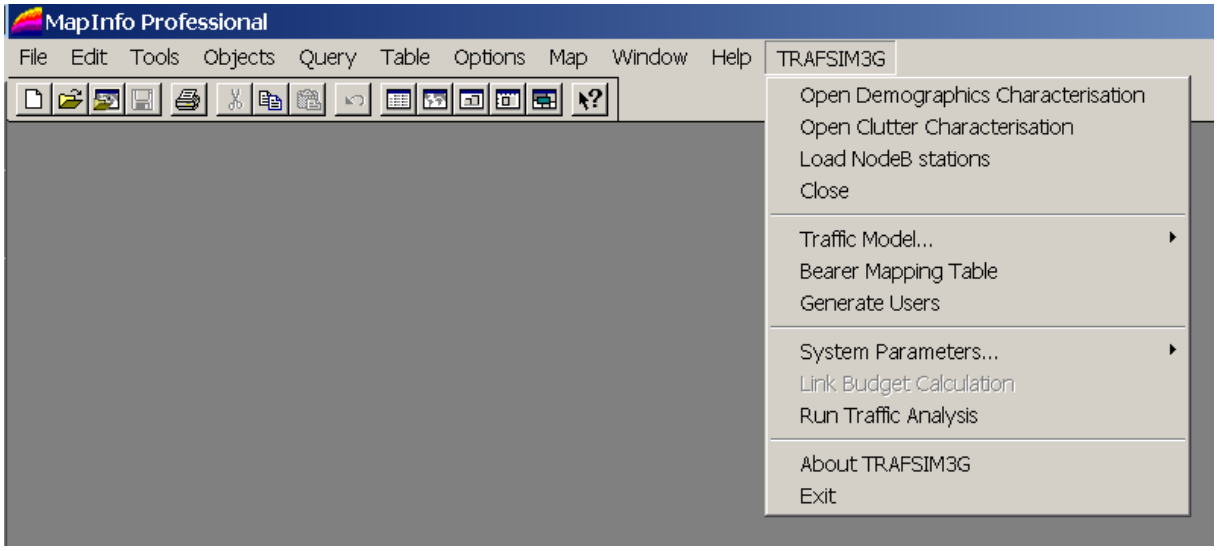

Figure Annex J.1 – TRAFSIM3G Main menu.

1. **Open Demographics Characterisation** (Load district information tables)

2. **Open Clutter Characterisation** (Load clutter information tables)

3. **Load NodeB stations**

4. **Generate Users** (user is prompted to a new generation of file import, if already created a user pattern. Traffic parameters shall be confirmed in advance before starting the generation process)

Traffic Model parameters, as penetration, demographic characterisation weights can be changed. Within this menu, user is also able to change the service table's definition, where the tool user can assign different weights for the several applications available. **Bearer mapping** option will show a read-only table including all the application to RB mapping considerations.

In **System Parameters** menu, the tool user can change the propagation model parameters (COST 231-WI), the E_b/N_0 values, the link budget parameters and load different antenna patterns (application considers a default 65º horizontal beam width antenna). After generating the users, the tool user shall verify the link budget assumptions, and if correct with the scenario chosen, to run the **Link Budget Calculation**, which will enable all link calculation and save it in the respective output file, finishing the user's generation process.

- **System Performance (VC++ Module)**

The tool user can run the VC++ module directly from the TRAFSIM3G menu (**Run Traffic Analysis**). This item will open the VC++ module user interface as shown in Figure Annex J.2.

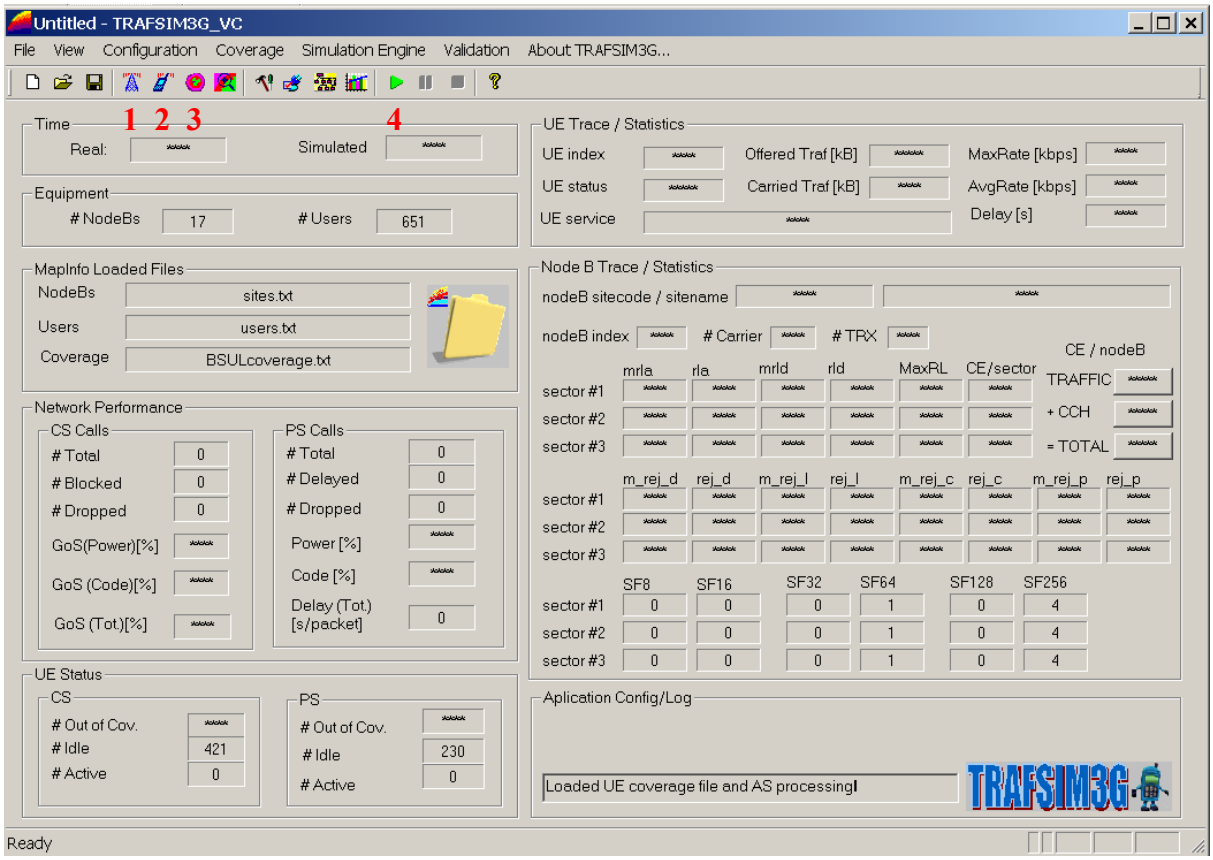

Figure Annex J.2 – VC++ module user interface.

Similar to the GIS module, a simple 4-click process was developed (see Figure Annex J.2):

1. **Load NodeB** data
2. **Load UEs** data
3. **Load UL coverage** data
4. Start time domain analysis (push **Play** button)

Along the input process, the application window provides status on the number of sites and UEs loaded (**Equipment**) as the validation of the input files by displaying its names in the **MapInfo® Loaded Files** area, and showing tasks conclusion in the **Application Config/Log** status window. Network and UE performance main indicators are also presented real-time, along with the NodeB/UE that can also be traced and its main performance indicators shown.

The user can easily access coverage information after loading the 3 files, by pushing the **Coverage Indicators button**. Information on RSCP and AS distribution is provided along with non-covered users percentage, and UL radius calculations from GIS module.

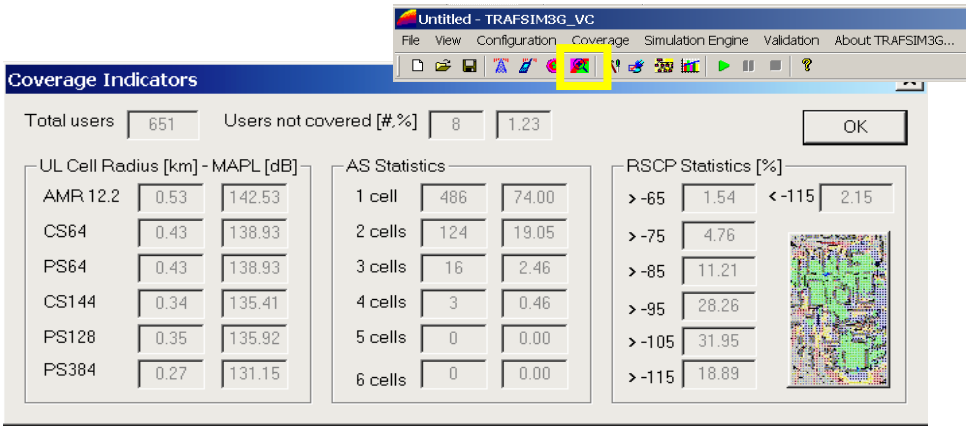

Figure Annex J.3 – Coverage indicators.

- **General Configuration**

This option enables the tool user to define input/output directories, along with the output file selection flags. The trace menu indicates which NodeB/UE will be displaying real-time (in the main application window) its performance indicators. The tool user is also requested to define the simulation time, and the data filter (only data after the defined time will be processed).

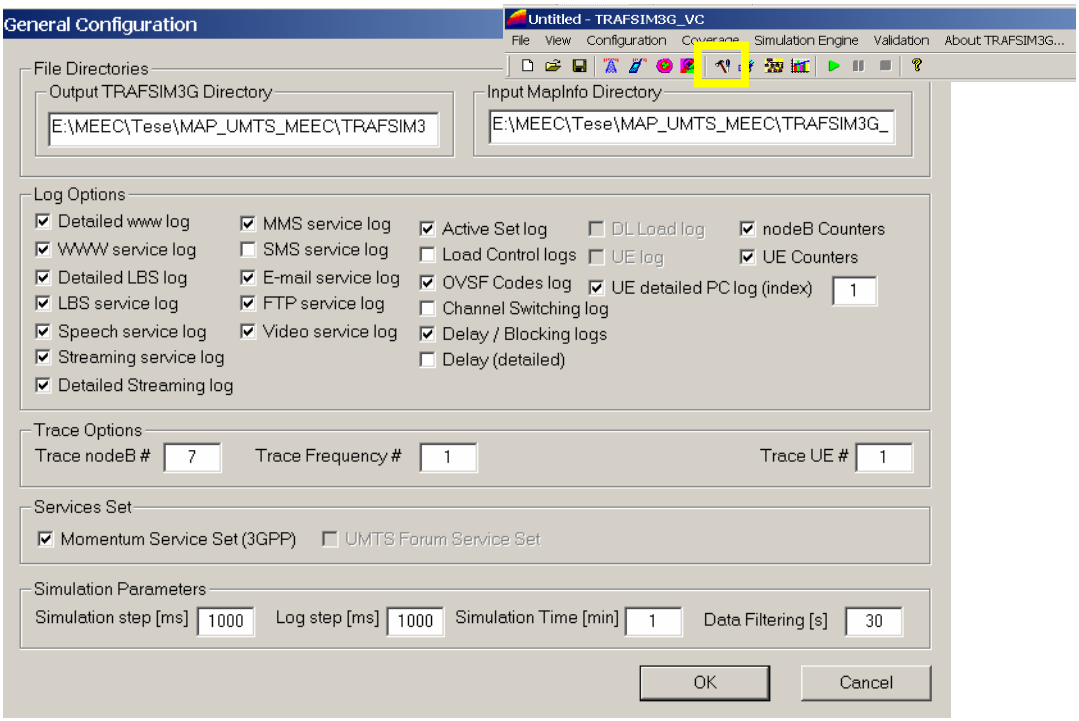

Figure Annex J.4 – General Options.

- **Services**

All services and traffic source model parametrisation can be defined in TRAFSIM3G. Source models were split by type as shown in :

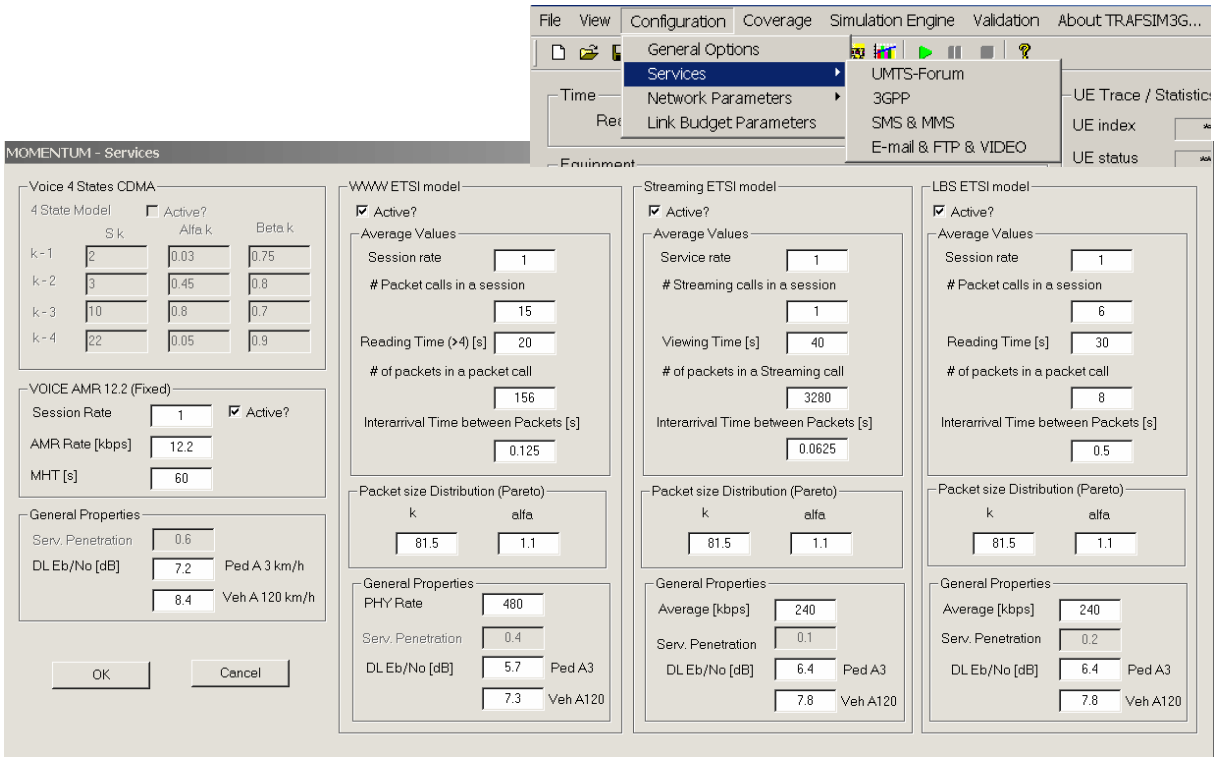

Figure Annex J.5 – Speech and WWW derived traffic source models.

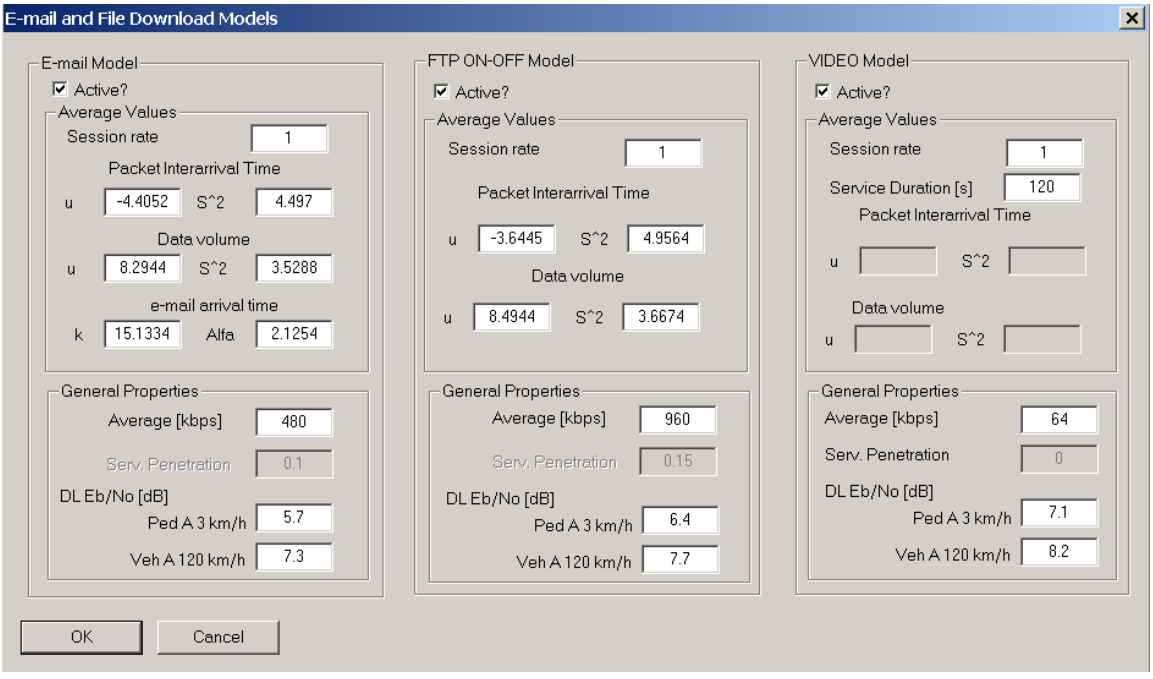

Figure Annex J.6 – E-mail, FTP and video traffic source models parametrisation.

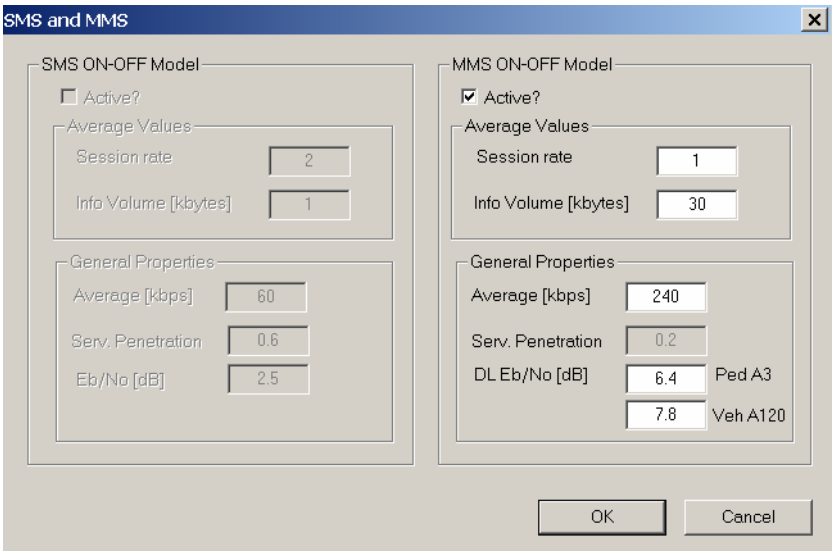

Figure Annex J.7 – MMS and SMS parameters.

- **Network Parameters – RRM**

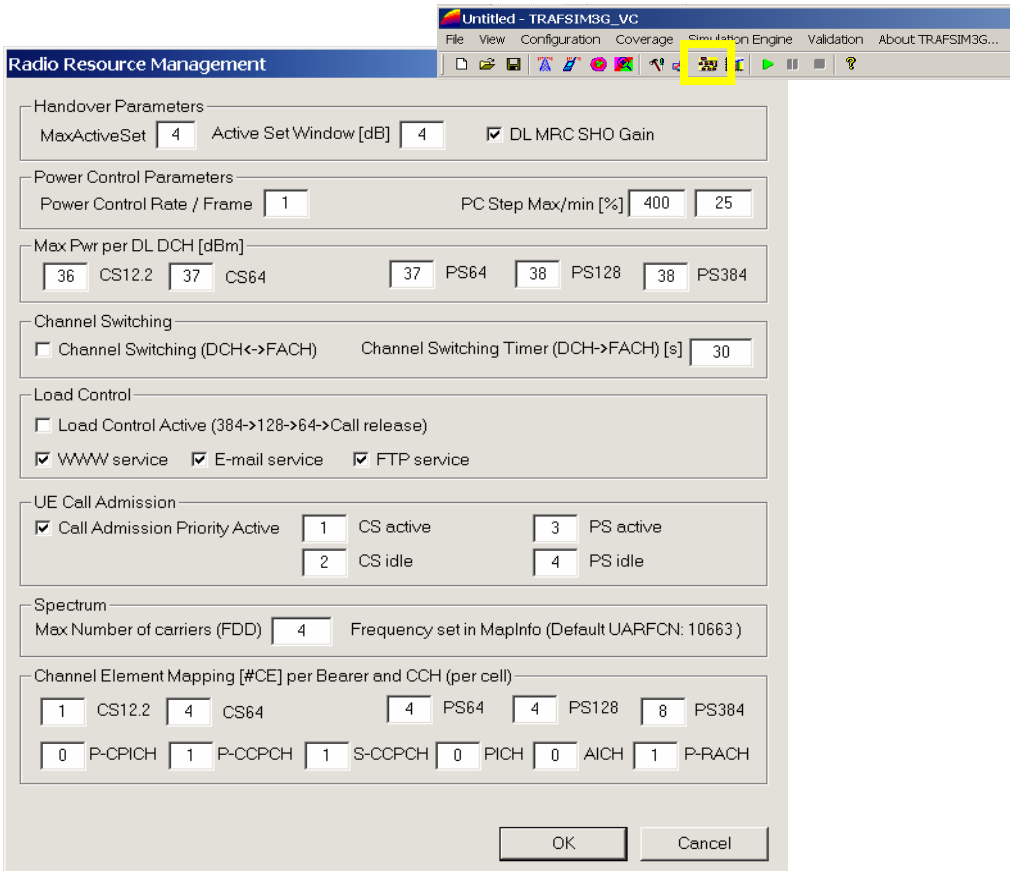

Figure Annex J.8 – RRM parameters.

This menu includes all RMM configurable parameters, for SHO, power control, admission and load control. Also includes CE mapping information.

- **Network Dimensioning**

This menu includes all the calculation process definitions, such as the definition of the interference calculation process, the inclusion of common channel CEs in final NodeB CE figures, inclusion of FFM variable algorithm or alternatively fixed margin approach. Number of considered carriers is also defined in this menu.

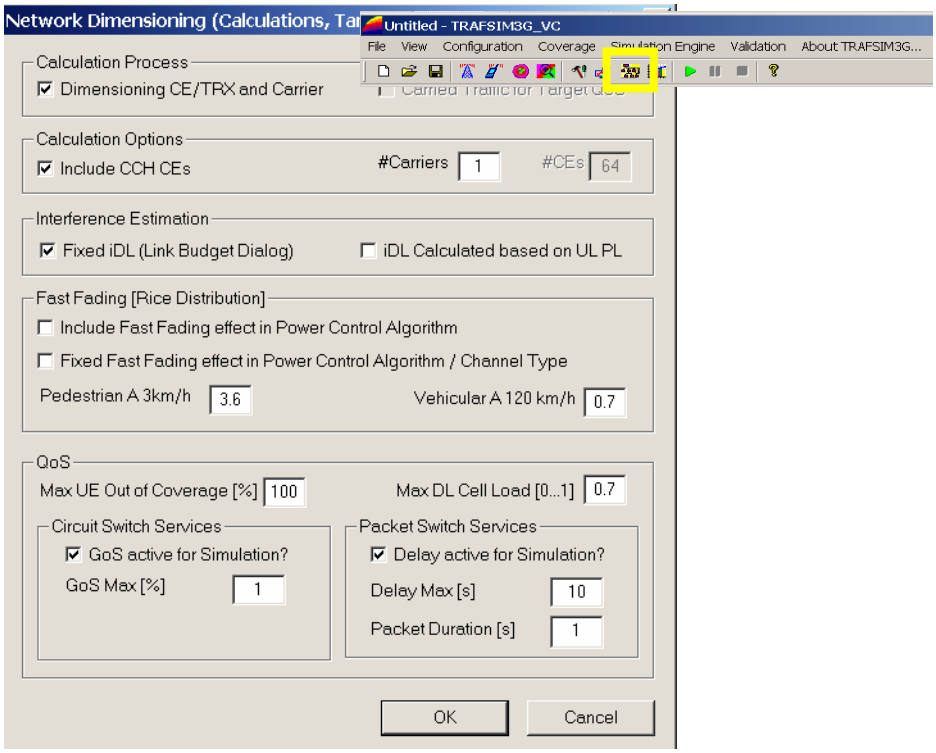

Figure Annex J.9 – Network dimensioning parameters.

- **(DL) Link Budget Parameters**

This menu includes all DL link budget parameters not defined in the GIS modules suc as the ortogonality factors, FFM *K* Rice coeficients and inter-to-intra cell intereference ratio.

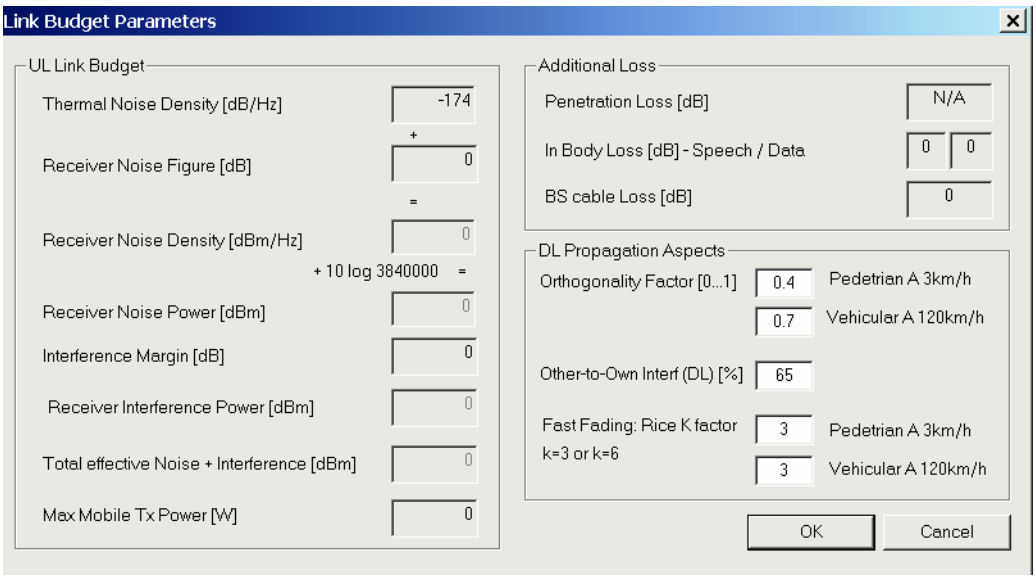

Figure Annex J.10 – DL link budget parameters.

K. Input/Output Files – MapBasic® Module

This annex includes the input/output format for files used in the MapBasic® module of TRAFSIM3G.

- **Input Files Format**

Table Annex K.1- Age table contents.

Header	Application	DL Rb [kbps] / CS,PS	Age<20	20<Age<64	Age>64
Unit	N/A	N/A	[%]	[%]	[%]
Type	string	string	float	float	float
Example	audio-on-demand	64 (PS)	14	3	0

Table Annex K.2 – Education and salary table contents.

Header	No Education	Basic	Complementary	Degree	Low	Medium	Medium-High	High
Unit	[%]	[%]	[%]	[%]	[%]	[%]	[%]	[%]
Type	float	float	float	float	float	float	float	float
Example	0	9	3	3	0	0	4	9

Table Annex K.3 – Scenarios table contents.

Header	Clutter	Penetration
Unit	N/A	[%]
Type	string	float
Example	Dense Residential	30

Table Annex K.4 – Antennas table contents.

Header	Azimuth	RefToMaxGain
Unit	º	[- dB]
Type	int	float
Example	0	0.02 (16.98 dBi)

Table Annex K.5 – Bearer mapping table.

Header	Applic.	Service Type	Bearer	Switch. Type	QoS	UL Rb	DL Rb	Traf. Model Momentum
Unit	N/A	N/A	N/A	N/A	N/A	[kbps]	[kbps]	N/A
Type	string	string	string	string	string	float	float	string
Example	audio_on demand	MUSIC_ON_ DEMAND	PS_IB_UL_64k bps_DL_64kbps	PS	I/B	64	64	streaming

Table Annex K.6 – Bearer mapping table (cont.).

Header	SF_UL	SF_DL	TTI_UL	TTI_DL	Coding_U L	Coding_ DL	PHY_UL_ Rb	PHY_DL_R b
Unit	N/A	N/A	[ms]	[ms]	N/A	N/A	[kbps]	[kbps]
Type	int	int	int	int	float	float	float	float
Example	16	32	20	20	1/3	0.333	240	240

Table Annex K.7 – E_b/N_0 table contents.

Header	Rb / Switch	Channel Type	UL	DL
Unit / Range	[kbps] / [CS, PS]	[Pedestrian, Vehicular, Indoor]	[dB]	[dB]
Type	int	string	float	float
Example	64 (CS)	Pedestrian	4.2	6.7

Table Annex K.8 – District table contents.

Header	District name	Present pop.	Age <20	20<Age <64	Age >64	No Educ.	Basic	Comple-mentary	Degree	Salary
Unit	N/A	N/A	[%]	[%]	[%]	[%]	[%]	[%]	[%]	List
Type		int	float	float	float	float	float	float	float	string
Example	S.João de Deus	33640	22.95	33.34	43.71	6.70	31.91	22.28	39.11	High

Table Annex K.9 – Clutter table contents.

Header	ID	Clutter	Clutter_ID
Unit	N/A	N/A	N/A
Type	int	string	int
Example	404	Dense Residential	1

Table Annex K.10 – Sites table contents

Header	Site code	Site name	City	X (Lon.)	Y (Lat.)	Z Height Azimuth	Sector 1,2,3 PA power	Sector 1,2,3 CPICH	Sect 1,2,3 CCH
Unit	N/A	N/A	N/A	dec W	dec N	m	º	W	W	W
Type	string	String	string	float	float	float	int	float	float	float
Example	10101	NodeB101	Lisbon	-9.096	38.75	0 (N/A)	0,120,240	20	2	6

- **Output Files Format**

Table Annex K.11 – Users txt file contents.

Header	User_Id	Long	Lat	Serv#1	Serv#2
Unit	N/A	dec	dec	list {PS64/128/384, CS64, None}	list {PS64/128/384, CS64, None}
Type	int	float	float	string	string
Example	1	-9.15	38.73	PS128	None

Table Annex K.12 – Users txt file contents (cont.).

Header	S1 Id	S2 Id	Clutter Id	Channel	Pen.	S1 Mom.	S2 Mom.
Unit	1- CS12.2 2- CS64 3- CS144 4- CS384 5- PS64 6- PS128 7- PS384	same as S1 Id	1- Dense Res. 2- Light Res. 3- Mixed B. 4- Tertiary B. 5- Industrial B. 6- Roads 7- Green Areas	1-Ped. 2- Veh.	[dB]	6- speech 7- WWW 8- VideoConf. 9- Streaming 10- LBS 11- SMS 12 - MMS 13- E-mail 14- FTP	same as S1 Momentum -99- none
Type	int	int	int	int	float	int	int
Example	6	0	7	1	0	7	-99

Table Annex K.13 – BSULCoverage txt file contents.

Header	UE_Id	BSnum	BSn	BSndist	BSnangle	Cell_n	Path_n
Unit	N/A	<9	N/A	[km]	º [0...359]	sitecode + cell_index)	[dB]
Type	int	int	string	float	float	string	float
Example	1	3	10007	0.43	205.6	100072	142.59

Table Annex K.14 – ExportLinkBudget txt file contents.

Parameter	Variable	Unit	Type	Example	Comments
RMAX_UL_service	cell radius	[km]	float	0.425	speech, CS or PS64/128/384
p_ue_tx	UE power	[dBm]	float	21	
ue_gain	UE ant. gain	[dBi]	float	0	
serv	Target Service	N/A	Int	1	1-Speech, 2-CS64, 3-PS64, 4–CS144, 5-PS128, 6-PS384
c_users	Flag	N/A		1	Show Users: informative
body_loss_voice	-	[dB]		3	
body_loss_data	-	[dB]		1	
deep_ind	Indoor Penetration	[dB]		0	Used for RMAX_UL
stdev_out	stdev outdoor	[dB]		7	
stdev_ind	stdev indoor	[dB]		6	
cov_prob	coverage probability	[%]		95	
dist_coef	distance coefficient	[dB/km]		3.8	
sho_gain	soft handover gain	[dB]		3	
ffm_marg	fast fading margin	[dB]		3.5	
NodeB_NF	noise figure	[dB]		3	
ant_gain	NodeB ant. gain	[dBi]		17	
tma	TMA existence	int		0	
cable_loss	-	[dB]		3	
tma_gain	-	[dB]		12	
tma_nf	TMA noise figure	[dB]		2	
load_marg	Load factor	[%]		0.5	

L. Input/Output Files – VC++ Module

This annex includes the input/output format for files used in the VC++ module of TRAFSIM3G.

- **Output Files Format**

Table Annex L.1 – TRAFSIM3G log file contents.

Parameter / File entry	Type	Example
Number of NodeB	string	Created 17 NodeB
NodeB object creation check	string	NodeB inputs and OVSF tree created
Number of UE and object check	string	Created 1382 UEs
UE inputs check	string	UE inputs loaded
Traffic vector creation check	string	Initiated 3GPP UE services
File load check	string	Link Budget from MapInfo® loaded
File load check	string	Services and Bearer mapping from MapInfo® loaded
File load check (BSULcoverage)	string	Loaded UE coverage file and AS processing
Start time	string	Simulation started at 19:53:40
Service assignment for UE (# sessions)	string	3GPP_SPEECH traffic created: Ns=0 for UE Id=5
Stop time	string	Simulation ended at 19:57:23

Table Annex L.2 – Application service log file contents.

Filename	Detailed	File contents
Speech		#sessions, start frame, duration [s]
WWW	Yes	#sessions, start frame, # occupied frames
Video Conference		#sessions, start frame, duration [s]
Streaming	Yes	#sessions, start frame, # occupied frames
LBS	Yes	#sessions, start frame, # occupied frames
SMS / MMS		#sessions, start frame, SMS / MMS size [kB], # occupied frames
E-mail		#sessions, start frame, E-mail size [B], # occupied frames
FTP		#sessions, start frame, FTP size [B], # occupied frames

Table Annex L.3 – UE power control file contents.

Parameter / File entry	Unit	Type	Example
UE Index	N/A	Int	23
Active Set link	N/A	Int (0...5)	0 (main link)
Timeslot	N/A	Int (0...14)	0 (see Section 4.3.3)
Frame Number	N/A	Int	2944
UE Rx Power	[dBm]	Float	-114.97
UE Power in NodeB PA	[W]	Float	0.0246
FFM attenuation	[dB]	Float	0
I_{oth}	W	Float	5.847E-14
I_{oth}/I_{own}	N/A	Float	0.65

Table Annex L.4 – UE counters (time filter) files contents.

Parameter / File entry	Unit	Type	Example
UE Index	N/A	Int	431
Offered volume	[kB]	float	29.6
Carried volume	[kB]	float	29.6
Maximum rate	[kbps]	float	128
Average rate	[kbps]	float	122.7
Service	N/A	Int	13
LC_384to128, LCxxtoyy	N/A	Int	0 (load control counters / service)
Number CS calls	N/A	Int	0
CS calls blocked	N/A	Int	0
PS packets	N/A	Int	32
Number delayed packets	N/A	Int	8
Total PS delay	[s]	float	0.08

Table Annex L.5 – NodeB counters (time filter) files contents.

File entry	Unit	Type	Description / Example
Time	s	float	0 - Only available in time and time filter files
NodeBcode	N/A	string	10101
Cell	N/A	Int	1
mrlaxx / mrldxx	N/A	Int	Main radio link addition/deletion (divided in total, CS and for each service: e.g., mrla6 for speech)
rlaxx / rldxx	N/A	Int	Radio link addition/deletion for SHO links (divided in total, CS and for each service: e.g., mrla6 for speech)
mrlarejdistxx / mrlarejdistxx	N/A	Int	Main radio link addition/deletion and Radio link addition/deletion links rejected due to high pathloss (distance)
mrlarej**pwr**xx / mrlarej**pwr**xx	N/A	Int	Main radio link addition/deletion and Radio link addition/deletion links rejected due to high load
mrlarej**ovsf**xx / mrlare**ovsf**xx	N/A	Int	Main radio link addition/deletion and Radio link addition/deletion links rejected due to shortage of OVSF codes
mrlarej**PA power**xx / mrlare**PA power**xx	N/A	Int	Main radio link addition/deletion and Radio link addition/deletion links rejected due to shortage of PA power
mrlarej**DLpwr**xx / mrlare**DLpwr**xx	N/A	Int	Main radio link addition/deletion and Radio link addition/deletion links rejected due to high DL link power (above value defined in RRM window per RB)
MaxTrafPA power	W	float	Maximum PA power value (traffic only) in BH
AvgTrafPA power	W	float	Average PA power value (traffic only) in BH
MaxRadioLinks	N/A	Int	Maximum number of simultaneous radio links (per sector)
MaxCE_T	N/A	Int	Maximum number of channel elements for traffic
CE_CCH	N/A	Int	Channel elements for common channels traffic processing
CE_Total	N/A	Int	Total channel elements number (traffic + CCH, per sector)
Max Carrier / (TRX)	N/A	Int	Maximum number of carriers / transceivers
Max_SFxx	N/A	Int	Maximum simultaneous code allocations of SFxx (4…512)
SP_kB_main, …	N/A	float	Traffic volume for main links (one per service)
SP_kB_sho, …	N/A	float	Traffic volume for soft handover (SHO) links (per service)
SP_kB_ssho, …	N/A	float	Traffic volume for softer handover (SSHO) links (per service)
P64_kB_main, …	N/A	float	Traffic volume for 64 kbps bearer (per PS RB)
PS64_kB_sho, …	N/A	float	Traffic volume for 64 kbps bearer SHO links (per PS RB)
PS64_kB_ssho, …	N/A	float	Traffic volume for 64 kbps SSHO links (per PS RB)

Table Annex L.6 – CodeAlloc and CodeDelloc files contents.

Parameter / File entry	Unit	Type	Example
Time	s	float	10
Sitecode	N/A	Int	10101
Sector	N/A	Int	1
Sitename	N/A	string	NodeB10101
# OVSF codes (per SF)	N/A	Int	2 (SF32)

Table Annex L.7 – Blocking and delay event files contents.

Parameter / File entry	Unit	Type	Example / Description
UE Index	N/A	Int	3 - UE identifier
Service	N/A	Int	6 – (speech)
Time	N/A	Int	2300 (frame number)
DropReason	1….5	Int	1 (1-load, 2-ovsf, 3-PA power, 4-DL pwr, 5-distance)
ASindex	N/A	Int	0 (active set index 0 is main, 1...5 are SHO links)
Value	[%, N/A, W, W, km]	float	0.72 (DL maximum load is 70%)

Table Annex L.8 – Active set file contents.

Parameter / File entry	Unit	Type	Example / Description
UE Index	N/A	Int	23
AS size	N/A	Int	2
cellcode (cell 0 to 5)	N/A	string	101012 , 101013 **(nocell** is used in case no cell in the active set)

M. VOC, REF, DAC and DAM Service Distribution Tables

This annex includes the services distribution for the VOC, REF, DAC and DAM scenarios used in simulation.

Table Annex M.1 – Service distribution for VOC scenario.

Service Distribution			Age [%]			Salary [%]				Education [%]			
Application	DLrate [kbps]	Traf. Model	<20	<64	>64	Low	Med.	M./H.	High	No Ed.	Basic	Compl.	Degree
voice	12,2 (CS)	speech	61	65	95	97	93	80	51	97	89	77	67
audio-on-demand	64 (PS)	streaming	6	1	0	0	0	1	5	0	2	3	1
video-telephony	64 (CS)	video	4	6	1	0	1	3	8	1	1	2	6
video-on-demand	384 (PS)	streaming	2	1	0	0	0	1	5	0	0	1	1
web-browsing	128 (PS)	WWW	4	8	3	0	1	2	8	0	1	5	8
chat	64 (PS)	WWW	6	3	0	1	1	4	4	0	1	4	3
personal LBS	64 (PS)	lbs	1	5	1	0	1	2	5	0	0	2	3
MMS	64 (PS)	mms_sms	9	3	0	2	3	4	5	0	4	3	3
interactive gaming	128 (PS)	streaming	3	1	0	1	2	3	4	2	3	3	1
FTP	384 (PS)	ftp	1	5	0	0	0	0	3	0	0	0	5
e-mail	128 (PS)	e-mail	3	3	1	0	0	1	4	0	1	1	3

Table Annex M.2 – Service distribution for REF scenario.

Service Distribution			Age [%]			Salary [%]				Education [%]			
Application	DLrate [kbps]	Traf. Model	<20	<64	>64	Low	Med.	M./H.	High	No Ed.	Basic	Compl.	Degree
voice	12,2 (CS)	speech	44	48	90	95	87	66	34	95	80	62	50
audio-on-demand	64 (PS)	streaming	9	2	0	0	0	2	7	0	3	4	2
video-telephony	64 (CS)	video	5	9	2	0	2	5	11	2	2	4	9
video-on-demand	384 (PS)	streaming	3	2	0	0	0	1	7	0	0	2	1
web-browsing	128 (PS)	WWW	6	12	5	0	1	4	10	0	2	9	13
chat	64 (PS)	WWW	9	5	0	1	2	6	5	0	1	6	4
personal LBS	64 (PS)	lbs	1	7	2	0	1	4	6	0	0	3	4
MMS	64 (PS)	mms_sms	13	4	0	3	5	6	7	0	7	4	4
interactive gaming	128 (PS)	streaming	4	2	0	1	3	4	5	3	5	4	2
FTP	384 (PS)	ftp	2	7	0	0	0	0	3	0	0	0	8
e-mail	128 (PS)	e-mail	4	4	1	0	0	2	5	0	1	2	4

Table Annex M.3 – Service distribution for DAC scenario.

Service Distribution			Age [%]			Salary [%]				Education [%]			
Application	DLrate [kbps]	Traf. Model	<20	<64	>64	Low	Med.	M./H.	High	No Ed.	Basic	Compl.	Degree
voice	12,2 (CS)	speech	28	31	82	90	76	50	20	90	67	45	33
audio-on-demand	64 (PS)	streaming	11	2	0	0	0	3	8	0	5	6	2
video-telephony	64 (CS)	video	7	11	4	0	3	8	13	4	3	5	12
video-on-demand	384 (PS)	streaming	3	2	0	0	0	1	8	0	0	3	1
web-browsing	128 (PS)	WWW	8	16	9	0	2	5	12	0	3	13	17
chat	64 (PS)	WWW	11	6	0	2	3	9	6	0	2	9	6
personal LBS	64 (PS)	lbs	1	9	4	0	2	5	7	0	0	4	6
MMS	64 (PS)	mms_sms	17	5	0	6	8	9	8	0	11	6	6
interactive gaming	128 (PS)	streaming	6	2	0	2	5	7	7	6	8	6	2
FTP	384 (PS)	ftp	2	9	0	0	0	0	4	0	0	0	10
e-mail	128 (PS)	e-mail	6	5	2	0	0	3	7	0	2	3	6

Table Annex M.4 – Service distribution for DAM scenario.

Service Distribution			Age [%]			Salary [%]				Education [%]			
Application	DLrate [kbps]	Traf. Model	<20	<64	>64	Low	Med.	M./H.	High	No Ed.	Basic	Compl.	Degree
voice	12,2 (CS)	speech	12	13	60	76	52	25	8	76	40	21	14
audio-on-demand	64 (PS)	streaming	14	3	0	0	0	4	9	0	9	9	3
video-telephony	64 (CS)	video	8	14	8	0	7	12	15	10	6	7	16
video-on-demand	384 (PS)	streaming	4	3	0	0	0	2	9	0	0	4	1
web-browsing	128 (PS)	WWW	10	20	20	0	3	8	14	0	6	18	21
chat	64 (PS)	WWW	14	8	0	5	7	14	7	0	3	13	7
personal LBS	64 (PS)	lbs	1	12	8	0	3	8	8	0	0	5	7
MMS	64 (PS)	mms_sms	21	7	0	14	17	14	9	0	20	9	7
interactive gaming	128 (PS)	streaming	7	3	0	5	10	10	8	14	14	9	3
FTP	384 (PS)	ftp	3	12	0	0	0	0	5	0	0	0	13
e-mail	128 (PS)	e-mail	7	7	4	0	0	4	8	0	3	4	7

N. DAC Scenarios Service Dist. Tables

This annex includes the services distribution for the VOC, REF, DAC and DAM scenarios used in simulation.

Table Annex N.1 – Service distribution for VC scenario.

Service Distribution			Age [%]			Salary [%]				Education [%]			
Application	DLrate [kbps]	Traf. Model	<20	<64	>64	Low	Med.	M./H.	High	No Ed.	Basic	Compl.	Degree
voice	12,2 (CS)	speech	28	31	82	90	76	50	20	90	67	45	33
audio-on-demand	64 (PS)	streaming	8	1	0	0	0	2	5	0	3	5	1
video-telephony	**64 (CS)**	**video**	**25**	**34**	**10**	**0**	**11**	**23**	**39**	**7**	**11**	**19**	**35**
video-on-demand	384 (PS)	streaming	2	1	0	0	0	1	5	0	1	2	1
web-browsing	128 (PS)	WWW	6	9	5	0	2	3	7	0	2	8	10
chat	64 (PS)	WWW	8	4	0	2	2	6	3	0	1	6	3
personal LBS	64 (PS)	lbs	1	6	2	0	1	3	4	0	0	3	3
MMS	64 (PS)	mms_sms	12	3	0	6	5	6	5	1	8	5	3
interactive gaming	128 (PS)	streaming	4	1	0	2	3	4	4	2	6	5	1
FTP	384 (PS)	ftp	2	6	0	0	0	0	4	0	0	0	6
e-mail	128 (PS)	e-mail	4	3	1	0	0	2	4	0	1	2	4

Table Annex N.2 – Service distribution for WW scenario.

Service Distribution			Age [%]			Salary [%]				Education [%]			
Application	DLrate [kbps]	Traf. Model	<20	<64	>64	Low	Med.	M./H.	High	No Ed.	Basic	Compl.	Degree
voice	12,2 (CS)	speech	28	31	82	90	76	50	20	90	67	45	33
audio-on-demand	64 (PS)	streaming	9	2	0	0	0	2	7	0	4	5	2
video-telephony	64 (CS)	video	5	9	2	0	3	6	11	4	3	4	9
video-on-demand	384 (PS)	streaming	3	2	0	0	0	1	7	0	0	2	1
web-browsing	**128 (PS)**	**WWW**	**12**	**24**	**12**	**0**	**3**	**8**	**20**	**0**	**6**	**18**	**25**
chat	**64 (PS)**	**WWW**	**18**	**9**	**0**	**3**	**6**	**14**	**9**	**0**	**3**	**13**	**8**
personal LBS	64 (PS)	lbs	1	7	2	0	1	4	6	0	0	3	4
MMS	64 (PS)	mms_sms	13	4	0	5	7	7	7	0	10	5	4
interactive gaming	128 (PS)	streaming	4	2	0	2	4	5	5	6	7	5	2
FTP	384 (PS)	ftp	2	7	0	0	0	0	3	0	0	0	8
e-mail	128 (PS)	e-mail	4	4	1	0	0	2	5	0	1	2	4

Table Annex N.3 – Service distribution for ST scenario.

Service Distribution			Age [%]			Salary [%]				Education [%]			
Application	**DLrate [kbps]**	**Traf. Model**	**<20**	**<64**	**>64**	**Low**	**Med.**	**M./H.**	**High**	**No Ed.**	**Basic**	**Compl.**	**Degree**
voice	12,2 (CS)	speech	28	31	82	90	76	50	20	90	67	45	33
audio-on-demand	**64 (PS)**	**streaming**	**21**	**5**	**0**	**0**	**0**	**5**	**15**	**0**	**8**	**12**	**6**
video-telephony	64 (CS)	video	4	9	4	0	2	5	8	2	2	3	10
video-on-demand	**384 (PS)**	**streaming**	**8**	**7**	**0**	**0**	**0**	**4**	**19**	**0**	**0**	**6**	**4**
web-browsing	128 (PS)	WWW	5	13	9	0	1	4	7	0	2	8	14
chat	64 (PS)	WWW	7	5	0	1	2	6	3	0	1	6	5
personal LBS	64 (PS)	lbs	1	8	4	0	1	4	4	0	0	2	5
MMS	64 (PS)	mms_sms	10	4	0	4	6	6	5	0	6	4	5
interactive gaming	**128 (PS)**	**streaming**	**10**	**5**	**0**	**4**	**11**	**14**	**12**	**8**	**13**	**12**	**6**
FTP	384 (PS)	ftp	1	8	0	0	0	0	2	0	0	0	8
e-mail	128 (PS)	e-mail	3	4	2	0	0	2	4	0	1	2	5

Table Annex N.4 – Service distribution for LB scenario.

Service Distribution			Age [%]			Salary [%]				Education [%]			
Application	**DLrate [kbps]**	**Traf. Model**	**<20**	**<64**	**>64**	**Low**	**Med.**	**M./H.**	**High**	**No Ed.**	**Basic**	**Compl.**	**Degree**
voice	12,2 (CS)	speech	28	31	82	90	76	50	20	90	67	45	33
audio-on-demand	64 (PS)	streaming	8	2	0	0	0	2	6	0	3	5	2
video-telephony	64 (CS)	video	5	8	3	0	2	5	10	4	2	4	9
video-on-demand	384 (PS)	streaming	2	2	0	0	0	1	6	0	0	2	1
web-browsing	128 (PS)	WWW	6	11	6	0	1	4	9	0	2	10	13
chat	64 (PS)	WWW	8	5	0	1	2	6	4	0	1	7	4
personal LBS	**64 (PS)**	**lbs**	**2**	**20**	**8**	**0**	**3**	**11**	**16**	**0**	**0**	**9**	**13**
MMS	**64 (PS)**	**mms_sms**	**30**	**9**	**0**	**8**	**13**	**16**	**15**	**0**	**18**	**12**	**11**
interactive gaming	128 (PS)	streaming	4	2	0	1	3	4	5	6	5	5	2
FTP	384 (PS)	ftp	2	7	0	0	0	0	3	0	0	0	8
e-mail	128 (PS)	e-mail	4	4	1	0	0	2	5	0	1	2	4

Table Annex N.5 – Service distribution for EM scenario.

Service Distribution			Age [%]			Salary [%]				Education [%]			
Application	**DLrate [kbps]**	**Traf. Model**	**<20**	**<64**	**>64**	**Low**	**Med.**	**M./H.**	**High**	**No Ed.**	**Basic**	**Compl.**	**Degree**
voice	12,2 (CS)	speech	28	31	82	90	76	50	20	90	67	45	33
audio-on-demand	64 (PS)	streaming	6	1	0	0	0	2	4	0	3	4	1
video-telephony	64 (CS)	video	4	6	2	0	3	5	7	4	2	3	6
video-on-demand	384 (PS)	streaming	2	1	0	0	0	1	4	0	0	2	1
web-browsing	128 (PS)	WWW	4	9	4	0	2	3	6	0	2	8	9
chat	64 (PS)	WWW	6	3	0	2	3	6	3	0	1	6	3
personal LBS	64 (PS)	lbs	1	5	2	0	2	3	4	0	0	3	3
MMS	64 (PS)	mms_sms	9	3	0	6	8	6	4	0	7	4	3
interactive gaming	128 (PS)	streaming	3	1	0	2	5	4	3	6	5	4	1
FTP	384 (PS)	ftp	1	5	0	0	0	0	2	0	0	0	5
e-mail	**128 (PS)**	**e-mail**	**36**	**34**	**10**	**0**	**0**	**20**	**41**	**0**	**12**	**20**	**35**

Table Annex N.6 – Service distribution for FT scenario.

Service Distribution			Age [%]			Salary [%]				Education [%]			
Application	**DLrate [kbps]**	**Traf. Model**	**<20**	**<64**	**>64**	**Low**	**Med.**	**M./H.**	**High**	**No Ed.**	**Basic**	**Compl.**	**Degree**
voice	12,2 (CS)	speech	28	31	82	90	76	50	20	90	67	45	33
audio-on-demand	64 (PS)	streaming	5	0	0	0	0	3	3	0	5	6	0
video-telephony	64 (CS)	video	3	2	4	0	3	8	4	4	3	5	2
video-on-demand	384 (PS)	streaming	2	0	0	0	0	1	3	0	0	3	0
web-browsing	128 (PS)	WWW	4	2	9	0	2	5	4	0	3	13	2
chat	64 (PS)	WWW	5	1	0	2	3	9	2	0	2	9	1
personal LBS	64 (PS)	lbs	1	1	4	0	2	5	2	0	0	4	1
MMS	64 (PS)	mms_sms	8	1	0	6	8	9	3	0	11	6	1
interactive gaming	128 (PS)	streaming	3	0	0	2	5	7	2	6	8	6	0
FTP	**384 (PS)**	**ftp**	**41**	**59**	**0**	**0**	**0**	**0**	**54**	**0**	**0**	**0**	**58**
e-mail	128 (PS)	e-mail	3	1	2	0	0	3	2	0	2	3	1

O. VOC, REF, DAC and DAM Output Analysis

This annex include all analysis performed and used in results summary of Chapter 5 to what regard the simulations on VOC, REF, DAC and DAM scenarios.

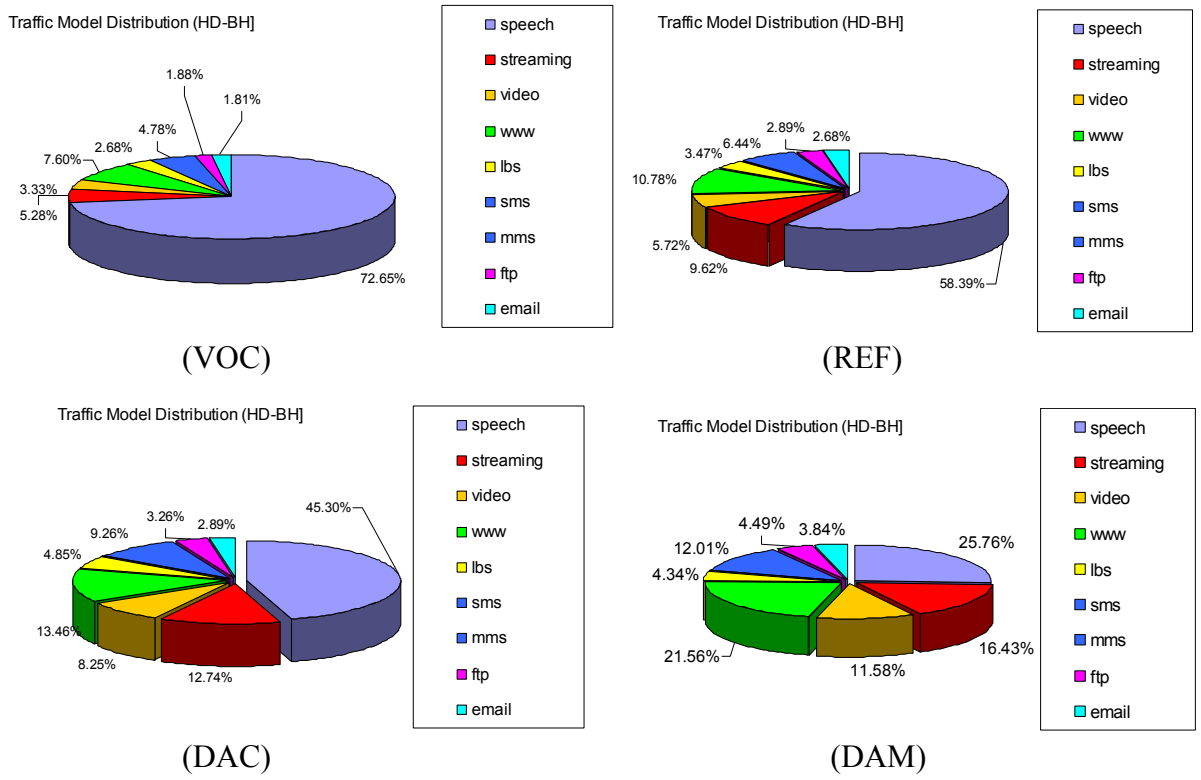

Figure Annex O.1 – Traffic Mix distribution (TRAFSIM3G traffic).

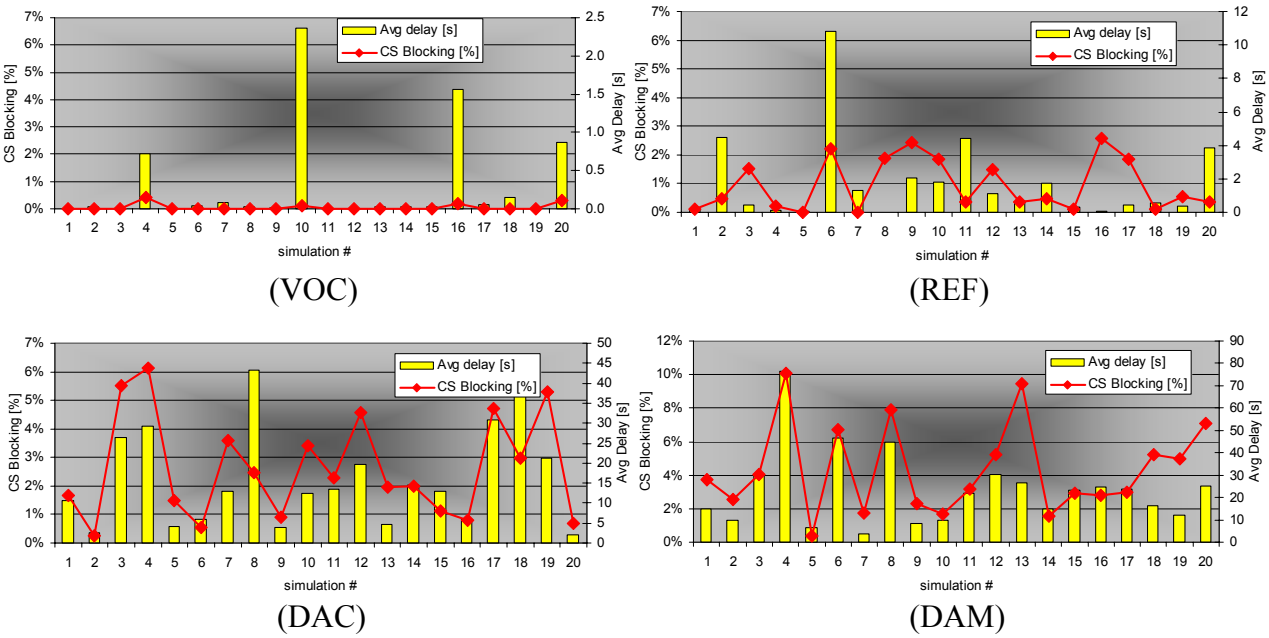

Figure Annex O.2 – Blocking and Average delay.

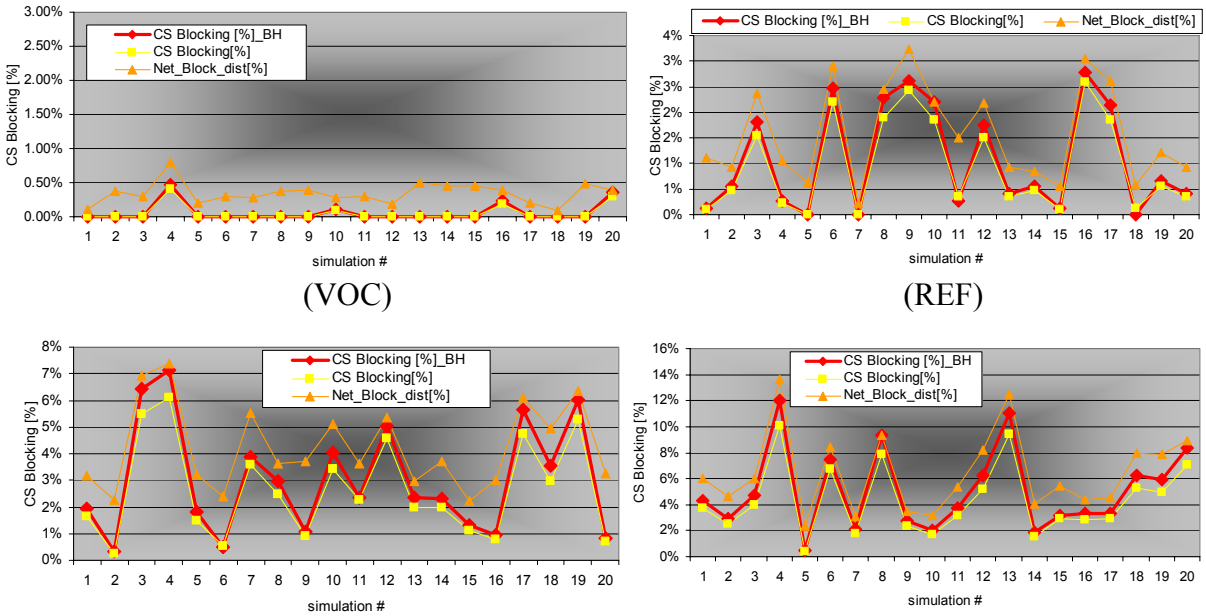

Figure Annex O.3 – Blocking in BH, 70 min and including distance blocks.

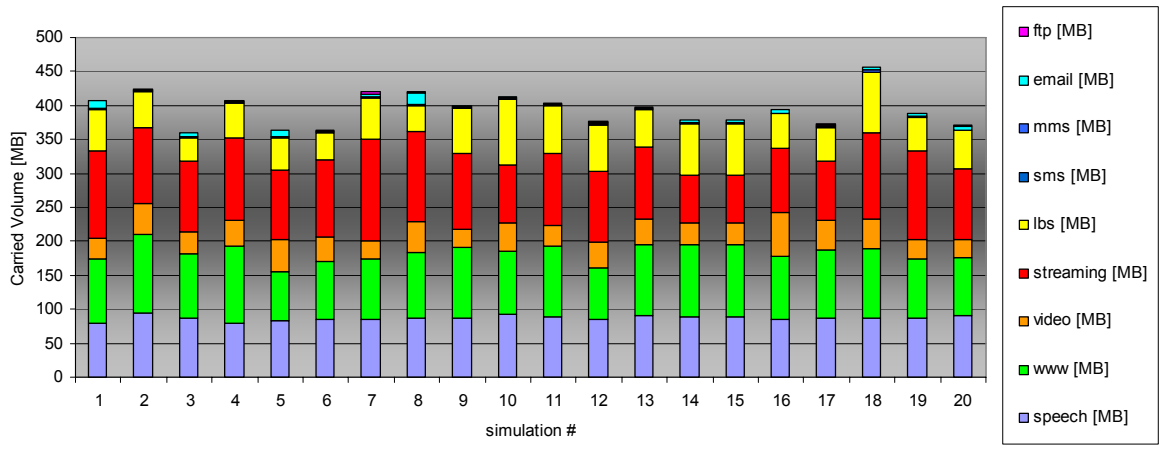

Figure Annex O.4 – Carried traffic volume in VOC scenario.

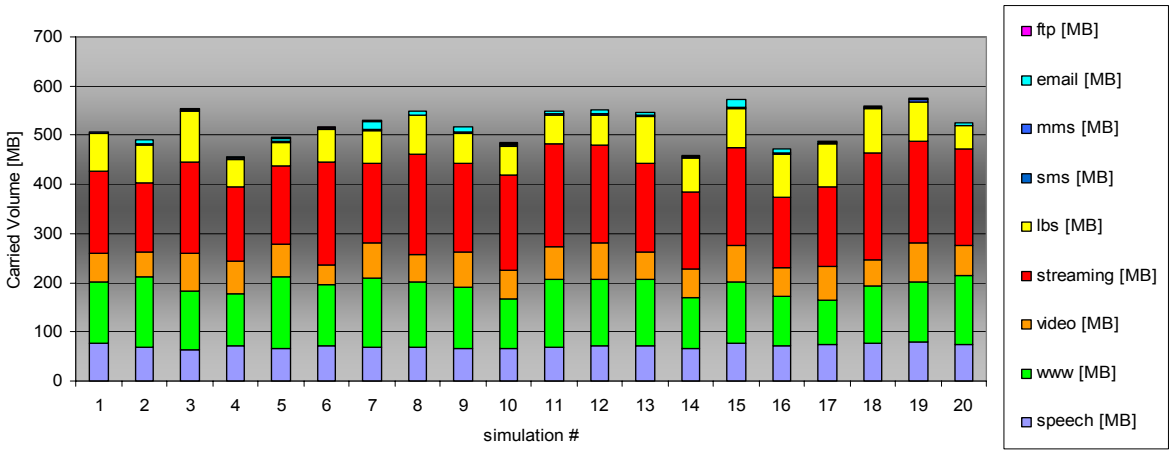

Figure Annex O.5 – Carried traffic volume in REF scenario.

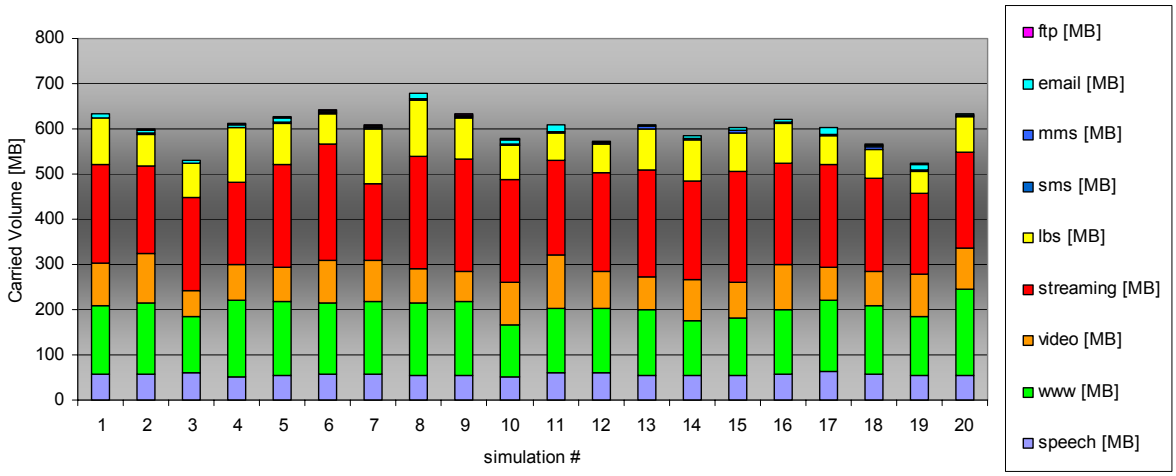

Figure Annex O.6 – Carried traffic volume in DAC scenario.

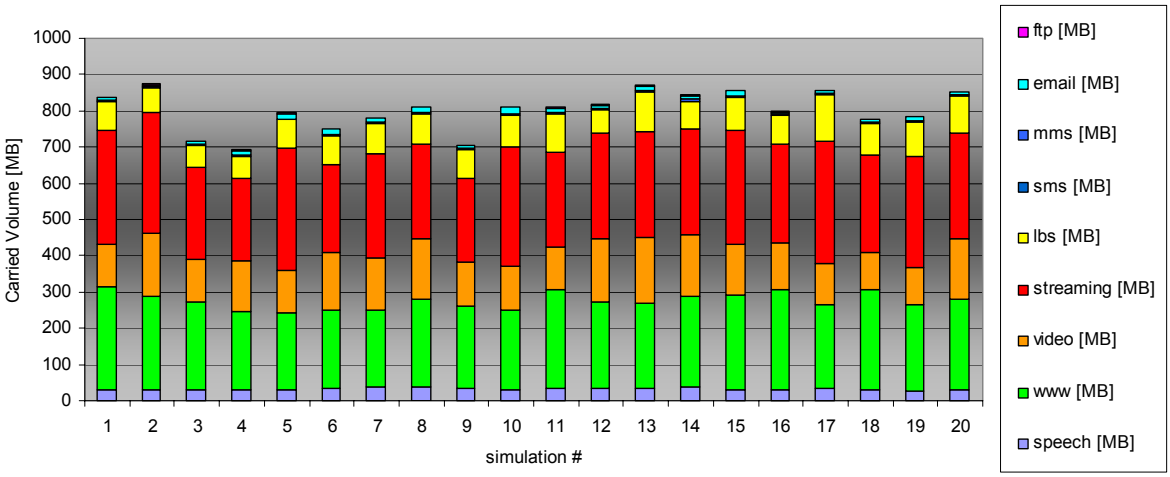

Figure Annex O.7 – Carried traffic volume in DAM scenario.

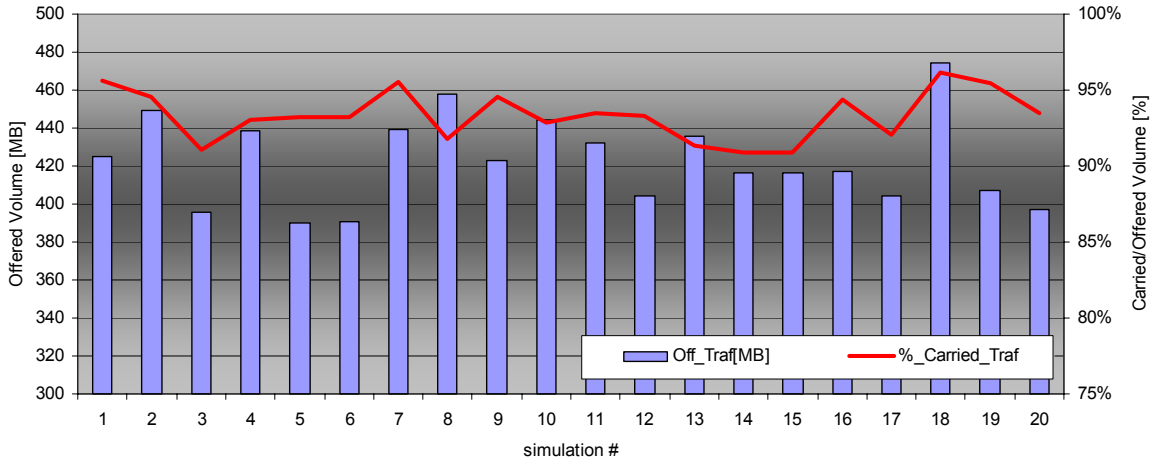

Figure Annex O.8 – Carried/Offered traffic volume ratio in VOC scenario.

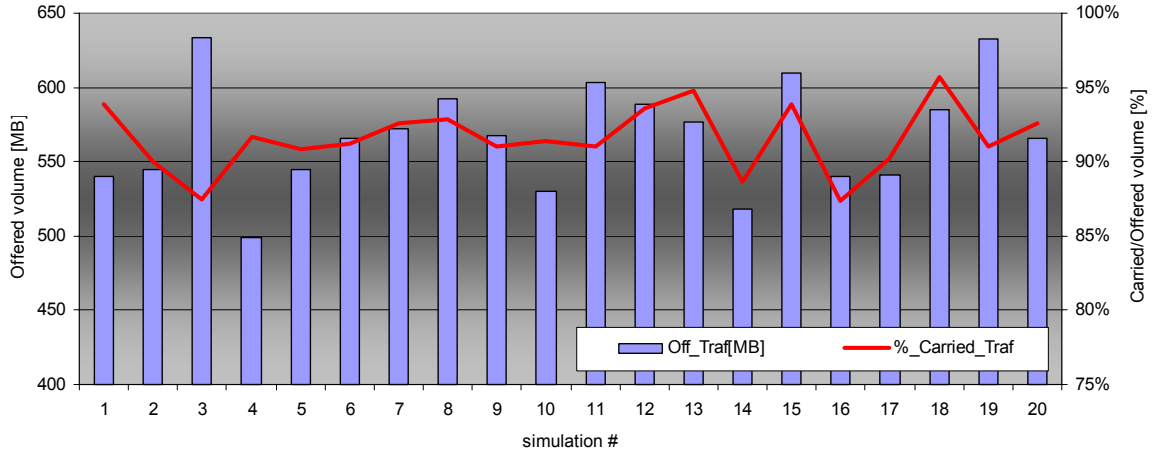

Figure Annex O.9 – Carried/Offered traffic volume ratio in REF scenario.

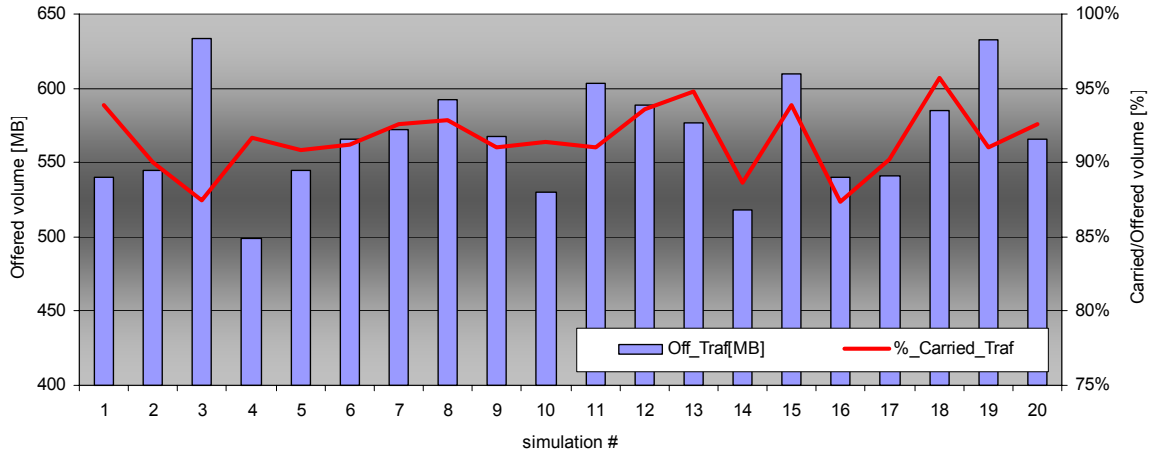

Figure Annex O.10 – Carried/Offered traffic volume ratio in DAC scenario.

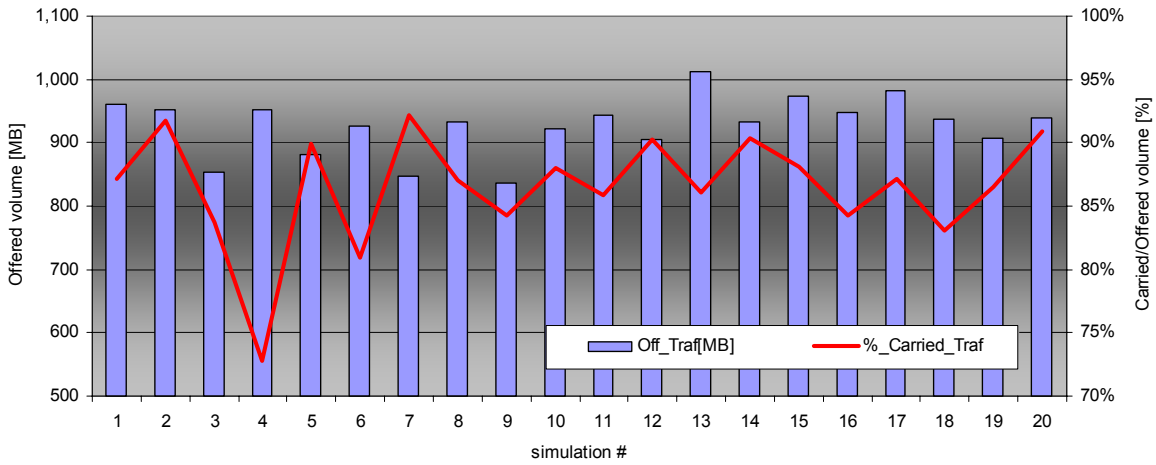

Figure Annex O.11 – Carried/Offered traffic volume ratio in DAM scenario.

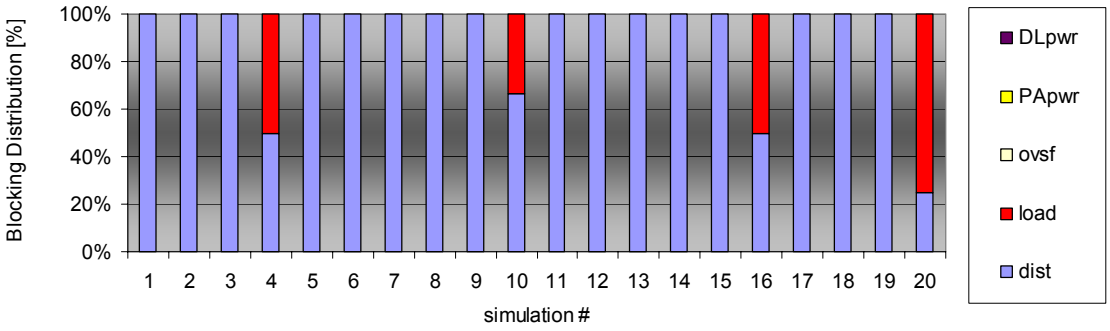

Figure Annex O.12 – Blocking cause's distribution (VOC).

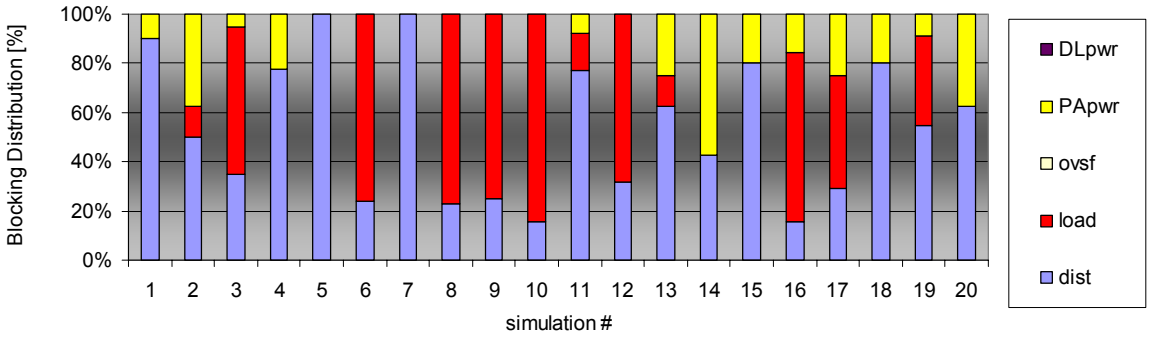

Figure Annex O.13 – Blocking cause's distribution (REF).

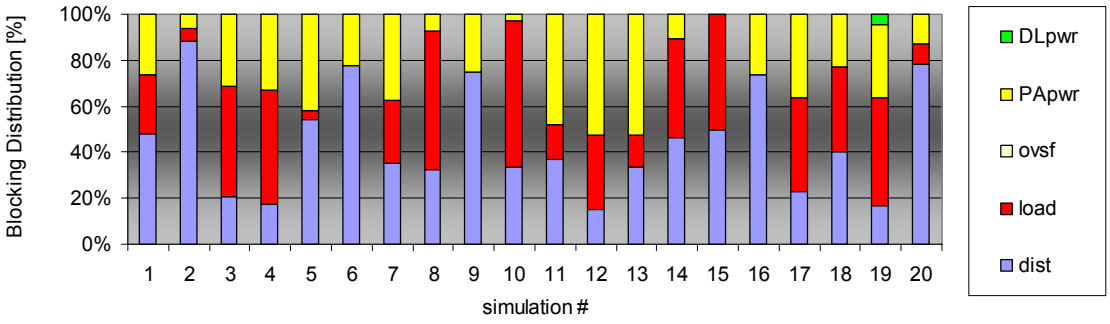

Figure Annex O.14 – Blocking cause's distribution (DAC).

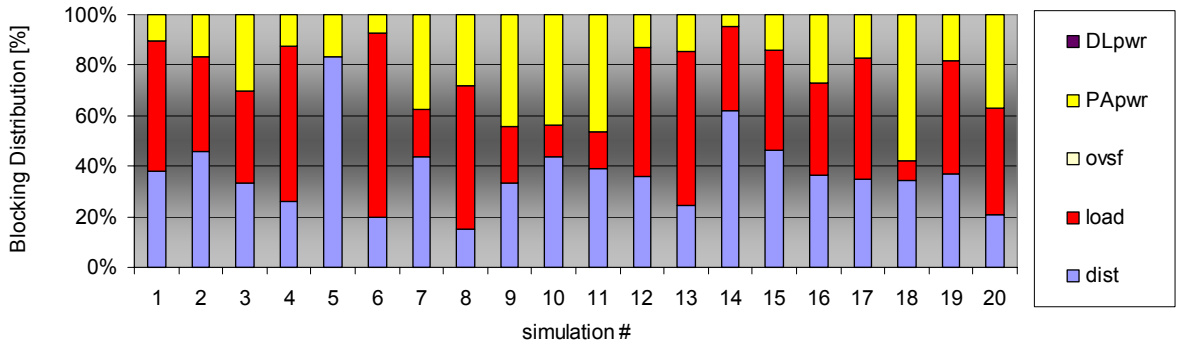

Figure Annex O.15 – Blocking cause's distribution (DAM).

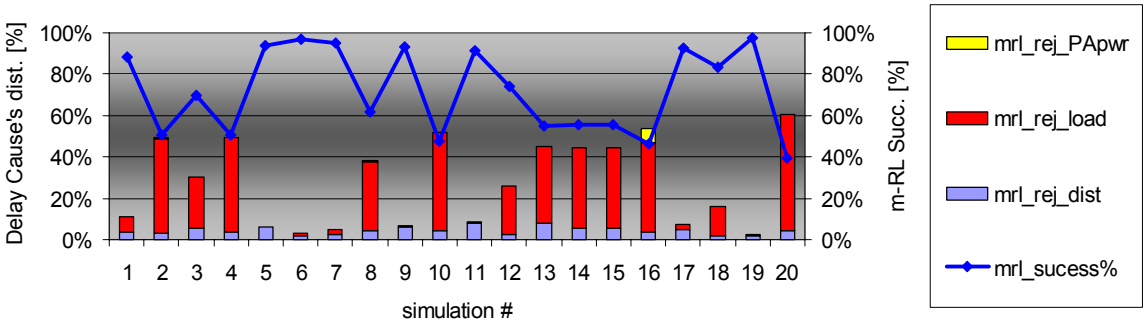

Figure Annex O.16 – PS delay cause's distribution (VOC).

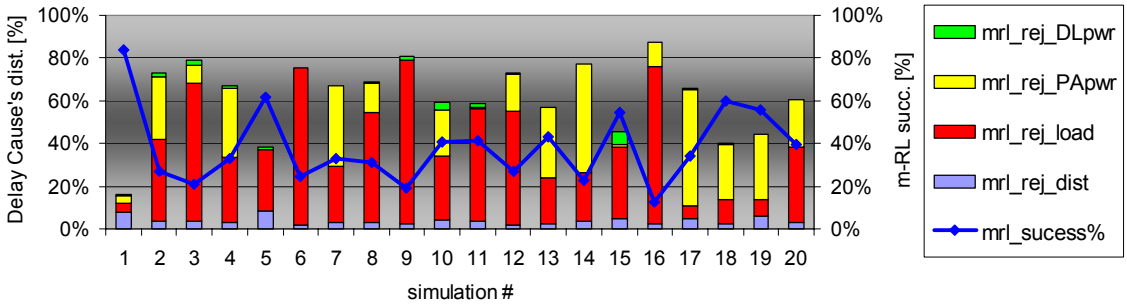

Figure Annex O.17 – PS delay cause's distribution (REF).

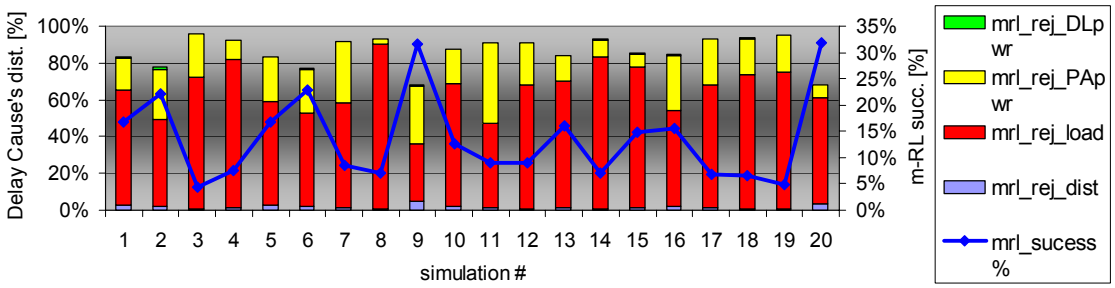

Figure Annex O.18 – PS delay cause's distribution (DAC).

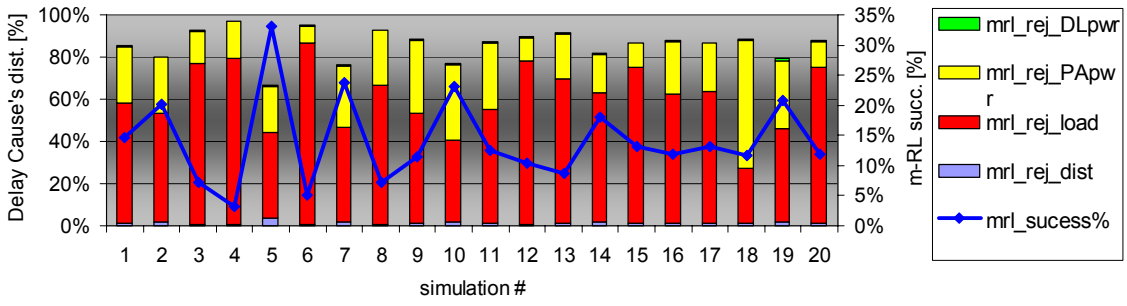

Figure Annex O.19 – PS delay cause's distribution (DAM).

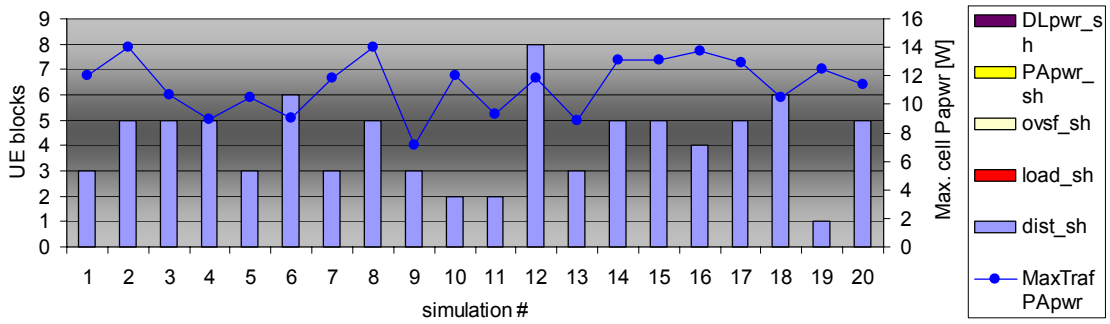

Figure Annex O.20 – Blocking cause's distribution SHO links (VOC).

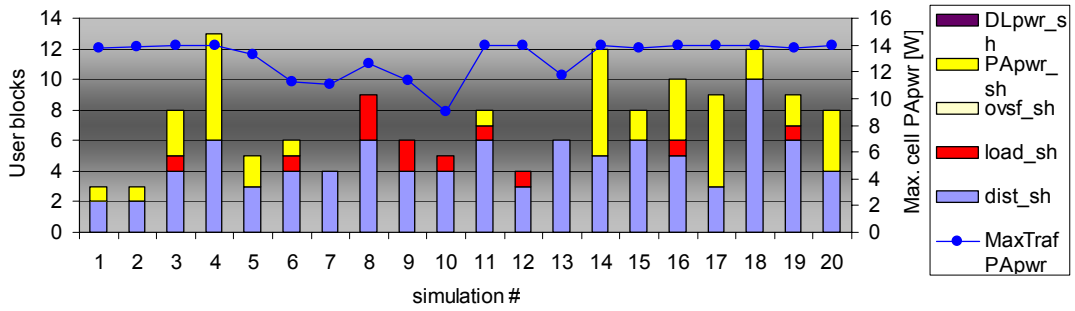

Figure Annex O.21 – Blocking cause's distribution SHO links (REF).

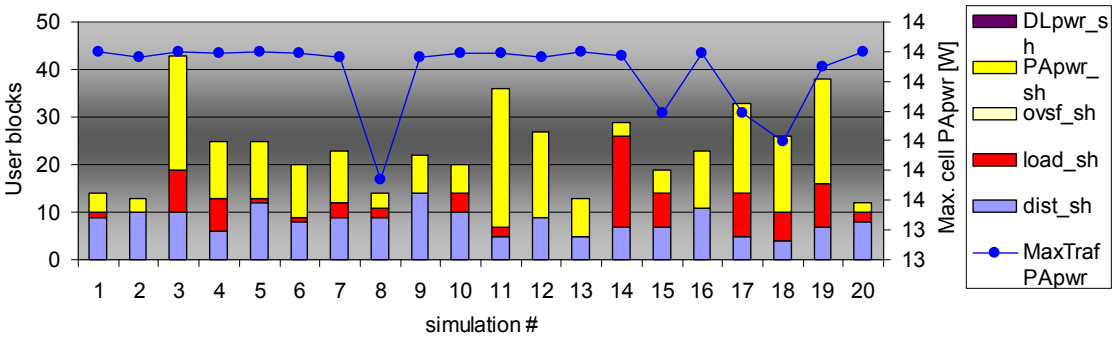

Figure Annex O.22 – Blocking cause's distribution SHO links (DAC).

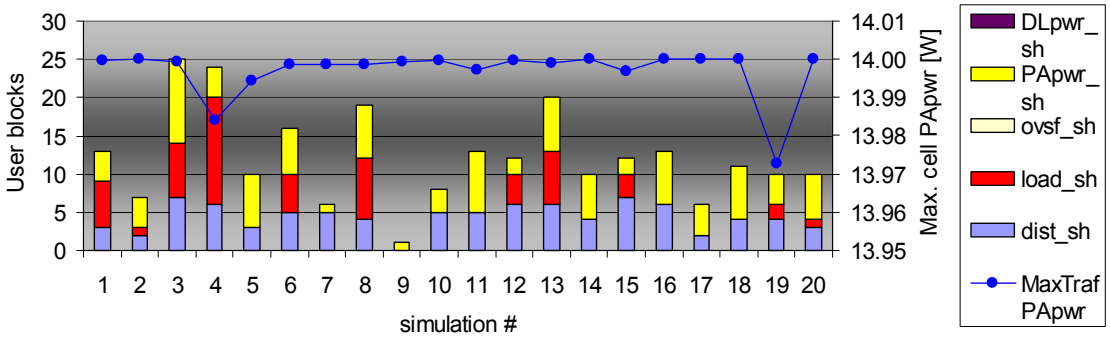

Figure Annex O.23 – Blocking cause's distribution SHO links (DAM).

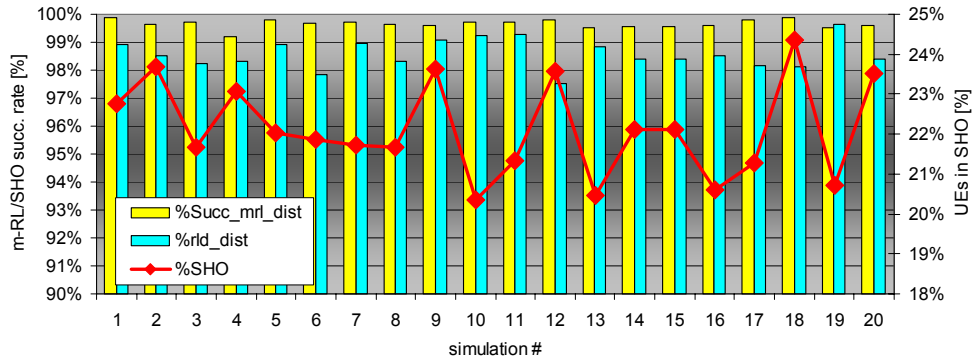

Figure Annex O.24 – CS Statistics: m-RL/SHO-RL succ. and SHO percentage (VOC).

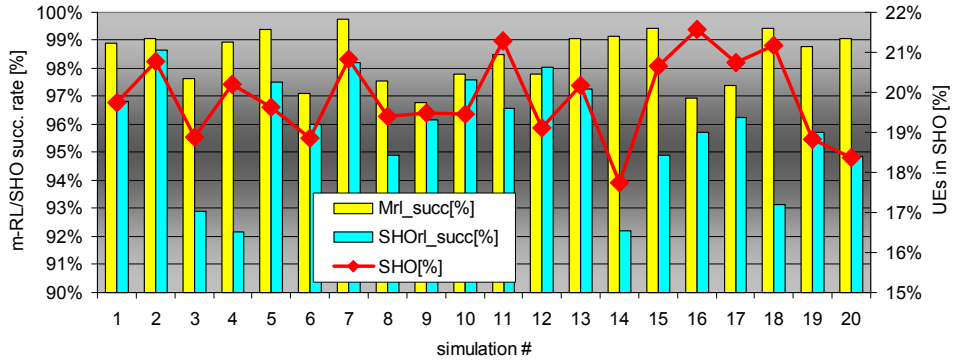

Figure Annex O.25 – CS Statistics: m-RL/SHO-RL succ. and SHO percentage (REF).

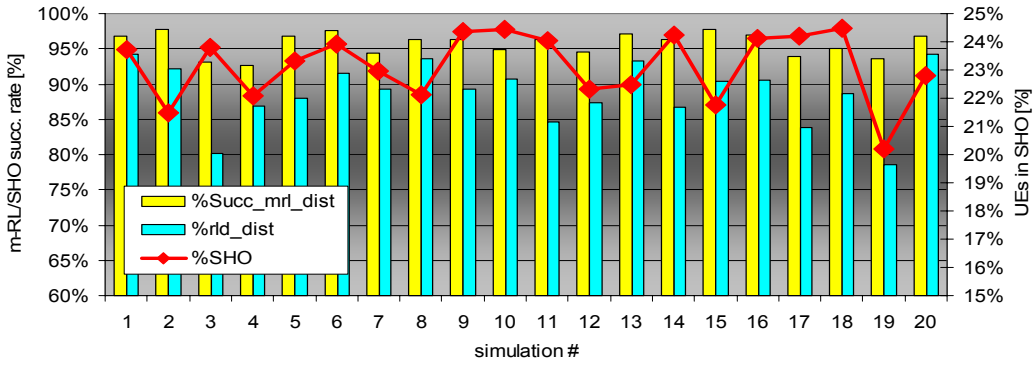

Figure Annex O.26 – CS Statistics: m-RL/SHO-RL succ. and SHO percentage (DAC).

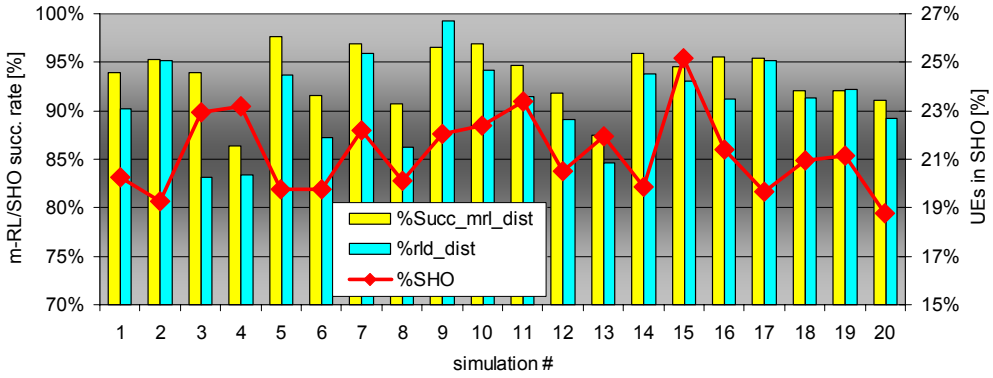

Figure Annex O.27 – CS Statistics: m-RL/SHO-RL succ. and SHO percentage (DAM).

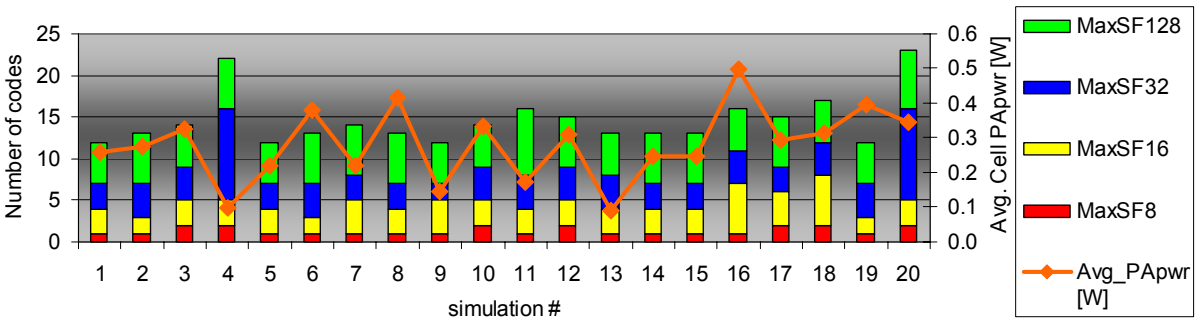

Figure Annex O.28 – SF code usage and Average Cell PA power (VOC).

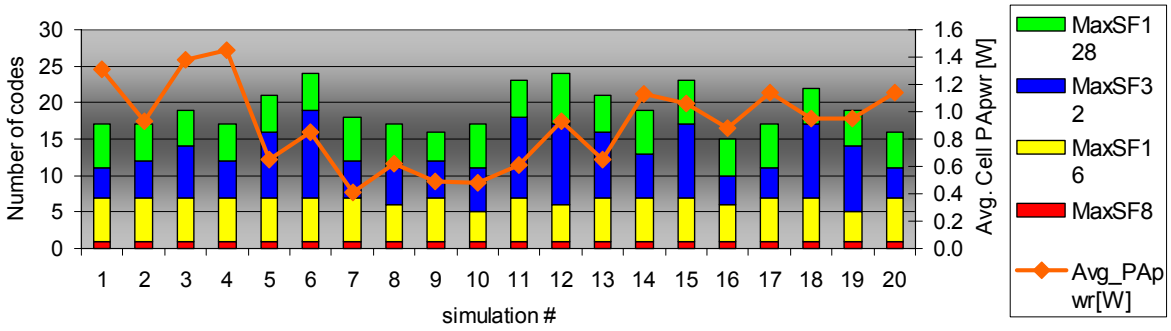

Figure Annex O.29 – SF code usage and Average Cell PA power (REF).

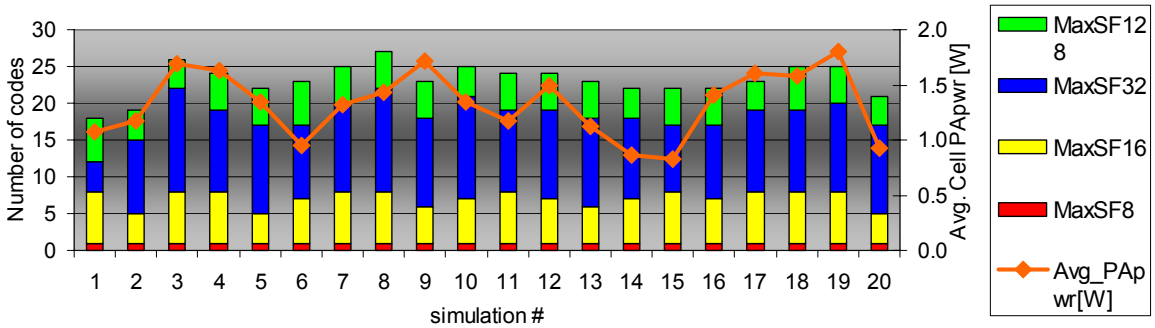

Figure Annex O.30 – SF code usage and Average Cell PA power (DAC).

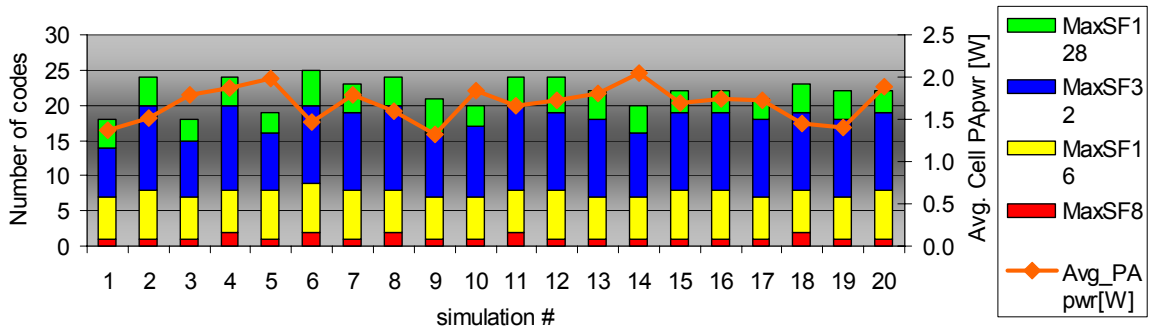

Figure Annex O.31 – SF code usage and Average Cell PA power (DAM).

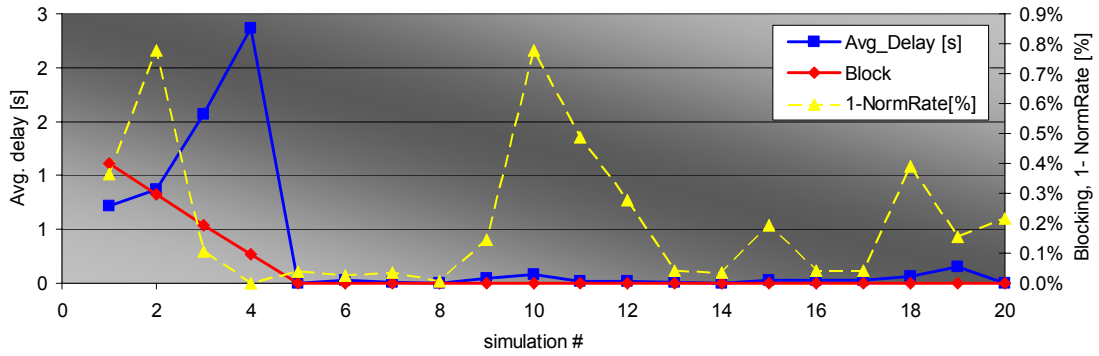

Figure Annex O.32 – Blocking, Average delay and Normalised rate correlation (VOC).

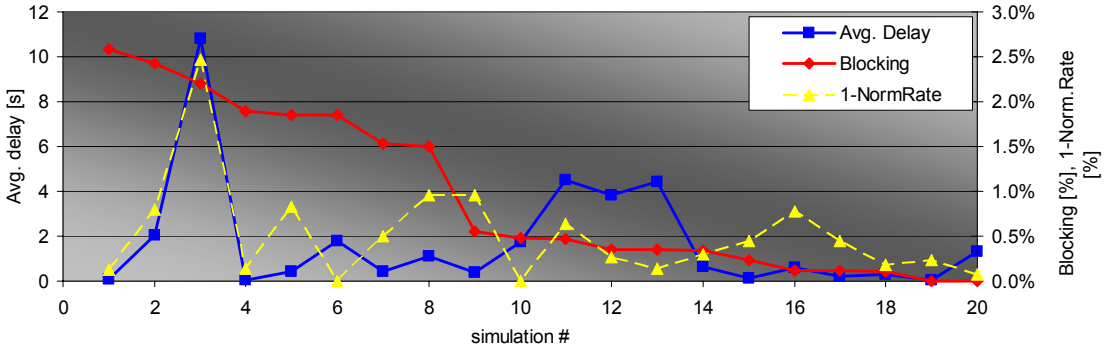

Figure Annex O.33 – Blocking, Average delay and Normalised rate correlation (REF).

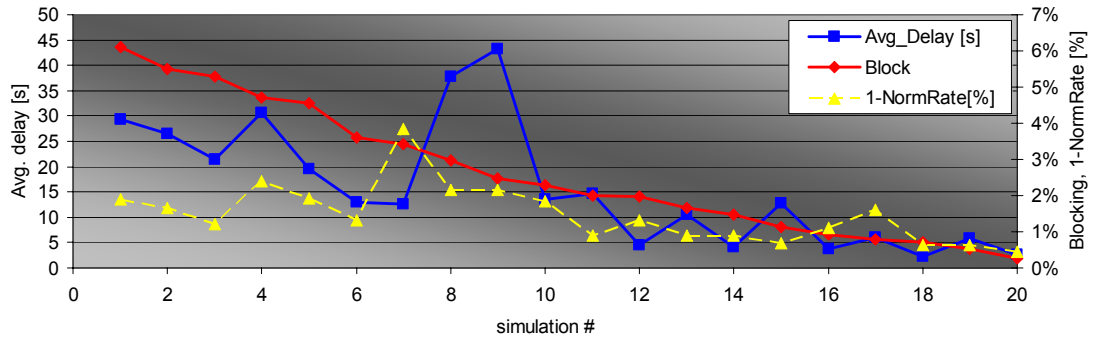

Figure Annex O.34 – Blocking, Average delay and Normalised rate correlation (DAC).

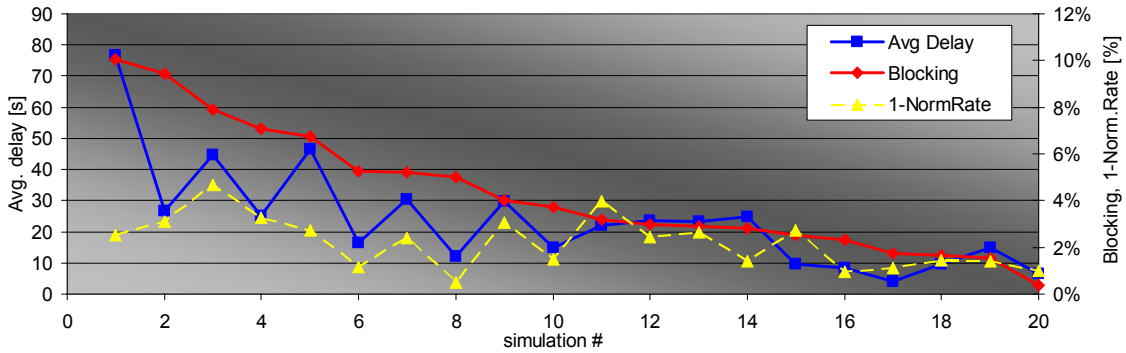

Figure Annex O.35 – Blocking, Average delay and Normalised rate correlation (DAM).

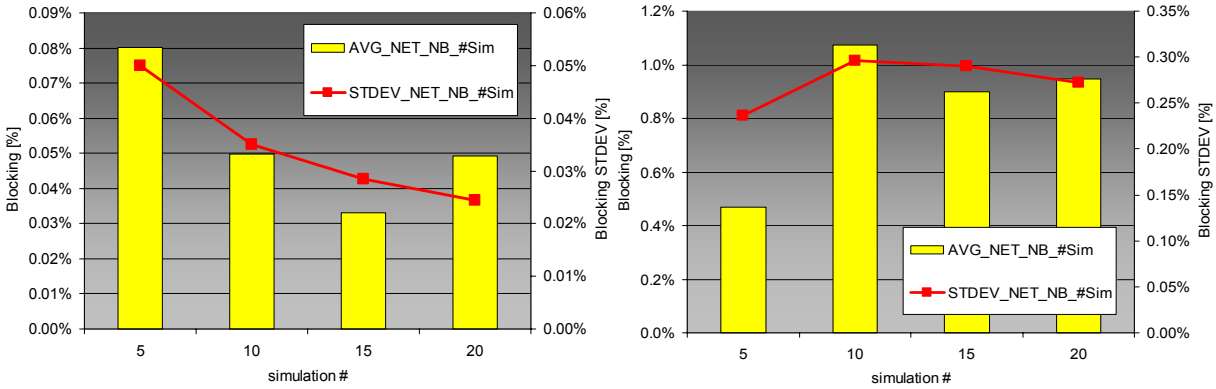

(VOC) (REF)

Figure Annex O.36 – Blocking Average and STDEV for VOC/REF simulations.

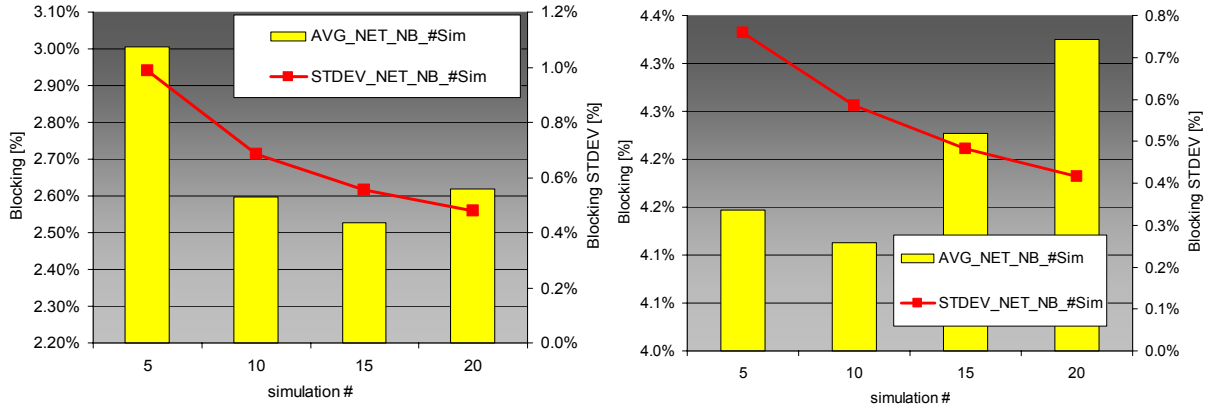

(DAC) (DAM)

Figure Annex O.37 – Blocking Average and STDEV for DAC/DAM simulations.

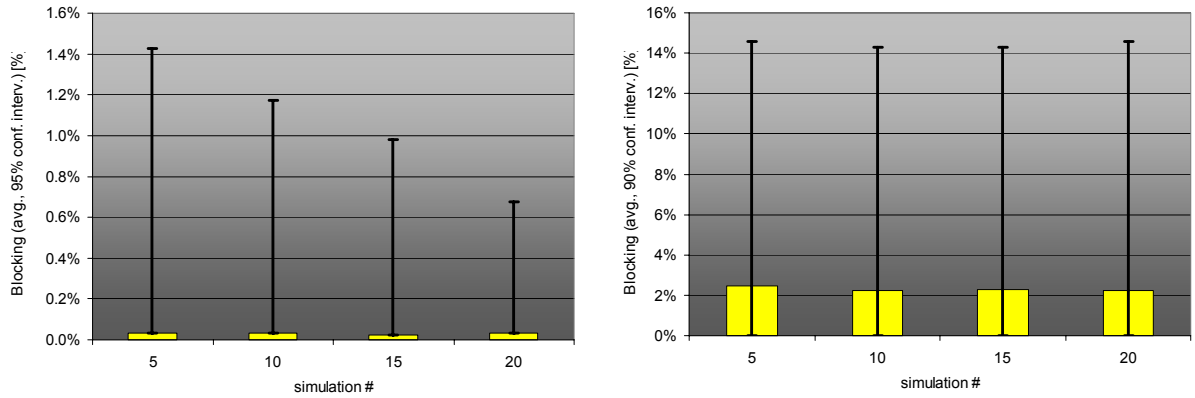

(VOC) (DAC)

Figure Annex O.38 – Blocking Average 95 %/90 % percentile for VOC/DAC simulations.

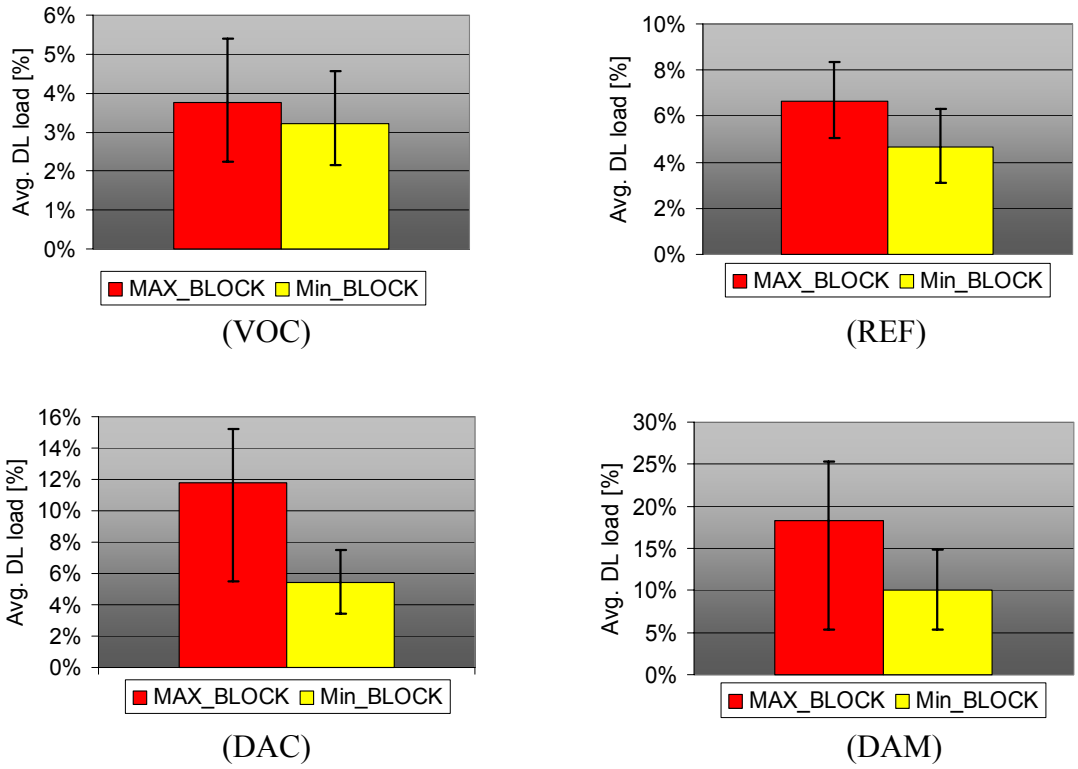

Figure Annex O.39 – Average DL load (90 % percentile).

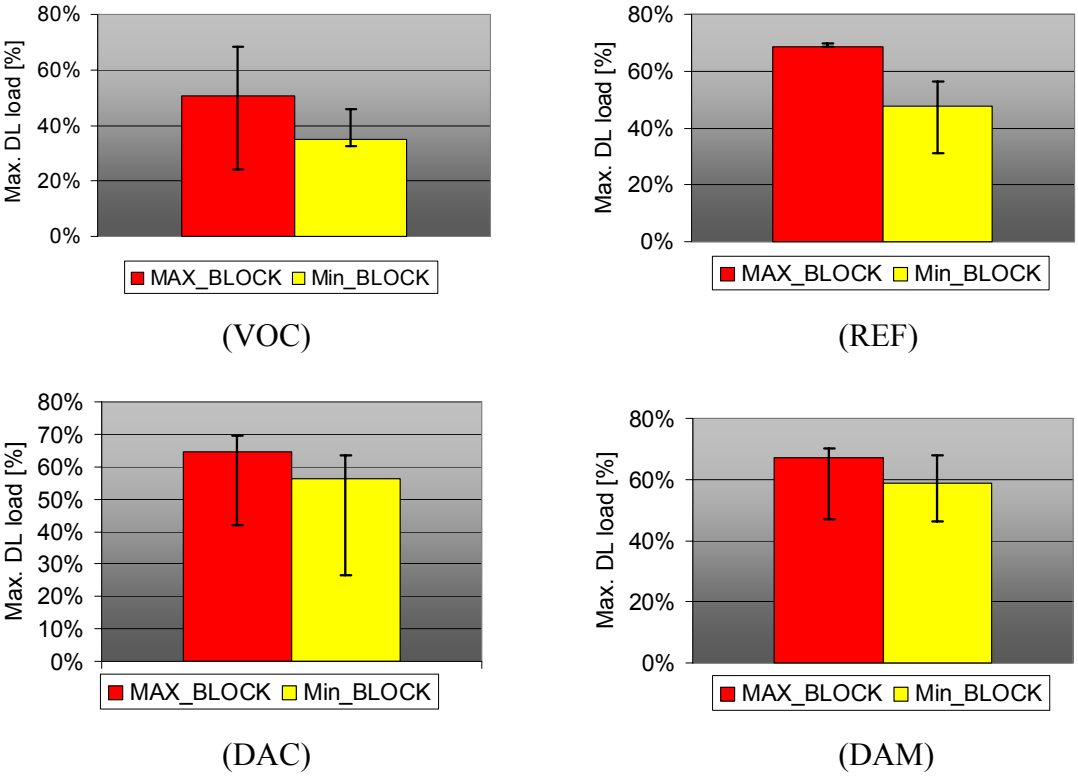

Figure Annex O.40 – Maximum DL load (90 % percentile).

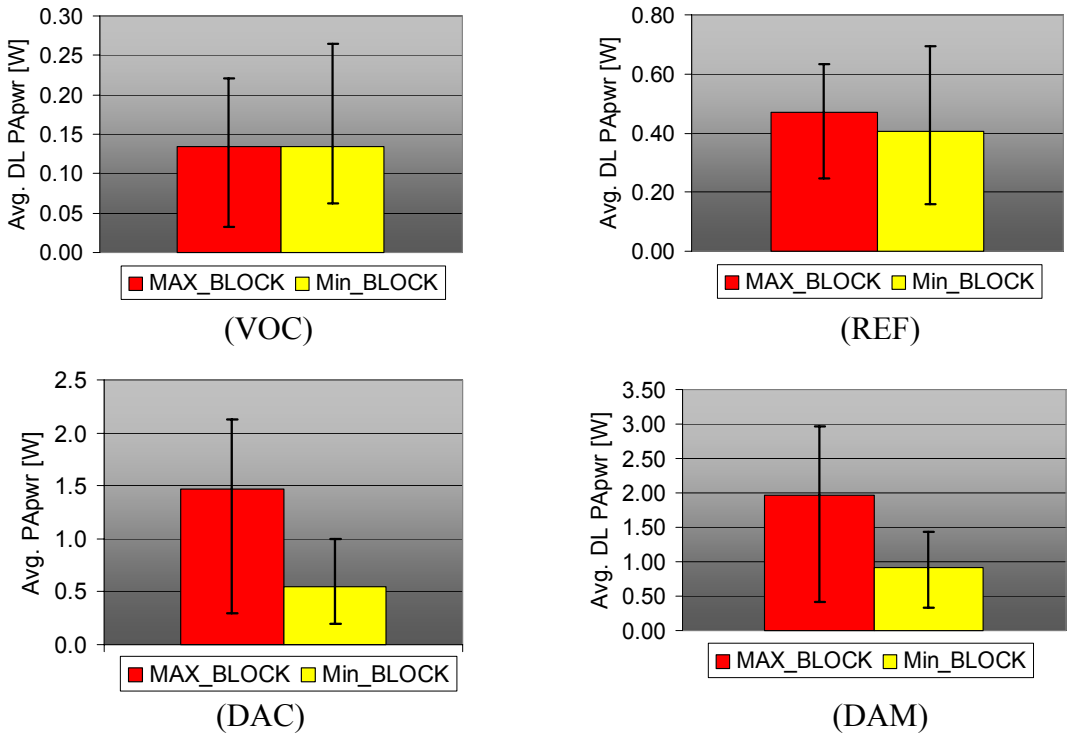

Figure Annex O.41 – Average DL PA power (90 % percentile).

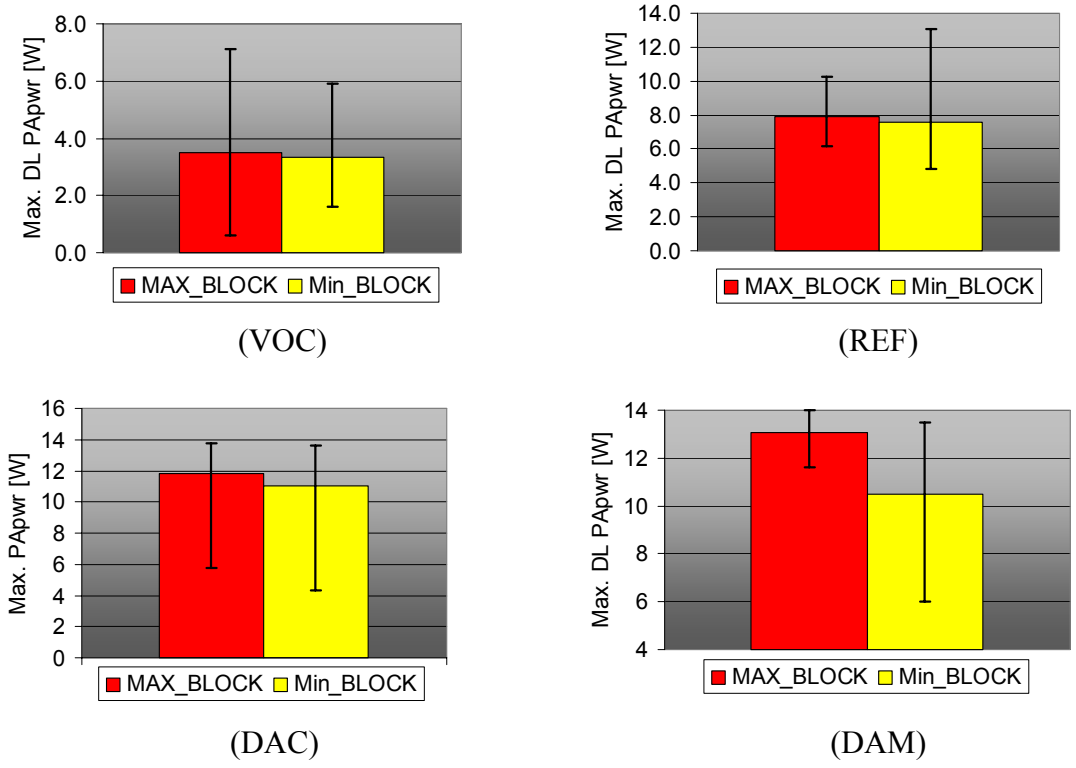

Figure Annex O.42 – Maximum DL PA power (90 % percentile).

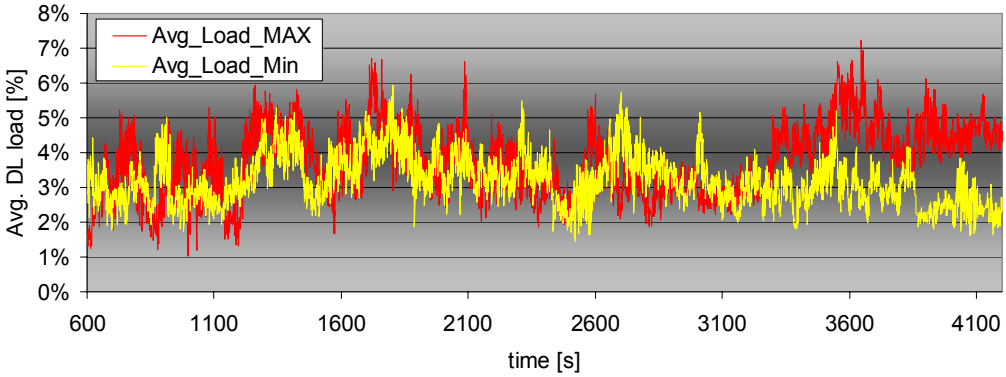

Figure Annex O.43 –Average DL load (eval. Period – VOC, min/max blocking).

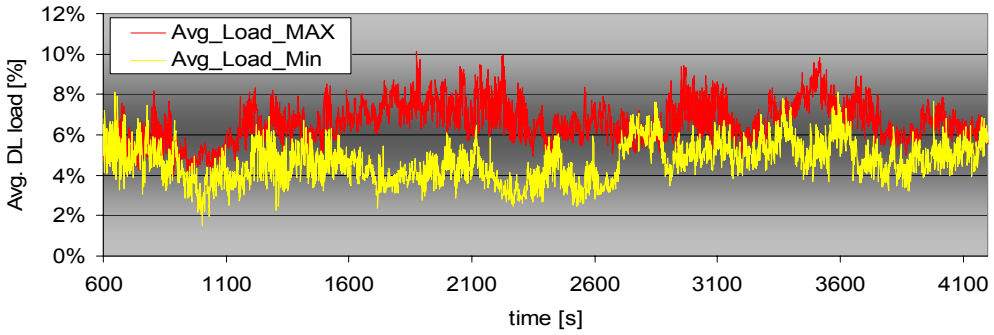

Figure Annex O.44 –Average DL load (eval. Period – REF, min/max blocking).

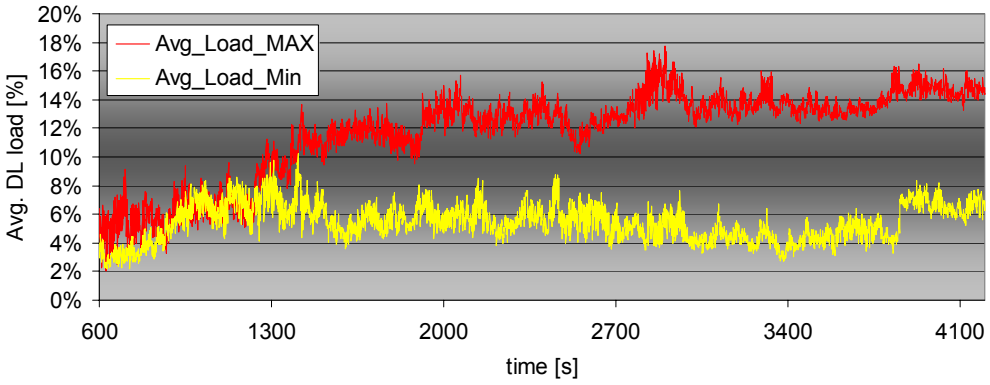

Figure Annex O.45 –Average DL load (eval. Period – DAC, min/max blocking).

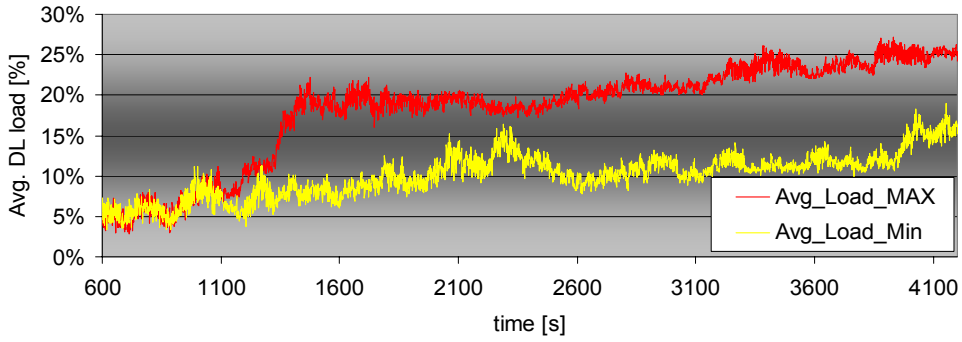

Figure Annex O.46 –Average DL load (eval. Period – DAM, min/max blocking).

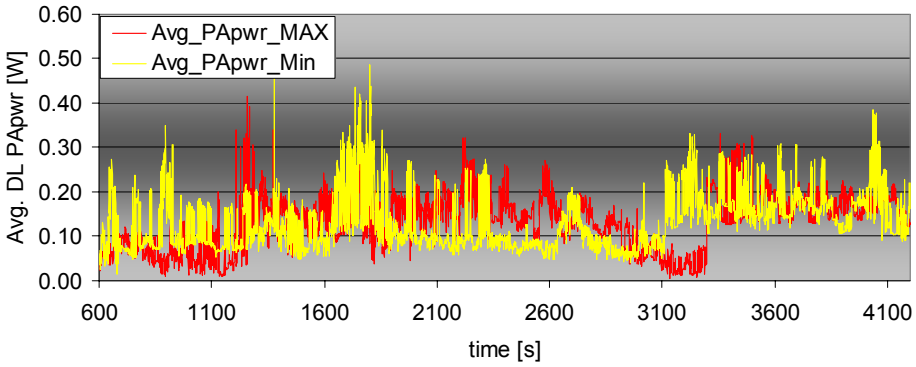

Figure Annex O.47 –Average DL PA power (eval. Period – VOC, min/max blocking).

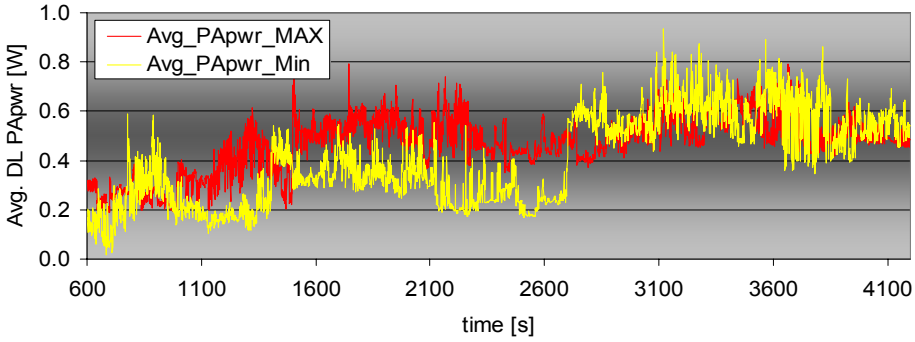

Figure Annex O.48 –Average DL PA power (eval. Period – REF, min/max blocking).

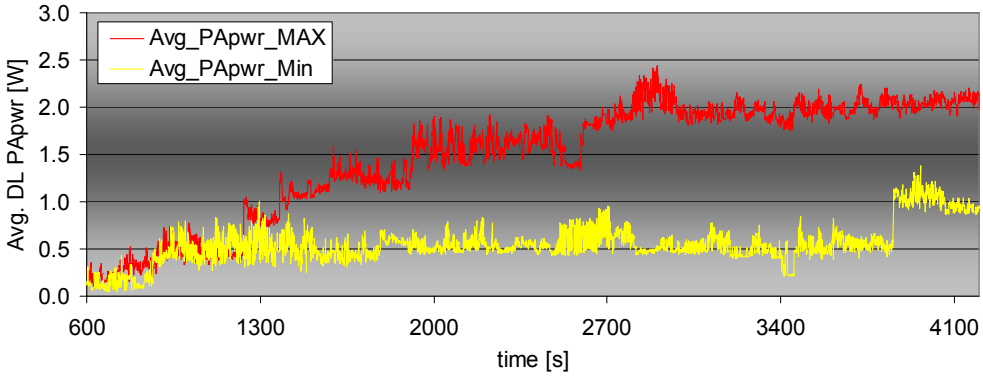

Figure Annex O.49 –Average DL PA power (eval. Period – DAC, min/max blocking).

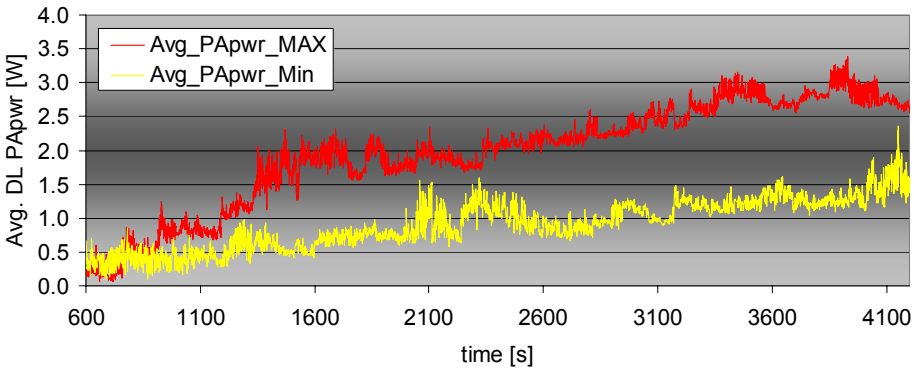

Figure Annex O.50 –Average DL PA power (eval. Period – DAM, min/max blocking).

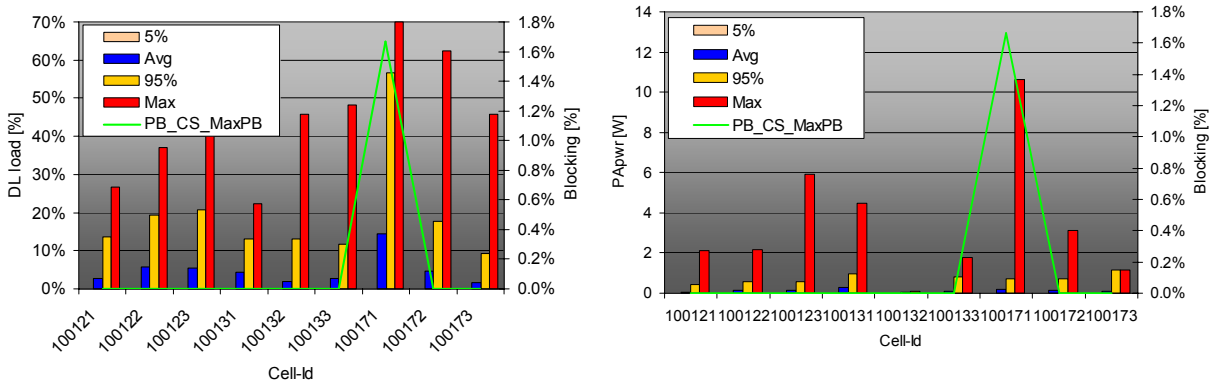

Figure Annex O.51 – Worst cells performance for VOC maximum blocking scenario.

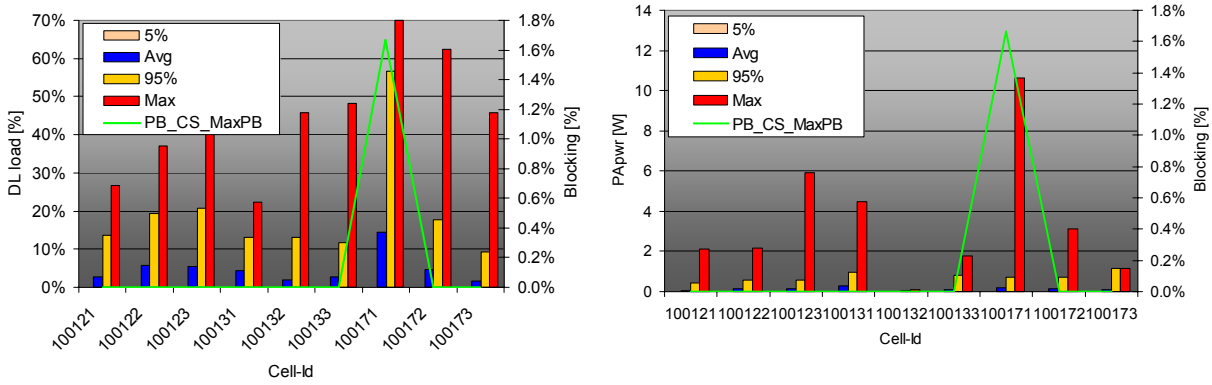

Figure Annex O.52 – Worst cells performance for REF maximum blocking scenario.

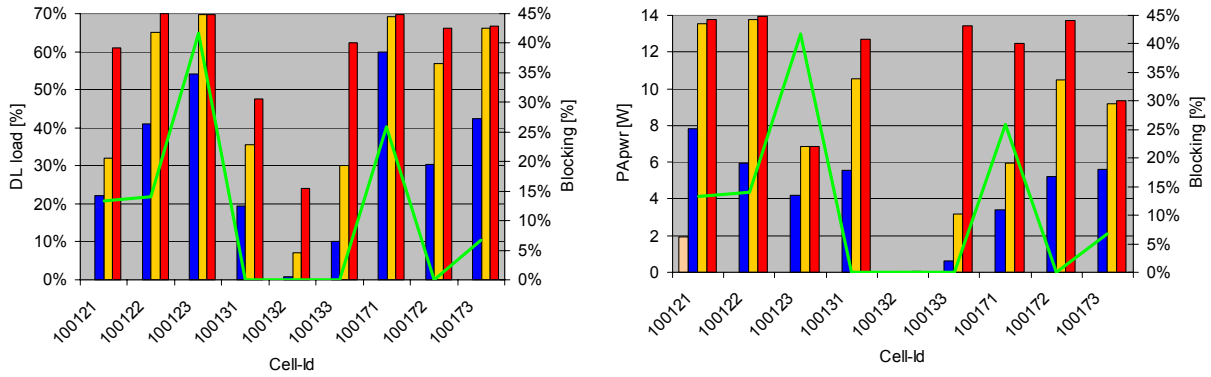

Figure Annex O.53 – Worst cells performance for DAM maximum blocking scenario.

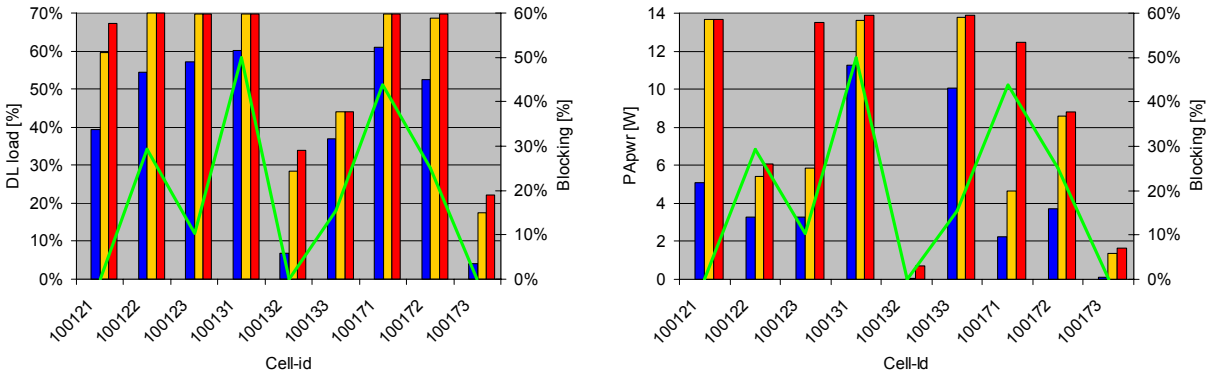

Figure Annex O.54 – Worst cells performance for DAM maximum blocking scenario.

P. DAC Scenarios Output Analysis

This annex includes all analysis performed and used in results summary of Chapter 5 to what regards the simulations on DAC scenarios with service dominance.

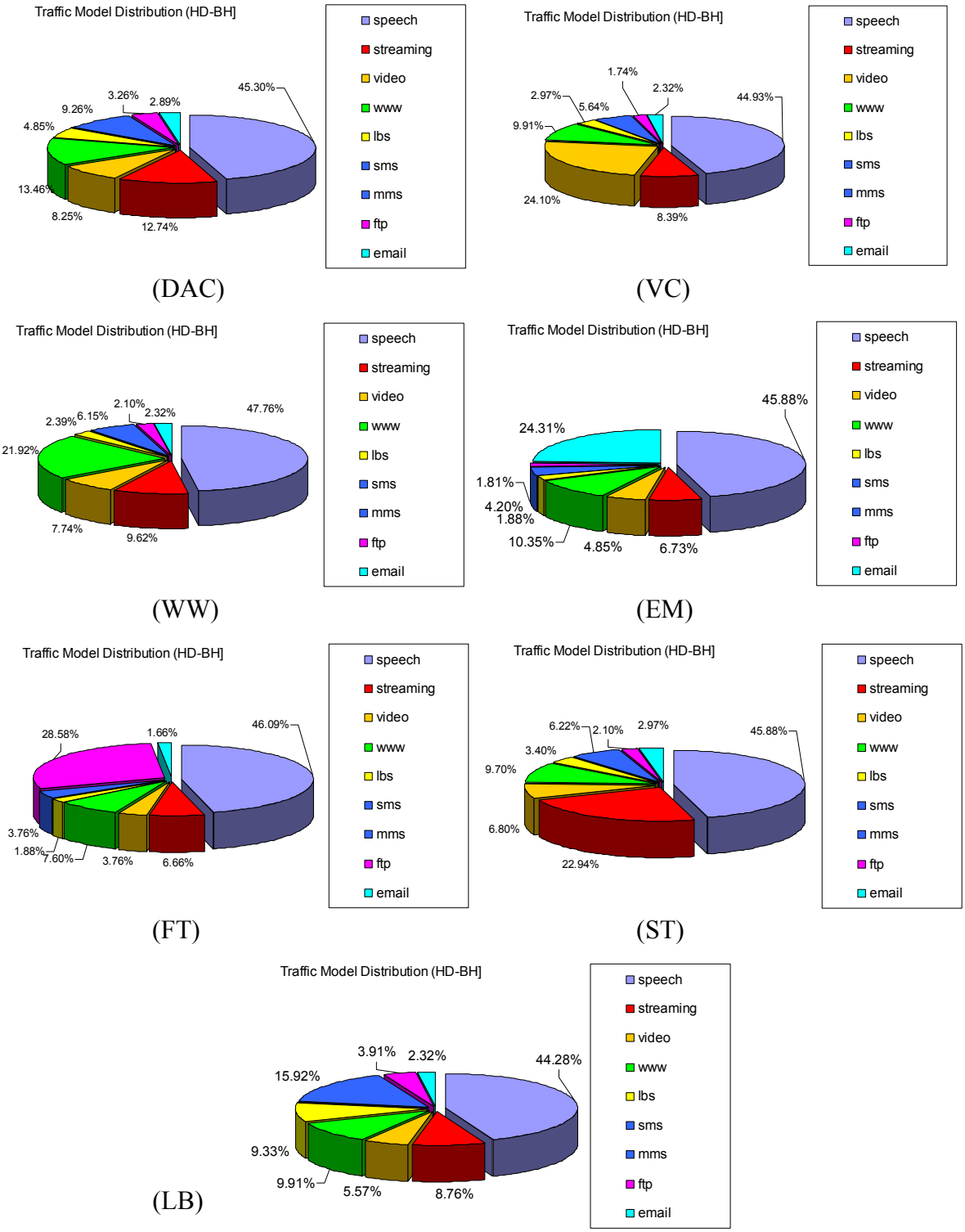

Figure Annex P.1 – Traffic Mix distribution (TRAFSIM3G traffic).

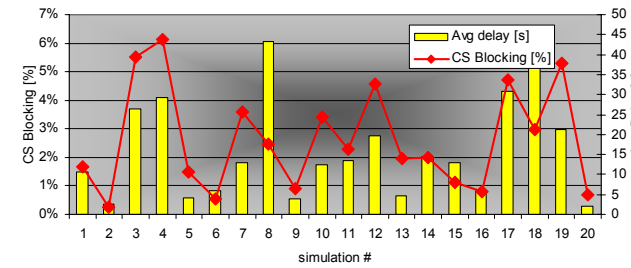

(DAC)

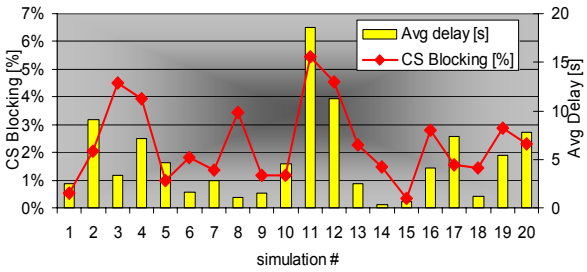

(VC)

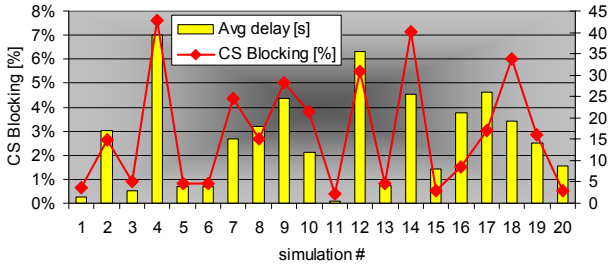

(WW)

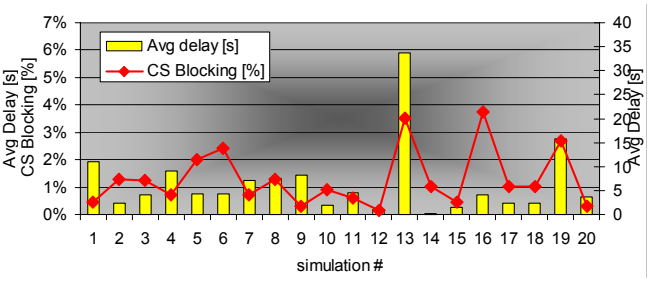

(EM)

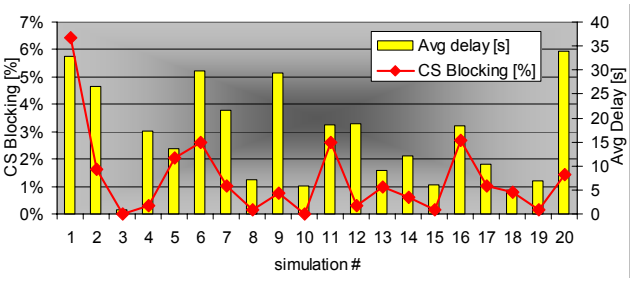

(FT)

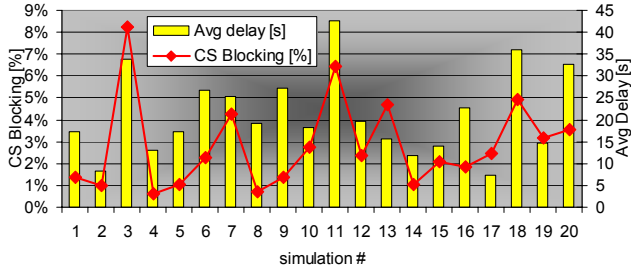

(ST)

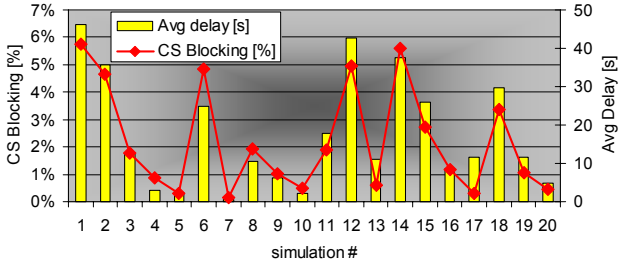

(LB)

Figure Annex P.2 – Blocking and Average delay.

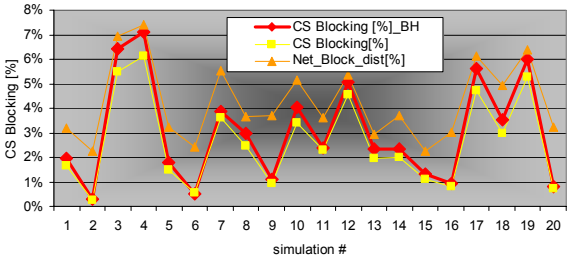

(DAC)

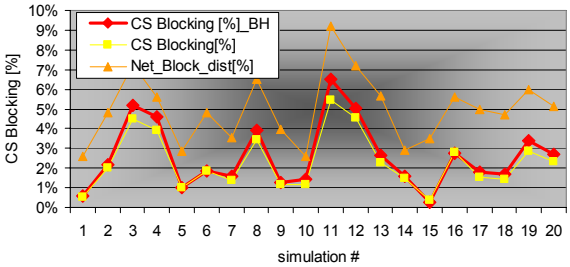

(VC)

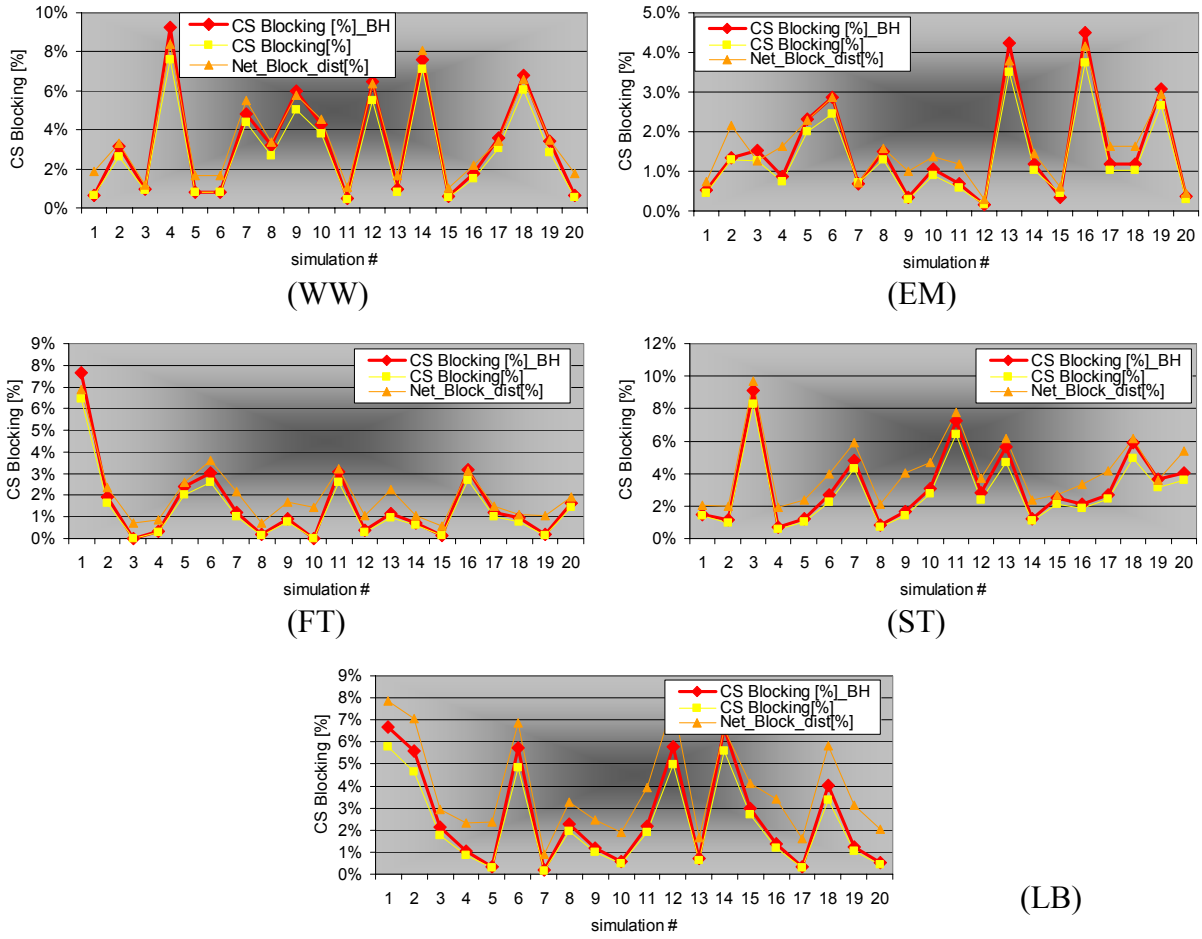

Figure Annex P.3 – Blocking in BH, 70 min and including distance blocks.

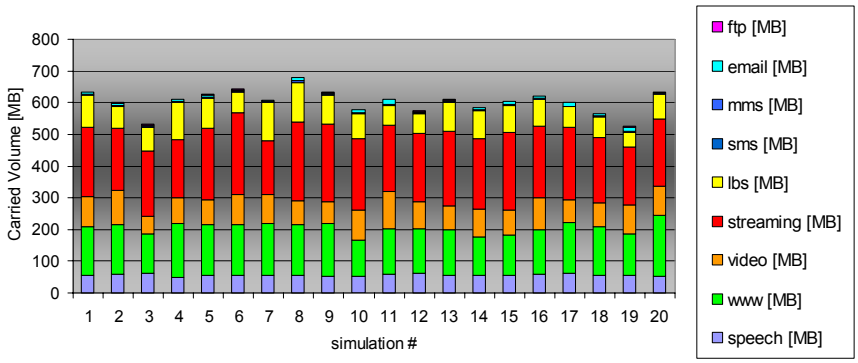

Figure Annex P.4 – Carried traffic volume in DAC scenario.

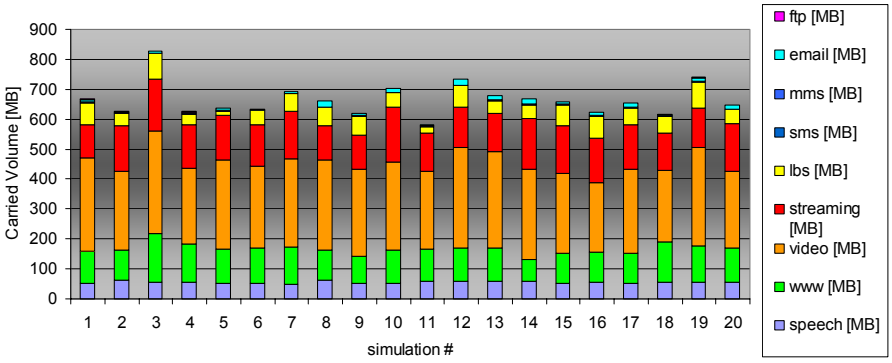

Figure Annex P.5 – Carried traffic volume in VC scenario.

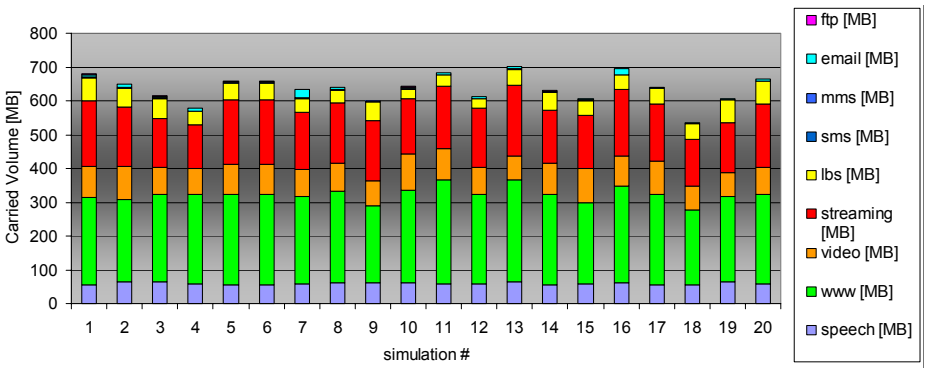

Figure Annex P.6 – Carried traffic volume in WW scenario.

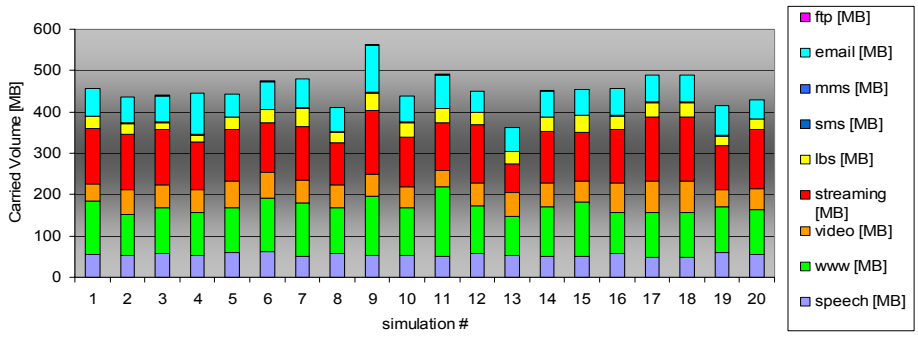

Figure Annex P.7 – Carried traffic volume in EM scenario.

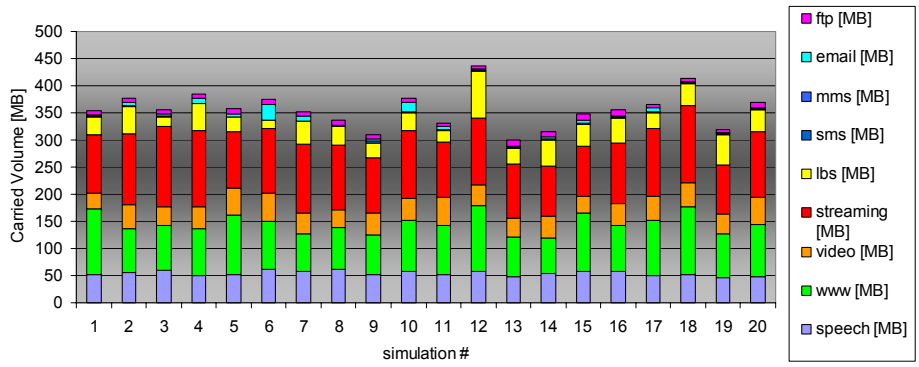

Figure Annex P.8 – Carried traffic volume in FT scenario.

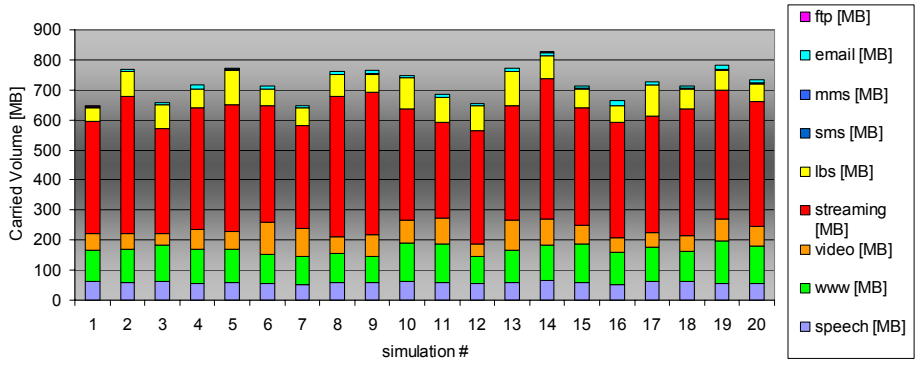

Figure Annex P.9 – Carried traffic volume in ST scenario.

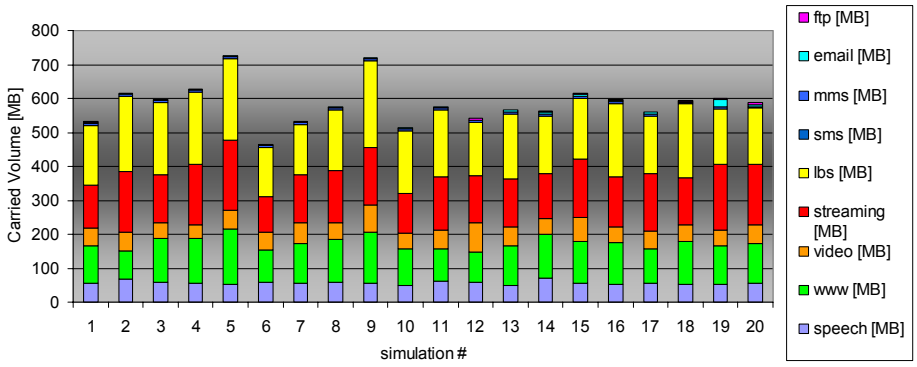

Figure Annex P.10 – Carried traffic volume in LB scenario.

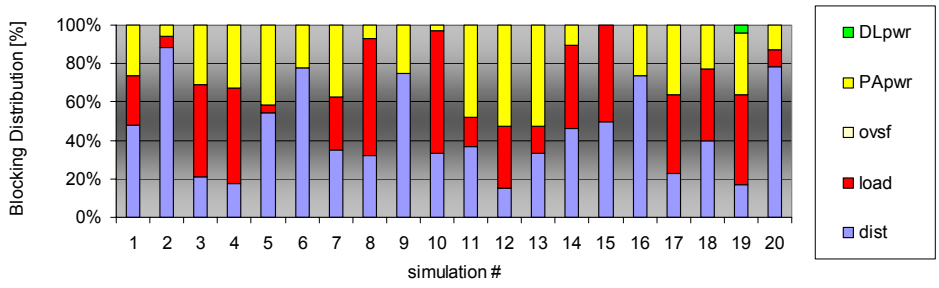

Figure Annex P.11 – Blocking cause's distribution (DAC).

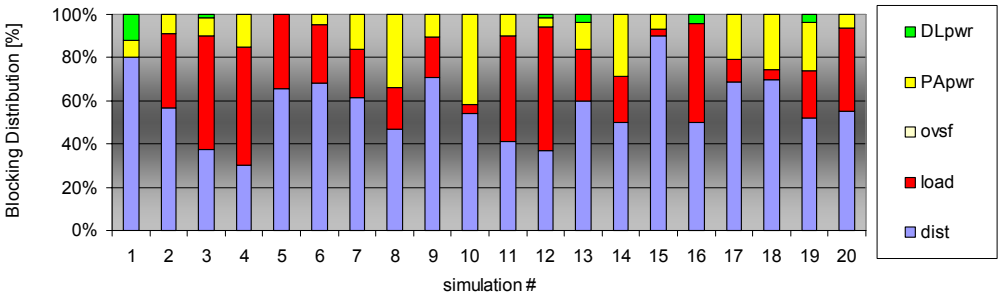

Figure Annex P.12 – Blocking cause's distribution (VC).

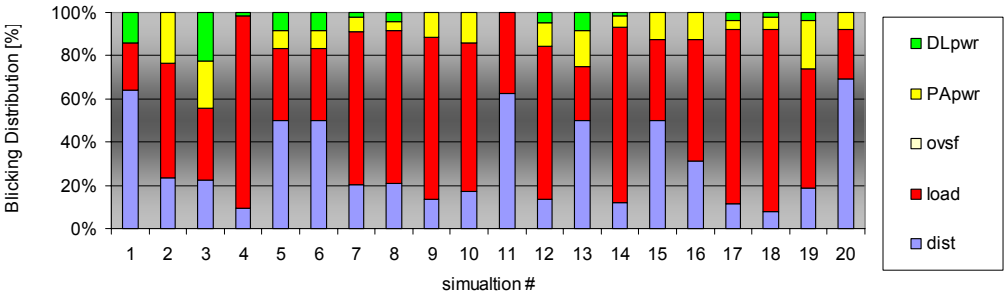

Figure Annex P.13 – Blocking cause's distribution (WW).

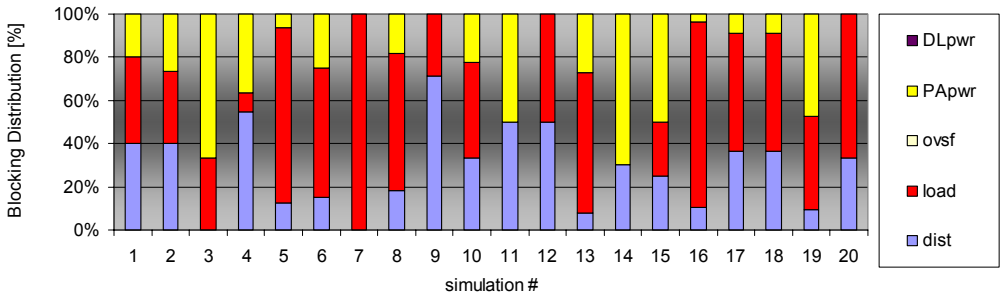

Figure Annex P.14 – Blocking cause's distribution (EM).

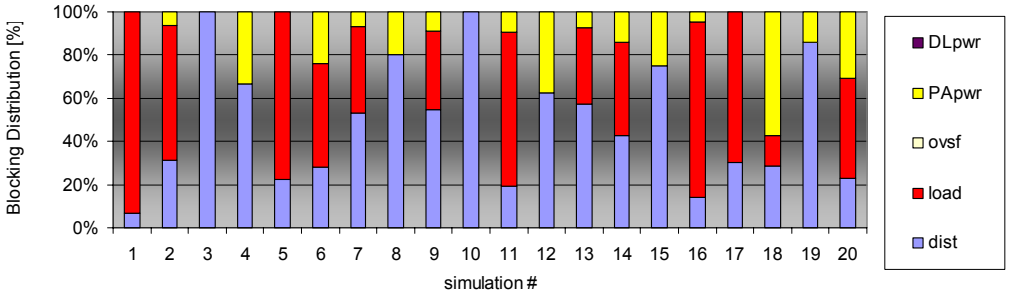

Figure Annex P.15 – Blocking cause's distribution (FT).

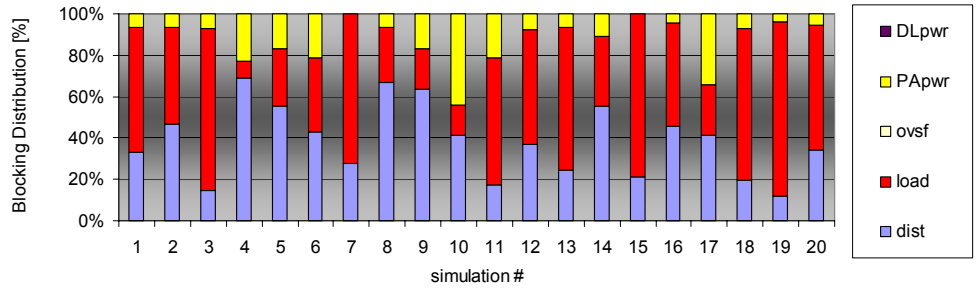

Figure Annex P.16 – Blocking cause's distribution (ST).

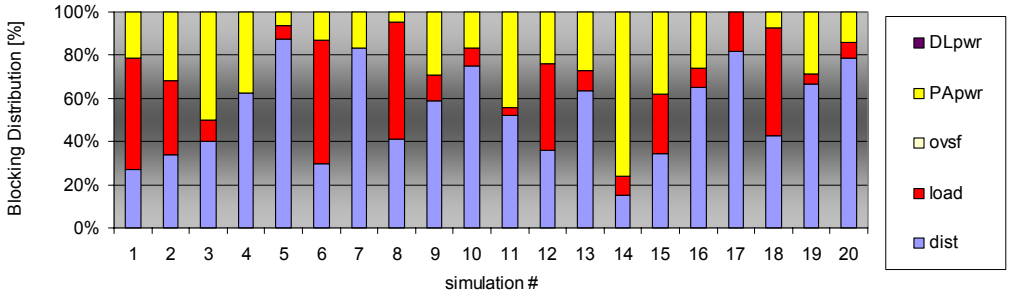

Figure Annex P.17 – Blocking cause's distribution (LB).

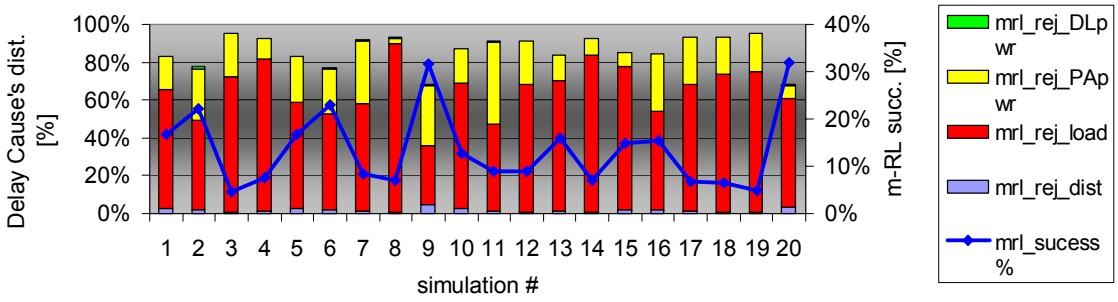

Figure Annex P.18 – PS delay cause's distribution (DAC).

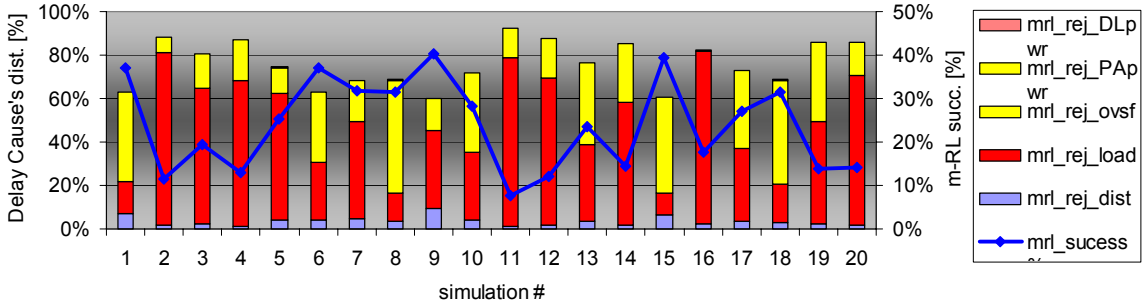

Figure Annex P.19 – PS delay cause's distribution (VC).

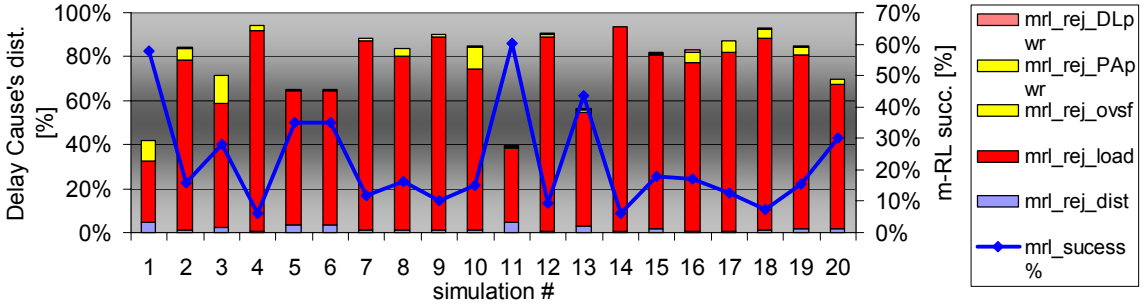

Figure Annex P.20 – PS delay cause's distribution (WW).

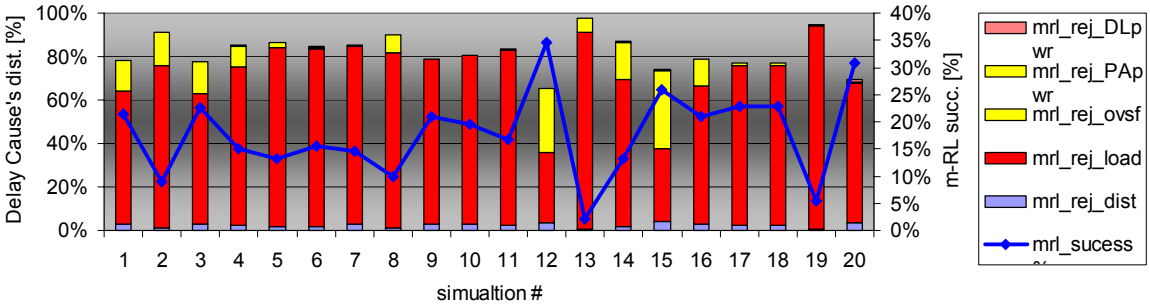

Figure Annex P.21 – PS delay cause's distribution (EM).

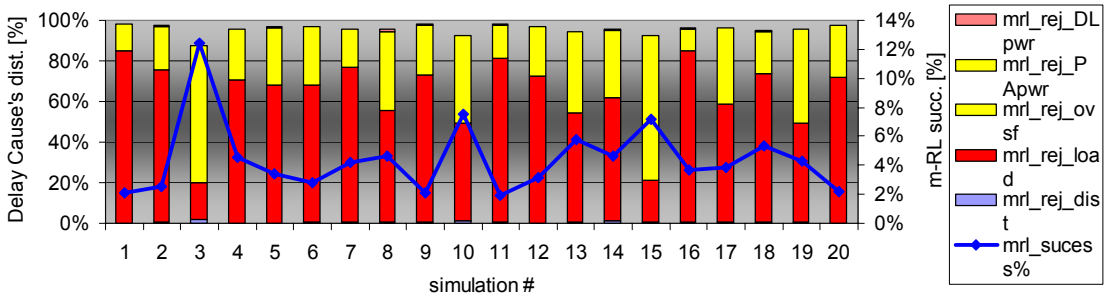

Figure Annex P.22 – PS delay cause's distribution (FT).

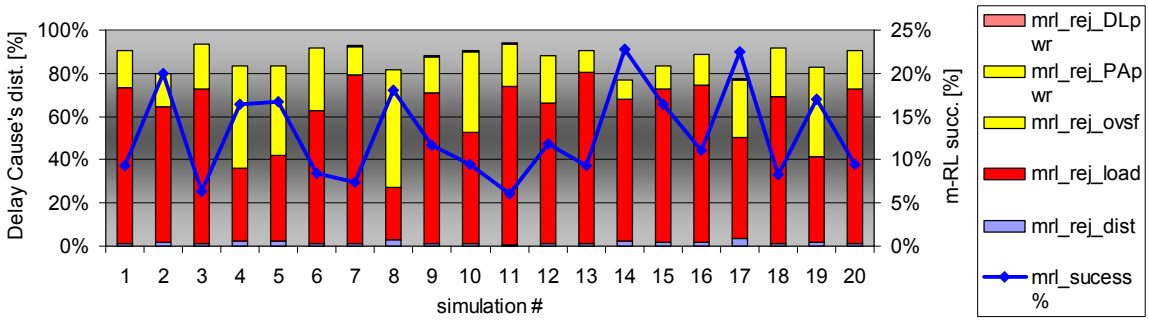

Figure Annex P.23 – PS delay cause's distribution (ST).

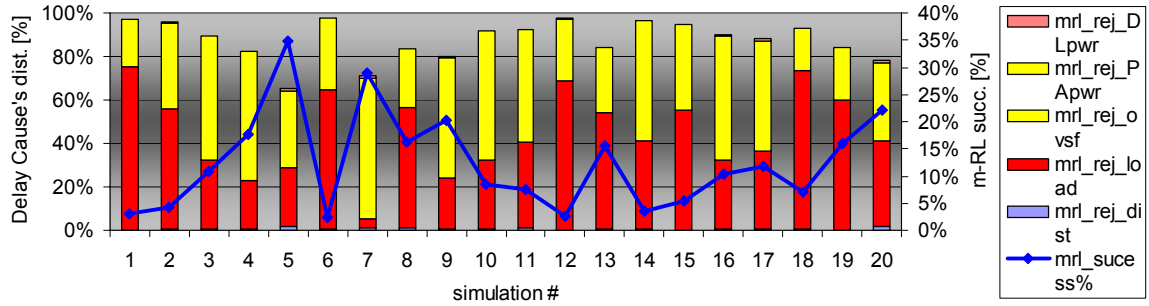

Figure Annex P.24 – PS delay cause's distribution (LB).

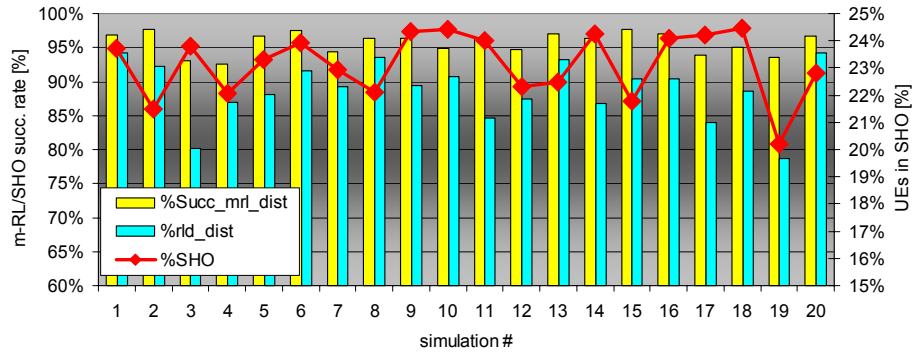

Figure Annex P.25 – CS Statistics: m-RL/SHO-RL succ. and SHO percentage (DAC).

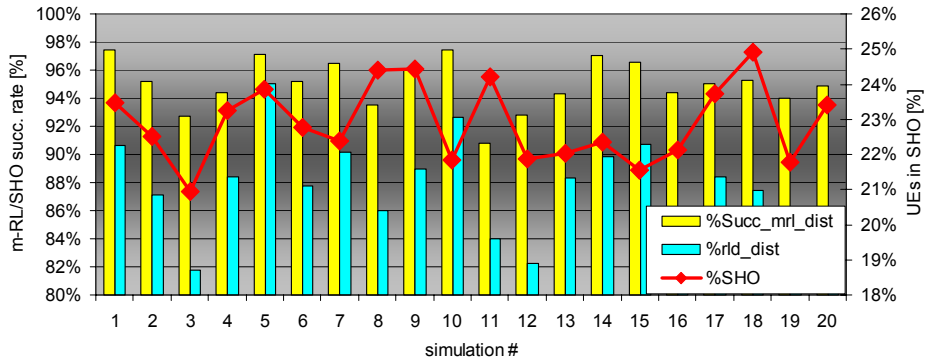

Figure Annex P.26 – CS Statistics: m-RL/SHO-RL succ. and SHO percentage (VC).

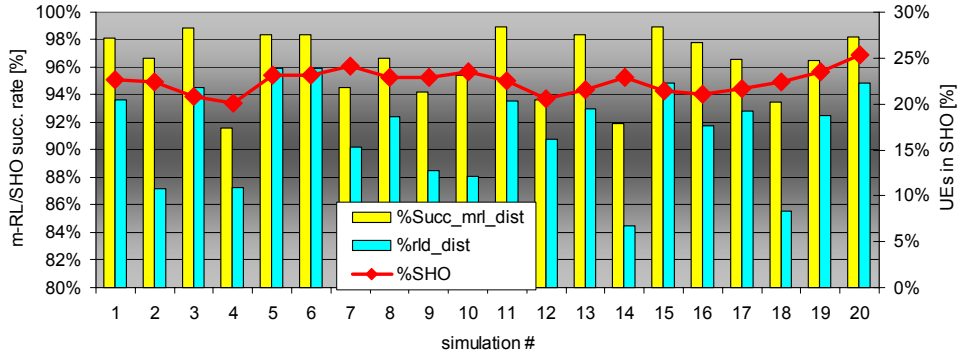

Figure Annex P.27 – CS Statistics: m-RL/SHO-RL succ. and SHO percentage (WW).

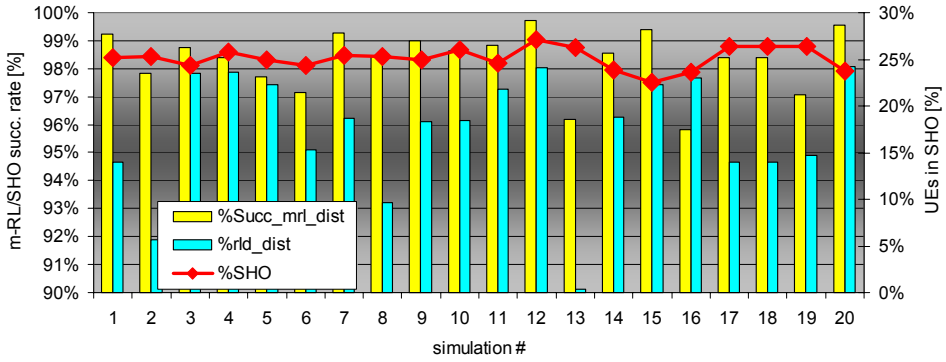

Figure Annex P.28 – CS Statistics: m-RL/SHO-RL succ. and SHO percentage (EM).

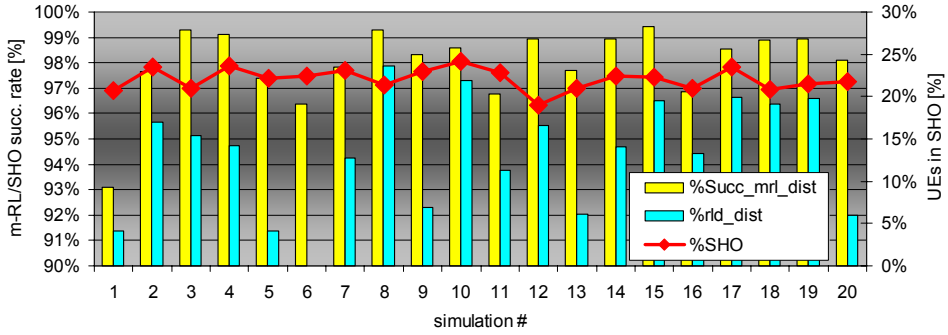

Figure Annex P.29 – CS Statistics: m-RL/SHO-RL succ. and SHO percentage (FT).

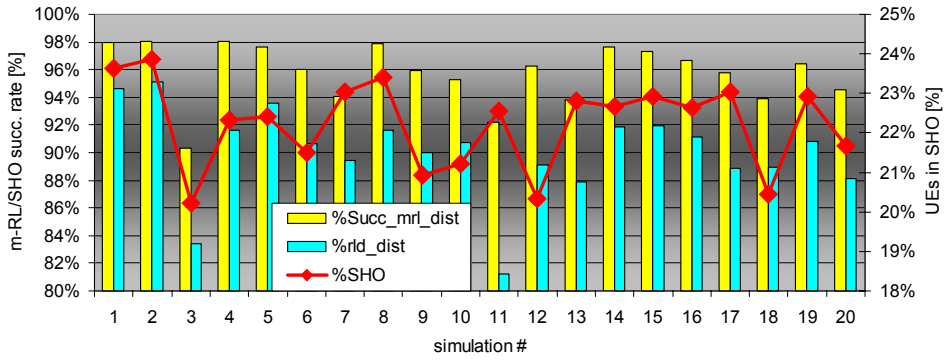

Figure Annex P.30 – CS Statistics: m-RL/SHO-RL succ. and SHO percentage (ST).

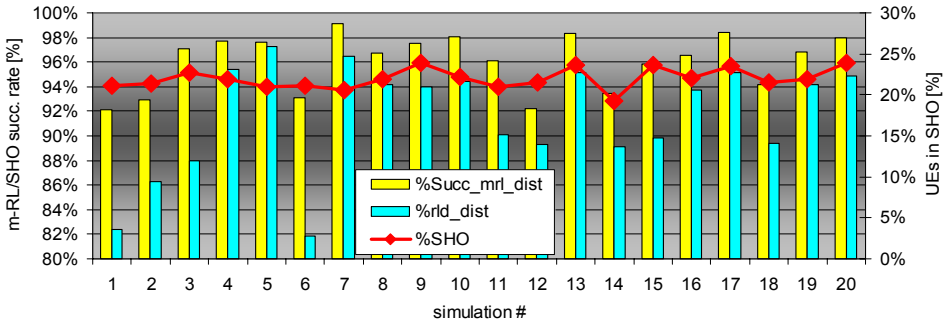

Figure Annex P.31 – CS Statistics: m-RL/SHO-RL succ. and SHO percentage (LB).

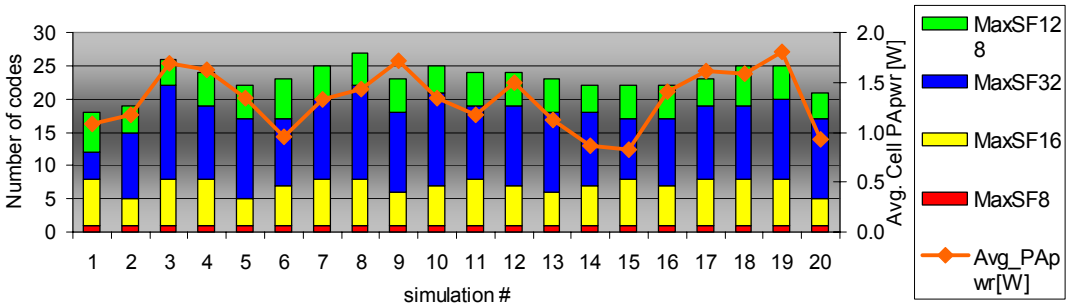

Figure Annex P.32 – SF code usage and Average Cell PA power (DAC).

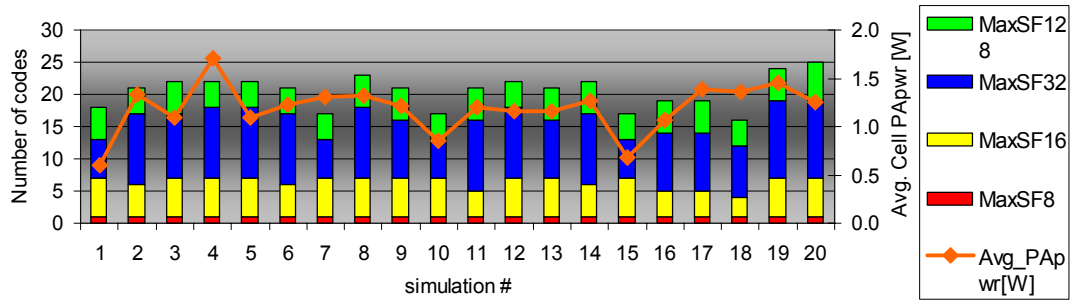

Figure Annex P.33 – SF code usage and Average Cell PA power (VC).

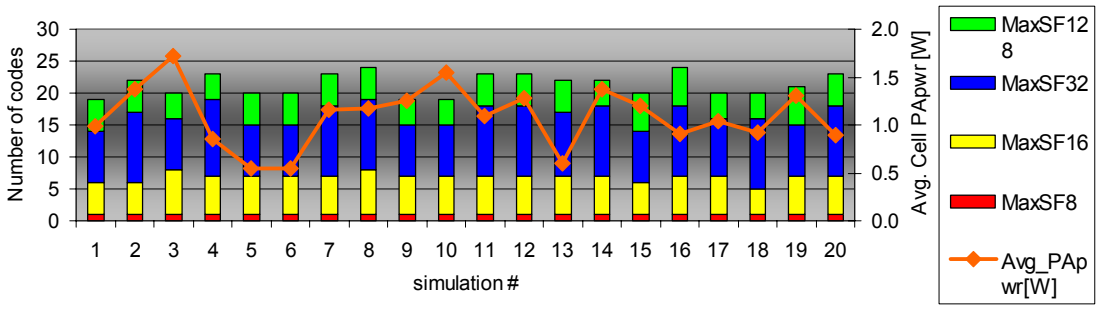

Figure Annex P.34 – SF code usage and Average Cell PA power (WW).

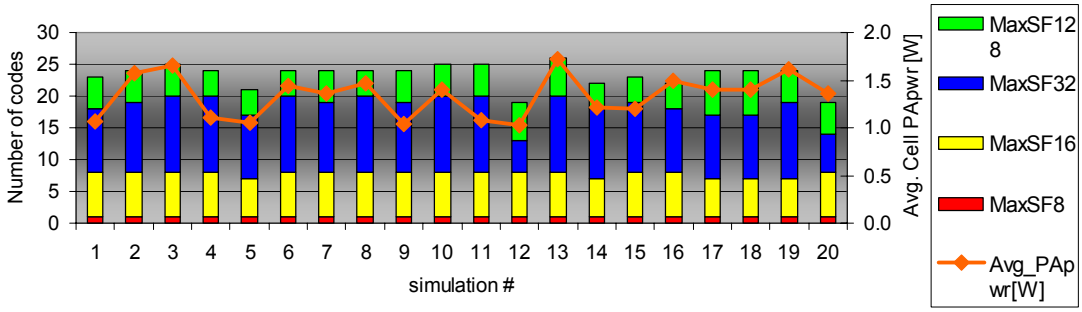

Figure Annex P.35 – SF code usage and Average Cell PA power (EM).

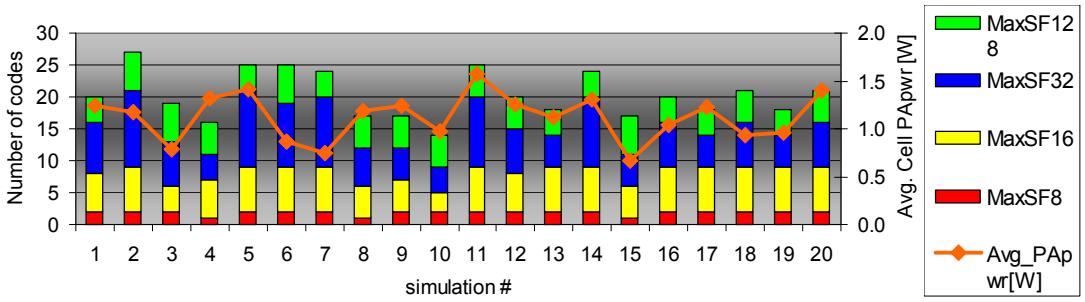

Figure Annex P.36 – SF code usage and Average Cell PA power (FT).

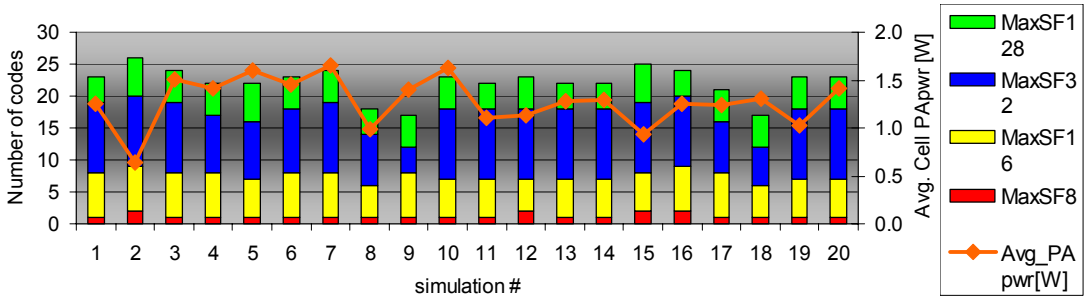

Figure Annex P.37 – SF code usage and Average Cell PA power (ST).

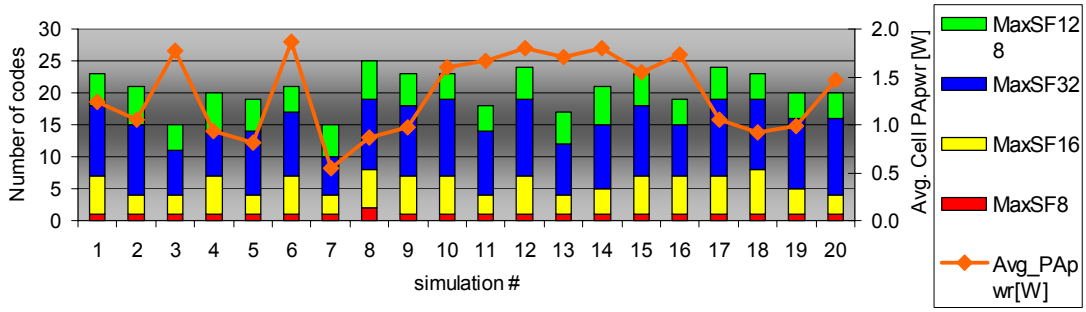

Figure Annex P.38 – SF code usage and Average Cell PA power (LB).

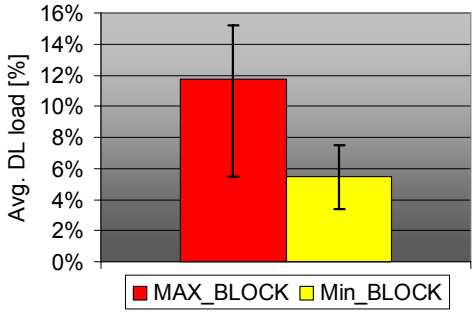

(DAC)

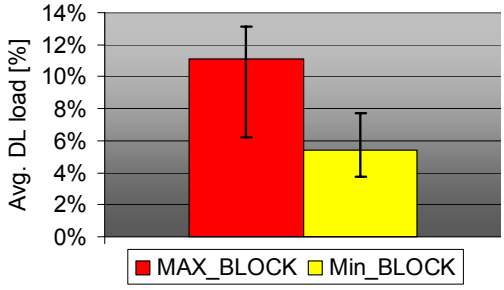

(VC)

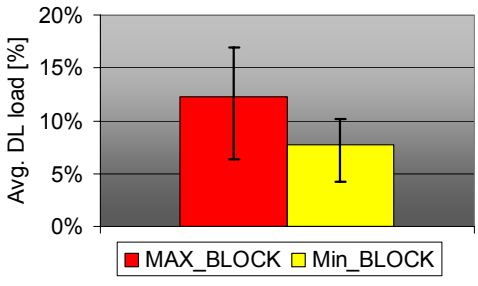

(WW)

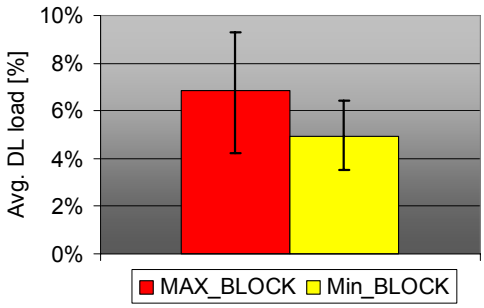

(EM)

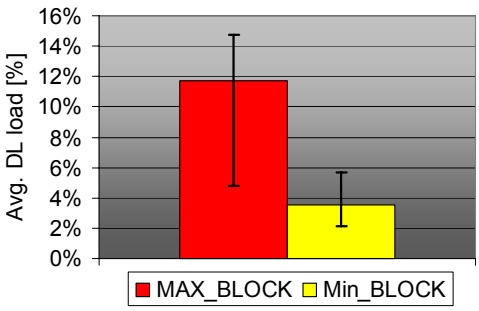

(FT)

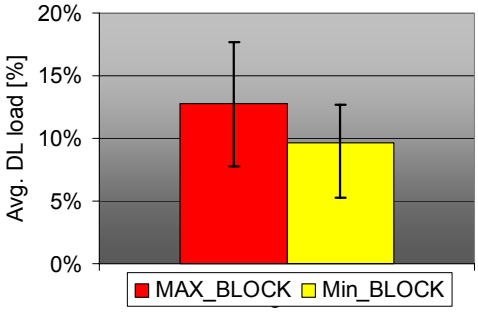

(ST)

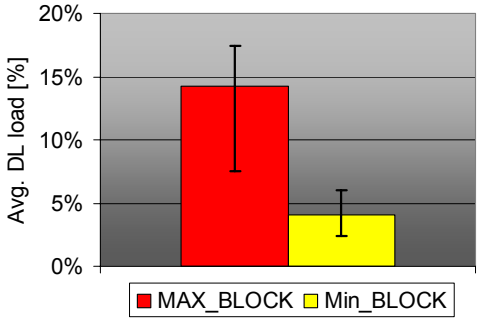

(LB)

Figure Annex P.39 – Average DL load (90% percentile).

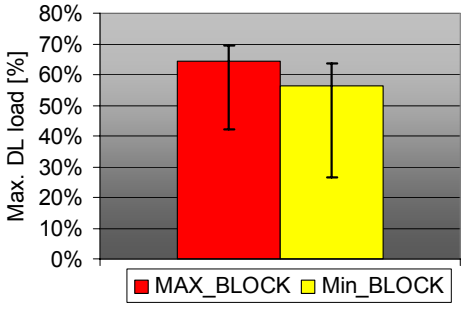

(DAC)

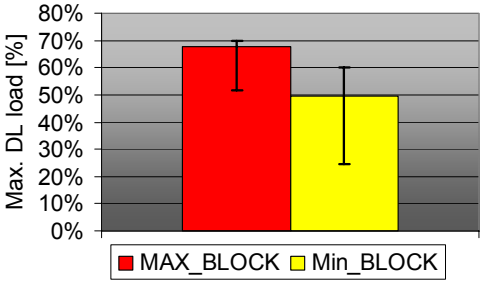

(VC)

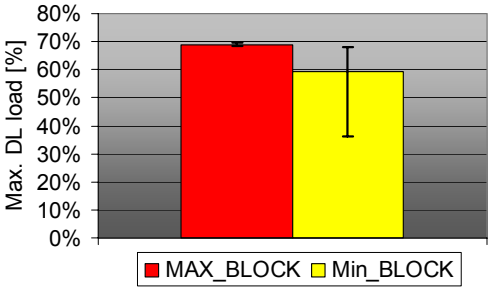

(WW)

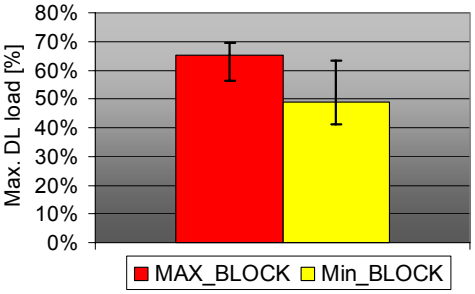

(EM)

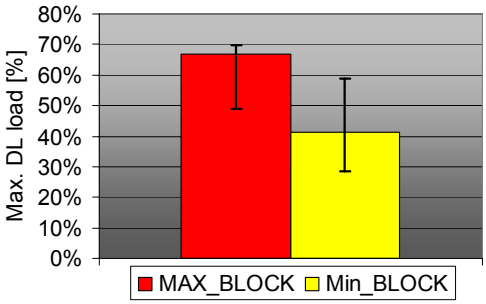

(FT)

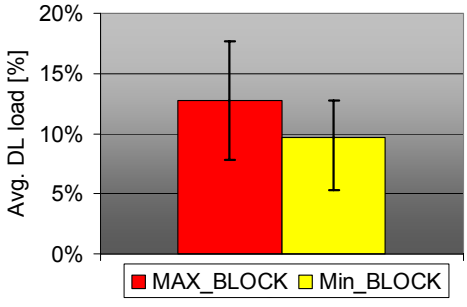

(ST)

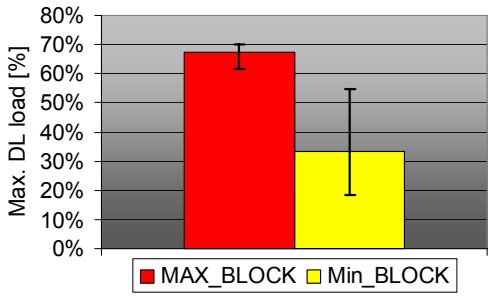

(LB)

Figure Annex P.40 – Maximum DL load (90% percentile).

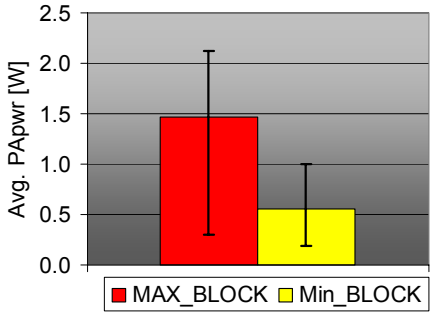

(DAC)

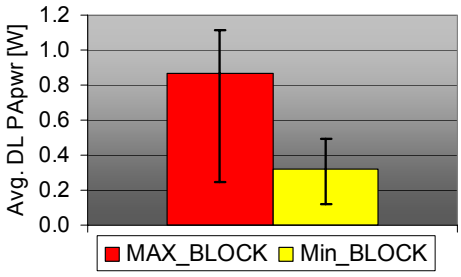

(VC)

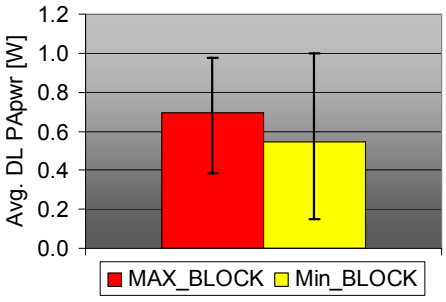

(WW)

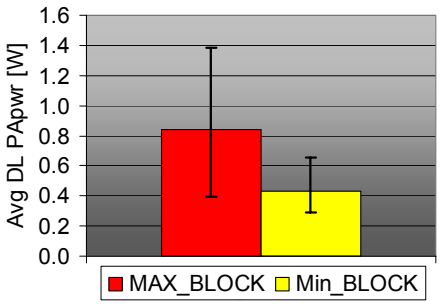

(EM)

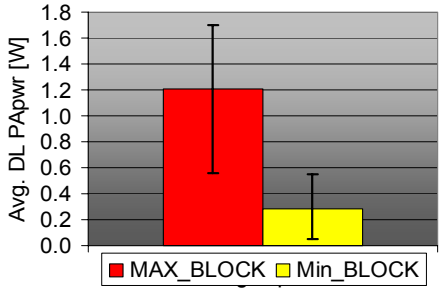

(FT)

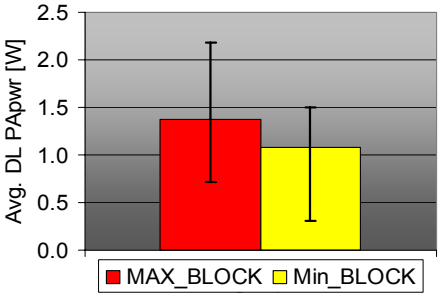

(ST)

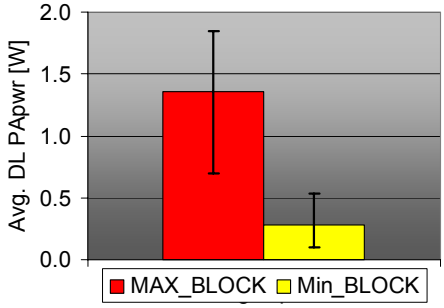

(LB)

Figure Annex P.41 – Average DL PA power (90% percentile).

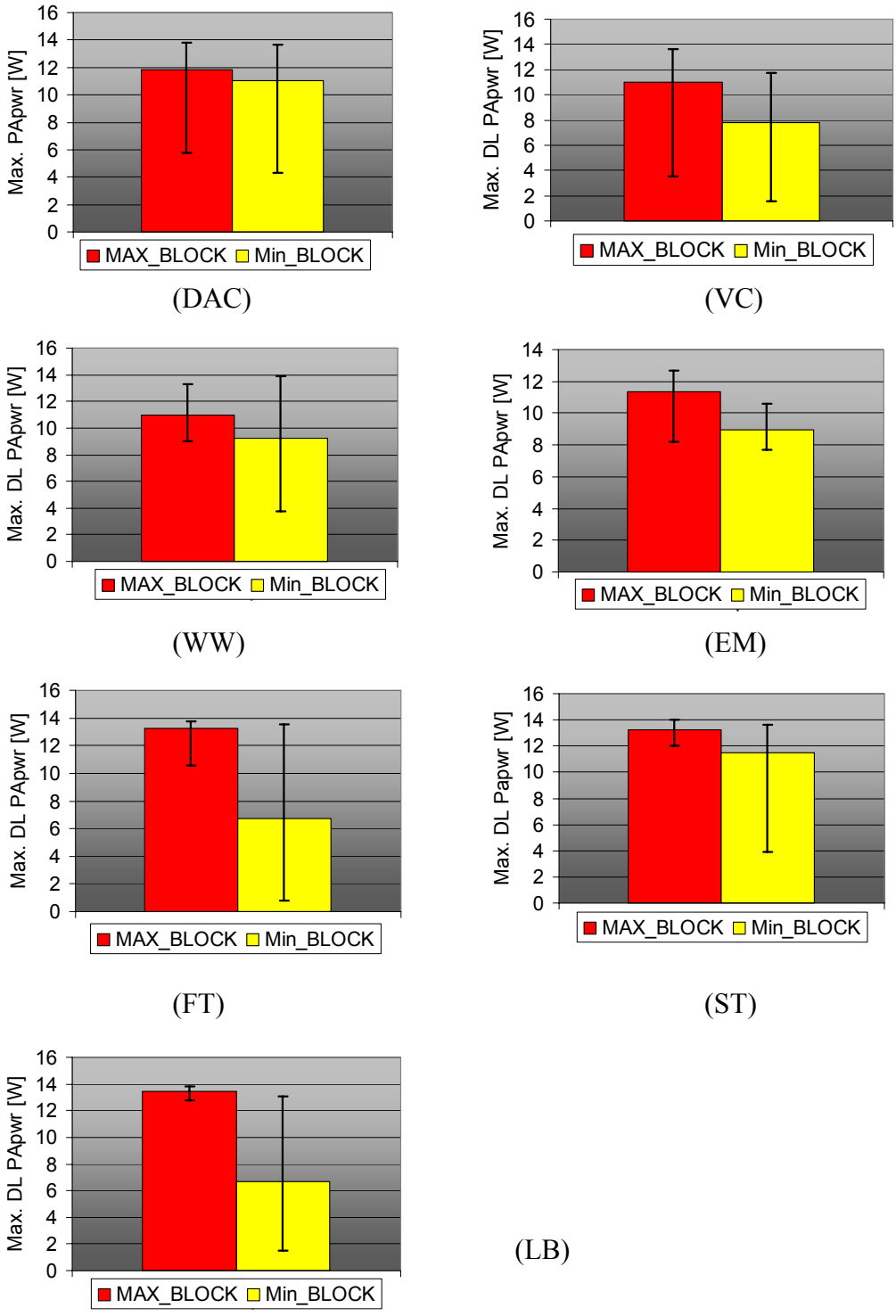

Figure Annex P.42 – Maximum DL PA power (90% percentile).

Q. LD Scenarios Output Analysis

This annex include all analysis performed and used in results summary of Chapter 5 to what regard the simulations on LD scenario, including TMA strategy impact analysis.

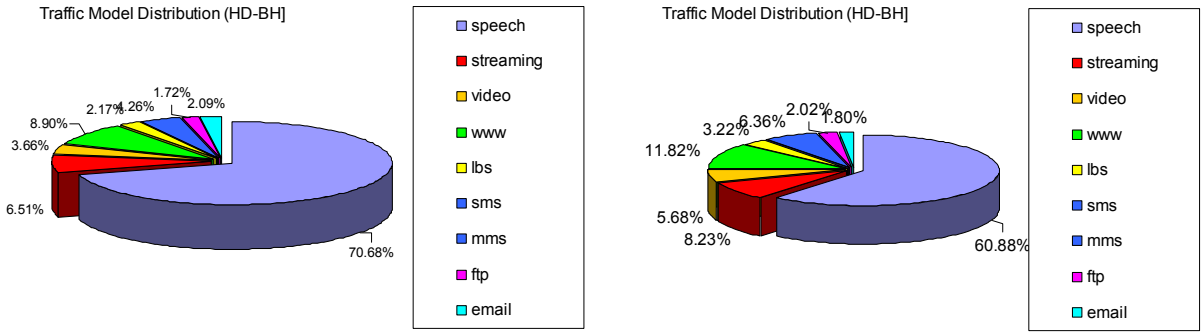

(REF)

(DAC)

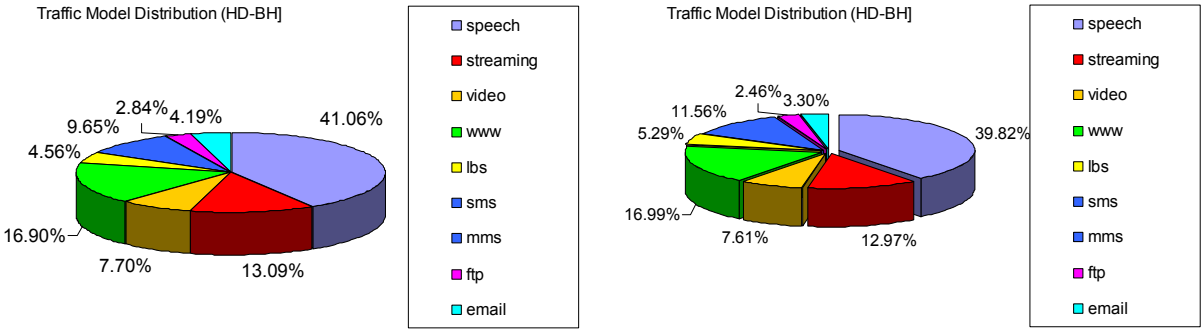

(DAM)

(DAM - 4 %)

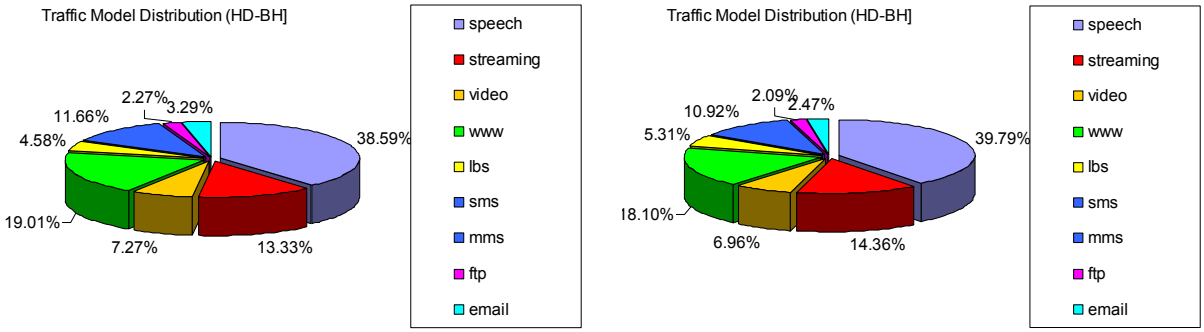

(DAM - 6 %)

(DAM - TMA)

Figure Annex Q.1 – Traffic Mix distribution (TRAFSIM3G traffic).

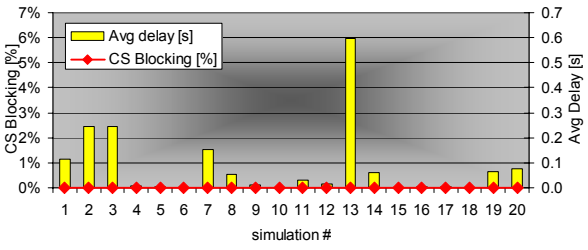

(REF)

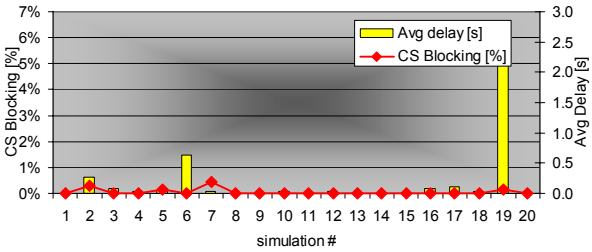

(DAC)

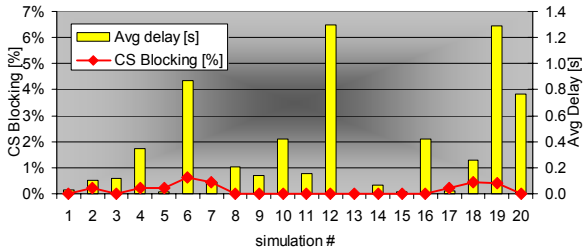

(DAM)

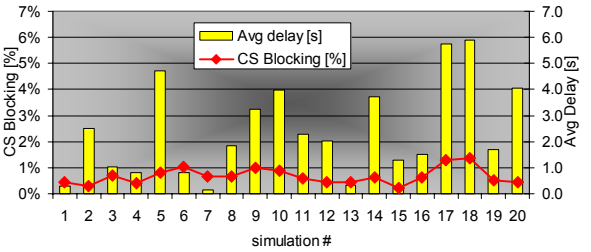

(DAM - 4 %)

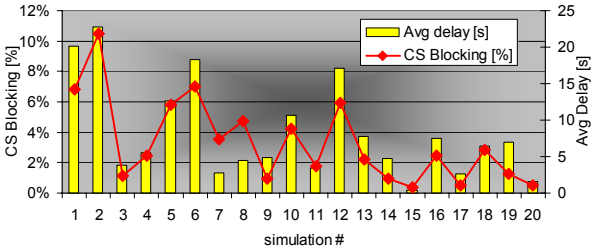

(DAM - 6 %)

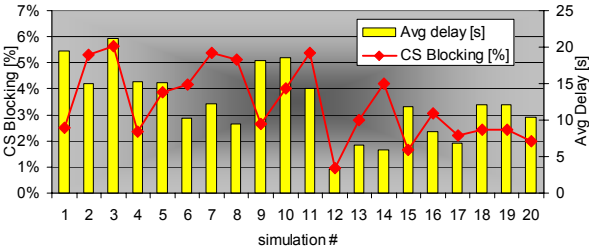

(DAM - TMA)

Figure Annex Q.2 – Blocking and Average delay.

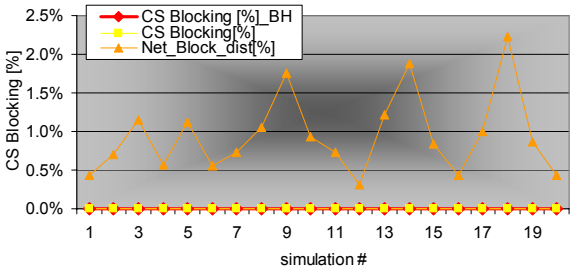

(REF)

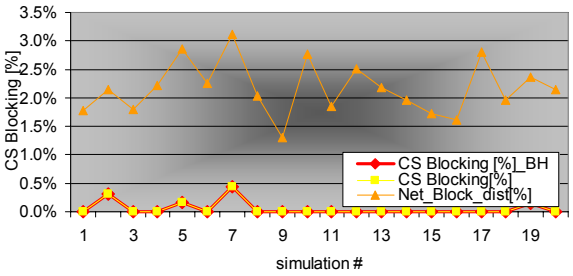

(DAC)

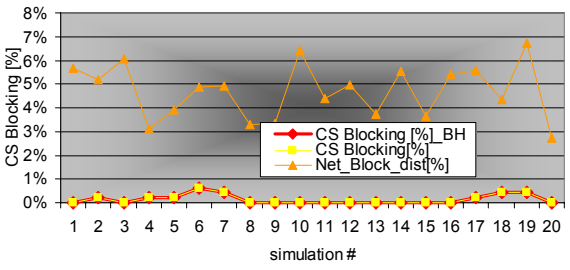

(DAM)

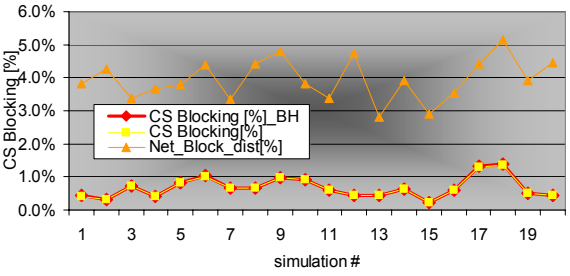

(DAM - 4 %)

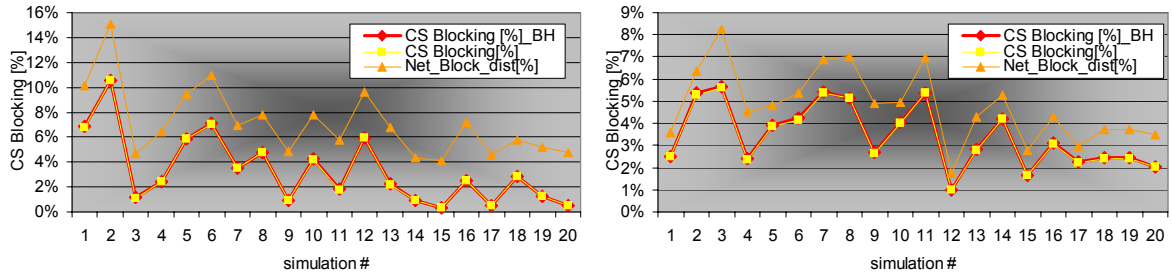

(DAM - 6 %) (DAM - TMA)

Figure Annex Q.3 – Blocking in BH, 70 min and including distance blocks.

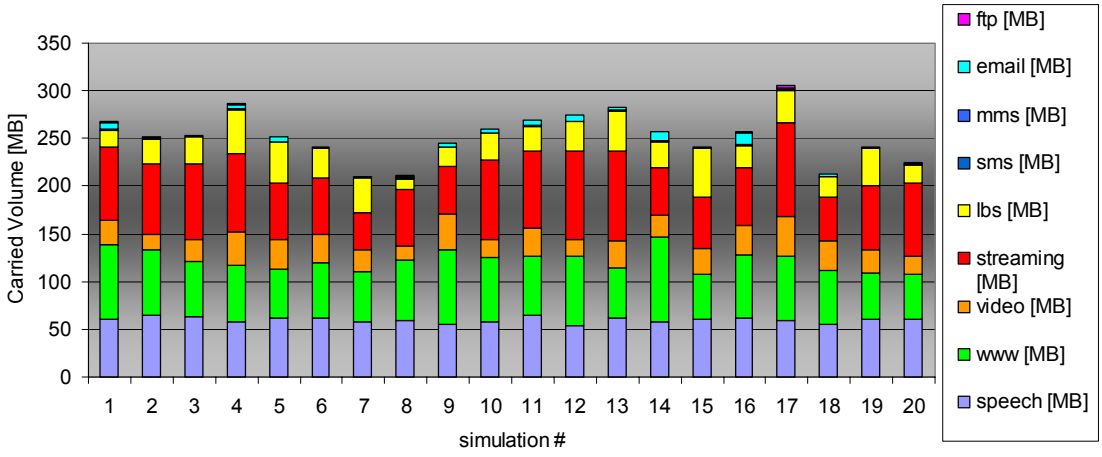

Figure Annex Q.4 – Carried traffic volume in REF scenario.

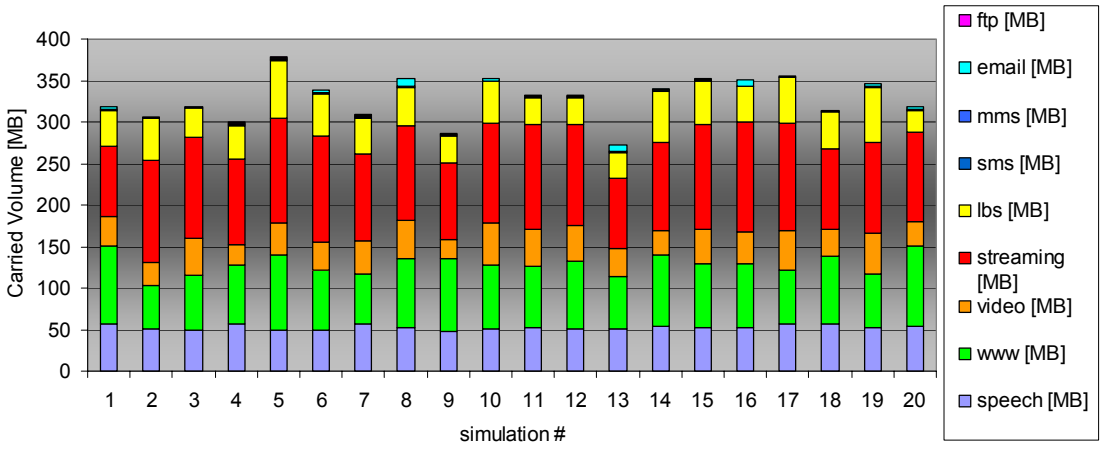

Figure Annex Q.5 – Carried traffic volume in DAC scenario.

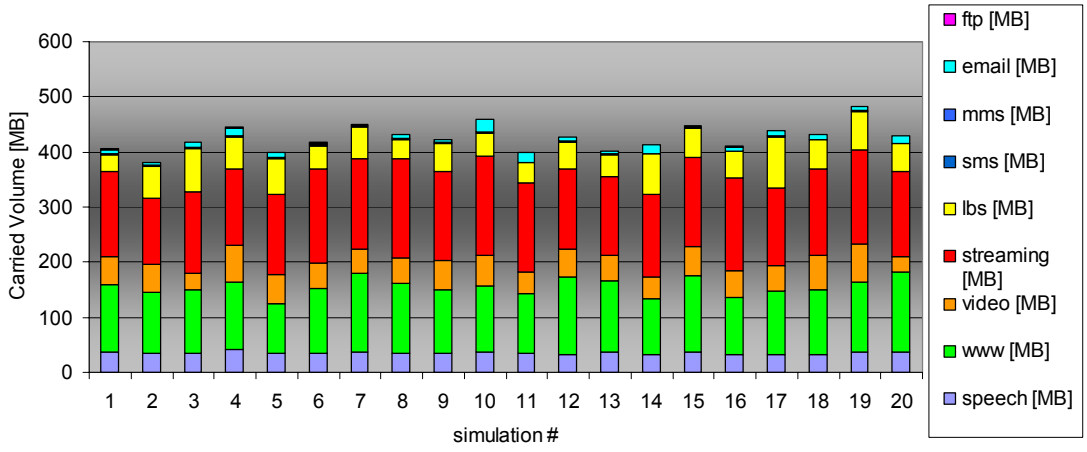

Figure Annex Q.6 – Carried traffic volume in DAM scenario.

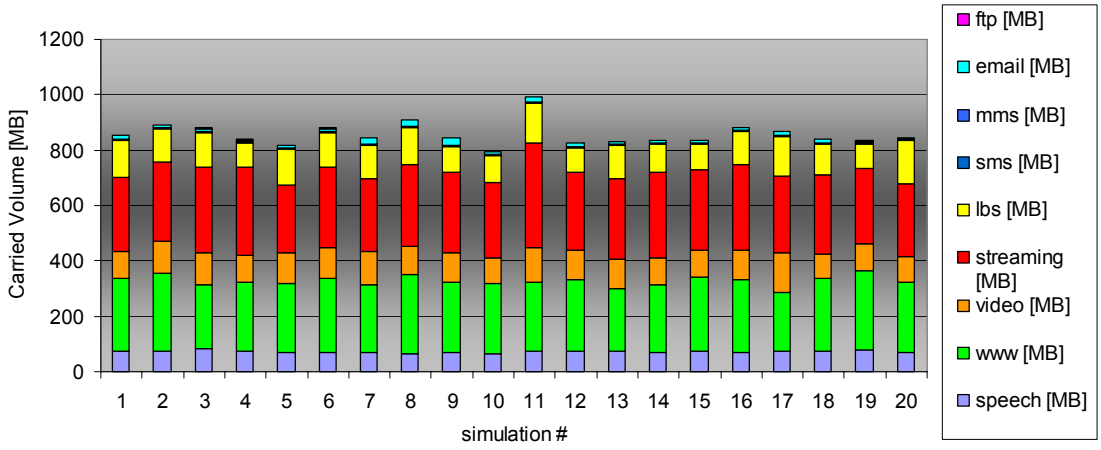

Figure Annex Q.7 – Carried traffic volume in DAM – 4 % scenario.

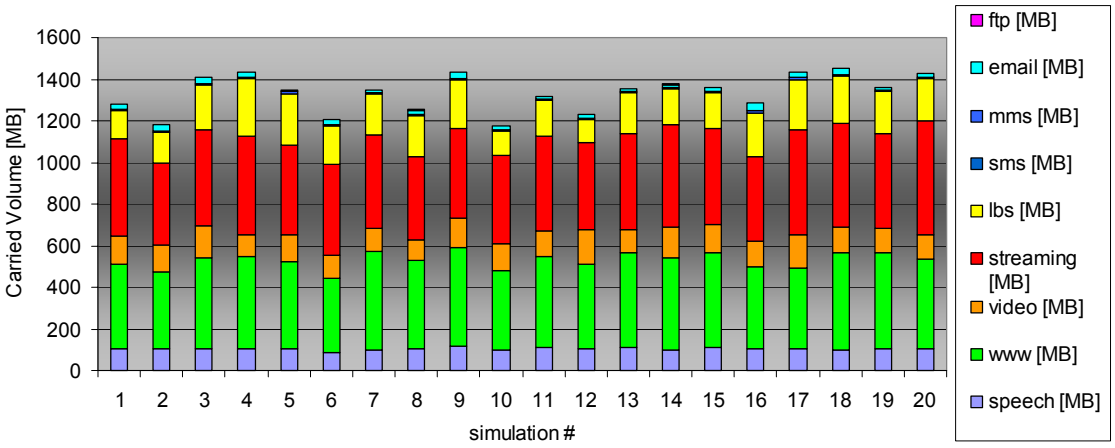

Figure Annex Q.8 – Carried traffic volume in DAM – 6 % scenario.

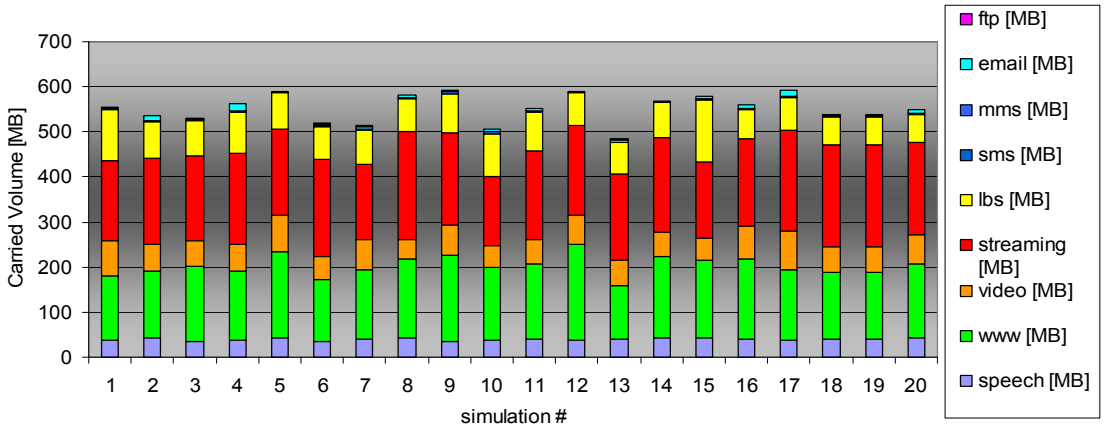

Figure Annex Q.9 – Carried traffic volume in DAM - TMA scenario.

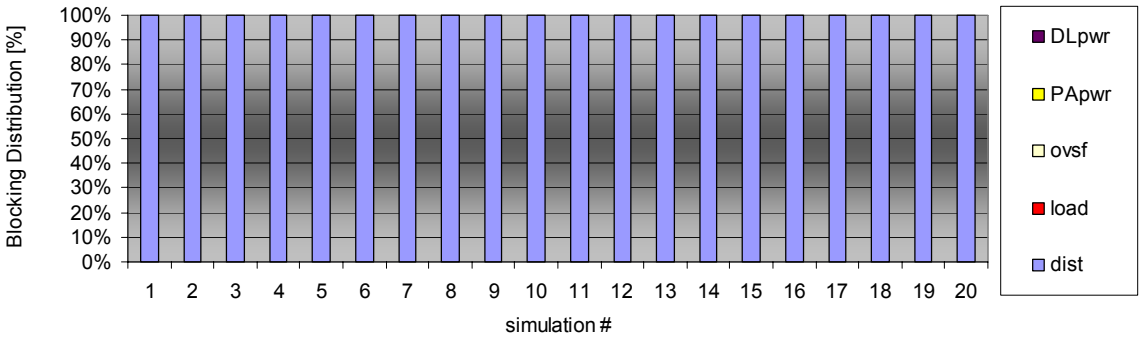

Figure Annex Q.10 – Blocking cause's distribution (REF).

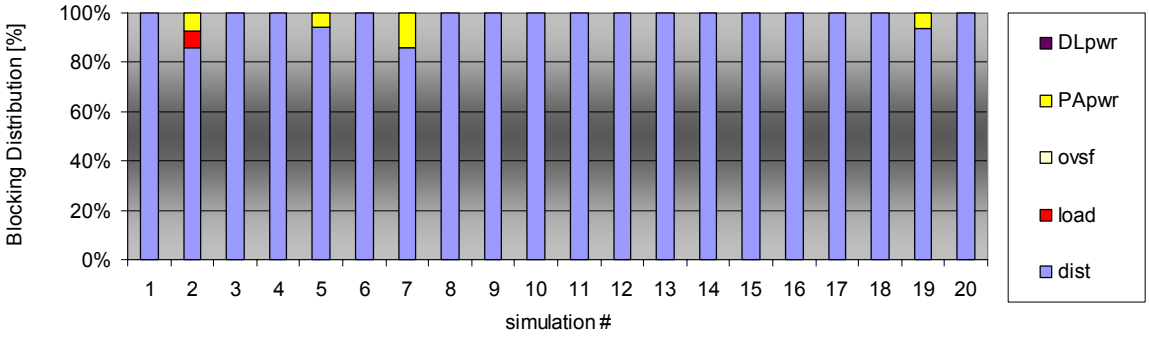

Figure Annex Q.11 – Blocking cause's distribution (DAC).

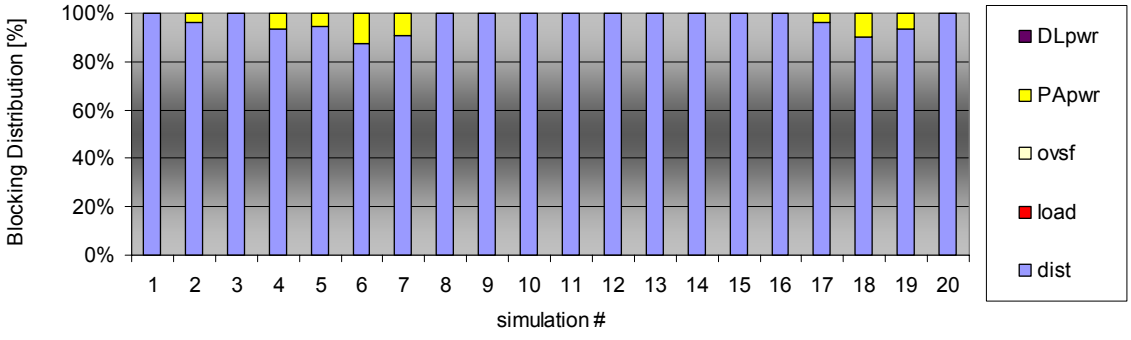

Figure Annex Q.12 – Blocking cause's distribution (DAM).

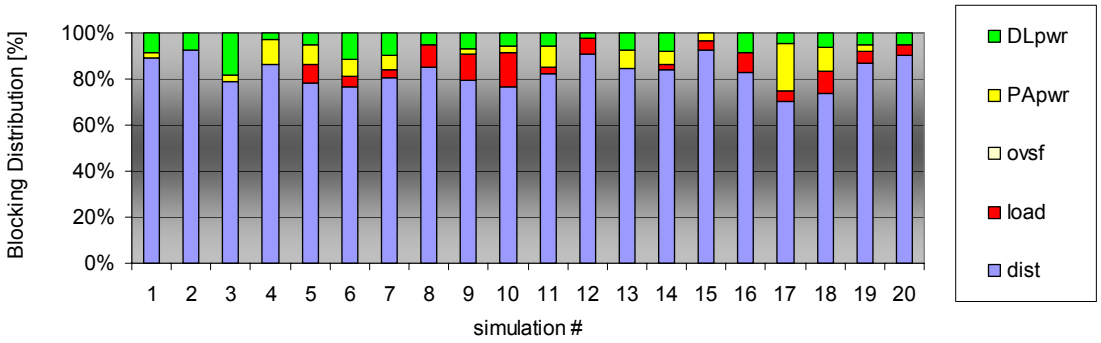

Figure Annex Q.13 – Blocking cause's distribution (DAM – 4 %).

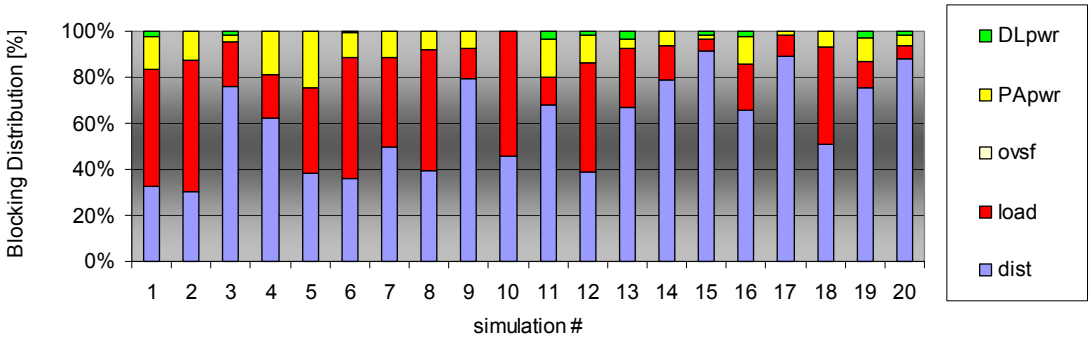

Figure Annex Q.14 – Blocking cause's distribution (DAM – 6 %).

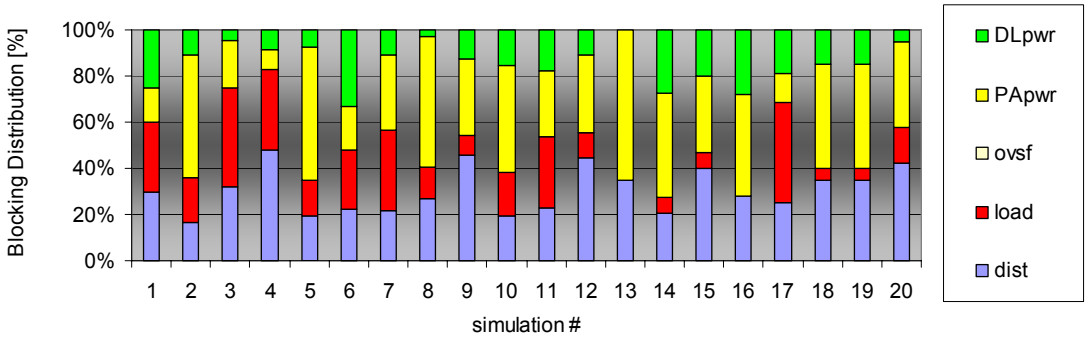

Figure Annex Q.15 – Blocking cause's distribution (DAM – TMA).

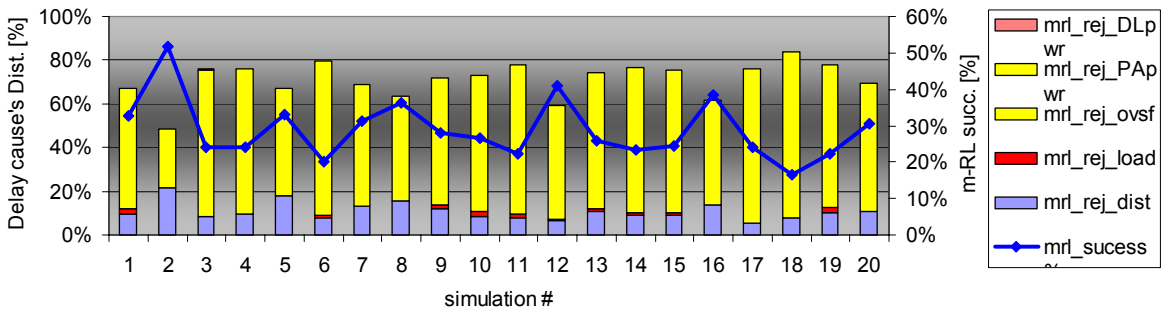

Fgure Annex Q.16 – PS delay cause's distribution (REF).

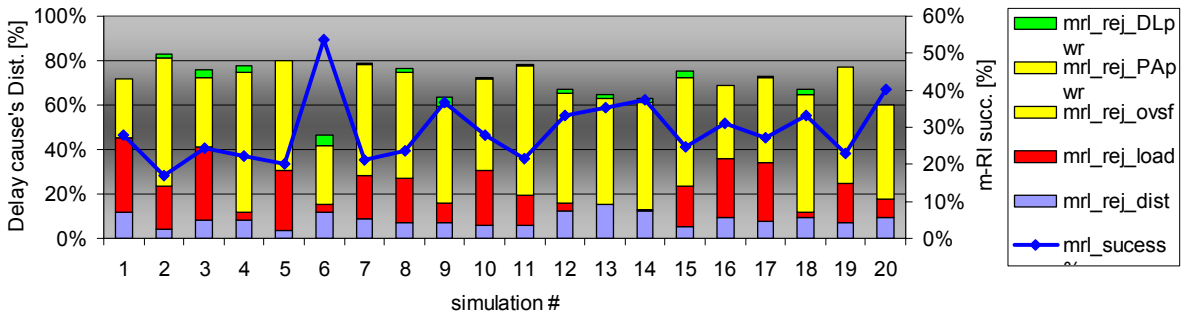

Figure Annex Q.17 – PS delay cause's distribution (DAC).

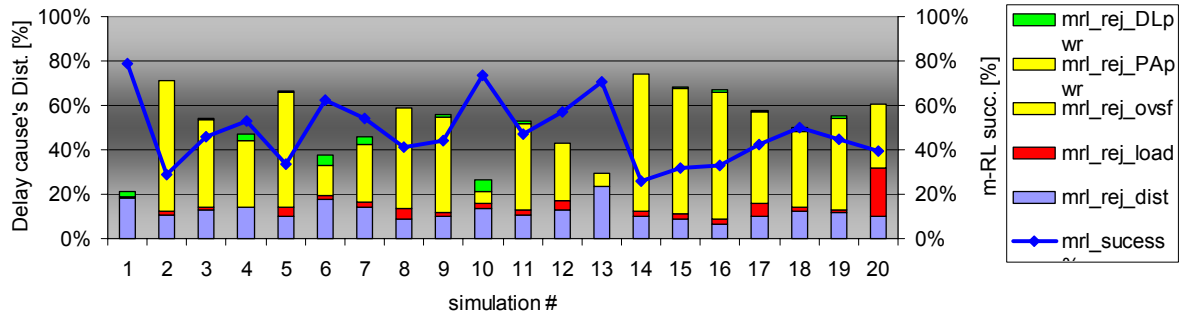

Figure Annex Q.18 – PS delay cause's distribution (DAM).

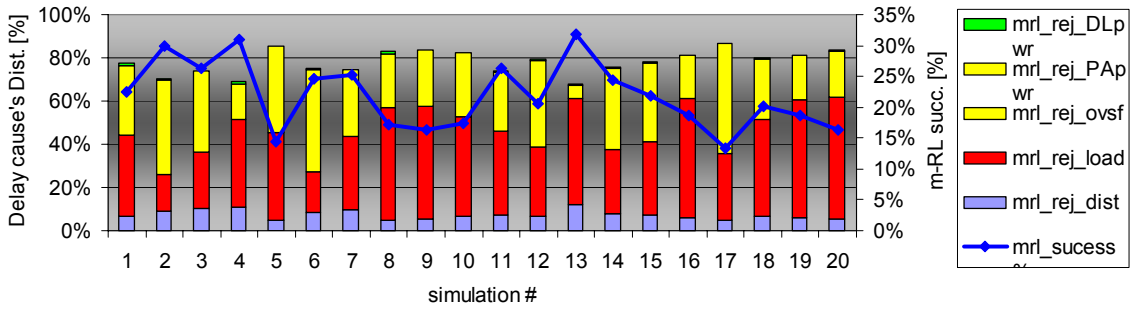

Figure Annex Q.19 – PS delay cause's distribution (DAM – 4 %).

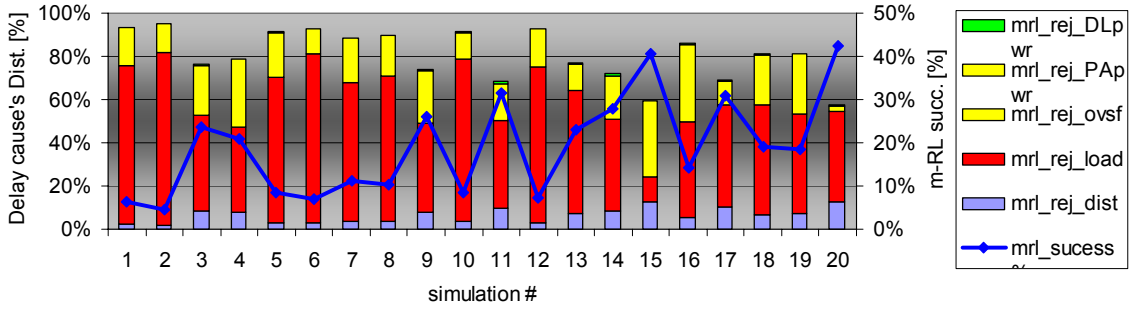

Figure Annex Q.20 – PS delay cause's distribution (DAM – 6 %).

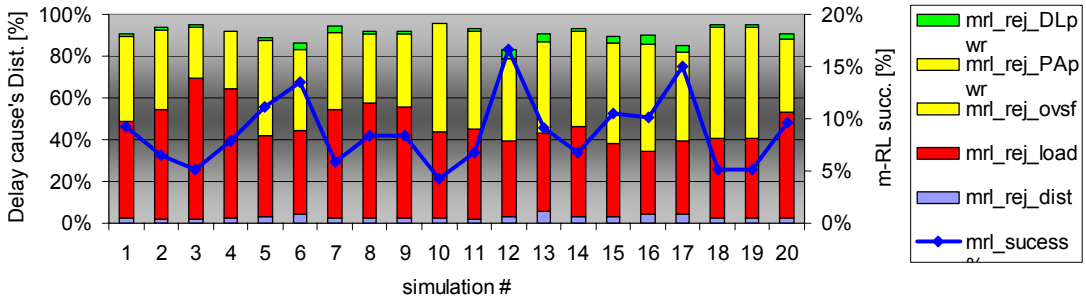

Figure Annex Q.21 – PS delay cause's distribution (DAM - TMA).

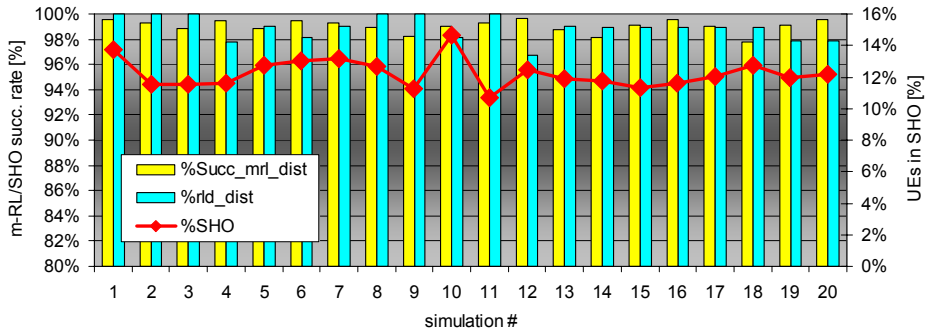

Figure Annex Q.22 – CS Statistics: m-RL/SHO-RL succ. and SHO percentage (REF).

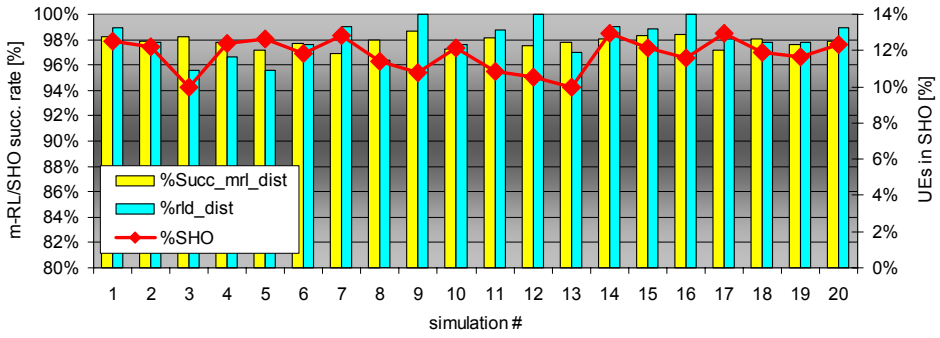

Figure Annex Q.23 – CS Statistics: m-RL/SHO-RL succ. and SHO percentage (DAC).

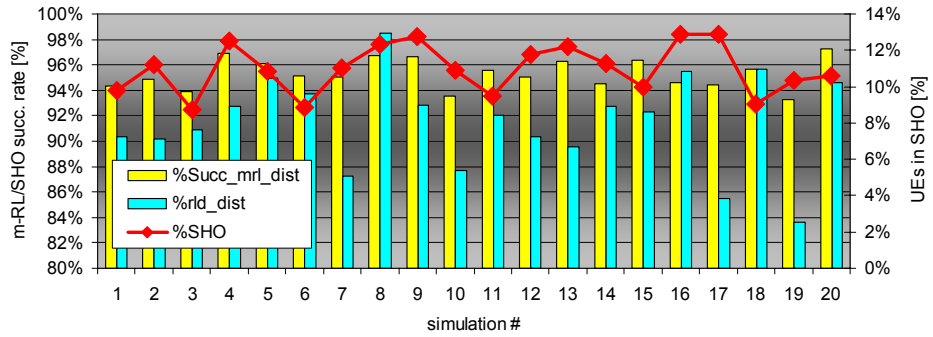

Figure Annex Q.24 – CS Statistics: m-RL/SHO-RL succ. and SHO percentage (DAM).

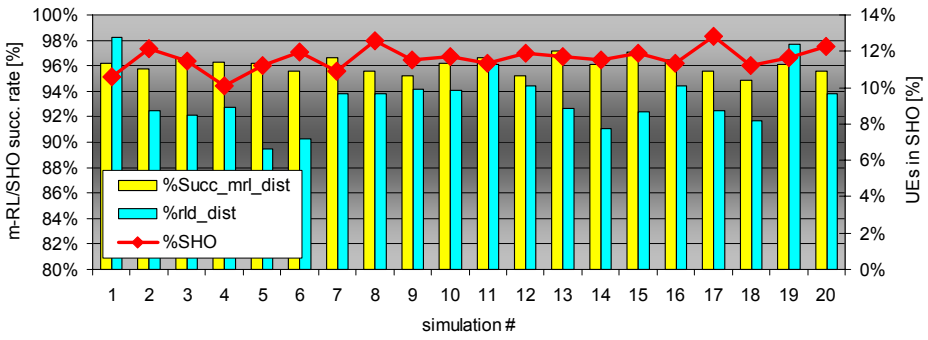

Figure Annex Q.25 – CS Statistics: m-RL/SHO-RL succ. and SHO percentage (DAM_4).

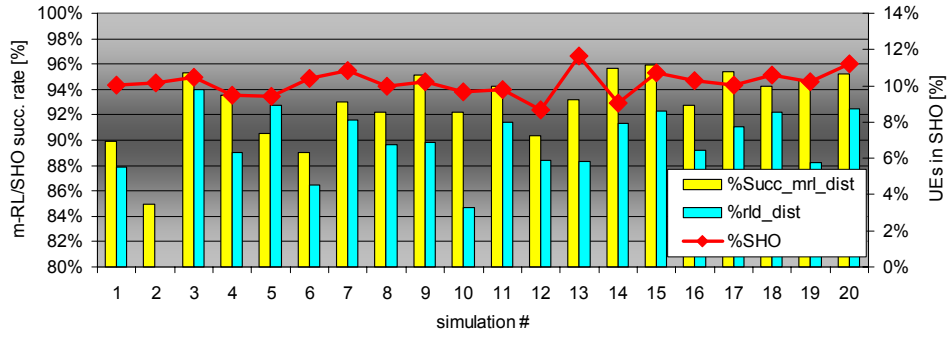

Figure Annex Q.26 – CS Statistics: m-RL/SHO-RL succ. and SHO percentage (DAM_6).

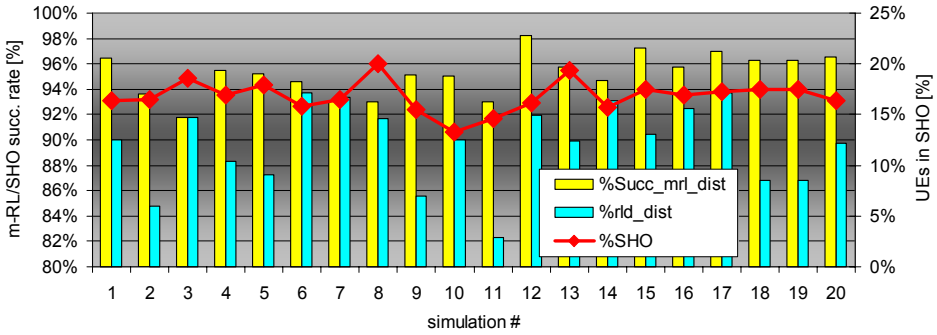

Figure Annex Q.27 – CS Statistics: m-RL/SHO-RL succ. and SHO perc.(DAM – TMA).

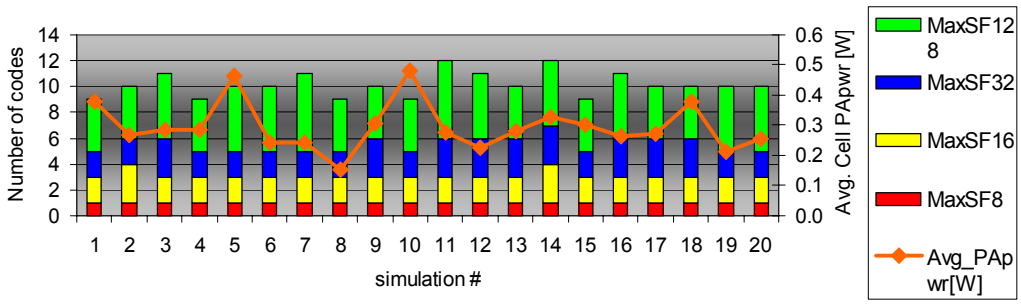

Figure Annex Q.28 – SF code usage and Average Cell PA power (REF).

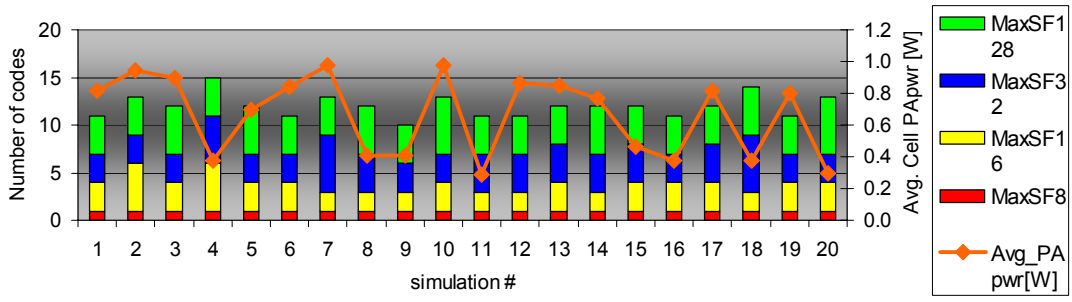

Figure Annex Q.29 – SF code usage and Average Cell PA power (DAC).

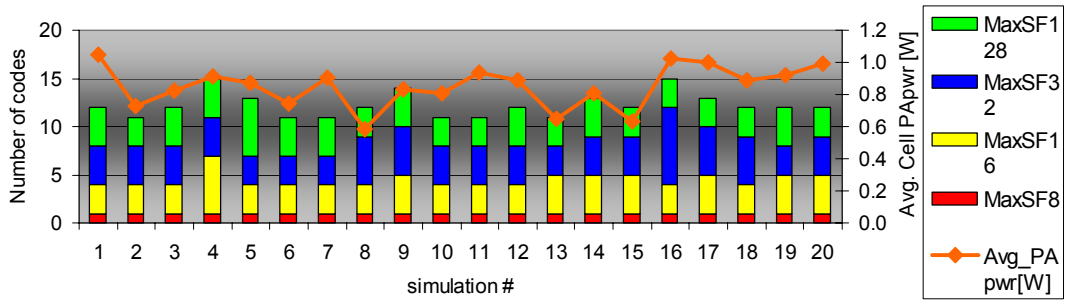

Figure Annex Q.30 – SF code usage and Average Cell PA power (DAM).

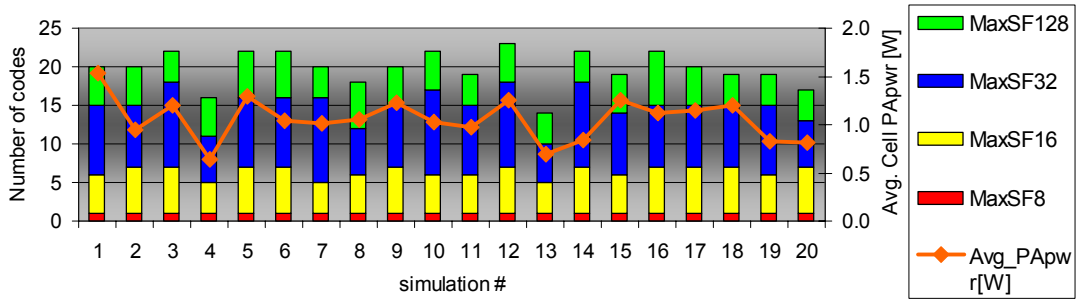

Figure Annex Q.31 – SF code usage and Average Cell PA power (DAM – 4 %).

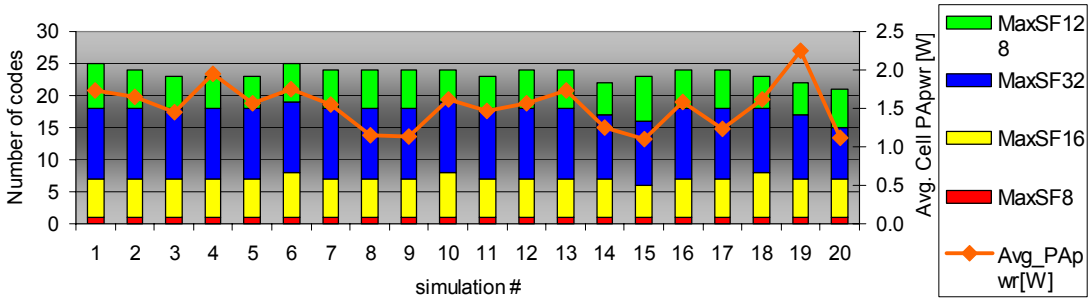

Figure Annex Q.32 – SF code usage and Average Cell PA power (DAM – 6 %).

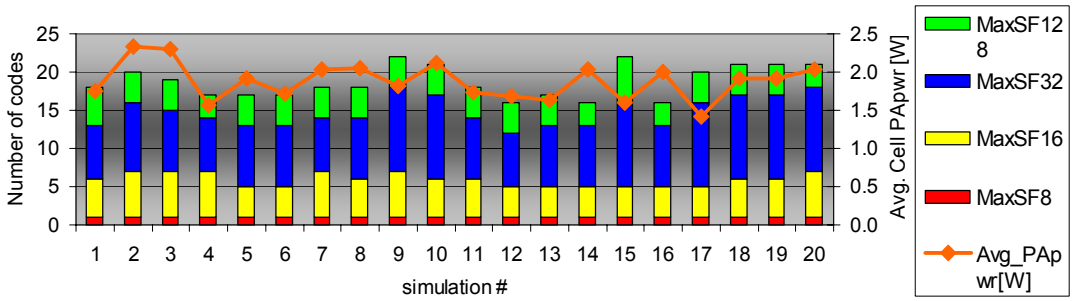

Figure Annex Q.33 – SF code usage and Average Cell PA power (DAM – TMA).

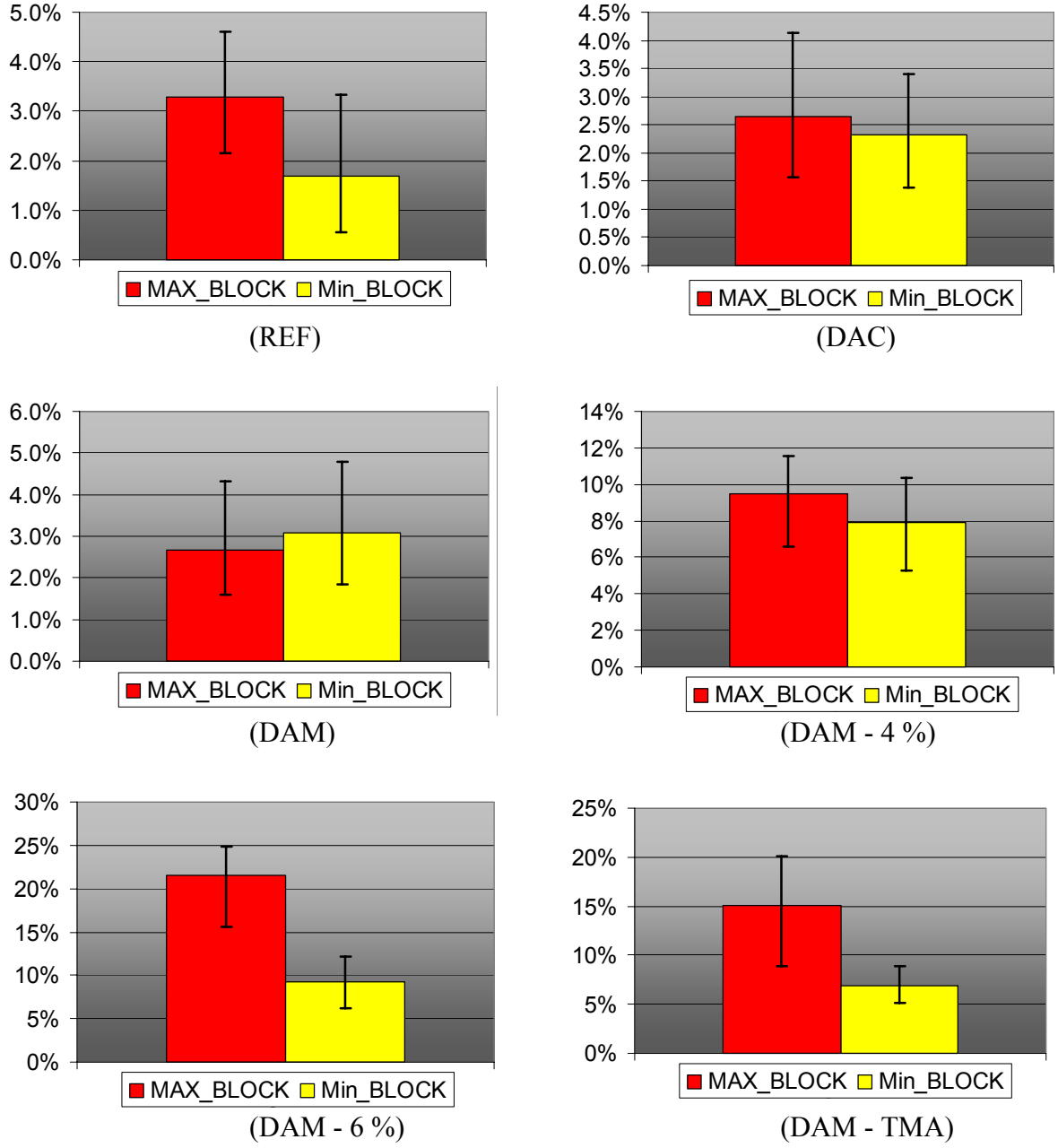

Figure Annex Q.34 – Average DL load (90% percentile).

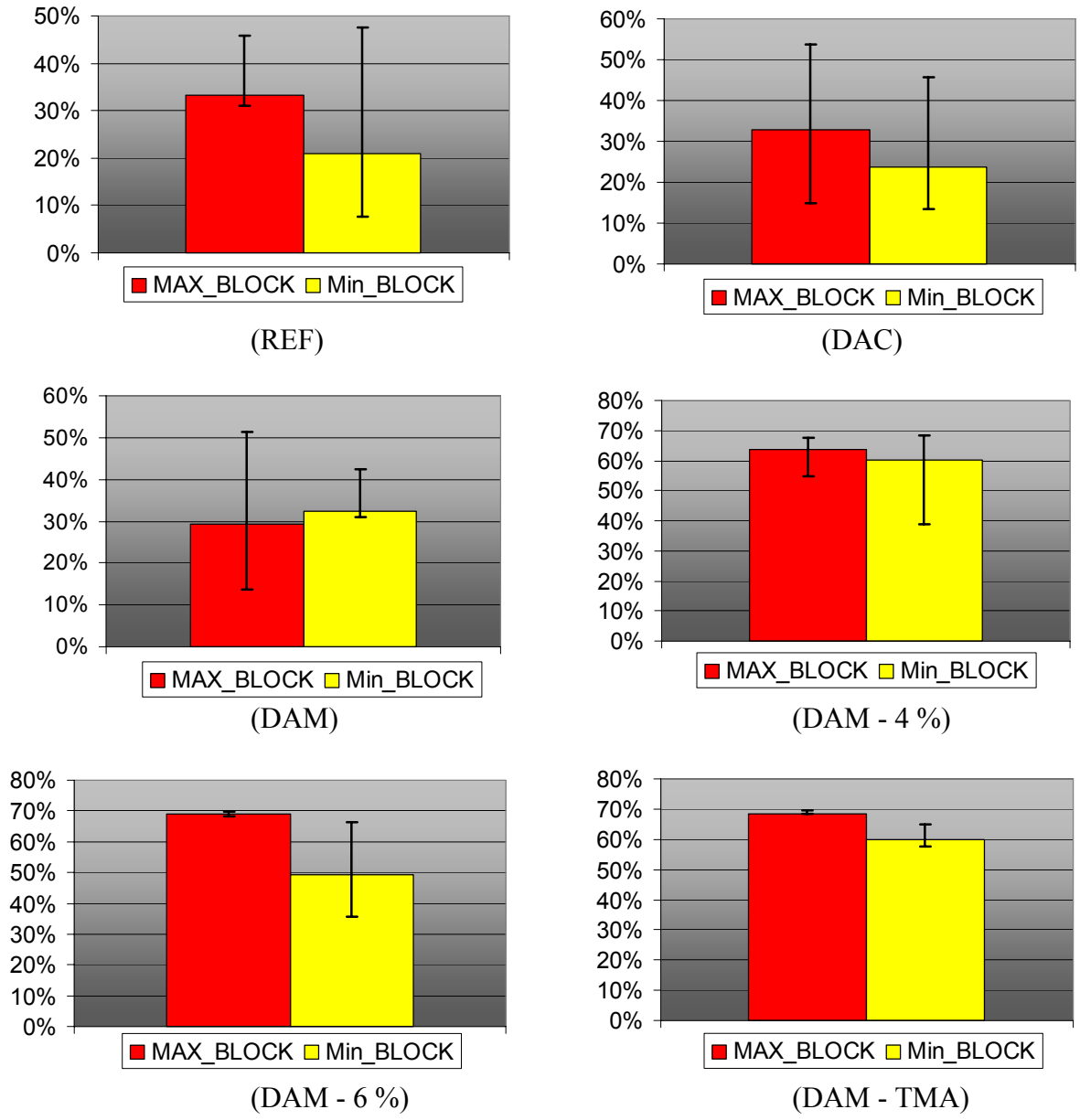

Figure Annex Q.35 – Maximum DL load (90% percentile).

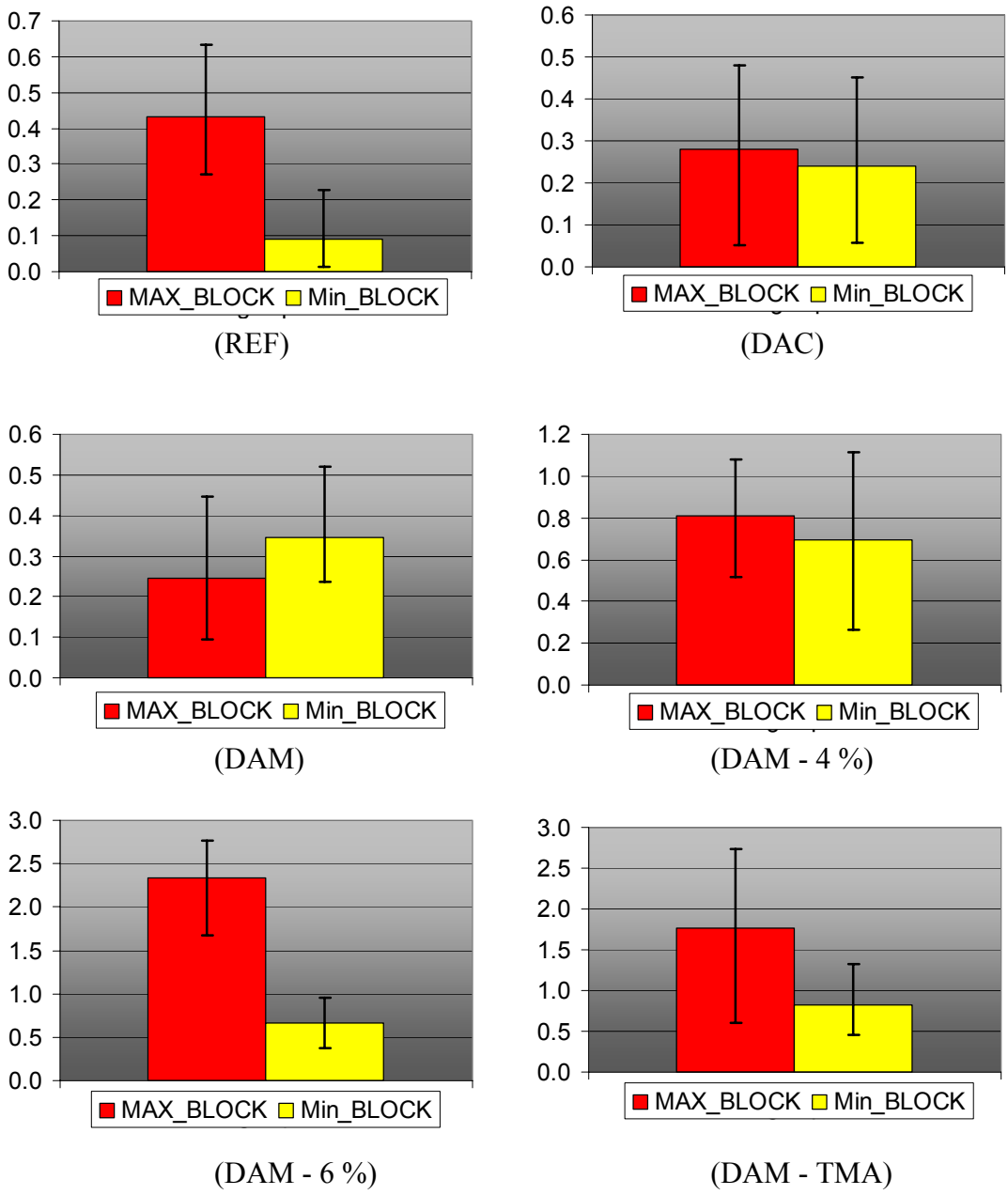

Figure Annex Q.36 – Average DL PA power (90% percentile).

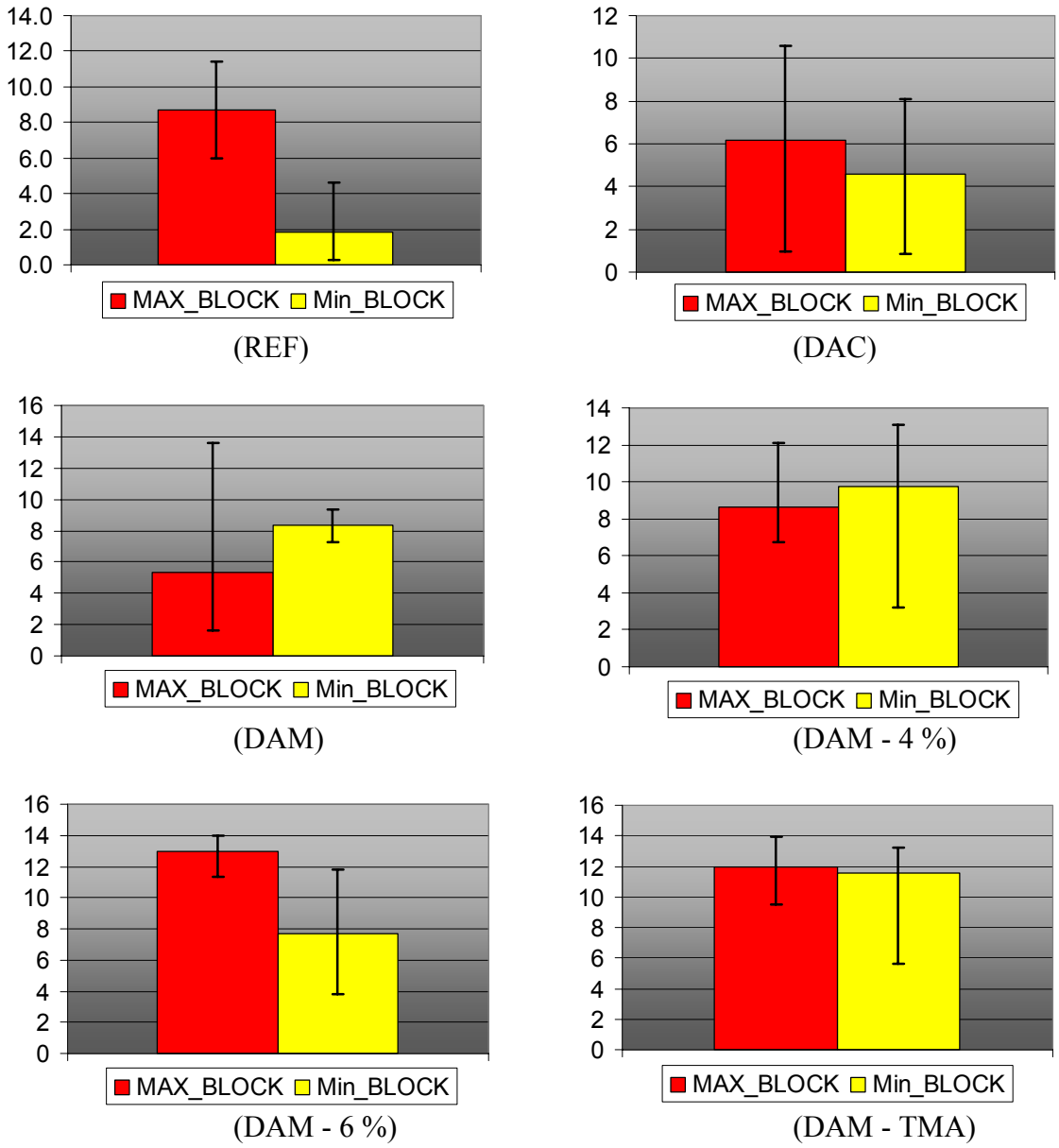

Figure Annex Q.37 – Maximum DL PA power (90% percentile).

References

[AdCo02] Adiego,D. and Cordier,C., "Multi-Service Radio Dimensioning for UMTS PS Services", *in Proc. of PIMRC*, Lisbon, Portugal, Sep. 2002.

[Agui03] Aguiar,A., Traffic Analysis at the Radio Interface in Converging Mobile and Wireless Communication Systems, Master Thesis, Instituto Superior Técnico, Lisbon, Portugal, Dec. 2003.

[NOKI04] http://www.nokia.com/

[ARCV03] ArcView (http://www.esri.com)

[ARRO04] http://www.arrows-ist.upc.es

[CaML02] Lisbon GIS Maps – Clutter and ground occupation, *Câmara Municipal de Lisboa*, 2002 (http://ulisses.cm-lisboa.pt).

[Card04] Cardoso,F.D., *Short-term Fading Characteristics in Wideband Mobile Communication Systems*, Ph.D. Thesis, Instituto Superior Técnico, Portugal, June 2004.

[Corr02] Correia,L.M., *Mobile Communication Systems* (in Portuguese), AEIST, Instituto Superior Técnico, Lisboa, Portugal, 2002.

[DaCo99] Damasso,E. and Correia,L.M., *Digital Mobile Radio Towards Future Generation,* COST 231 Final Report, 1999 (http://www.lx.it.pt/cost231/).

[DGCI02] Direcção Geral de Impostos, 2001 (http://www.dgci.min-financas.pt/).

[Dias03] Dias,M.C., *Traffic Analysis at the Radio Interface in UMTS FDD*, Master Thesis, Instituto Superior Técnico, Lisbon, Portugal, Dec. 2003.

[DiLS01] Dillinger,M., Luo,J. and Schulz,E., "Radio Resource Scheduling Algorithms for Mixed VoIP and HTTP Traffic in HIPERLAN/2 System", in *Proc. of IST Mobile Communications Summit*, Sitges, Spain, Sep. 2001.

[ETSI98a] ETSI, *"Evaluation Report for ETSI UMTS Terrestrial Radio Access (UTRA) ITU-R RTT Candidate"*, Technical Report, France, Apr. 1998 (http://www.etsi.org).

[ETSI98b] ETSI, *Universal Mobile Telecommunications System (UMTS); Selection procedures for the choice of radio transmission technologies of the UMTS (UMTS 30.03 version 3.2.0),* Technical Report, No. TR 101 112, Ver. 3.2.0 , France, Apr. 1998 (http://www.etsi.org).

[EURE00] EURESCOM P921, *UMTS radio access, D2: Guidelines For UMTS Radio Access Network Design*, Germany, Oct. 2000 (http://www.eurescom.de/public/projects/p900-series/P921/).

[FeAl02] Félix,A. and Almeida,J., *Traffic Prediction Models in UMTS (in Portuguese)*, Graduation Thesis, Instituto Superior Técnico, Lisbon, Portugal, September 2002.

[FeCo03] Correia,L.M. and Ferreira,L., "Generation of Traffic Demand Scenarios for UMTS", in *Proc. of IST Mobile & Wireless Communications Summit 2003*, Aveiro, Portugal, June 2003.

[FORU02] UMTS Forum, *"UMTS Forum Position White Paper Nº 1 – Evolution to 3G/UMTS Services"*, August 2002 (http://www.umts-forum.org)

[FrNg00] Frey,M. and Nguyen-Quang,S., "A Gamma-Based Framework for Modelling Variable-Rate MPEG Video Sources: The GOP GBAR Model", *IEEE/ACM Transactions on Networking*, Vol. 8, No. 6, Dec. 2000, pp. 710-719.

[Hata80] Hata,M., "Empirical Formula for Propagation Loss in Land Mobile Radio Services", IEEE Trans. Veh. Technol., Vol. VT-29, No. 3, Aug. 1980, pp. 317-325.

[Heym97] Heyman,D., "The GBAR Source Model for VBR Videoconferences", *IEEE/ACM Transactions on Networking*, Vol. 5, No. 4, Aug. 1997, pp. 554-560.

[HoTo01] Holma,H. and Toskala,A., *WCDMA for UMTS*, John Wiley et Sons, UK, 2001 (Revised Edition).

[IIRC03] Santo,L., *Traffic Modelling: Developing a Cell Plan for Multi-Service 3G Traffic*, IIR GPRS & WCDMA Technical Forum, Madrid, Spain, July 2003 (www.iir-telecoms.com).

[IkYU84] Ikegami,F., Yoshida,S. and Umehira,M., "Propagation factors controlling mean field strength on urban streets," IEEE Trans. on Antennas and Propagation, Vol. 32, No. 8, Aug. 1984, pp. 822-829.

[InNE01] Population Census 2001, INE, Lisbon, 2001 (http://www.ine.pt/censos2001).

[IPWL04] IPWireless web site – news (http://www.ipwireless.com).

[KlLL01] Klemm,A., Lindemann,C. and Lohmann,M., "Traffic Modelling and Characterisation for UMTS Networks", in *Proc. of GLOBECOM'01 - IEEE Global Telecommunications Conference*, San Antonio, Texas, USA, Nov. 2001.

[LaWN02] Laiho-Steffens,J., Wacker,A. and Novosad,T., *Radio Network Planning and Optimisation for UMTS*, UK, 2002.

[MAPI03] MapInfo® (http://www.MapInfo.com)

[MaZe02] Malik,S. and Zeghlache,D., "DL Capacity and Performance Issues in Mixed Services UMTS WCDMA Networks", in *Proc. of VTC2002 Spring,* Birmingham-Alabama, USA, May 2002.

[MOME00] MOMENTUM (MOdels and SiMulations for NEtwork PlaNning and ConTrol of UMTS) research project, EU - IST Programme, contract number IST-2000-28088, http://momentum.zib.de.

[NyJO01] Nyberg,H., Johansson,C. and Olin,B., "A streaming Video Traffic Model for the Mobile Access Network", in *Proc. of VTC'2001 - IEEE 54th Vehicular Technology Conference*, Atlantic City, New Jersey, USA, Oct. 2001.

[OOKF68] Okumura,Y., Ohmori,E., Kawano,T. and Fukuda,K., "Field Strength and Its Variability in VHF and UHF Land-Mobile Radio Service", Rev. Elec. Commun. Lab., Vol. 16, Sep.-Oct. 1968, pp. 825-873.

[PMCS02a] PMC-Sierra web site, 3G Base Transceiver Station (NodeB), (http://www.pmc-sierra.com/pdf/diagrams/3G_Base_transceiver_station.pdf)

[RaMe01] Rábanos,J. and Mesquida,C., *Mobile Communications of Third Generation* (in Spanish), Telefónica Móviles España, Madrid, Spain, 2001.

[Ribe03] Ribeiro,L.Z., *Traffic Dimensioning for Multimedia Wireless Networks*, Ph.D. Thesis, Virginia Polytechnic Institute, Virginia, USA, April 2003.

[SEAC04] http://seacorn.ptinovacao.pt.

[SeCo03] Serrador,A. and Correia,L.M., *UMTS Traffic Source Modelling*, COST 273, Deliverable TD(03)118, Paris, France, May 2003.

[Serr02] Serrador,A., *Optimisation of Cell Radius in UMTS-FDD Networks*, Master Thesis, Instituto Superior Técnico, Lisbon, Portugal, December 2002.

[SHLW00] Sipilä,K., Honkasalo,Z., Laiho-Steffens,J. and Wacker,A., "Estimation of Capacity and Required Transmission Power of WCDMA DL Based on a DL Pole Equation", *in Proc. of VTC2000*, Tokyo, Japan, 2000.

[SiLW99] Sipilä,K., Laiho-Steffens,J. and Wacker,A., "Soft Handover Gains in a Fast Power Controlled WCDMA UL", *in Proc. of VTC'99,* Houston, USA, 1999.

[SLWJ99] Sipilä,K., Laiho-Steffens,J., Wacker,A. and Jäsberg,M., "Modelling the Impact of the Fast Power Control on the WCDMA UL", *in Proc. of VTC'99,* Houston, USA, 1999.

[SoLa03] Soldani,D. and Laiho-Steffens,J., "User Perceived Performance of Interactive and Background Data in WCDMA Networks with QoS differentiation", *in Proc. of WPMC'03,* Kanagawa, Japan, October 2003.

[SOQU04] http://www.soquet.leeds.ac.uk/

[UMFo03] UMTS Forum, *3G Offered Traffic Characteristics*, UMTS Forum Report No.33, November 2003 (www.umts-forum.org/reports.html).

[UTRA04] http://www.sommiel.com/planning_tools.htm

[VaCa02] Vasconcelos,A., Carvalho,P., *Modelos de Tráfego para Estações de Base em UMTS*, Graduation Thesis, Instituto Superior Técnico, Lisbon, Portugal, September 2002.

[VaRF99] Valkó,A.G., Rácz,A. and Fodor,G., "Voice QoS in Third-Generation Mobile Systems", *IEEE Journal on Selected Areas in Communications*, Vol. 17, No. 1, Jan. 1999, pp. 109-123.

[WaBe88] Walfisch,J. and Bertoni,H. L., "A theoretical model of UHF propagation in urban environments," IEEE Trans. on Antennas and Propagation, Vol. 36, No. 12, Dec. 1988, pp. 1788-1796.

[WLSH99] Wacker,A., Laiho-Steffens,J., Sipilä,K. and Heiska,K., "The Impact of the Base Station Sectorisation on WCDMA Radio Network Performance", *in Proc. of VTC'99,* Amsterdam, The Netherlands, September 1999.

[Wool02] Woolfrey,M., *2003 make or break for UMTS?*, EMC, October 2002 (http://www.emc-database.com/website.nsf/index/pr021007#this-page)

[3GPP02a] 3GPP Management, (http://www.3gpp.org/Management/Management.htm)

[3GPP02b] 3GPP TS 25.401, *UTRAN Overall Description*,V3.10.0, http://www.3gpp.org/[7]

[3GPP02c] 3GPP TS 25.430, *UTRAN Iub Interface: General Aspects and Principles*, V3.8.0

[3GPP02d] 3GPP TS 23.101, *General UMTS Architecture*, V3.1.0

[3GPP02e] 3GPP TS 25.410, *UTRAN Iu Interface: General Aspects and Principles*, V3.8.0

[3GPP02f] 3GPP TS 21.111, *USIM and IC card requirements*, V3.4.0

[3GPP02g] 3GPP Specifications - Releases, http://www.3gpp.org/specs/releases.htm

[3GPP02h] 3GPP TS 21.101, *Release 1999 Specifications*, V3.9.0

[3GPP02i] 3GPP TS 21.102, *3rd Generation mobile system Release 4 specifications,* V4.6.0

[3GPP02j] 3GPP TS 21.103, 3rd Generation mobile system Release 5 specifications, V5.1.0

[3GPP02k] 3GPP TS 25.420, *UTRAN I_{ur} Interface General Aspects and Principles*, V3.5.0

[3GPP02l] 3GPP TS 25.331, *Radio Resource Control (RRC)*, V3.12.0

[3GPP02m] 3GPP TS 25.413, *UTRAN Iu Interface RANAP Signalling*, V3.11.0

[3GPP02n] 3GPP TS 25.201, *Physical layer - General description*, V3.4.0

[3GPP02o] 3GPP TS 25.104, *BS Radio transmission and Reception (FDD)*, V3.10.0

[3GPP02p] 3GPP TS 25.301, *Radio Interface Protocol Architecture,* V3.11.0

[3GPP02q] 3GPP TS 25.213, *Spreading and modulation (FDD),* V3.8.0

[3GPP02r] 3GPP TS 25.211, *Physical channels and mapping of transport channels onto physical channels (FDD)*, V3.12.0

[3GPP02s] 3GPP TS 25.214, *Physical Layer Procedures (FDD),* V3.11.0

[3GPP02t] 3GPP TS 25.215, *Physical layer - Measurements (FDD),* V3.11.0

[3GPP02u] 3GPP TS 22.105, *Services and Service Capabilities,* V3.10.0

[3GPP02v] 3GPP TS 23.107, *Quality of Service (QoS) concept and architecture,* V3.9.0

[3GPP02x] 3GPP TS 22.002, *Circuit Bearer Services (BS) supported by a Public Land Mobile Network (PLMN),* V3.6.0

[3GPP02y] 3GPP TS 22.060, *General Packet Radio Service (GPRS); Service description, Stage 1,* V3.5.0

[3GPP02w] 3GPP TS 25.306, *UE Radio Access capabilities,* V3.6.0

[3GPP02z] 3GPP TS 25.101, *UE Radio Transmission and Reception (FDD),* V3.11.0

[7] All 3GPP specifications are retrieved from latest R99 ftp folder in http://www.3gpp.org/

[3GPP04a] 3GPP TS 34.108, *Common test environments for User Equipment (UE)* conformance testing, V5.1.0

[3GPP04b] 3GPP TS 26.071, *Mandatory Speech Codec speech processing functions - AMR Speech Codec; General Description*, V3.0.1

[3GPP04c] 3GPP Web site, (http://www.3gpp.org)